

Berichte

zur Polar-
und Meeresforschung

583

2008

**Reports
on Polar and Marine Research**



**The Expedition of the Research Vessel "Polarstern"
to the Antarctic in 2007 (ANT-XXIII/9)**

**Edited by
Hans-Wolfgang Hubberten
with contributions of the participants**

 **HELMHOLTZ
| GEMEINSCHAFT**

**ALFRED-WEGENER-INSTITUT FÜR
POLAR- UND MEERESFORSCHUNG**
In der Helmholtz-Gemeinschaft
D-27570 BREMERHAVEN
Bundesrepublik Deutschland

ISSN 1866-3192

Hinweis

Die Berichte zur Polar- und Meeresforschung werden vom Alfred-Wegener-Institut für Polar- und Meeresforschung in Bremerhaven* in unregelmäßiger Abfolge herausgegeben.

Sie enthalten Beschreibungen und Ergebnisse der vom Institut (AWI) oder mit seiner Unterstützung durchgeführten Forschungsarbeiten in den Polargebieten und in den Meeren.

Es werden veröffentlicht:

- Expeditionsberichte (inkl. Stationslisten und Routenkarten)
- Expeditionsergebnisse (inkl. Dissertationen)
- wissenschaftliche Ergebnisse der Antarktis-Stationen und anderer Forschungs-Stationen des AWI
- Berichte wissenschaftlicher Tagungen

Die Beiträge geben nicht notwendigerweise die Auffassung des Instituts wieder.

Notice

The Reports on Polar and Marine Research are issued by the Alfred Wegener Institute for Polar and Marine Research in Bremerhaven*, Federal Republic of Germany. They appear in irregular intervals.

They contain descriptions and results of investigations in polar regions and in the seas either conducted by the Institute (AWI) or with its support.

The following items are published:

- expedition reports (incl. station lists and route maps)
- expedition results (incl. Ph.D. theses)
- scientific results of the Antarctic stations and of other AWI research stations
- reports on scientific meetings

The papers contained in the Reports do not necessarily reflect the opinion of the Institute.

The „Berichte zur Polar- und Meeresforschung“
continue the former „Berichte zur Polarforschung“

* Anschrift / Address

Alfred-Wegener-Institut
Für Polar- und Meeresforschung
D-27570 Bremerhaven
Germany
www.awi.de

Editor in charge:
Dr. Horst Bornemann

Assistant editor:
Birgit Chiaventone

Die "Berichte zur Polar- und Meeresforschung" (ISSN 1866-3192) werden ab 2008 ausschließlich elektronisch als Open-Access-Publikation herausgegeben (URL: <http://epic.awi.de>).

**The Expedition of the Research Vessel "Polarstern"
to the Antarctic in 2007 (ANT-XXIII/9)**

**Edited by
Hans-Wolfgang Hubberten
with contributions of the participants**

**Ber. Polarforsch. Meeresforsch. 583 (2008)
ISSN 1866-3192**

ANT-XXIII/9

**02 February 2007 - 10 April 2007
Punta Arenas - Cape Town**

**Fahrtleiter / Chief Scientist:
Hans-Wolfgang Hubberten**

**Koordinator / Coordinator:
Eberhard Fahrbach**

CONTENTS

1.	Zusammenfassung und Fahrtverlauf	5
	Summary and itinerary	9
2.	Weather and ice conditions	11
3.	Marine geophysics	15
4.	Marine geology in the Prydz Bay - Kerguelen Plateau area	37
5.	Mapping the distribution of Si and N isotopes in Southern Ocean surface waters and their relation to trace element availability	54
6.	The carbonate system and the carbon isotopic composition of particulate organic matter in southern ocean surface waters	59
7.	The influence of sediment transport on $^{230}\text{Th}_{\text{xs}}$ inventories and ^{14}C ages of organic matter in individual sediment fractions	62
8.	Documentation of the holocene and pleistocene variability of paleo-environmental conditions within the Antarctic Circumpolar Current (ACC)	67
9.	Deployment of Argo-floats	69
10.	<i>Phaeocystis antarctica</i> in a water transect from South America to South Africa	73
11.	High resolution bathymetry of the Prydz Bay and the Southern Ocean	75
12.	Late Quaternary environmental history of the Rauer Group, Prydz Bay region, as deduced from lake and marine basin sediments	80
13.	Functional microbial diversity in extreme antarctic habitats: abundance, phylogeny and ecology	95

14.	Petrology of Prydz Bay granulites (Larsemann Hills and Rauer Islands)	102
15.	MABEL: Multidisciplinary Antarctic Benthic Laboratory	107
	APPENDIX	114
A.1	Beteiligte Institute / participating institutes	115
A.2	Fahrtteilnehmer / cruise participants	118
A.3	Schiffsbesatzung / ship's crew	120
A.4	Station list PS 69	122
A.5	List of samples	131
A.6	Graphical core description	148

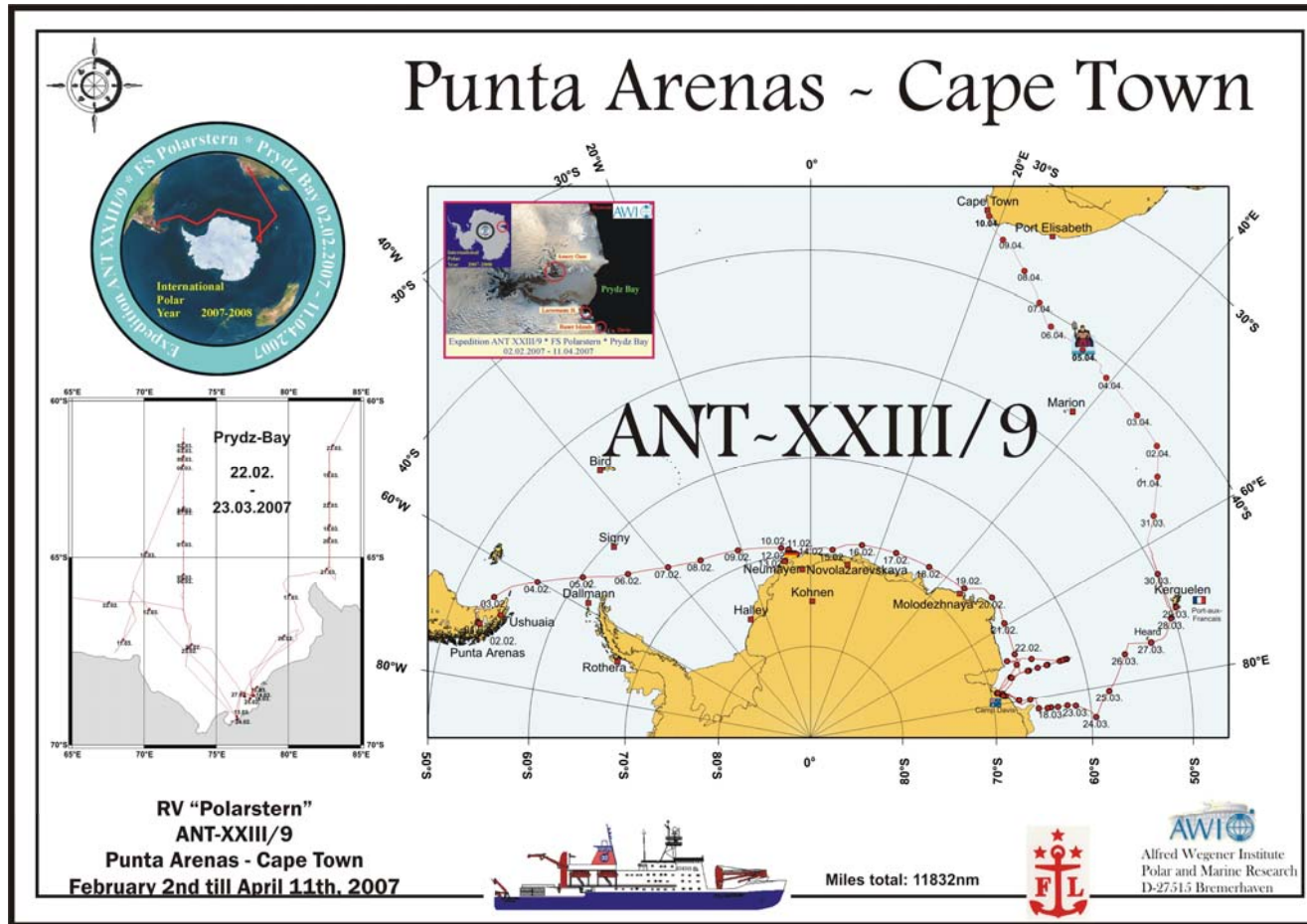


Abb. 1.1: Fahrtroute ANT-XXIII/9
Fig. 1.1: Cruise track ANT-XXIII/9

1. ZUSAMMENFASSUNG UND FAHRTVERLAUF

Hans-Wolfgang Hubberten
Alfred-Wegener-Institut für Polar- und Meeresforschung (AWI), Potsdam

Wissenschaftliche Schwerpunkte der Expedition ANT-XXIII/9 des Forschungsschiffs *Polarstern* waren geophysikalische und meeresgeologische Untersuchungen zur Erkundung der geodynamischen und tektonischen Entwicklung des Kontinentalrandes im Gebiet der Prydz-Bucht sowie die Rekonstruktion der glazial-marinen Umweltgeschichte dieses Gebiets im Spätquartär. In Ergänzung dazu wurden Feldarbeiten zur Klima- und Umweltrekonstruktion in eisfreien Gebieten in der Umgebung der Prydz-Bucht durchgeführt und die Entwicklung des antarktischen Permafrosts und seiner Lebensformen studiert. Ozeanographische Untersuchungen ergänzten das überwiegend geowissenschaftliche Programm der Expedition.

Die Expedition begann am 02. Februar 2007 in Punta Arenas, Chile, und führte nach Durchfahren der Magellanstraße auf direktem Kurs in Richtung Neumayer Station (Abb. 1.2). Vor Erreichen der Schelfeiskante wurde der Versuch unternommen, das italienische Ozeanbodenobservatorium MABEL aufzunehmen, welches am 05. Dezember 2005 ebenfalls von der *Polarstern* ausgesetzt worden war. Aufgrund von technischen Problemen an dem Aufnahmegerät MODUS war dieser Einsatz erfolglos, so dass MABEL bis zu einem zukünftigen Versuch am Meeresboden verbleiben musste. Danach nahm *Polarstern* Kurs auf die Atka-Bucht und machte nach Durchbrechen eines dichten Eisgürtels am Nordanleger fest. Die anschließend durchgeführte Versorgung der Neumayer Station erfolgte in Rekordzeit von nur einem Tag.

Auf der Fahrt zu dem Hauptarbeitsgebiet der Expedition, der Prydz-Bucht, wurden 14 automatische Driftbojen im Rahmen des internationalen Argo-Projekts ausgesetzt.

Nach dem Eintreffen in der Prydz-Bucht wurde an den Larsemann Bergen mit dem Ausfliegen von zwei Landgruppen begonnen. Die erste Gruppe führte geomikrobiologische Untersuchungen in Permafrostböden durch, von denen wichtige Erkenntnisse für die Entwicklung von Lebensformen unter extremen klimatischen Bedingungen erwartet werden. Die zweite Gruppe konzentrierte sich auf petrologische Untersuchungen der metamorphen Komplexe an der Ostseite der Prydz-Bucht. Parallel dazu erfolgten Besuche an den Stationen Progress (Russland) und Zhongshan (China). Zu der chinesischen Station wurden per Helikopter Deichseln und Ersatzteile für Schlitten geflogen. Mit den russischen Partnern wurden logistische Fragen einer für das Jahr 2007/2008 geplanten Landtraverse diskutiert. Nachdem der geplante Aufbau eines Feld-

camps in der Amery-Oase aus Wettergründen gestrichen werden musste, erfolgte das Ausfliegen der dritten Landgruppe auf die Rauer-Inseln. Diese Gruppe konzentrierte sich auf die Gewinnung von Sedimenten aus Frischwasser- und Epi-Schelfseen zur Rekonstruktion der Klima- und Umweltgeschichte dieser Region. Auf einer Insel wurden eine seismische und eine magnetische Station aufgebaut. Parallel zu den Flugaktivitäten wurden einige meeresgeologische Beprobungen in der Prydz-Bucht durchgeführt.

Anschließend begann das umfangreiche geophysikalische Programm, welches die Untersuchung der geodynamischen und tektonischen Entwicklung des Kontinentalrands zwischen Prydz-Bucht und Kerguelen-Plateau zum Ziel hatte (Abb. 1.3). In einem ersten seismischen Profil wurden bei 72°43'E vom Kontinentalrand nach Norden 19 OBS und 3 OBH ausgesetzt. Gemeinsam mit dem russischen FS *Akademik Alexander Karpinsky* wurden in einem Zweischiif-Unternehmen seismische Linien mit einem Mehrkanalseismiksystem unter Nutzung eines 5 km langen digitalen Streamers vermessen. Ein zweites seismisches Profil wurde nach Verlassen der Prydz-Bucht weiter östlich bei 82°50'E abgefahren.

Danach wurden entlang des seismischen Profils mehrere meeresgeologische Stationen durchgeführt, bei denen Oberflächenproben und lange Sedimentkerne geborgen wurden.

Zurück in der Prydz-Bucht konnten aufgrund von starker Neueisbildung keine OBS ausgesetzt werden. Das geplante seismische Profil über den Lambert-Graben musste folglich gestrichen werden. Für einige Tage konzentrierten sich die Arbeiten deshalb auf das Umsetzen, Ausfliegen und Einholen der Landgruppen. Während dieser Zeit wurde auch ein IPY Gipfeltreffen mit den Leitern der Stationen Davis (Australien), Progress (Russland) und Zhongshan (China) auf der *Polarstern* abgehalten. Ein Besuch an der australischen Davis-Station wurde zur Eichung der magnetischen Daten von *Polarstern* sowie für Referenzmessungen für das gravimetrische Messprogramm genutzt. Weitere gravimetrische Anschlussmessungen wurden noch an der Station Port-aux-Francais und der historischen Drygalsky Station auf den Kerguelen-Inseln sowie am Ende der Reise in Kapstadt durchgeführt.

Parallel zu den seismischen Arbeiten wurde ein engmaschiger magnetischer Survey unter Nutzung eines Hubschraubers der *Polarstern* geflogen, um die Messungen des Bordmagnetometers zu ergänzen.

Nach Beendigung des zweiten seismischen Profils wurde eine umfangreiche meeresgeologische Beprobung vom Kontinentalrand bis auf das Kerguelen-Plateau vorgenommen, wobei mit einem Kerngewinn von 28,15 m der bisher längste Kern gewonnen wurde. Weitere geplante Stationen westlich der Kerguelen mussten wegen Sturm gestrichen werden.

Fast auf der gesamten Fahrtstrecke von Punta Arenas über das Weddellmeer zur Prydz-Bucht und weiter über das Kerguelen-Plateau Richtung Kapstadt wurden Proben zur Untersuchung der Konzentration von Nährstoffen und Eisen sowie der Si und N Isotope in Diatomeen genommen.

Auf dem Transit nach Kapstadt wurde die verbleibende Schiffszeit genutzt, um zwei kurze geophysikalische Messprogramme über dem Kerguelen-Plateau durchzuführen (Magnetik, Schweremessungen, Parasound, Hydrosweep). Diese dienten zum einen zur Ergänzung früherer Untersuchungen, die mit dem Forschungsschiff *Sonne* im Jahr 2005 durchgeführt wurden, und zum zweiten für einen „Pre-Site-Survey“ für eine Bohrlokation im Rahmen des Internationalen Ozeanbohr-Projekts (IODP) genutzt werden.

Die Expedition ANT-XXIII/9 endete aus logistischen Gründen einen Tag früher als geplant am 10. April 2007 in Kapstadt.

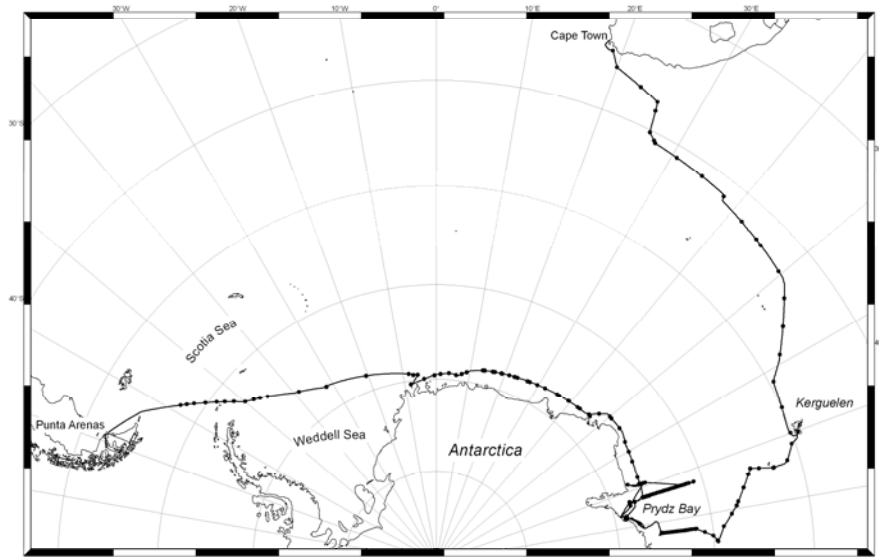


Abb. 1.2: Übersicht der Fahrtroute der Polarstern Expedition ANT-XXIII/9
Fig. 1.2: Overview of track chart of Polarstern expedition ANT-XXIII/9

SUMMARY AND ITINERARY

Hans-Wolfgang Hubberten
Alfred-Wegener-Institut (AWI), Potsdam

The scientific programme of the Antarctic expedition ANT-XXIII/9 of *Polarstern* concentrated mainly on geophysical and marine geological studies to investigate the geodynamic and tectonic development of the continental margin of the region as well as to reconstruct the glaciomarine environmental history of the late Quaternary. In addition, studies of the climatic and environmental reconstruction have been carried out on the ice-free areas surrounding the Prydz Bay, which were complemented by investigations on the development of permafrost and primitive life as well as on petrologic studies. In addition to these major research topics, smaller programmes on oceanographic and chemical studies were carried out.

The expedition started on 02 February 2007 in Punta Arenas, Chile, and took direct course to the Neumayer Station after leaving the Magellan Strait (Fig. 1.2). Before arriving at the ice shelf border, the Italian ocean floor observatory MABEL, which was deployed from *Polarstern* on 05 December 2005, could not be recovered as planned due to technical problems of the system. The subsequent annual supply of the German over-wintering station Neumayer was undertaken in a record time of only one day.

On transect from Neumayer Station to Prydz Bay, 14 floats were deployed under the umbrella of the Argo project, accompanied by several CTD casts.

After arrival in Prydz Bay the first land groups were flown out with the helicopters to the Larsemann Hills in order to start with geomicrobiological studies in permafrost soils as well as with sampling of rocks for petrological investigations. Parallel to these activities the permanent stations Progress (Russia) and Zhongshan (China) were visited. As the planned field work in the Amery Oasis had to be cancelled due to bad weather conditions, a larger group was transported to the Rauer Islands to sample lake sediments from freshwater and epishelf lakes. A seismological "Reftec" station and a magnetometer were installed on one of the Rauer islands. Marine geological sampling was carried out at several stations during this period.

After these operations the comprehensive geophysical programme began which was focused on the investigation of the geodynamic and tectonic development of the continental margin in the Prydz Bay area (Fig. 1.3). In the first deep crustal seismic refraction profile at 72°43'E, 19 OBS and 3 OBH were deployed from the continental boundary to the north. The profile was studied in a two-vessel experiment together with the Russian RV *Akademik Alexander Karpinsky*

using a state-of-the-art seismic reflection system including a 5 - 6 km long digital streamer. A second seismic profile was measured after leaving the Prydz Bay area, in a S-N transect east of the first profile at 82°50'E. On the track of the first seismic profile and closer to the continent west of this line, several marine geological stations were realized. Parallel to the seismic studies, densely-spaced parallel magnetic survey lines were flown by the *Polarstern* helicopters equipped with a towed Caesium magnetometer system and completed by the shipboard fluxgate magnetometer system.

Returning to Prydz Bay, a seismic profile planned in this area with the aim to study the structure of the Lambert Graben had to be cancelled due to strong new ice formation. The work in the Bay was concentrated on flight operations for investigations on land and the final transport of all land camps back to *Polastern*. An Antarctic IPY summit was held on board *Polarstern* with the leaders of the stations Davis (Australia), Progress (Russia), and Zhongshan (China). A later visit of the Australian Davis Station was used for the calibration of the magnetic and gravimetric measurements. Further gravimetric reference measurements were undertaken at Port-aux-Francais Station and the historical Dyrygalsky Station on Kerguelen Islands and after the end of the cruise at Cape Town.

After finishing the second seismic profile, an intensive marine geological sampling started from the continental margin to the Kerguelen Islands with a maximum recovery of 28.15 m of sediment with a piston corer. Further stations planned west of Kerguelen had to be cancelled due to bad weather conditions.

On the transit to Cape Town remaining ship time was used for two short geophysical surveys at the Agulhas Plateau using gravimetric, magnetic, parasound and hydrosweep measurements for complementing geophysical studies carried out with the German research vessel RV *Sonne* in 2005 and to obtain information for a pre site survey for the International Ocean Drilling Program (IODP).

Surface water samples were taken to support paleoceanographic reconstructions of nutrient cycling in the Southern Ocean and their impact on atmospheric CO₂ over past climate cycles almost continuously along the cruise track from Punta Arenas to Cape Town via Prydz Bay and the Kerguelen Plateau.

The *Polarstern* expedition ANT-XXIII/9 ended in Cape Town on 10 April 2007, due to logistic reasons one day earlier than planned.

2. WEATHER AND ICE CONDITIONS

Reinhard Strüfing, Hartmut Sonnabend
DWD Hamburg

Polarstern left Punta Arenas on 2 February. En route to Neumayer weak air pressure differences prevailed at first, except two hours of westerly winds with Bft 8 to 9 near Cape Horn. On 5 February, south-east of Elephant Island, first icebergs appeared in the fog over the northern outflow of the Weddell gyre. Later the first gale force low moved into the Weddell Sea and *Polarstern* encountered easterly winds force 9 with waves of 6 or 7 meter sideways on 7 to 8 February. On 10 February, reduced swell enabled an attempt to raise MABEL, the ocean bottom observatory near Neumayer.

The final approach to Neumayer on 12 February took place during whiteout conditions. The handling of the supplies to Neumayer had to be postponed until the following day when the weather improved due to katabatic air motions dissolving the clouds. During the evening of February 13 *Polarstern* already pushed its way through the ice near Atka Bay, now heading for its destination Prydz Bay near 75°E, 2,000 miles away.

During the first 4 days the depressions of the subantarctic low pressure belt were too weak to affect *Polarstern's* journey. At this stage a helicopter flight took place from Casey Bay near 50°E in order to sample rocks from the mountains of Enderbay Land. Once again katabatic air flow caused the clouds to dissolve over the Antarctic coast despite adverse weather conditions over the sea.

Later on an extended ice belt near the coast and strong, sometimes gale force easterly winds lead to reduced ship's speed, uncomfortable movements by the ship und icing. The ice coverage of the summer season 2006/2007 mainly near the entrance to the bay was considered as abnormally high, (see Fig 2.1) for its stage on 22 February.

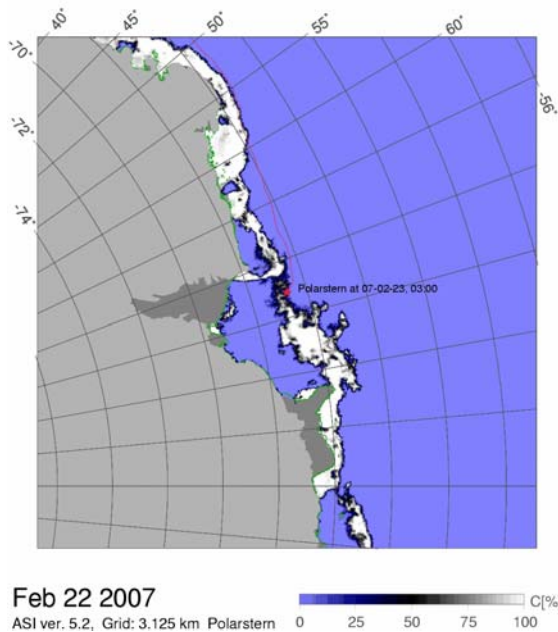


Fig. 2.1: Ice conditions in Prydz Bay region on 22 February

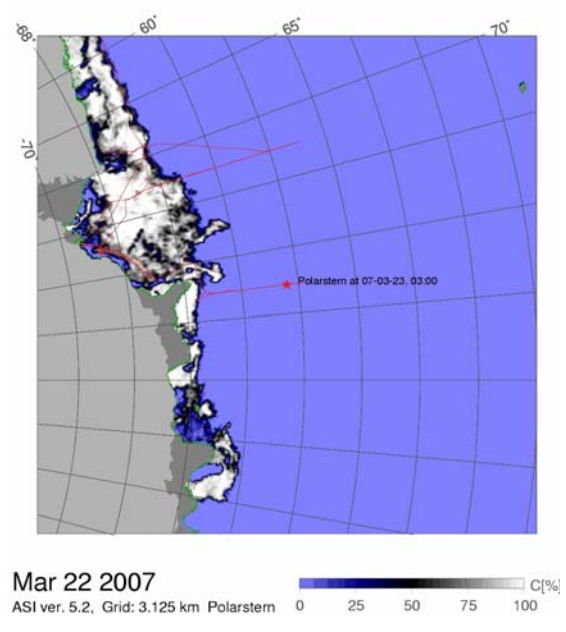


Fig. 2.2: Ice conditions in Prydz Bay region on 22 March

The disembarkation of the groups destined for the Larsemann hills and the Rauer islands, part of the eastern area of Prydz Bay, started on 24 February. The helicopter flights happened during easterly winds with mostly low cloudiness. When on 27 February a hurricane force low moved into Prydz Bay it was decided to tackle the forecast winds of force 10 inside the bay. On 28 February isolated force 11 and gusts of force 12 were encountered with a wave height of only 7 meter. The land groups had to rest meanwhile. Otherwise, these land groups took advantage of the katabatic downward motion in the easterly air flow which frequently dissolved the clouds.

Polarstern met the start of the International Polar Year (IPY) on 1 March outside Prydz Bay when dealing with seismic traverses. The weather consisted of a mixture of rather weak lows and unpronounced high wedges, but a lot of clouds. Therefore the flights with the magnetometer were partly hampered by low clouds, freezing drizzle und light snow. During this time *Polarstern* cooperated with the Russian RV *Akademik Alexander Karpinsky*.

After geo stations near the northwest area of Prydz Bay *Polarstern* returned into the bay on 13 March in order to fetch land groups for embarkation or shift other groups to different areas. The helicopter flights benefited from the mostly sunny weather conditions. At this time three other ships could be observed in the vicinity busy with the winter supplies of the three stations there. With the dominant southerly airflow over the western parts of Prydz Bay quite a lot of new ice had formed. Therefore, the inshore seismic traverse had to be cancelled.

Because of IPY delegations of the Australian Station Davis, the Chinese station Zhongshan and Russian station Progress were invited to a reception aboard

Polarstern on 14 March. In return the Australians invited crew and scientists to visit their station which took place on 15 March. One day later the remaining scientists returned from Rauer Islands, the ship left Prydz Bay and, at temperatures near minus 10° C, made its way through fast growing new ice, a lot of multi-annual sea ice and many icebergs of an almost completely frozen Prydz Bay (see Fig 2.2).

With mostly southerly winds and waves not higher than 3 meter the weather during the following second seismic traverse along the 83°E was quite similar to the situation at the first measurements. During 24 March *Polarstern* reached its easternmost position in the southern hemisphere ever, when a geo-station was held near the 86°E.

When continuing in direction to Kerguelen Plateau frontal systems of an extended gale force low passed. However, on 27 March the low clouds broke and opened the view at Heard Island. The smoke plume of its 2,800 m high volcano could be seen quite clearly. During the following night *Polarstern* went through a southerly gale force 9 with waves of 7 meter height. Only 12 hours later the waves had ceased to an extent that the piston corer released a record sediment core of 28.15 meter, the longest ever aboard this ship.

At dawn of 29 March *Polarstern* sailed into Golf de Morbihan, part of the Kerguelen Islands, and dropped anchor near Port-aux-Francais, the French station. The predicted high pressure had verified, so crew and scientist could experience this barren part of the world under relatively comfortable conditions. During the early afternoon *Polarstern* put out to sea for the last leg of this cruise heading for cape town, against the prevailing westerly winds. However, at first advantage could be taken of the easterly winds caused by an approaching gale force low.

During the evening of March 30 a westerly gale up to Bft 10 developed with a wave maximum of 10 meter and ship's speed reduced. This situation happened again with slightly less intensity on 2 April. Thereafter wind and waves decreased though the swell continued at high level for some time. On 4 April, the thermometer first time showed temperatures above 10° C, on 5 even almost 20° C when the polar baptism took place with perfect weather conditions. Few hours later a cold front with heavy thunderstorms passed with temperatures decreasing to 11° C on 6 April.

After the passage of another high and the following easterly winds near force 7 on Easter Sunday, 8 April, *Polarstern* put into Cape Town harbour during the evening of 10 April.

Figures 2.3, 2.4 and 2.5 indicate the distribution of wind and waves during cruise ANT-XXIII/9.

Distribution of Wind Direction 02.02.-06.04.07

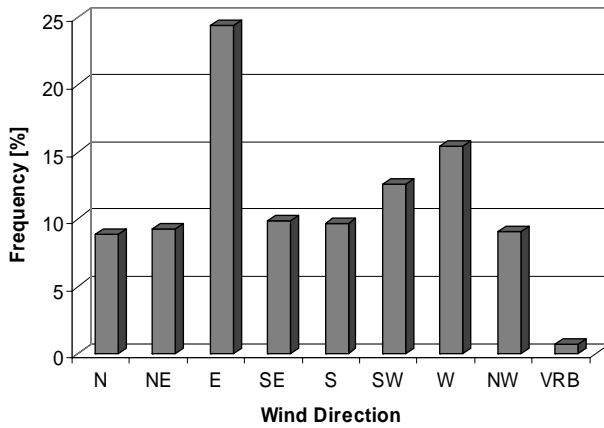


Fig. 2.3: Frequency distribution of wind conditions during the cruise (wind direction)

Distribution of Wind Force 02.02.-06.04.07

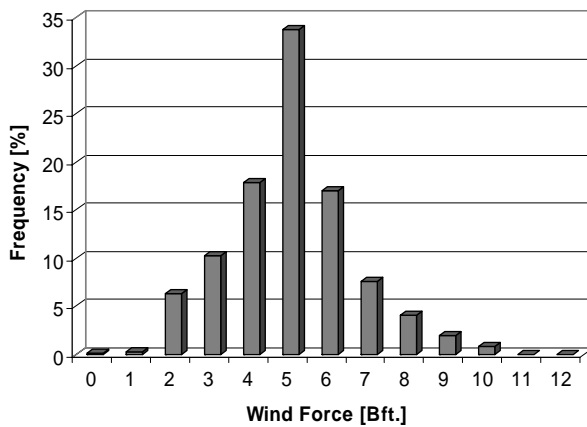


Fig. 2.4: Frequency distribution of wind conditions during the cruise (wind force)

Distribution of Wave Height 02.02.-06.04.07

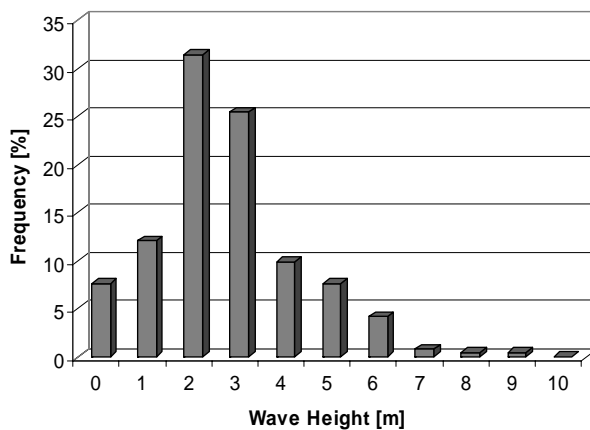


Fig. 2.5: Frequency distribution of wave conditions during the cruise (wave height)

3. MARINE GEOPHYSICS

Geodynamic and tectonic evolution of the continental margin of the Prydz Bay area

Karsten Gohl¹⁾, Nicole Parsieglä¹⁾,
Birte-Marie Ehlers¹⁾, Conrad
Kopsch²⁾, Detlef Damaske⁴⁾, Norbert
Lensch¹⁾, Martin Hansen⁶⁾, Christina
Bienhold¹⁾, Kristin Daniel¹⁾, Joshua
Knight⁵⁾, Kristina Meier¹⁾, Florian
Stark¹⁾, Morelia Urlaub¹⁾

¹⁾Alfred-Wegener-Institut (AWI),
Bremerhaven

²⁾Alfred-Wegener-Institut (AWI),
Potsdam

³⁾VNII Okeangeologia, St. Petersburg,
Russia

⁴⁾Federal Institute for Geosciences
and Resources (BGR), Hanover

⁵⁾University of Sydney, School of
Geosciences (USYD), Australia

⁶⁾K.U.M. Umwelt- und Meerestechnik
GmbH (KUM), Kiel

(German Leitchenkov³⁾, on board RV *Karpinsky*)

Objectives

The separation of Greater India from Antarctica in early Cretaceous time and the break-up of Australia from Antarctica since the Late Cretaceous led to the formation of the modern Indian Ocean and a continuous oceanic passage between the southern Atlantic (Weddell Sea), the Southern Indian Ocean and the western Pacific. The Cretaceous Gondwana break-up was accompanied by enormous volcanic extrusions of so-called Large Igneous Provinces (LIP), such as the Kerguelen Plateau in the Southern Indian Ocean. The geodynamic and depositional record of these events, which largely affected the Earth's climate, is best preserved in the crustal structure and sedimentary record of the marine region juxtaposed to the Amery Ice Shelf and includes the continental shelf, slope and rise of Prydz Bay, the eastern Cooperation Sea, the eastern Enderby Abyssal Plain, Southern Kerguelen Plateau and the Princess Elizabeth Trough between the Southern Kerguelen Plateau and Princess Elizabeth Land (Stagg et al., 2005).

The Kerguelen Plateau marks one of the two most voluminous LIPs in oceanic setting and is attributed to the Kerguelen mantle hotspot emplaced 120 million years ago, about 15 million years after the onset of seafloor spreading between India and Antarctica (Gaina et al., in press). Earlier studies and ODP Leg 183 drill data have shown that the Southern Kerguelen Plateau and Elan Bank are partly underlain by continental crust affected by Cretaceous extension (e.g. Operto & Charvis, 1996; Gladczenko & Coffin, 2001). It is unclear, how far south the plateau maintains possible continental origin and how its igneous activity affected the apparent oceanic crust between the plateau and the East Antarctic continent. Despite continuous subsidence from early Late Cretaceous

to Eocene time, the Kerguelen Plateau has remained a shallow marine feature that influences the oceanic circulation in the Indian Ocean. For instance, the Antarctic Circum-Polar Current (ACC) is deflected by the topography of the plateau.

Prydz Bay lies at the offshore continuation of the Lambert Graben that marks one of the most prominent intracontinental rifts. The Lambert Graben is coupled with a deeply submerged peri-continental rift system beneath the continental slope and rise of the Cooperation Sea whose highly extended crust has been suggested to form a transition to the Enderby Abyssal Plain seafloor formed by Early Cretaceous spreading. The Cenozoic sedimentary cover of the deep-water basins contains a complete distal record of the earliest glacial events and associated climate changes known in Antarctica. Yet, the origin, evolution and tectonic activity of the Lambert Rift region is hardly understood. Equally unknown are the consequences of lithospheric dynamics and crustal tectonics for the dynamics of the East Antarctic Ice-Sheet in the area of the Lambert Graben, Prydz Bay and the adjacent continental margins of Mac Robertson Land and Princess Elizabeth Land. The following questions are addressed by this project:

- structural parameters, physical properties and interrelations of rifted continental, oceanic and volcanic crust in the Prydz Bay area;
- mechanism of extension of continental crust, geometry of rifting and time (onset and duration) of rifting stage;
- position and nature of the continent-to-ocean transition, timing and geodynamic regime of seafloor formation, particularly the position of rotation poles at early stages of seafloor spreading between India and Antarctica;
- subsidence history of Prydz Bay and the Cooperation Sea basin and its evolution as deep oceanic gateway;
- tectonic nature of the southern Kerguelen Plateau (oceanic edifice or continental sliver) and the relationship between seafloor spreading and LIP formation.

This objectives and goals of this geophysical programme are integral components of the *International Polar Year* (IPY 2007/08) project “Plate Tectonics and Polar Gateways in Earth History” (PLATES & GATES).

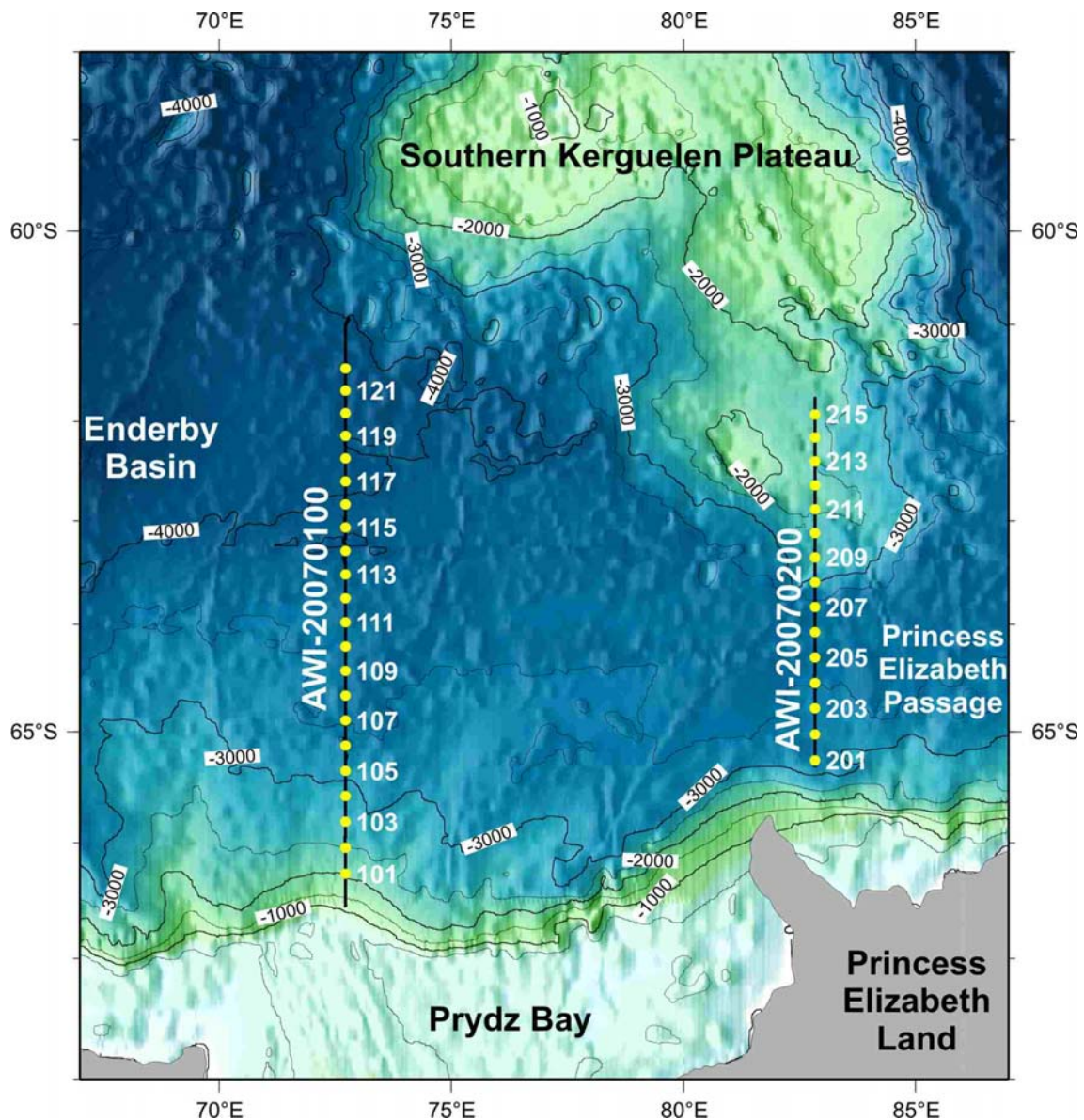


Fig. 3.1: Topographic map of working area with OBS/OBH stations (yellow dots and station numbers - complete PS69/...) along deep crustal seismic profiles AWI-20070100 and AWI-20070200 (black lines)

Work at sea

The geophysics programme of the *Polarstern* expedition ANT-XXIII/9 was conducted as a cooperative IPY 2007/08 project between AWI and the 52th Russian Antarctic Expedition of VNIIOkeangeologia and *Polar Marine Geological Expedition* (PMGE) (both St. Petersburg, Russia) with the RV *Akademik Alexander Karpinsky*. Further cooperation partner was the *School of Geosciences* of the *University of Sydney* (Australia). The expertise of geoscientists of *Geoscience Australia*, who have previously done extensive geophysical work in this area, helped in planning this project. This international cooperation allowed additional and complementary data acquisitions and a two-ship seismic experiment. The geophysical data acquisition on *Polarstern*

included (a) deep crustal refraction/wide-angle reflection seismics, (b) helicopter and shipboard magnetics and (c) gravimetrics.

The originally proposed project plan consisted of three deep crustal seismic profiles using ocean-bottom seismometers (OBS) off the Mac Robertson Land margin, across the Princess Elizabeth Trough (Fig. 3.1) and across the Lambert Graben of Prydz Bay, with all profiles accompanied by parallel heli-magnetic flight tracks. However, a tight cruise schedule and the fast growth of new sea ice at this time of the season prevented us from deploying OBS systems in the inner Prydz Bay. Therefore, the deep seismic profile across the Lambert Graben had to be cancelled. The wide sea ice cover at this time of the season also prevented us from extending the two remaining profiles onto the continental shelf. Profile AWI-20070100 followed the multichannel seismic reflection line RAE-5206 collected by the RV *Karpinsky* in the same season. Profile AWI-20070200 followed mostly the multichannel seismic reflection line RAE-3910 collected by the RV *Karpinsky* in 1994.

a) Deep crustal seismics

Methods and equipment

Standard seismic refraction and wide-angle reflection techniques were applied along two profiles using ocean-bottom hydrophone (OBH) and ocean-bottom seismometer (OBS) systems in order to collect P- and S-wave phases from the crust and upper mantle. Profile AWI-20070100 was occupied with 22 OBH/OBS systems at a nominal spacing of 25.5 km along a 625.6 km long shot profile (Tab. 3.1). On profile AWI-20070200, we deployed 15 OBH/OBS systems at a nominal spacing of 26.5 km along a shot profile of 398.5 km length (Tab. 3.2). We used two different ocean-bottom seismic data acquisition systems during this cruise: 20 LOBSTER (Long-term Ocean-Bottom Seismometer for Tsunami and Earthquake Research) type OBS systems of the DEPAS equipment pool and 3 OBH systems of AWI.

The LOBSTER systems consist of syntactic foam floats mounted on a steel frame together with the data logger and batteries in a pressure cylinder, an acoustic release, a seismometer, a hydrophone, a radio beacon, a xenon flash light and a flag (Fig. 3.2). The system is tightly connected to an anchor frame via the acoustic releaser. The anchor type depends on the weight of the LOBSTER, i.e. on the number of floats and the number of pressure cylinders. We used anchor type 4 (85 kg) for LOBSTERs with two pressure cylinders and anchor type 3 (62 kg) for systems with a single pressure cylinder. The first pressure cylinder contains the SEND Marine Compact Seismocorder (MCS) data logger and a pack of 48 alkali batteries. For short-term deployments, the additional pressure cylinder contains battery dummies. The acoustic/time release unit KUMQuat 562 is attached to the frame with the corresponding clamp and to the anchor frame hook through a hook and the releaser latch. The 3-component broadband Guralp CMG-40T (30 s natural period) seismometer is mounted to the frame. A clamp bolt of the anchor plate is pushed against the seismometer to achieve a good coupling. The HighTech hydrophone is attached to the upper part of the frame. The acoustic release communicates via the

K/MT 8011M deck unit. The recording parameters are set via the Linux programme SENDCOM3 which also controls the time synchronisation of the internal clock with the external GPS clock (Motorola M12 Plus Oncore). For both profiles, the sampling frequency was set to 250 Hz, and the gain was set to 16 for the hydrophone channel and to 4 for the seismometer channels, respectively. The data were stored on 20 GB hard disks of the MCS.

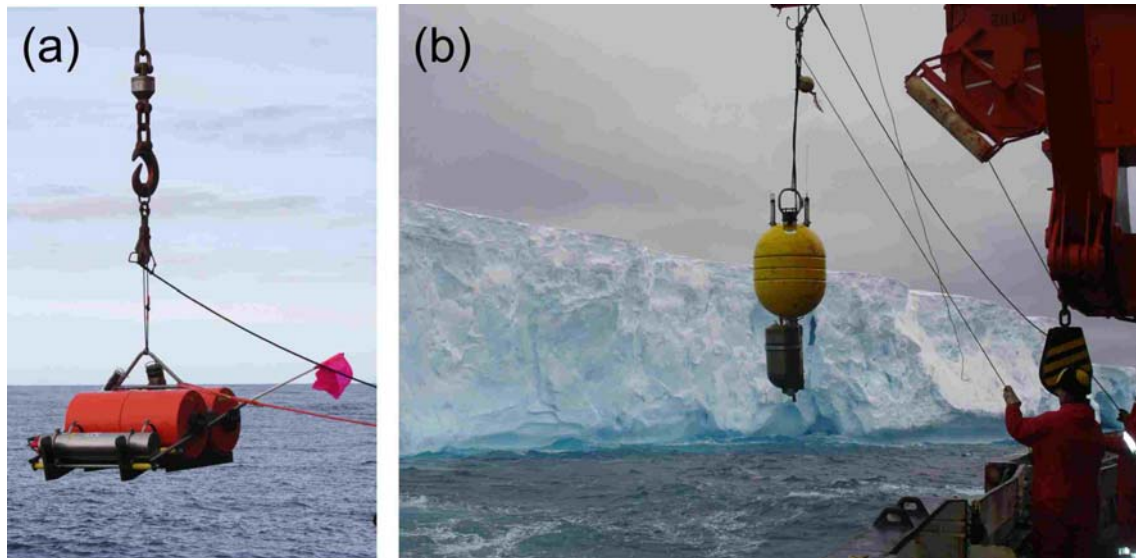


Fig. 3.2: (a) Deployment of an OBS system (type LOBSTER) and (b) recovery of an OBH system

The components of an OBH are mounted on a steel rack (Fig. 3.2). Beneath a ring for deployment and retrieval purposes, the steel construction holds a floating body consisting of syntactic foam and a pressure chamber holding the power supply and seismic recording unit. The seismic hydrophone is an E-2PD sensor made by OAS Inc. The acoustic/time release unit, made by MORS/OCEANO (type RT-661 CE), is mounted next to the recording pressure chamber. A ground weight of 60 kg as anchor is suspended 2.5 m below the release system. Communication with the release system is transmitted via a hydrophone mounted on top of the buoyancy body next to a Xenon flashlight, radio beacon of NOVATECH type, flag and a length of floating rope. The acoustic release communicates with the K/MT 8011M deck unit. The pressure cylinder contains a 1-channel Marine Broadband Seismic Recorder (MBS) manufactured by SEND GmbH, powered by a rechargeable lead-acid battery (12 V, 33 Ah). The pre-amplified (SN21 preamplifier) analogue input signal is digitized by the 16-bit analogue-digital converter (ADC) of the MBS. The recording parameters are set via the control programme SENDCOM2 which also controls the time synchronisation of the internal clock with the external GPS clock. During this survey, the sampling frequency was set to 250 Hz for the hydrophone channel. From a possible scale of 1-31, the gain was set to 5. The data were stored on 1 GB FlashCards connected to the MBS via a PCMCIA socket. For time synchronisation, we used a Meinberg GPS-166 clock which also provided the signal for the airgun trigger pulse.

As seismic source for the OBS/OBH profiles (Tab. 3.3), we used a cluster of 8 G.Guns™ (8 x 520 in³ = 4160 in³ = 68.17 liters in total) mounted on a steel frame and lowered into the water from the A-frame (Fig. 3.3). The cluster was towed 15 m behind the vessel at a depth of 10 m. For profile AWI-20070100, the airguns were fired once per minute at an operation air-pressure of 180-190 bar, leading to a nominal shot spacing of 150 m. For profile AWI-20070200, we added a single Bolt™ 800CT airgun of 2,000 in³ (32.8 liters) volume to the G.Guns™ on starboard side for increased volume and lower frequency. The airgun was towed 15 m behind the vessel at a depth of 13 m. In this configuration, the operation air-pressure was set to 130 - 140 bar for both the Bolt™ airgun and the G.Guns™. With a hydrophone towed at about 200 m distance, we measured the relative shots delays between the two airguns systems. The G.Gun™ trigger was set between 25 and 35 ms in order to be in sync with the Bolt airgun firing. The G.Gun™ cluster had to be repaired three times along profile AWI-20070100. During two of these shot gaps, the RV *Karpinsky* deployed 2 airguns (type 6PI-20) of 40 liters each and fired them with 140 bar at the same rate of 60 s. An AWI-owned Meinberg GPS-166 clock was installed on the *Karpinsky* for the two-ship experiment and provided the trigger time. Shot delay times were continuously recorded.



Fig. 3.3: G.Gun™ cluster used as seismic source

We deployed a 3-channel Reftek™ 72-A seismic recorder (AWI-11) with a 1-Hz 3-component seismometer (Mark-4L) on Hop Island (coordinates 68°49.80' S, 77°40.67' E) of the Rauer Island group on 25 February 2007 in order to record airgun shot arrivals along a landward extension of the planned OBS profile in Prydz Bay (which was eventually not conducted) and, at the same time, record

any possible seismicity over several weeks after its deployment. Recording started on 25 February 06:02 UTC. The recording is continuous with a sampling rate of 100 Hz. Accurate time information is provided through an external GPS antenna. The RefTek™ with its batteries and a solar panel was housed in a weather-tight aluminium box. The seismometer was covered with a turned-over bucket. Both items were covered with loose rocks to avoid movements and destruction from strong winds. During collection of the instrument on 14 March, we noted that the Reftek™ failed to communicate with the connected Epson™ handheld control terminal. Batteries were still well charged. As data could not be downloaded with board means, power was disconnected on 20 March. Another attempt to save any data will have to be made at the institute.

Two-ship wide-angle reflection recordings

For the purpose of continuous recordings of pre-critical wide-angle reflection data of the lower crust and crust-mantle boundary, the RV *Karpinsky* deployed its seismic streamer and followed *Polarstern* on shot profile AWI-20070100 at a distance between 15 and 30 km while recording the airgun shots of *Polarstern*. The distance varied according to assumed crustal thickness. The seismic reflection equipment of *Karpinsky* consists of a 4,400 m long digital streamer (type Input/Output MSX-6000M™) with 352 channels (hydrophone group spacing of 12.5 m) and an MSX-6000™ recording system. Each shot was recorded with a trace length of 40 s and a sampling rate of 2 ms and was then converted to SEG-Y format. The trigger time for the recording unit was provided by the Meinberg GPS-166 clock in order to be on the same time basis with the airgun trigger of *Polarstern*. From a total of 4,029 records, 3,636 wide-angle shots by the *Polarstern* airguns were recorded. The remaining 393 shot records contain normal-incidence reflection data of the *Karpinsky* airguns when substituting for *Polarstern* shot gaps.

Processing of OBH/OBS data

The OBH/OBS data acquired from all 36 stations were subject to onboard processing consisting of the following steps:

- 1) The MBS/MCS recorders were connected to the GPS clock and the DEPAS Linux laptop computer running the programmes *SENDCOM2* or *SENDCOM3*, respectively. Recording was ended and time skew was taken to obtain the time drift of the internal clock of the recorder compared to GPS time. This closes the data file.
- 2) The data and log files were copied to the Linux PC via an external hard disk. The data files were pre-processed with the Linux version of the *send2x* programme package (version 2.X). The routines *mbsread* (for MBS recorders) or *mcsread* (for MCS recorders) extract the data from the raw files. The routine *seg-ywrite* demultiplexes the data, adds shot and station coordinates to the trace headers and converts the data to the SEG-Y format according to a given time window provided by a shot point coordinate file. A SEG-Y file with constant trace lengths of 60 s was extracted, beginning at the exact shot time.
- 3) Using *CWP/SU* (SeismicUnix) software, the data were converted from SEG-Y to SU format. Shot-receiver offsets were calculated and written, together with

water depths at the receiver, into the file header. After bandpass filtering (4-17 Hz), travel-time reduction and optimising display parameters, the OBH/OBS records were displayed for a first data analyses.

- 4) For archiving purposes, the data were transferred to the UNIX server 'wega'.
- 5) For the calculation of velocity-depth models, the data were re-converted from SU to SEG-Y format and further into the ZP format. Using the programme ZP, refraction and reflection phases were picked from the records.

b) Helicopter and shipboard magnetics

We collected 8,056 km of aeromagnetic data with a Scintrex[®] caesium vapour magnetometer, towed 30 m below the helicopter in a 'bird'. Inside the cockpit, the magnetometer was connected to the PICODAS[™] data acquisition system, consisting of a PC connected with a GPS-antenna and a radar altimeter. Daily flight planning was done on a laptop using prepared grids. Waypoints were generated in a separate programme and entered into the helicopter's GPS to navigate along the planned flight paths. The GPS was recorded with the PICODAS[™] data acquisition system with an antenna installed on the front panel of the helicopter. In addition, GPS was recorded on a laptop using software written by Conrad Kopsch which allowed recording the flight tracks independently. This proved to be of importance when the PICODAS[™] system failed to record GPS positions at a few occasions. In order to achieve survey lines being parallel to the seismic profiles, we used a Lambert conformal projection. A minimum of two lines (at a line spacing of 5 km) to the east and west of the central ship's track were flown so that a 20 km wide swath was surveyed over the entire length of each profile. In some profile segments, depending on weather and area of interest, the swath was widened to 30 km, or to 50 km on the northern end of seismic profile AWI-20070200. Whenever possible, tie lines perpendicular to the survey lines were flown.

Shipboard magnetic measurements were made by two fluxgate vector magnetometers, which are permanently installed on the crow's nest. The data are directly loaded into the ship's archiving system PODAS at one-second intervals. To take account of the influence of the metallic bulk of the ship, the ship undertook figure-eight compensation loops on 14 February, 13 March and 10 April. In the small area of a compensation loop, the variations of the magnetic field due to crustal magnetisation are assumed to be negligible. The loops thus provide coefficients which relate the ship's heading, roll and pitch movements to the variations in magnetometer measurements. These coefficients allow the correction of the shipboard magnetic measurements in the wider area around the compensation loop.

The recorded magnetic field shows not only geographical but also temporal and diurnal variations due to solar radiation and other influences. This variation can be removed by subtracting continuous measurements taken at base stations deployed within or near the survey area. We installed a base station magnetometer on Hop Island of the Rauer Island group about 50 m from the seismic land-recorder during the period of 25 February and 14 March 2007. The magnetometer used for this purpose is an Overhauser effect proton precession

magnetometer GSM-19, manufactured by GEM Systems. Power supply to the magnetometer was achieved using two car batteries and a solar panel. The magnetometer sensor was mounted on a pole tightened by ropes. Unfortunately, the magnetometer failed to collect data shortly after installation, probably due to dysfunction of the regulator between the solar panel and batteries. Thanks to the staff of Davis Station, we obtained data from their permanently installed fluxgate magnetometer observatory. From comparison of these data with the magnetic field recordings during our survey flights we can conclude that no special magnetic disturbances in the variations recorded at Davis affected our data. Data processing normally includes the direct removal of the diurnal variations using the base station, but we found that this was not applicable because of the large distances between our two survey areas to Davis Station. We therefore will rely on the shipboard magnetic data for correcting the heli-mag data.

c) Gravimetric surveying

Marine gravity data were continuously acquired during the expedition using the ship's permanently installed Bodenseewerke KSS-31 gravity meter, which is 1 m above sea-level. The data were directly archived in the PODAS system at one-second intervals. The gravity data acquisition worked without major problems for most parts of the cruise, except for short periods when PODAS was shut down or a few times in the beginning of the cruise when data of the gravity meter were not logged by PODAS. We conducted land reference measurements with the LaCoste & Romberg gravity meter G-877 in Punta Arenas, Davis Station (Prydz Bay), Port-aux-Francais and historic Drygalsky Station (both on Kerguelen Islands), and in Cape Town in order to tie the shipboard data to the International Gravity Station Network (IGSN) (Tab. 3.4).

The marine gravity data were processed using the AWI-own programmes *REDUCE* and *GRAVCORR* to apply the Eötvös and latitudinal corrections and to reduce the gravity reference field according to the IGNS reference station readings of Punta Arenas. The result is a file with free-air gravity anomaly values along the entire ship track. Exact corrections for instrument drift will have to be performed at the institute using all relevant land reference measurements.

Added short programme: Geophysical surveys of Agulhas Plateau

During *Polarstern's* return transit to Cape Town, we crossed the Agulhas Plateau which is another Large Igneous Province in the Indian Ocean and a region of long-term research focus at AWI. This plateau, whose oceanic or continental origin is strongly debated, has been at an important location for the interocean exchange of water masses around southern Africa. Remaining ship-time allowed us to conduct two short geophysical surveys on the plateau using shipboard magnetic and gravity measurements as well as Hydrosweep multibeam bathymetric and Parasound sub-bottom mapping:

1) A cross-profile survey was conducted as a pre-site survey for drill site APT-02 (40°52.14' S, 27°21.34' E) proposed in the submitted IODP proposal '*Southern African Climates, Agulhas Warm Water Transports and Retroflexion, and Interocean Exchanges (SAFARI)*' (by Zahn et al.). Limited time did not permit to survey the proposed drill site APT-01.

2) A profile was surveyed across the southern and central Agulhas Plateau from 40°12.2' S and 26°18.2' E to 37°27.1' S and 25°36.6' E on the location of the deep crustal seismic line AWI-20050200 acquired during the RV *Sonne* cruise SO-182 in 2005 as part of the *Agulhas-Karoo Geoscience Transect* (component of German-South African cooperative project *Inkaba ye Africa*). This profile adds important, and previously missing, magnetic and gravity data along the southern part of the transect.

Preliminary results*Seismic profile AWI-20070100*

Of the 19 OBS and 3 OBH systems deployed, 21 stations were recovered from which data were downloaded. The OBS at station 119 could not be recovered, in spite of numerous attempts to send release codes. Even at the time when the time-release should have been activated, the system did not return to the surface. The OBH systems recorded useful hydrophone data with source-receiver offsets up to 30 km. Good quality hydrophone and seismometer data with source-receiver offsets up to 70 km were recorded by the OBS systems across the eastern Enderby Basin (data example in Fig. 3.4). This deep crustal seismic dataset includes refracted P-wave phases from at least two sedimentary layers and at least two layers of the crystalline crust. Reflection phases from the crust-mantle boundary (P_mP) are observed on five recordings. Ten recordings show a low-amplitude refracted phase from the upper mantle (P_n).

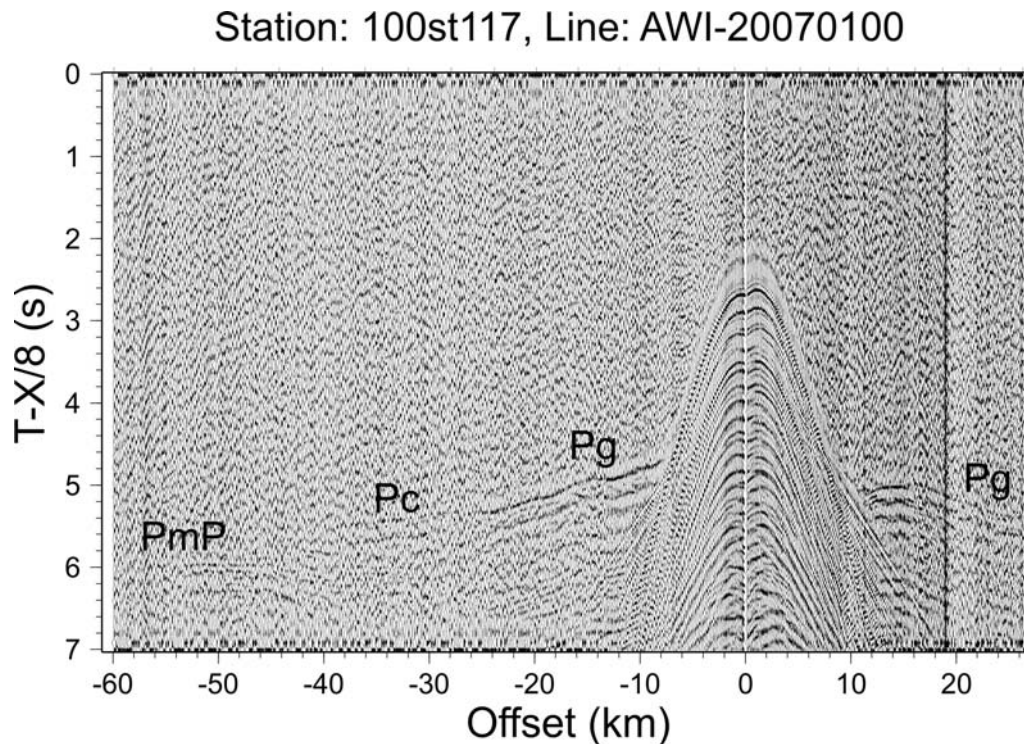


Fig. 3.4: Data example of OBS station 117 of profile AWI-20070100 with identified phases from the upper crust (P_g), lower crust (P_c) and crust-mantle boundary (P_{mP})

After we had picked P-wave arrivals from the records and digitized a strong mid-sedimentary reflector and the top of basement from the Russian RAE-5206 seismic reflection line, a first attempt was made to generate a velocity-depth model using the raytracing and travel-time inversion routine *RAYINV*R by Zelt & Smith (1992) and the first-arrival travel-time tomography *FAST* by Zelt & Barton (1998). In the resulting preliminary model of *RAYINV*R (Fig. 3.5), sediment velocities were modelled with 1.8 - 2.8 km/s for the upper sediment layer and 2.4 - 4.2 km/s for second sediment layer. The upper sediment layer has an almost uniform thickness of about 1 km along the profile, whereas the second layer is thin on the northern part of the profile and thickens distinctively towards the south reaching a thickness of more than 4 km. The upper crystalline crust shows significant lateral variations in the P-wave velocity from 5.5 - 6.5 km/s in the northern half of the profile to 5.0 - 6.0 km/s in its southern half. The velocities in the middle and lower crust range from 6.2 km/s at the top to 7.6 km/s at the bottom. They exhibit less lateral variations but also decrease in southward direction. The Moho depth increases from about 14 km at the northern end of the profile to about 16 km in the south. By subtracting the water column, these depths correspond to crustal thicknesses between 10 km in the north and 13 km in the south. P-wave velocities of the uppermost mantle are modelled with 8 km/s.

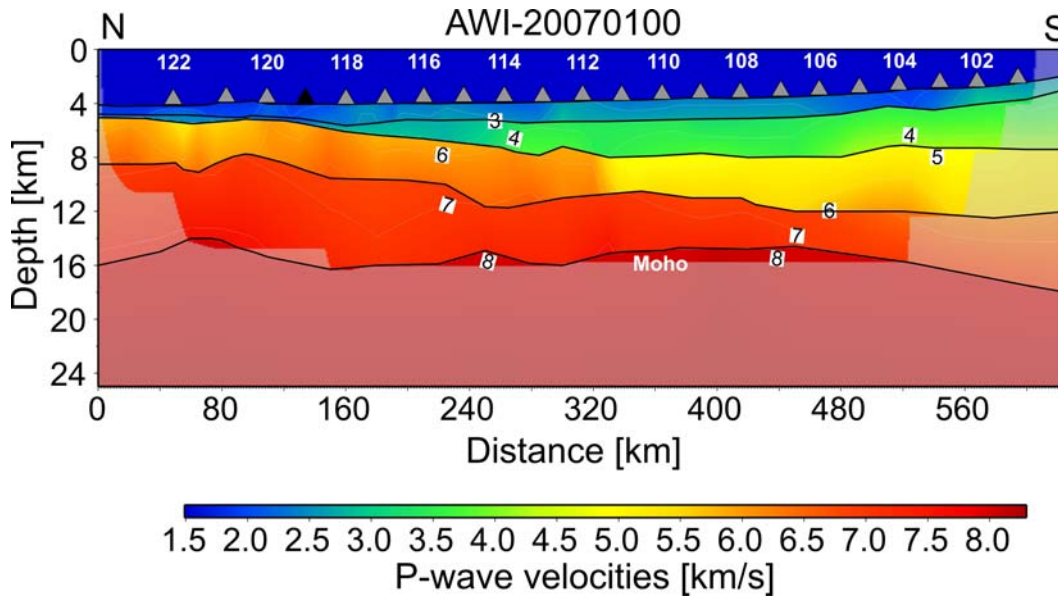


Fig. 3.5: Preliminary P-wave velocity-depth model of profile AWI-20070100

This profile covers the crust of the eastern Enderby Basin from the foot of the continental slope to an area just off the south-western edge of the Kerguelen Plateau (Fig. 3.1). While crustal thickness remains almost constant along the profile, we observe a distinct, almost abrupt change in mid-crustal seismic P-wave velocities and a smoother change in velocity in the lower crust in the centre of the profile. The mid-crustal velocities in the southern part of the profile correspond to those of intermediate to felsic composition, thus, continental origin. The P-wave velocities of the northern profile half are interpreted to stem from oceanic crustal composition. The mid-crustal velocity change coincides with the location of the Magnetic Coastal Anomaly (MCA) (Stagg et al., 2005; Gaina et al., in press) which has been suggested to mark the continent-ocean boundary. A more detailed analysis of the data in the months to follow will include the S-wave arrivals and the data of the wide-angle two-ship experiment as well as the magnetic and gravity survey. However, if this first analysis and interpretation can be confirmed, the rifted continental margin of Mac Robertson Land underwent enormous crustal thinning before break-up from India or the continental fragments of the Kerguelen Plateau.

Seismic profile AWI-20070200

Of the 2 OBH and 13 OBS systems deployed, all 15 systems were recovered and recorded good quality data from the airgun shots across the Princess Elizabeth Passage and on to the Southern Kerguelen Plateau. The records of this profile (data example in Fig. 3.6) exhibit a significantly better data quality than those of profile AWI-20070100. Nine recordings show refracted P-wave phases from the upper mantle (P_n) at source-receiver offsets up to 85 km. P_n phases of records from the northern stations arrive are offset in time to the first-arrival travel-time branches by more than a second, indicating a possible low-velocity zone in the crust.

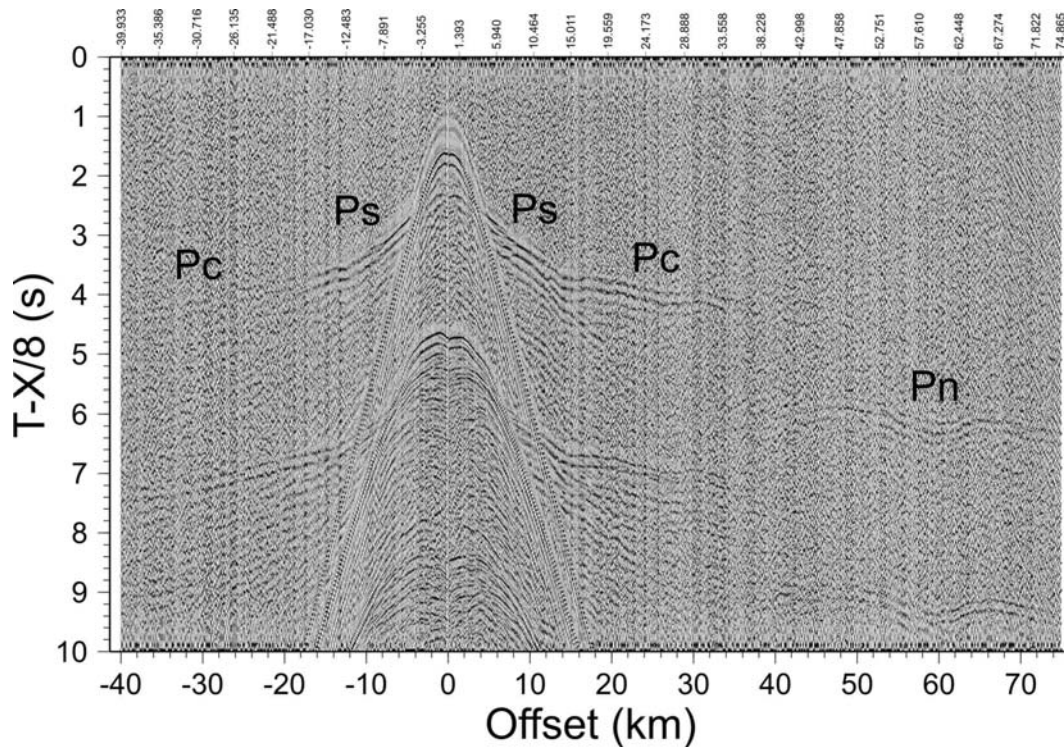


Fig. 3.6: Data example of OBS station 213 of profile AWI-20070200 with identified phases from the sediments (Ps), crystalline crust (Pc) and uppermost mantle (Pn)

A first raytracing and inversion model was calculated with the programmes *FAST* and *RAYINV* using P-wave arrivals of all 15 stations and with the basement being identified from the coincident Russian seismic reflection line RAE-3910 (Figs. 3.7 and 3.8). The upper sediment layer can be modelled with velocities between 1.8 and 2.5 km/s. Velocities between 2.5 and 4.4 km/s are modelled for the second sediment layer. Basement highs separate the sedimentary section into four sub-basins. The thickness of the sediments increases from 1.5 km in the north to 3.5 km in the south. The upper crustal velocities range from 4.2 to 6.4 km/s. The thickness of upper crystalline crust is about 4 km, except for the basement highs where it is about 5 km thick. The thickness of the lower crust decreases from 8 km in the north to 4 km in the south. Its velocities vary in the south from 6.3 km/s at the top of this layer to 7.6 km/s at the base of the crust. In the north, the lower crust consists of a low-velocity zone with velocities between 6.5 and 6.9 km/s. The Moho depth increases from about 17 km in the north to 12 km in the south. The uppermost mantle has velocities of about 8 km/s. It must be noted that, in particular, the results of the lower crust are still very preliminary which will need to be verified by further analysis.

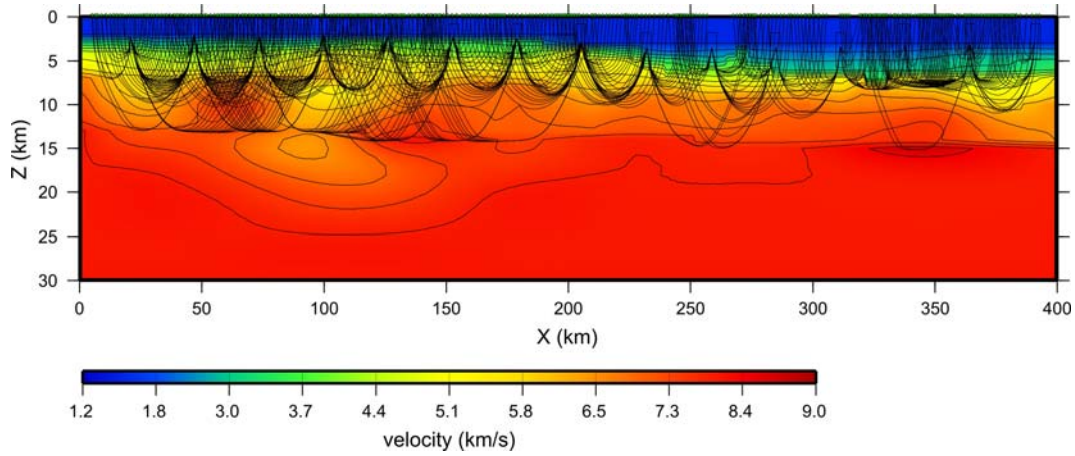


Fig. 3.7: Preliminary first-arrival tomography model of profile AWI-20070200

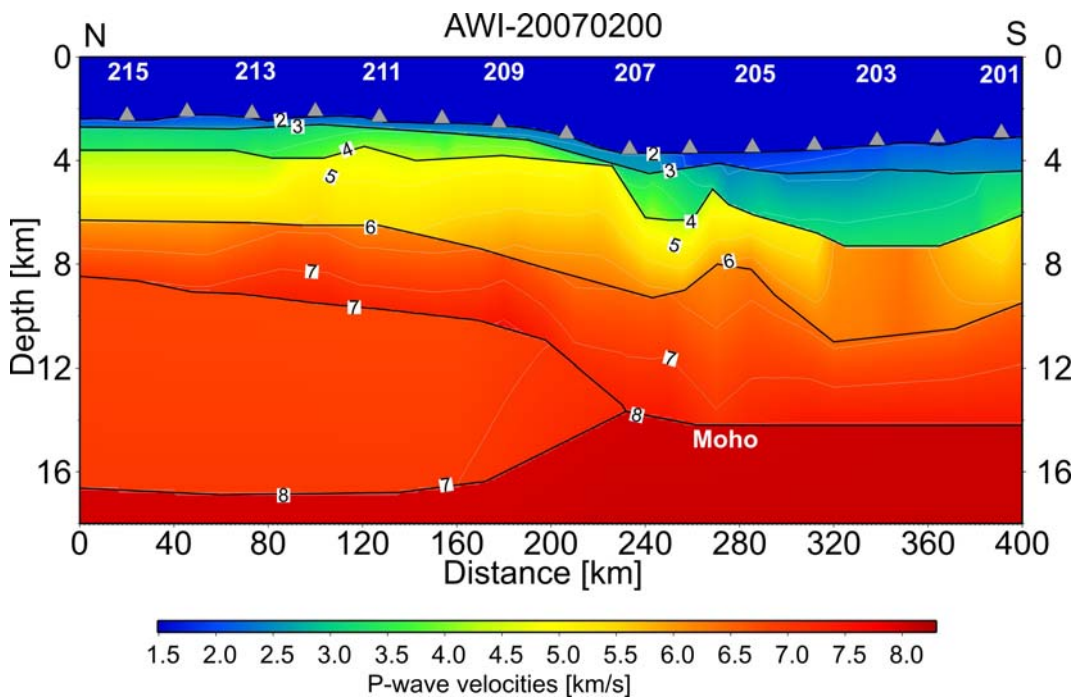


Fig. 3.8: Preliminary P-wave velocity-depth model of profile AWI-20070200

These preliminary results of the velocity-depth model are dominated by the structure of the Southern Kerguelen Plateau to the north. The vertical crustal velocity distribution changes from the thick crust of the plateau to that of the thin oceanic crust beneath the Princess Elizabeth Trough. The P-wave data from the plateau indicate that a good portion of the lower crust consists of low-velocity continental-type rock composition. This means that the partial continental affinity of the Southern Kerguelen Plateau, as indicated by seismic data and ODP drill samples further north (e.g. Operto & Charvis, 1996; Gladchenko & Coffin, 2001), continues to its southernmost limit. Here, the continental crust must have been enormously thinned and fragmented as part of the rifting process between India and Antarctica. Later, with the onset of the Kerguelen hotspot activity, this region was subject to accretion and extrusion of voluminous amounts of igneous material from the mantle, including parts of the

oceanic crustal Princess Elizabeth Trough. However, more detailed data analyses have to be performed by integrating S-wave phases of the OBS recordings, pre-existing regional seismic reflection lines, magnetic and gravity survey data.

Magnetic survey

At the end of each survey day, data were retrieved from the PICODAS™ data acquisition system and stored on the ship server 'wega'. The binary data-files were converted to ASCII-files (including reduction of the sampling rate to 1 Hz) using the REPLOT programme of the PICODAS™ system. For further processing, we used the GEOSOFT® software package *OasisMontaj™* installed on a laptop. After transferring the data into a database, spikes were removed manually. A preliminary map was created which included the flight path (to check against the pre-planned survey grid) and a first visualisation of the magnetic field data. In cases when the system's GPS failed, the coordinates were taken from the additional laptop which recorded the GPS data separately. These data had to be prepared separately and later merged into the data base. A correction for regional effects of the earth's magnetic field was made by calculating the IGRF (International Geomagnetic Reference Field) value at all survey points and at the survey altitude of 100 m. The IGRF value was calculated using IGRF model 2005 at a mean date of 5 March 2007 for profile AWI-20070100 (profile A) and 21 March for profile AWI-20070200 (profile C). To prepare for a levelling procedure and also for easier presentation of the data, the flights were cut into normal survey lines (parallel to the seismic profile) and tie-lines (perpendicular to survey lines, in some cases also flight-sections connecting survey lines in a more irregular pattern were used). At the same time, we eliminated sections of the flights not needed, such as in turns from one line to the next. After removal of IGRF, the resulting values of the survey lines were gridded using the minimum curvature algorithm of the GEOSOFT® package. The grid mesh was 500 m x 500 m. To obtain a smooth basis for the modelling of spreading anomalies with the magnetic spreading anomaly programme *MAGBATH983*, the gridded data were re-sampled with a regular 100 m x 100 m cell size stored in a new database. Lines at distance of 5 km and 10 km to the east and west of the seismic profiles (thus approximating the original survey lines) were exported to be used for anomaly modelling.

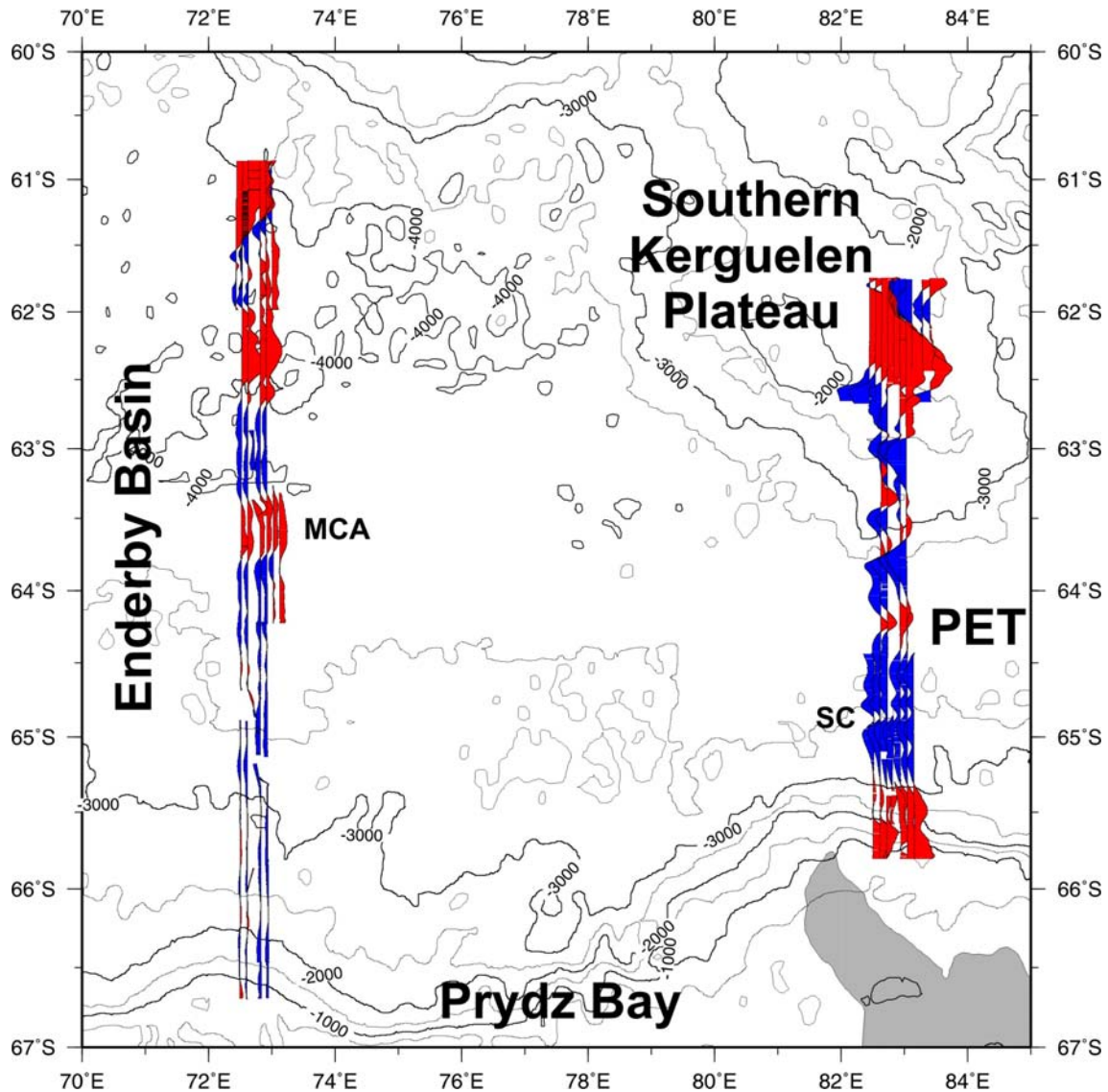


Fig. 3.9: Map with amplitude wiggles of the heli-magnetic surveys parallel to profiles AWI-20070100 (west) and AWI-20070200 (east). Negative amplitudes of total intensity anomalies are in blue and positive amplitudes are in red. PET = Princess Elizabeth Trough, MCA = Magnetic Coastal Anomaly, SC = former spreading centre

The gridded data as well as the amplitude wiggles (Fig. 3.9) show clear several linear trends in the surveyed swaths. The southern half of the magnetic anomaly swath along profile AWI-20070100 exhibits very low amplitude anomalies without any distinct pattern. The middle of the profile is characterized by the dominant positive Magnetic Coastal Anomaly (MCA) which has been well observed through the Enderby Basin (Gaina et al., in press). North of the MCA, a pattern of east-west trending anomalies appears which are subject of detailed modelling to derive a crustal age and structural model. The swath data along profile AWI-20070200 show linear anomaly trends in east-west direction, changing to northwest strike direction in the north where the profile crosses the southernmost Kerguelen Plateau. As our seismic data of this profile indicate fragmented continental crust under the southern Kerguelen Plateau, we tried to fit only the southern part of the profile to seafloor spreading

anomalies within the isochron range of M11 to M2 (about 137.0 - 127.5 Ma) according to a previously published age model for this part of the crust (Gaina et al., in press). By assuming that there must be a former spreading centre in the Princess Elizabeth Trough if the Kerguelen Plateau is continental and the trough is oceanic (as suggested from our seismic model), we found the best fit of synthetic data to the observed magnetic profile data between chrons M6 and M10 on both sides of a spreading centre (Fig. 3.10). Such a spreading centre is also indicated at this position in the Russian seismic reflection data profile RAE-3910. Our analysis and age model is only a preliminary result which needs to be tested and confined with more data analyses and model calculations in the months to follow.

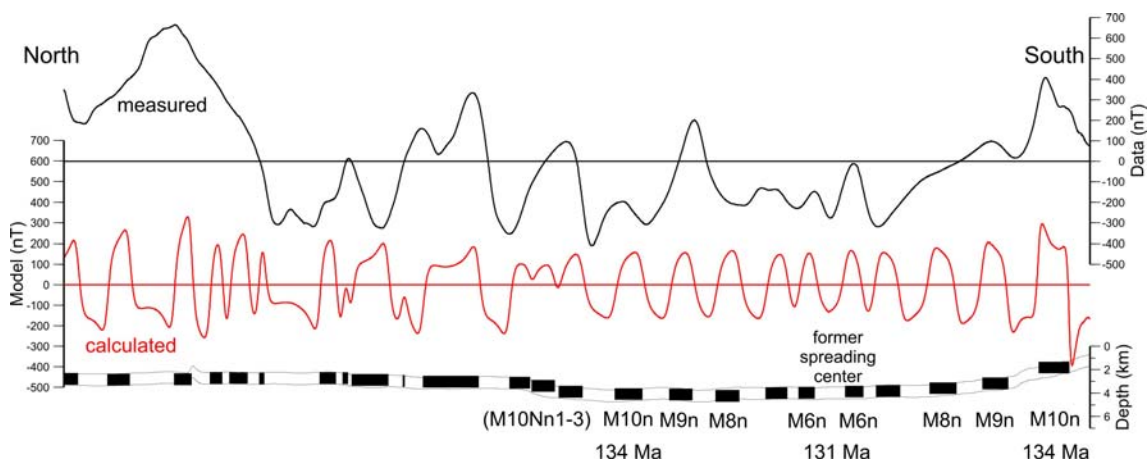


Fig. 3.10: Preliminary model of magnetic seafloor spreading anomalies along profile AWI-20070200 with indications of a former spreading centre in the Princess Elizabeth Trough (PET) at anomaly M6 (131 Ma). Modelled spreading half-rate is 3.3 cm/yr to the north and 3.7 cm/yr to the south of the ridge. The anomalies in the northern half of the profile do not correspond to spreading anomalies because of the continental crust underneath the Southern Kerguelen Plateau.

References

- Gaina, C., Müller, R.D., Brown, B., Ishihara, T. & Ivanov, S., in press. Breakup and early seafloor spreading between India and Antarctica, *Geophys. J. Int.*
- Gladchenko, T.P. & Coffin, M.F., 2001. Kerguelen Plateau crustal structure and basin formation from seismic and gravity data, *J. Geophys. Res.*, 106, B8, 16583-16601.
- Operto, S. & Charvis, P., 1996. Deep structure of the southern Kerguelen Plateau (southern Indian Ocean) from ocean-bottom seismometer wide-angle seismic data, *J. Geophys. Res.*, 101, 25077-25103.
- Stagg, H.M.J., Colwell, J.B., Direen, N.G., O'Brien, P.E., Brown, B.J., Bernadel, G., Borissova, I., Carson, L. & Close, D.B., 2005. Geological Framework of the Continental Margin in the Region of the Australian Antarctic Territory, *Geoscience Australia Record 2004/25*.

Zelt, C.A. & Barton, P.J., 1998. Three-dimensional seismic refraction tomography: A comparison of two methods applied to data from the Faeroe Basin, *J. Geophys. Res.*, 103, 7187-7210.

Zelt, C.A. & Smith, R.B., 1992. Seismic travelttime inversion for 2-D crustal velocity structure, *Geophys. J. Int.*, 108, 16-34.

Tab. 3.1: Deployment coordinates and instrument description of OBH/OBS profile AWI-20070100

Station no. PS69/	Instr. type	Lat South	Lon East	Depth (m)	Deployment date	UTC	Recovery date	UTC	Remarks
101	OBH	66°16.210'	72°43.020'	2100	28.02.2007	22:15	06.03.2007	04:02	weak signal
102	OBH	66°02.349'	72°42.800'	2540	01.03.2007	00:06	06.03.2007	08:03	
103	OBH	65°49.054'	72°43.080'	2820	01.03.2007	01:41	06.03.2007	10:29	
104	OBS	65°34.702'	72°43.243'	2930	01.03.2007	03:55	06.03.2007	13:25	
105	OBS	65°21.114'	72°43.104'	3057	01.03.2007	05:22	06.03.2007	15:24	weak signals
106	OBS	65°07.483'	72°42.800'	3297	01.03.2007	06:53	06.03.2007	18:09	
107	OBS	64°53.774'	72°43.112'	3466	01.03.2007	08:43	06.03.2007	20:50	
108	OBS	64°40.081'	72°43.174'	3572	01.03.2007	10:58	06.03.2007	23:55	
109	OBS	64°26.234'	72°43.276'	3610	01.03.2007	12:46	07.03.2007	02:20	no data on seismometer channels
110	OBS	64°12.518'	72°43.142'	3615	01.03.2007	14:20	07.03.2007	05:00	
111	OBS	63°58.784'	72°43.071'	4034	01.03.2007	15:57	07.03.2007	07:58	only direct wave on Y-channel
112	OBS	63°44.880'	72°43.338'	3380	01.03.2007	17:39	07.03.2007	10:23	
113	OBS	63°31.348'	72°43.119'	3861	01.03.2007	19:19	07.03.2007	13:25	no data on Y-channel
114	OBS	63°17.583'	72°43.214'	3941	01.03.2007	20:58	07.03.2007	16:05	
115	OBS	63°03.482'	72°43.209'	3973	01.03.2007	22:36	07.03.2007	18:50	no data on seismometer channels
116	OBS	62°49.979'	72°43.097'	4004	02.03.2007	00:09	07.03.2007	21:19	only direct wave on X-channel
117	OBS	62°36.102'	72°43.166'	4003	02.03.2007	01:43	07.03.2007	23:47	
118	OBS	62°22.494'	72°43.212'	4149	02.03.2007	03:27	08.03.2007	02:22	no data on hydrophone channel, shot gap
119	OBS	62°08.756'	72°43.161'	4045	02.03.2007	05:30	-	-	OBS lost
120	OBS	61°55.043'	72°43.277'	4096	02.03.2007	07:32	08.03.2007	16:05	shot gap
121	OBS	61°41.300'	72°43.218'	4147	02.03.2007	09:32	08.03.2007	19:00	shot gap
122	OBS	61°22.448'	72°43.271'	4157	02.03.2007	11:31	08.03.2007	21:58	no data on hydrophone channel

Tab. 3.2: Deployment coordinates and instrument description of OBH/OBS profile AWI-20070200

Station no. PS69/	Instr. type	Lat South	Lon East	Depth (m)	Deployment date	UTC	Recovery date	UTC	Remarks
201	OBH	65°15.718'	82°50.014'	3150	18.03.2007	03:41	21.03.2007	00:15	
202	OBH	65°01.363'	82°50.012'	3340	18.03.2007	05:36	21.03.2007	15:40	
203	OBS	64°47.105'	82°49.885'	3409	18.03.2007	07:09	21.03.2007	18:10	
204	OBS	64°32.825'	82°50.027'	3593	18.03.2007	08:44	21.03.2007	20:53	
205	OBS	64°18.636'	82°50.050'	3667	18.03.2007	10:20	21.03.2007	23:28	
206	OBS	64°04.383'	82°50.140'	3712	18.03.2007	11:48	22.03.2007	02:35	
207	OBS	63°50.075'	82°49.985'	3713	18.03.2007	13:16	22.03.2007	05:35	
208	OBS	63°35.566'	82°50.111'	3065	18.03.2007	14:47	22.03.2007	09:45	
209	OBS	63°21.318'	82°50.006'	2646	18.03.2007	16:11	22.03.2007	11:58	
210	OBS	63°07.110'	82°50.002'	2552	18.03.2007	17:36	22.03.2007	14:10	no data on X-channel; only direct wave on Y
211	OBS	62°52.826'	82°50.027'	2423	18.03.2007	18:59	22.03.2007	16:07	
212	OBS	62°38.562'	82°49.942'	2302	18.03.2007	20:24	22.03.2007	23:34	
213	OBS	62°24.338'	82°49.925'	2386	18.03.2007	21:47	23.03.2007	02:59	
214	OBS	62°09.902'	82°50.034'	2257	18.03.2007	23:12	23.03.2007	05:17	
215	OBS	61°55.775'	82°49.999'	2445	19.03.2007	00:42	23.03.2007	07:32	

Tab. 3.3: Airgun shot profiles for OBH/OBS recordings

Profile	Lat South	Lon East	Date	UTC	Press. (bar)	Active airguns	Volume (liters)	Remarks
AWI-20070100	60°56.43'	72°48.19'	03.03.2007	04:58	190	8 G.Guns	68.0	start shot profile
			03.03.2007	08:06	190	7 G.Guns	59.5	some airguns lose air
	61°40.59'	72°43.19'	03.03.2007	13:00				trigger stopped; repairs of umbilicals
	61°24.67'	72°43.19'	03.03.2007	13:00	140	2 airguns 6PI-20	80.0	begin shooting from Karpinsky
	61°47.16'	72°43.20'	03.03.2007	17:29				end shooting from Karpinsky
	61°52.36'	72°43.21'	03.03.2007	17:30	190	8 G.Guns	68.0	trigger started
			03.03.2007	22:55	180	8 G.Guns	68.0	1 airgun loses air but shoots with 150 bar
			03.03.2007	23:45	185	7 G.Guns	59.5	
			04.03.2007	00:25	185	6 G.Guns	51.0	
	62°50.19'	72°43.22'	04.03.2007	04:00				trigger stopped; repairs of umbilicals
	63°10.37'	72°43.03'	04.03.2007	07:21	190	8 G.Guns	68.0	trigger started
			04.03.2007	07:56	180	8 G.Guns	68.0	
			04.03.2007	09:50	180	7 G.Guns	59.5	
			05.03.2007	07:53	180	6 G.Guns	51.0	
	65°13.74'	72°44.04'	05.03.2007	09:24				trigger stopped; repairs of umbilicals
	65°08.95'	72°43.20'	05.03.2007	10:17	140	2 airguns 6PI-20	80.0	begin shooting from Karpinsky
	65°19.01'	72°43.19'	05.03.2007	12:19				end shooting from Karpinsky
	65°31.52'	72°43.19'	05.03.2007	12:20	180	8 G.Guns	68.0	trigger started
	66°33.16'	72°43.49'	06.03.2007	01:00				end shot profile
AWI-20070200	61°44.98'	82°50.06'	19.03.2007	04:22	135	8 G.Guns & 1 Bolt	101.0	start shot profile
			19.03.2007	04:50	130	7 G.Guns & 1 Bolt	92.0	
			19.03.2007	10:00	135	6 G.Guns & 1 Bolt	83.5	
			20.03.2007	19:29	135	6 G.Guns	51.0	
	65°19.49'	82°49.77'	20.03.2007	22:30				end shot profile

Tab. 3.4: Gravity land reference measurements (n.a. means non-applicable)

land gravity reference location	elev. (m)	dist. from ship (m)	date	UTC (mean)	absolute gravity (mgal)	G-877 relative gravity (mgal)	KSS-31 value (mgal)
Punta Arenas, Port Admin.	32.9	n.a.	01.02.07	12:14	981320.810 (IGSN 1971)	4964.159	n.a.
Punta Arenas, Madones Pier	4.0	n.a.	01.02.07	15:27	981315.968 (derived)	4959.317	n.a.
Punta Arenas, Cabo Negro	4.5	400	01.02.07	16:05	981297.878 (derived)	4941.227	1032.37
Davis Station Base Trig. Pnt	28.7	5450	15.03.07	07:30	982573.120 (IGSN 1971)	6215.441	2315.99
Kerguelen Isl. Drygalski Stat.	15.0	n.a.	29.03.07	06:28	981061.637 (derived)	4705.025	n.a.
Kerguelen Isl. Port-Francais	22.0	1480	29.03.07	09:45	981059.355 (EOST2005)	4702.743	797.07
Cape Town Duncan Pier Poller 72	3.0	5	10.04.07	19:51	979636.567 (derived)	3280.324	-633.06

4. MARINE GEOLOGY IN THE PRYDZ BAY - KERGUELEN PLATEAU AREA

East Antarctic ice-sheet dynamics and variability of the glaciomarine environment

Bernhard Diekmann¹, Janine Bardenhagen², Andreas Borchers¹, Kristin Daniel², Antje Eulenburg¹, Christina de la Rocha², Hannes Grobe², Conrad Kopsch¹, Sven Kretschmer², Norbert Lensch², Peter Sperlich³, Ines Voigt¹

¹Alfred-Wegener-Institut (AWI), Potsdam

²Alfred-Wegener-Institut (AWI), Bremerhaven

³University of Bremen

Objectives

The working programme of the marine-geology group was dedicated to the recovery of marine sediment records for later land-based studies. The study is supported by DFG funding and integrated into the research activities of the International Polar Year (IPY 2007/2008), as part of the programme BIPOMAC (Bipolar Climate Machinery), coordinated by R. Gersonde (AWI Bremerhaven). It contributes to the AWI research programme MARCOPOLI, topic POL6 "Palaeoclimate since the Pliocene". The marine-geology work programme was devoted to the following scientific objectives:

- Reconstruction of East Antarctic ice-sheet dynamics during the last 40 kyr through the characterization of the glaciomarine environment, the identification of the glacial detrital supply, and the inference of Antarctic Bottom Water variability between Prydz Bay and the Kerguelen Plateau. The question of ice-sheet stability in Antarctica has attracted palaeoclimatic research during the recent past, because of its potential impact on changes in global sea level and thermohaline ocean circulation. Apart from the dramatic hypotheses of possible total ice-sheet decay in western Antarctica in the face of present global warming, the knowledge of fluctuations of the voluminous East Antarctic Ice Sheet (EAIS) is crucial for the understanding of the late Quaternary global climate system.
- Documentation of the Holocene and Pleistocene Variability of the Antarctic Circumpolar Current (ACC), by palaeoceanographic approaches on a transect across the ACC frontal system in the Kerguelen Plateau area. These studies comprise the reconstruction of variations in biological productivity and the evaluation of environmental proxy data from bioindicators to infer changes in sea-surface conditions, comprising variations in palaeotemperature, sea ice distribution, and nutrient inventories (see De la Rocha et al., chapter 8). Grain-size and mineralogical/geochemical characteristics of the detrital sediment fraction will be used for the reconstruction of bottom-water flow variability and to

distinguish the supply and dispersal of terrigenous sediments by aeolian input, hemipelagic settling, and ice-rafting.

- Assessment of the effect of current-driven sediment transport on thorium nuclide inventories and radiocarbon ages of organic matter (see Kretschmer & Mollenhauer, chapter 7).

Work at sea

The selection of appropriate sites for the marine geological studies concentrated on proximal locations near Antarctica, the Prydz Bay shelf and the MacRobertson shelf and continental slope, as well as distal locations on the Kerguelen Plateau (Fig. 4.1). The cruise-related studies comprised the identification of characteristic depositional units, as displayed in sections obtained from sub-bottom profiling with the Parasound system, and the recovery of representative marine sediment records (sea-bottom surface sediments and sediment cores), using multicorer, box corer, piston corer, and gravity corer equipment. Shipboard studies comprised whole-core measurements of geophysical sediment properties (magnetic susceptibility, p-wave velocity, gamma-ray density) with a GEOTECH Multi-Sensor Core Logger, sediment-core splitting, description and sampling, and x-ray imaging of sediment slices from the core sections. At representative sites, on-site studies were conducted in association with oceanographic CTD measurements (see Klatt & Muhle, chapter 9).

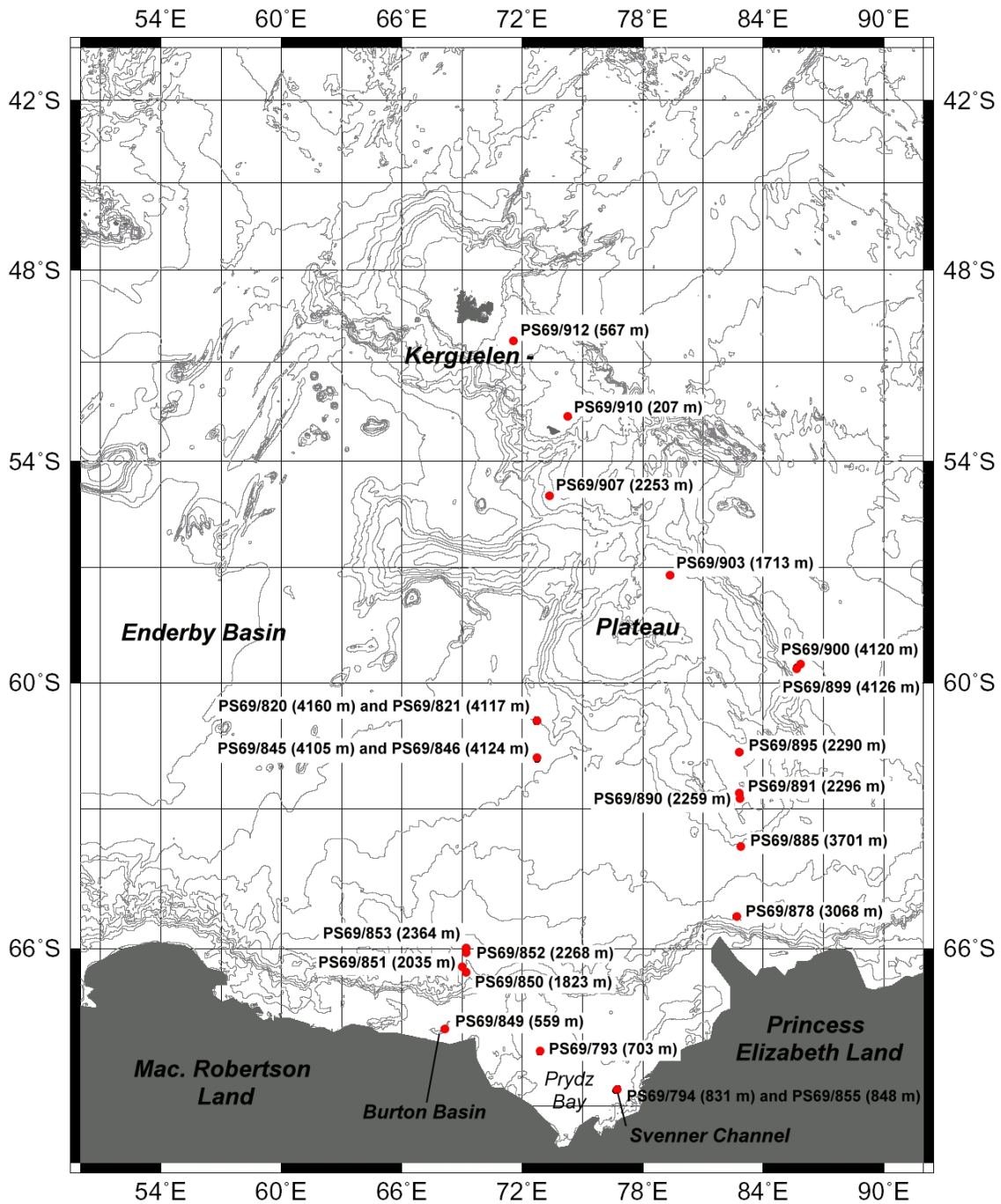


Fig. 4.1: Overview of the study area with indications of marine-geological sites with station numbers and related water depths (m). Isobaths at 500 m-intervals

Sediment Echography with the Parasound system

The Parasound system (ATLAS Hydrographic, GmbH, Bremen, Germany) is a ship-based sub-bottom echosounder, used for the survey of the acoustic characteristics and spatial and depth-related distribution of sea-floor sediments. Examples are presented in section 3. During cruise ANT-XXIII/9, Parasound profiling was dedicated to the following tasks:

- selection of appropriate study sites for the recovery of marine sediments,

- recognition of sediment architecture and thickness of the upper depositional units,
- characterization of the glaciomarine depositional environment,
- documentation of Parasound profiling data for the planning of future expeditions.

The hull-mounted Parasound sediment echosounder was run around the clock along all cruise tracks beyond the 200 mile zones of Chile and South Africa, amounting to a total track length of about 10.500 nm. Data collection started on 4 February 2007, 17:15 UTC (57° 31.179' S, 58° 53.771' W) and was finished on 8 April 2007, 12:30 UTC (37° 35.784' S, 25° 38.970' E). The Parasound system generates two primary frequencies between 18 and 23.5 kHz, transmitted at high power in a narrow beam with an angle of 4°. As a result of the interaction of the primary frequencies within the water column, a secondary frequency at 2.5 to 5.5 kHz results from the parametric effect and can be used for sub-bottom profiling. During the whole cruise, the following settings were used: PAR frequency 4 kHz, 2 periods/pulse length, A/D frequency 50 kHz and frequency filter at 4.0-5.5 kHz. Depending on water depth, the sensor operation mode was PAR or PAR-Pilot. In case of rough seas, above steep submarine flanks and sea mounts, and severe sea ice condition, as encountered in the Weddell Sea, the Atka Bay, and the Prydz Bay, the depth signal was missing and thus the NBS/PAR mode was used.

By the terms of the UBA permission (Umwelt-Bundesamt), the Parasound system was switched off during non-geology stations and during the presence of whales. A whale watch was organized on board (for location details see figure 11.2, chapter 11). After a standby time of more than one hour, the Parasound system was softly restarted (Tab. 4.1). For system control, data acquisition, storage, and visualization of data in the online-mode, we have used the operator PC. The PC for data storage was used for data management and post processing with the software Parastore-3 and SENT (H. Van Loom, University of Bremen). The parametric and the NBS signals were recorded and saved on different data storage units as *.asd and *ps3 files. All files were copied to the data storage PC. After sorting the files in directories at 4-hour intervals, they were saved on the main *Polarstern* server and on LTO-Tapes.

Tab. 4.1: Parasound Soft-Start after a standby time longer than one hour

Step	Time	Settings		
1	0 min	Narrow Beam Sounder	18 kHz	20 deg
			Transmit Power	1 %
		Sensor Operation	NBS	
2	5 min	Narrow Beam Sounder	18 kHz	20 deg
			Transmit Power	10 %
		Sensor Operation	NBS	
3	5 min	Narrow Beam Sounder	18 kHz	20 deg
			Transmit Power	100 %
			Receiver Pre-Gain	26 dB
		Sensor Operation	NBS	
4	10 min	Narrow Beam Sounder	18 kHz	4 deg
			Transmit Power	100 %
			Receiver Pre-Gain	26 dB
		Sensor Operation	NBS	
5	5 min	Parametric	No. Of periods per pulse	1
		Sensor Operation	NBS/PAR or PAR PILOT	
6	5 min	Parametric	No. Of periods per pulse	2
		Sensor Operation	NBS/PAR or PAR PILOT	

Sampling of sea-bottom surface sediments

For the characterization of modern sedimentary facies and biological export production in the study area, sea-bottom surface sediments at most stations were sampled with a multicorer (MUC). At some sites, where the multicorer did not penetrate stiff or sandy sediments, a box corer was used instead. The MUC was equipped with twelve core liners, each 60 cm in length and 6 cm in diameter. The MUC provided both undisturbed surface sediments with an overlying fluff layer and original bottom water from the sea ground. The recovered MUC sediments were sampled as outlined in Table 4.2.

Tab. 4.2: Sampling scheme of short sediment cores taken with the multicorer (MUC)

Core No.	Analysis	Sample Intervals	Storage	Principal Investigator
1	Water Concentr. Bulk Composition	1-cm slices at 1-5, 9, 14, 19, 24 cm, ...	4°C	Kuhn
2	Sedimentology	1-cm slices at 1-5, 9, 14, 19, 24 cm, ...	4°C	Diekmann
3	Sand	5-cm slices at 0-5, 5-10, 10-15 cm, ...	4°C	Diekmann
4	Diatoms/Rads/Opal	Fluff layer, 0-0.5 cm, 0.5-1.0 cm, 1-cm slices to core base	4°C	Gersonde/ De La Rocha
5	Diatoms/Rads/Opal	fluff layer, 0-0.5 cm, 0.5-1.0 cm	4°C	Gersonde/ De La Rocha
6	Diatoms/Rads/Opal	fluff layer, 0-0.5 cm, 0.5-1.0 cm	4°C	Gersonde/ De La Rocha
7	Opal / Th 230	0-0.5 cm, 0.5-1.0 cm	4°C	Gersonde/ Geibert
8	Diatoms/Rads	full core in tube bag	-25°C	Gersonde
9	Radiocarbon Dating	full core in 1cm slices	-25°C	Mollenhauer
10	Thorium	full core in 1cm slices	4°C	Kretschmer
11	Microbiology	full core in tube bag	-25°C	Wagner
12	Archive	full core in tube bag	-25°C	AWI Repository

At the different stations, sediment recovery of the MUC varied significantly in both the total number of sediment-filled liners and the average length of the obtained sediment cores, as shown in Table 4.3. Therefore, the general sampling scheme was modified at stations with low recovery and restricted to selected analytical purposes that appear to be most important for the realization of the scientific programmes.

Tab. 4.3: Overview of recovery and sample distribution of multicorer (MUC) sediment profiles

Station	No. of Cores	Average Core Length	1. Water / Bulk	2. Sedimentology	3. Sand	4. Diat/Rads/Opal	5. Diat/Rads/Opal	6. Diat/Rads/Opal	7. Opal / Th 230	8. Diat / Rads	9. Radiocarbon	10. Thorium	11. Microbiology	12. Archive
PS69/793-1	11	20 cm	X	X	X	X	X	X	X	X	X	X	X	
PS69/794-2	10	55 cm	X	X	X	X	X		X	X	X	X	X	
PS69/820-2	11	35 cm	X	X	X	X	X	X	X	X	X	X	X	
PS69/847-1	9	30 cm	X	X	X	X			X	X	X	X	X	
PS69/849-1	5	25 cm	X	X	X	X			X		X		X	
PS69/851-2	11	25 cm	X	X	X	X	X	X	X	X	X	X	X	
PS69/853-2	12	30 cm	X	X	X	X	X	X	X	X	X	X	X	X
PS69/855-2	6	30 cm				X	X	X	X	X			X	
PS69/891-3	5	12 cm				X	X	X			X	X		
PS69/895-1	7	15 cm	X	X	X	X	X	X	X	X		X		
PS69/899-1	9	25 cm	X	X	X	X	X	X	X	X	X	X	X	
PS69/903-1	3	15 cm	X	X		X								
PS69/907-3	7	25 cm	X	X	X	X	X	X	X	X	X			
PS69/912-5	8	25 cm	X	X	X	X	X		X	X	X		X	

In case of poor sediment recovery, an additional giant box corer (Großkastengreifer = GKG) was deployed and sampled with MUC liner tubes afterwards (Tab. 4.4). The liner tubes were sampled according to the MUC sampling scheme. In contrast to the MUC sediments, the GKG sediments did not yield undisturbed surface sediments, because the upper few cm of the top layers may have been washed off during the GKG's ascent. Evidence for sediment wash-off was given for instance at station PS69/885-1, where a worm tube stuck out several centimetres above the sediment surface and coarse clasts together with sand-agglutinated sediment burrows were concentrated as an artificial lag deposit on the sediment surface.

Tab. 4.4: Sample Tubes taken from Giant Box Corer (GKG)

Station No.	No. of Cores	Average Core Length	1. Water / Bulk	2. Sedimentol.	3. Sand	4. Diat/Rads/Onal	5. Diat/Rads/Onal	6. diat / rad / onal	7. opal / Th 230	8. Diat / Rads	9. Radiocarbon	10. Thorium	11. Microbio	12. Archive
PS69/855-3	5	45 cm	X	X	X						X			X
PS69/878-4	12	35 cm	X	X	X	X	X	X	X	X	X	X	X	X
PS69/885-1	12	45 cm	X	X	X	X	X	X	X	X	X	X	X	X
PS69/891-5	8	20 cm	X	X	X					X	X	X	X	X

Retrieval of long sediment cores

From 19 stations, a total of 20 sediment cores has been retrieved, 14 sediment cores with the gravity corer (8-, 10-, 15- m lengths) and 6 sediment cores with the piston corer (20-, 25-, 30- m lengths). The choice of gear depended on acoustic wave penetration and the intensity of hard reflections, displayed by Parasound. The piston corer was mainly chosen at stations with thick sediment sequences composed of diatom-rich muds and oozes, which occurred on the Prydz Bay shelf in the Svenner Channel and at most sites on the Kerguelen Plateau. The longest sediment core was taken at station PS69/912-3 with a 30 m long piston corer and yielded a 28.15 m long sediment recovery. Total sediment recovery amounts to 230.79 m core length, 100.24 m by gravity corer, and 130.55 m by the piston corer. Average core recovery was 7.16 m for the gravity corer, and 21.76 m for the piston corer. Relative average recovery in relation to core length and penetration was 66 % for the gravity corer, and 84 % for the piston corer. Three gravity corers were bent during operation, but yielded undisturbed recovery. Problems with the piston corer at some stations arose from the implosion of short liner intervals (< 1 m), caused by the sucking effect (under pressure) of the piston. MSCL data, however, only indicate locally restricted sediment disturbance within the whole cores, respectively. These problems were overcome by the selection of twin stations or the repetition of coring operations at one site. This approach allows the splicing of disturbed with undisturbed sections in the respective sediment cores from closely located stations. Details of sediment recovery and site data are compiled in the cruise station list in the appendix.

All retrieved sediment cores have been logged as whole-core sections with a Multi-Sensor-Core-Logger (MSCL) to determine petrophysical properties of the sediment cores (see following section). Six sediment cores were opened and examined on-board. Visual description was supported by smear-slide analysis and the evaluation of radiographs, obtained from 1-cm slices taken between the work and archive halves of the sediment cores. The radiographs yield a picture of vertical variations in clast concentrations, bedding features, and the intensity of bioturbation. Colour description is according to the colour coding of the

Munsell Soil Colour Chart. Additional colour scans were conducted with a Minolta photospectrometer at 1-cm steps. Samples for the determination of water contents were taken at 10-cm steps for each sediment core. Thorough sampling procedures for the forthcoming on-shore studies will be conducted after the cruise in the AWI laboratories in Bremerhaven and Potsdam.

Petrophysical Properties of Sediment Cores

The physical properties of sediment cores (gravity cores, piston cores, and box cores) were measured on whole-core sections at 1.0-cm steps, using a GEOTEK Multi-Sensor-Core-Logger (MSCL) (Tab. 4.5). The individual core sections are usually 1 m long, apart from end pieces of the cores that might be shorter. Examples of the obtained logging data are outlined in section 3. P-wave travel time, magnetic susceptibility, and gamma-ray absorption were measured simultaneously, including control measurements of core diameter and sediment temperature. From these data, bulk-wet density, magnetic susceptibility, fractional porosity, P-wave velocity, and impedance was calculated, using the MSCL software package. For calibration, the following parameter were used in the logger settings of the MSCL software (version 7.5):

- temperature sensor, calibrated with a Hg-thermometer,
- core thickness (displaceElement), calibrated with defined distance pieces,
- P-wave travel time, calibrated with a water core of known temperature and theoretical sound velocity,
- density calibration was carried out, using a set of defined mixtures of aluminium and distilled water in a gravity- and piston-core liner, respectively.

In addition to the MSCL measurements, all split-core surfaces from sediment cores, opened during the cruise, were colour-scanned at 1-cm resolution with a MINOLTA Spectrophotometer CM-2002.

Tab. 4.5: Sensor and parameter settings for measurements with the GEOTEK MSCL during ANT-XXIII/9

P-wave velocity and core diameter Plate-transducer diameter: 4 cm Transmitter pulse frequency: 500 kHz Pulse repetition rate: 1 kHz Received pulse resolution: 50 ns Gate: 2000 Delay: 10 s
Density Gamma ray source: Cs-137 (1983) Activity: 356 MBq Energy: 0.662 MeV Collimator diameter: 5.0 mm (KOL+SL) Gamma detector: Gammasearch2, Model SD302D, John Count Scientific Ltd., 10 s counting time
Fractional porosity Mineral grain density = 2.65, water density = 1.026
Temperature Bimetal sensor
Core thickness measurement Penny + Giles, Type HLP190, Ser. No. 92730147
Magnetic susceptibility Loop sensor: BARTINGTON MS-2C, Ser. No. 130 Loop sensor diameter: 14 cm Alternating field frequency: 565 Hz, counting time 10 s, precision $0.1 \cdot 10^{-5}$ (SI) Magnetic field intensity: ca. 80 A/m RMS Krel: 1.56 (SL, 12 cm core- \varnothing), 1.44 (KOL, 8.46 cm core- \varnothing) Loop sensor correction coefficient: 6.391 (SL) for 10^{-6} (SI), 16.689 (KAL) for 10^{-6} (SI)

Preliminary Results

The marine geology programme was designed to recover sediment records from representative regions of the glaciomarine study area in terms of environmental conditions that are suited for palaeoenvironmental reconstructions (Fig. 4.1).

Prydz Bay shelf

The wide Prydz-Bay shelf area in front of the large Amery Ice Shelf was investigated to gain insight into Holocene environmental history and small-scale glacial fluctuations during the younger past, and to find evidence for bottom-water formation. Our findings are consistent with observations undertaken by former marine-geological surveys. Subbottom profiling revealed a softly inclined shelf from 400 m to 600 m water depth towards the inner Prydz Bay. The sea ground to a wide extent showed a rugged topography with abundant iceberg plough and keel marks. In most places, only a thin drape of modern sediments could be identified. At station PS69/793 in central Prydz Bay, the sea floor consists of stiff pebbly muds overlain by 80 cm of diatomaceous oozes. The diamictic texture and presence of large crystalline clasts from the Prydz Bay hinterland suggest an glacial origin of the pebbly muds, deposited during a

former glacial advance as subaquatic or lodgement till (morainic sediments), while the biogenic sediments possibly represent the postglacial stage with increased biological productivity during the sea-ice-free seasons.

Two sediment cores were taken from the 850 m deep Svenner Channel, situated in the vicinity of the Rauer Islands. In the Parasound profiles (Fig. 4.2), a pronounced palaeo-topography is displayed by the interface between the basal morainic deposits and the cover sediments, pointing to glacially incised troughs. The cover sediments show marked lateral thickness variations and are even absent in the western part of the channel, suggesting the presence of strong bottom currents. Blank channels without any younger sediment drape were also encountered in the eastern part of the Prydz enbayment and possibly hold clues for modern deep-water formation in the Prydz Bay. Sediment core PS69/794-3 was taken from an expanded section of postglacial sediments and provided a 10 m long sediment record, consisting of diatomaceous oozes that show faint laminations and include conspicuous amounts of organic matter, as indicated by a strong hydrogen sulfide smell. Another sediment core (PS69/855-1) was taken from a more condensed section and successfully penetrated the underlying morainic sediments. The recovered postglacial section is about 14 m thick. A minimum in magnetic susceptibility in the middle part of the section may be attributable to the deposition of almost pure diatomaceous oozes, while increased values indicate the dilution of oozes by detrital components (Fig. 4.3).

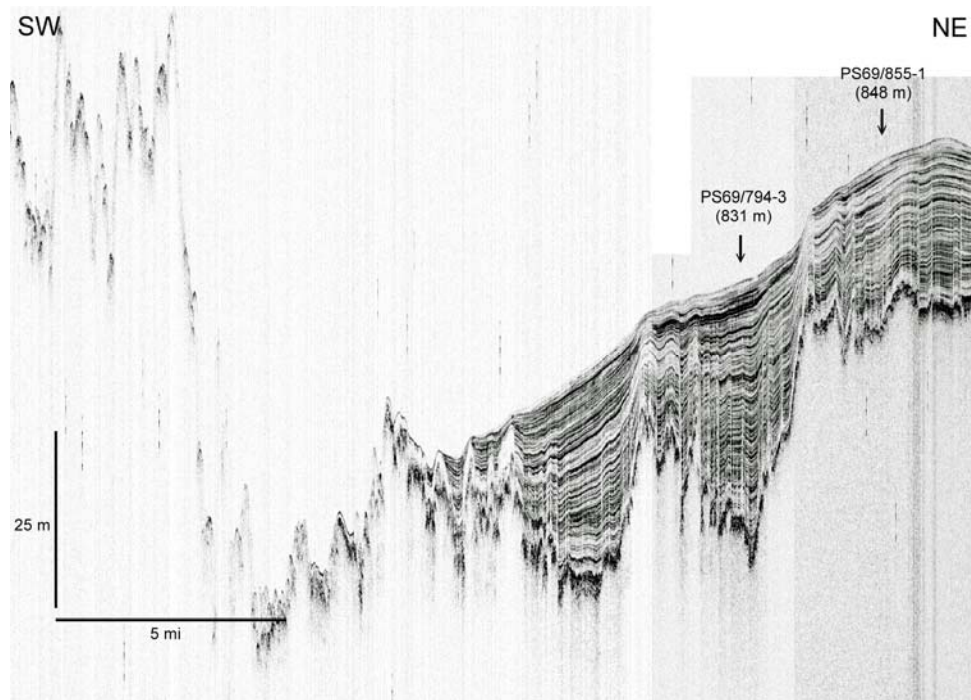


Fig. 4.2: Parasound section through the Svenner Channel on the Prydz-Bay shelf on a southwest-northeast transect, showing rugged topography of the glacially carved basal morainic deposits. The postglacial cover sediments show marked thickness variations and are absent in parts of the channel.

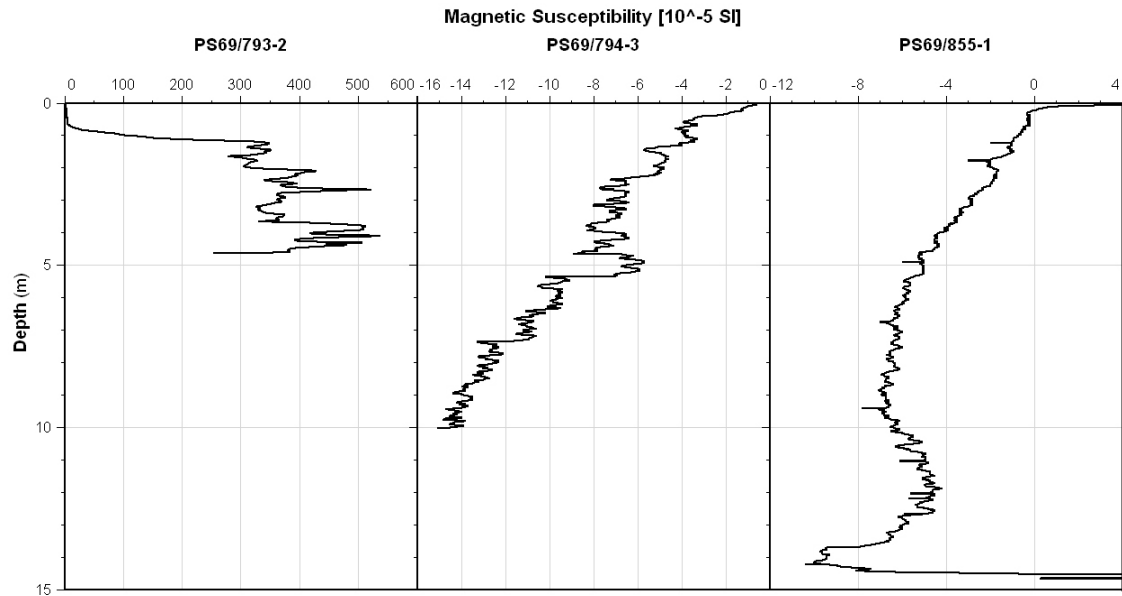


Fig. 4.3: Downcore variability of magnetic susceptibility (MS) in sediment cores from the Prydz Bay shelf. Postglacial diatom oozes are characterized by low MS values, while the morainic sediments exhibit increased values. Sediment core PS69/793-2 only shows a condensed postglacial section. Sediment cores PS69/794-3 and PS69/855-1 were taken from the Svenner Channel, including thick postglacial sequences. The latter penetrated into the basal morainic sediments and reveals marked downcore variability of MS values, possibly inversely related to opal concentrations in the sediments.

Mac Robertson continental margin

This area is situated beneath the near-coast iceberg track originating in Prydz Bay. A depth transect from the shelf across the continental slope was undertaken in order to get suitable records for the reconstruction of IRD (ice-rafted debris) fluxes through time and to gain insight into the variability of deep- and bottom water activity. Depending on the density of palaeo deep water masses, contourites may occur at different depth levels. The identification of gravitational sediment reworking (deposits that result from slumping, debris flows, or turbidity currents) may give clues for ice-sheet grounding and sediment bulldozing across the shelf edge during glacial advances and sea-level low stands in the past.

The Mac Robertson shelf is characterized by the presence of several deeply incised glacial troughs (down to 1,500 m water depth) that are known to include thick Holocene sediment sequences. During the cruise, the easternmost trough, the Burton Basin, was investigated. The Parasound survey revealed the absence of postglacial sediments in that area, apart from a local spot at 559 m water depth in the inner shelf, six miles offshore the Mac Robertson Coast. At this site, station PS69/849-2 yielded a 3 m long record of postglacial diatomaceous oozes with underlying morainic sediments. Beyond the shelf, the upper continental slope is characterized by steep flanks that are almost sediment-barren. At four stations (PS69/850-853) sediment retrieval was undertaken at the middle slope between 1820 and 2364 m water depth. Station PS69/852-1 at 2,268 m water depth was located on a levee structure and

yielded a 6.4 m long section of hemipelagic muds (Fig. 4.4). The upper two metres of the section include high proportions of sand and clasts admixed with biosiliceous remains (diatoms and radiolarians), underlain by fine-grained muds with low amounts of coarse material and rare biogenic remains. This lithology suggests the presence of interglacial sediments in the upper part and older glacial sediments in the lower part (see core description in the appendix). The succession may provide a good record of IRD and bottom-water variability at the Mac Robertson continental margin. Nearby station PS69/853-1 was situated on a drift deposit at 2,364 m water depth (Fig. 4.4) and revealed a more heterogenous lithology. The upper one metre thick unit resembles the interglacial sediments recovered from the levee structure. The underlying sediments in analogy are also finer grained with low abundances of biogenic remains, but show signs of sediment reworking by the appearance of graded sandy layers (turbidites) and contorted and mottled intervals (debris-flow deposits). The base of the sediment core includes an exotic 60 cm thick reddish layer of clay-rich sediment that stands in contrast to the otherwise greyish coloured sediments of the whole sediment core.

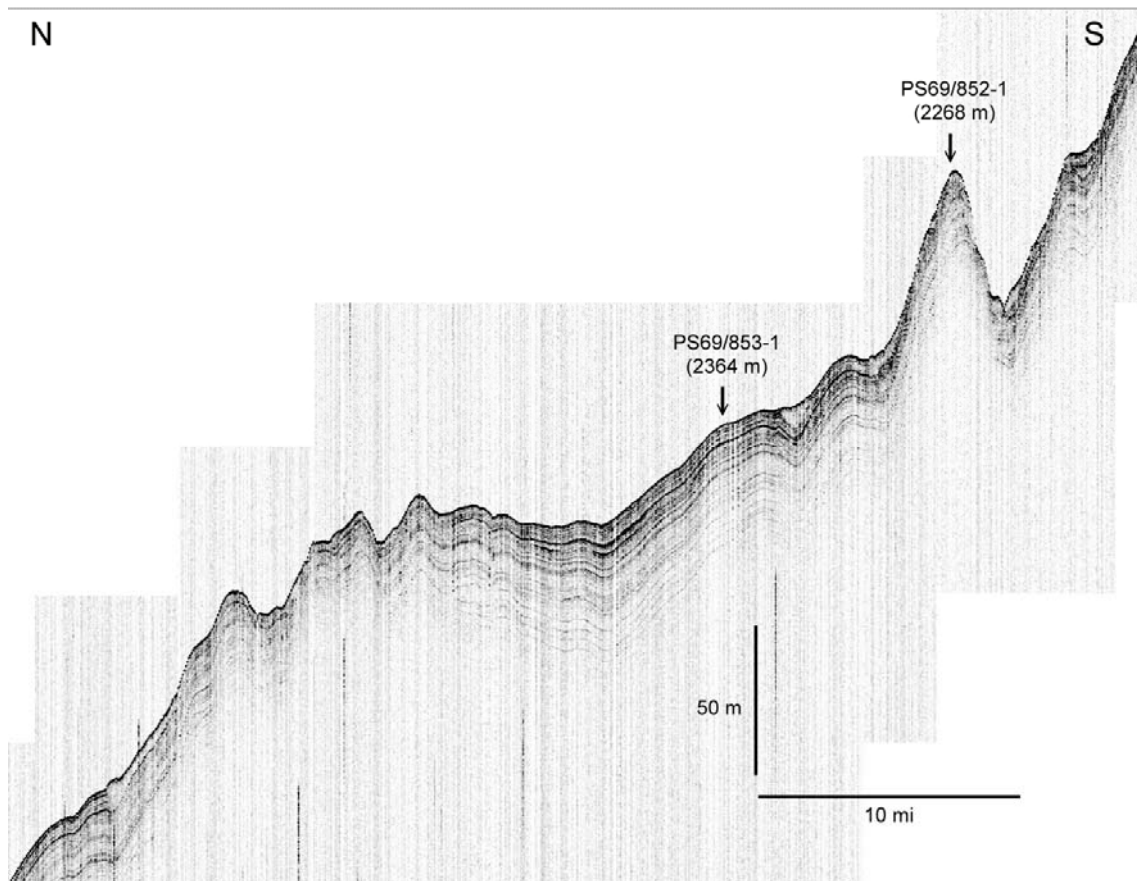


Fig. 4.4: North-south oriented Parasound section across the mid-slope of the Mac Robertson continental margin with location of marine-geological stations on drift and levee deposits.

Eastern Prydz Bay continental slope

The Parasound survey in that area revealed a lack of suitable sediment sequences for coring, apart from very restricted and local occurrences of small sediment nests. Only one station (PS69/878) was cored on a levee deposit at the lower continental slope at 3,067 m water depth and yielded a 6.4 m long record of possibly hemipelagic sediments.

Eastern Enderby Basin

Along the seismic line A of the geophysical working programme, four sediment cores were taken from pelagic deep-sea sediments, located west of the southern Kerguelen Plateau (Stations PS69/820, /821, /846, /847). The selection of coring stations followed the strategy to obtain both expanded and condensed sediment sequences, which are used for the reconstruction of thorium fluxes in relation to different sedimentation rates (see Kretschmer & Mollenhauer, chapter 7). Sediment core PS69/820-3 from 4,160 m water depth provided a rather homogenous, 13.9 m long section of brownish-gray diatom oozes and muds with dispersed clasts and sand grains. The presence of manganese nodules and incrustations on dropstones points to low sedimentation rates at this site. The dropstones consist of crystalline rock clasts, consistent with their origin from East Antarctic continental sources. The recovered sediments can be used for the reconstruction of long-term IRD variability and the inference of palaeo bottom-water dynamics in the deep water masses of the southern Antarctic Circumpolar Current.

Southern Kerguelen Plateau

The Kerguelen Plateau is situated at the return loop of iceberg drift from Prydz Bay. IRD records from there are needed to verify the IRD patterns observed in the ice-proximal position, particularly on the higher positions that are not influenced by abyssal currents. Two stations were investigated in 2,250 m water depth, where two sediment cores were recovered (PS69/890-1, /891-1) from 2,259 and 2,296 water depth, respectively. Sediment core PS69/890-1, 7.5 m in length, shows the principal composition of the exposed sediments on the southern Kerguelen plateau that consist of calcareous oozes. They are dominated by planktonic foraminifera and coccoliths, with variable amounts of biosiliceous remains and low concentrations of terrigenous muds. Dispersed dropstones are distributed throughout the section.

Kerguelen Drift

The Kerguelen Drift represents a thick sediment body located east of the southern Kerguelen Plateau at around 4,100 m water depth. The Parasound profiles show the presence of a deep channel at the foot of the Kerguelen Plateau that passes over to the drift deposits (Fig. 4.5). The cover sediments show marked lateral thickness variations that document the dynamics of Antarctic Bottom Water flow in the past. Sediment cores PS69/899-1 and PS69/900-1 were taken from sites with contrasting sedimentation rates to get a high-resolution record of the younger sediments and to penetrate into deeper sequences (Figs. 4.5, 4.6). Both sites are well suited for the reconstruction of current related particle fluxes (see also Kretschmer & Mollenhauer, chapter 7).

Surficial bottom sediments, obtained with the MUC, exhibit the sediment composition of the drift deposits, including high concentrations of both diatoms and detrital clays and silts. The sediments are admixed with IRD constituents that together with the sediment records from the other pelagic sites can provide insights into Antarctic glacial dynamics.

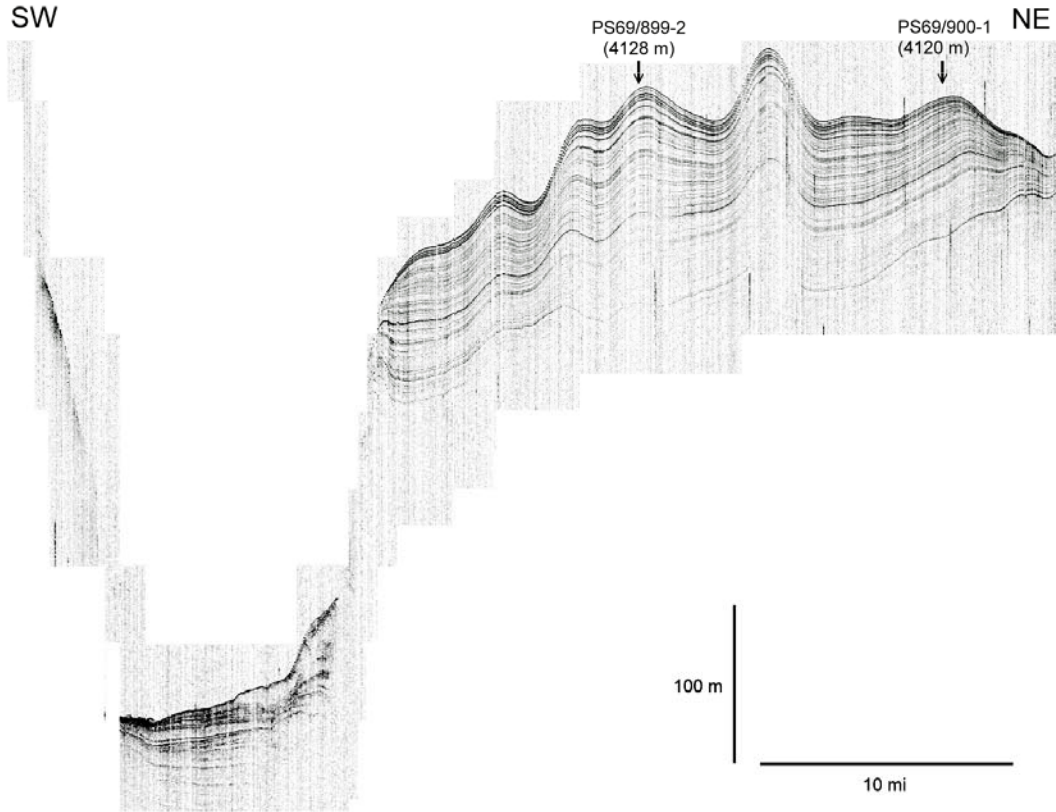


Fig. 4.5: West-east oriented Parasound transect across the Kerguelen Drift, showing sites of marine-geological stations. The upper sediment units display marked thickness variations.

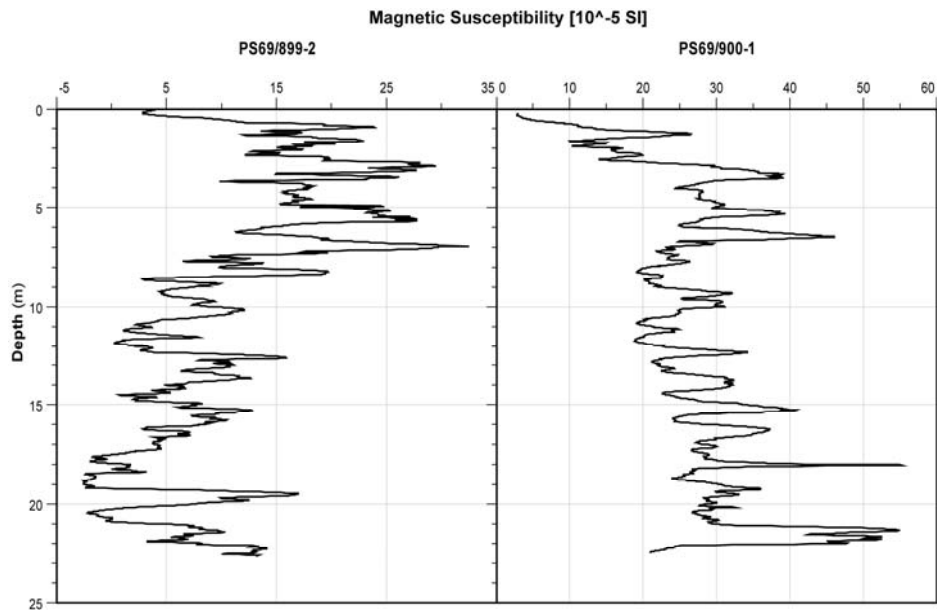


Fig. 4.6: Downcore variations in magnetic susceptibility (MS) in sediment cores taken from the Kerguelen Drift. The uppermost sections can be correlated, while the lower sections show marked differences in their individual MS pattern.

Central Kerguelen Plateau

A 22.9 m long sediment record of diatomaceous oozes and muds was retrieved at station PS69/907-2 situated closely south of the modern Polar Front at 55-degree southern latitude. Colour variations at the end pieces of core sections, ranging from tannish brown to dark grayish colours, together with alternating variations in physical properties (Fig. 4.7) suggest the documentation of glacial-interglacial climate cycles, possibly back to mid-Pleistocene times. Another station (PS69/912) was located north of the modern Polar Front southeast of the Kerguelen Islands at approximately at 50-degree southern latitude. Two 28.1 and 18.9 m long sediment cores were taken from there and possibly cover the late Pleistocene and Holocene at high resolution. The recovered sediment cores will be used for palaeoceanographic reconstructions of the Antarctic Circumpolar Current (see De La Rocha et al., chapter 8).

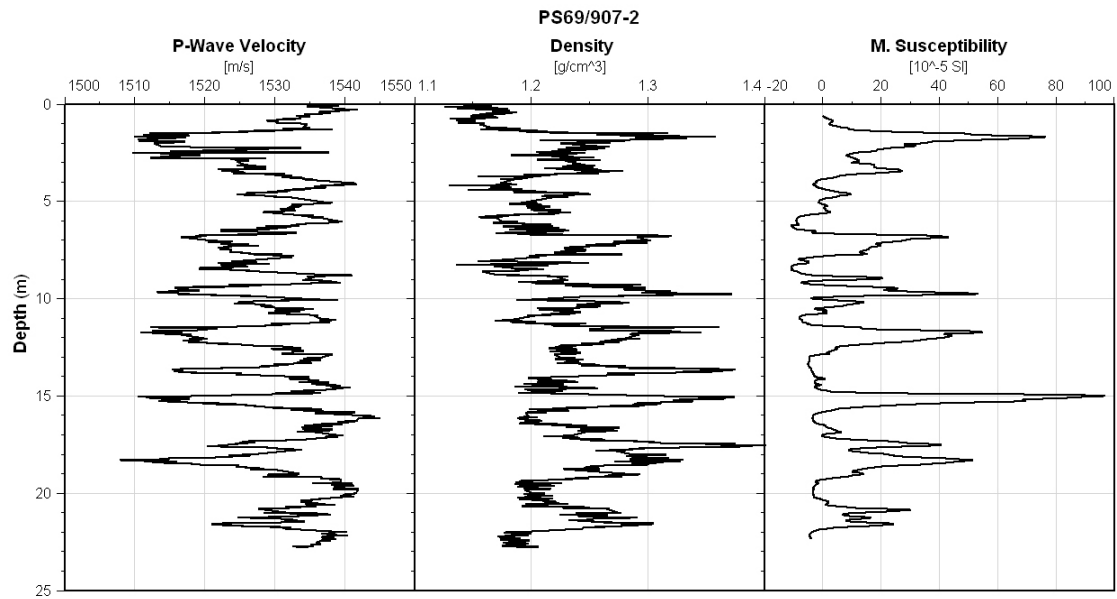


Fig. 4.7: Downcore fluctuations in physical properties in sediment core PS69/907-2 from the central Kerguelen Plateau. The cyclic fluctuations can be related to the alternation of diatom oozes and muds at glacial-interglacial time scales.

Outlook

Later onshore sediment-core studies will be focussed on the provenance and dispersal of ice-rafted debris (IRD) and the sedimentology of contourite/drift deposits in space and time, as indicators of palaeo iceberg drift tracks and AABW activity, respectively. Analyses on the concentration and composition of biogenic matter (carbonate, opal, organic carbon) will provide insights into the modes of biological productivity in the past. In addition to the proxy data inferred from individual samples, high-resolution measurements of downcore compositional variations will be carried out by multispectral colour logging and XRF element scanning of half-core splits at 1-mm resolution, to track environmental changes at sub-Milankovitch time scales. Cooperation is intended with associated scientists, dealing with stratigraphic items, marine particle fluxes, fossil bioindicators, and land records:

- Rainer Gersonde & Andrea Abelmann, AWI Bremerhaven (siliceous bioindicators)
- Gerhard Kuhn, AWI Bremerhaven (glacialmarine sedimentology)
- Martin Melles & Bernd Wagner, University Cologne (land-ocean linkages)
- Gesine Mollenhauer, AWI Bremerhaven (thorium-normalized particle fluxes, radiocarbon dating)
- Andreas Mackensen, AWI Bremerhaven (stable-isotope stratigraphy)

5. MAPPING THE DISTRIBUTION OF SI AND N ISOTOPES IN SOUTHERN OCEAN SURFACE WATERS AND THEIR RELATION TO TRACE ELEMENT AVAILABILITY

Christina L. De La Rocha¹⁾, Eleni Anagnostou²⁾, Christian Schlosser³⁾ ¹⁾ Alfred-Wegener-Institut (AWI), Bremerhaven
²⁾ Institute of Marine and Coastal Sciences, Rutgers University, New Jersey (RUNJ), USA
³⁾ Leibniz-Institute of Marine Sciences (IfM-GEOMAR), FB2 Marine Biogeochemie, Kiel

Objectives

The Si and N isotopic composition of sedimentary diatoms are key proxies for reconstructing nutrient cycling in the Southern Ocean and its impact on atmospheric CO₂ over past climate cycles. They are respectively considered to reflect the extent to which the nutrients, silicic acid and nitrate, are removed from the euphotic zone in support of primary production. The extent of CO₂ uptake during primary production relative to the upwelling of CO₂-rich deep waters in the Southern Ocean, in turn, has a strong influence on atmospheric concentrations of CO₂.

To date paleoceanographic reconstructions of silicic acid and nitrate draw down in the Southern Ocean, south of the present day Antarctic polar front (APF), have produced conflicting results. The Si isotopic composition of diatoms has suggested that silicic acid is more completely consumed during interglacials, and is utilized to a significantly lesser extent during glacials, especially the last glacial maximum (LGM) and the maximum of the penultimate glacial cycle. The nitrogen isotopic composition of organic matter trapped within the siliceous framework of diatoms, however, suggests the opposite pattern for nitrate utilization.

One possible solution to this conundrum lies with the availability of the micronutrient, Fe, which should have been in greater supply in the glacial Southern Ocean due to enhanced deposition of Patagonian dust, alleviating phytoplankton growth from the widespread Fe limitation that is observed in the present interglacial. In addition to being crucial for growth, nitrate utilization, and photosynthesis, Fe plays a key role in diatom silicification. Diatoms that are Fe limited are hampered in their ability to take up and utilize nitrate but are at the same time prone to excessive uptake and incorporation of silicon. Thus the two nutrient cycles may be decoupled over time as Fe levels fluctuate. Although the impact of Fe on Si and N uptake has been studied in diatoms both in culture and in various ocean regimes (including the Southern Ocean), the impact of Fe

limitation and recovery from Fe limitation on Si and N isotopes in diatoms and seawater has never been investigated.

In addition, while it is established that Fe can be a (co)limiting nutrient for phytoplankton in HNLC regions of the world, few details of the processes by which Fe is supplied to the ocean are known. Nor is there yet a fundamental understanding of marine processes involved with Fe scavenging and uptake, solubility, and remineralization. By examining Fe chemistry in the Southern Ocean during ANT-XXIII/9, an overview of the key processes controlling the biogeochemistry of Fe in seawater can be put together. From this a first attempt at quantifying the fluxes involved in each individual process can be made.

Thus objectives of this work are threefold. First, they are to map both the distribution of Fe and other trace elements and of Si and N isotopes in dissolved nutrients in surface waters in the Southern Ocean, providing information as to the range and variability of the variations (especially of the isotopic composition of nutrients) over a fine spatial scale. Secondly, they are to examine the relationship between Fe distributions, nutrient concentrations, algal physiology and morphology, and the Si and N isotopic composition of seawater and diatoms in the Southern Ocean. And lastly, there are to provide fundamental information on the rates and impact of various chemical and biological processes impacting Fe concentrations, solubility, and speciation.

This work was carried out in collaboration with Dr Peter Croot of IfM-GEOMAR and Dr Robert Sherrell of Rutgers University (USA).

Work at Sea

Surface water samples were taken by any of three different means: via a snorkel deployed through the "Brunnenschacht" in the ship's hull, via a "fish" deployed over the portside rail, or via the bow intake pumping system built in to the ship. The first two methods had the capacity to provide trace metal clean samples. The last method was good enough only for nutrient, chlorophyll, and Si and N isotope samples.

The snorkel consisted of a 1.5 meter long steel tube extended below the keel. At the tip of the pipe was a teflon "nose" through which water could be taken up, when the ship was steaming faster than 5 knots, without coming into contact with metal or water that had itself come into contact with metal. This water was taken on board using plastic tubing and a teflon membrane pump, and, on demand, filled two carboys- one with the water as is and the other with the water filtered first through an 0.2 um cartridge filter.

The snorkel could only be deployed in relatively ice-free areas, leaving broad stretches of the cruise unavailable for trace metal sampling (during these times the bow pump was used to continue the chlorophyll and isotope work as useful). Despite the caution observed with deployment of the snorkel, an errant ice floe did catch the snorkel, bend it up against the hull, and rip off the teflon nose cone sometime around 9 March. The bend had to be cut out of the tube and a new

nose cone had to be made. The snorkel, approximately 30 centimetres shorter, was then redeployed several days later (18 March).

An unsuccessful attempt was made to use the stainless steel "fish" (with plastic nose cone and teflon sipper) for a while in icier areas. Unfortunately the air temperature was cold enough to freeze solid the water in the tubing running between the sea surface and the wet lab (where the teflon pump was sitting). In addition, frequent dismantling of the system to accommodate other items on the sliding beam from which the fish was hung, introduced frequent trace metal contamination into the system. As a sampling system on this cruise, the fish was quickly abandoned.

Once filtered and prefiltered water was obtained in the sampling carboys, aliquots were immediately taken for a number of samples. The suite of samples taken includes chlorophyll concentrations; biogenic (BSi) and lithogenic (LSi) silica concentrations; dissolved silicon, nitrate, and soluble reactive phosphate concentrations; particulate organic carbon (POC), particulate organic nitrogen (PON), $\delta^{13}\text{C}$ of POC, and $\delta^{15}\text{N}$ of PON; $\delta^{30}\text{Si}$ of dissolved silicon and $\delta^{15}\text{N}$ of nitrate; dissolved, particulate, and total Fe; Fe solubility; Fe ligands; misc trace elements (Fe, Al, Ti, Zn, Cd, Co, etc) in dissolved, colloidal, and particulate phases; total intracellular Fe (and other intracellular trace metals); pigment concentrations; diatom morphometrics (size and shape of *Fragilariopsis kerguelensis*); and phytoplankton number and species composition.

Samples of chlorophyll, nutrients, BSi and LSi, POC and PON, $\delta^{30}\text{Si}$ of dissolved silicon, $\delta^{15}\text{N}$ of nitrate, and Fe solubility were also taken from 8 different CTD casts from depths ranging from 20 meters at the shallowest down to 4,000 meters at the deepest (although most sites were shallower than this).

Expected Results

All told, nearly 70 localities were sampled for surface waters (Fig. 5.1 in this chapter and Tab. A.5.1 in the appendix) and 76 depths were sampled from 8 different CTD casts (Fig. 5.1 in this chapter and Tab. A.5.2 in the appendix). These samples fall along a cruise track (Fig. 1.1) that covered temperate to polar regimes, crossed over the Antarctic Divergence, the Antarctic Polar Front, and the Subantarctic Front, regions of low Fe availability as well as those (down wind of land masses or on the Kerguelen Plateau) where Fe may be abundant, and both open and coastal waters. The samples taken (Fig. 5.1) should allow for documentation of shifts in nutrients, trace elements, physiology, morphology, and isotopes over a broad range of conditions. Such ground-truthing of the relationships between isotopes, trace elements, nutrient concentrations, and diatom morphometrics will help us to improve Si and N isotope-based paleoceanographic reconstructions of nutrient utilization and CO_2 removal. The data sets produced, in addition to enhancing our understanding of two proxies fundamental to reconstructions of Southern Ocean paleoceanography, fall under the auspices of the IPY umbrella project, BIPOMAC, and will also contribute to the trace metal and isotope mapping efforts of GEOTRACES.

5. Mapping the distribution of Si and N isotopes in Southern Ocean surface waters and their relation to trace element availability

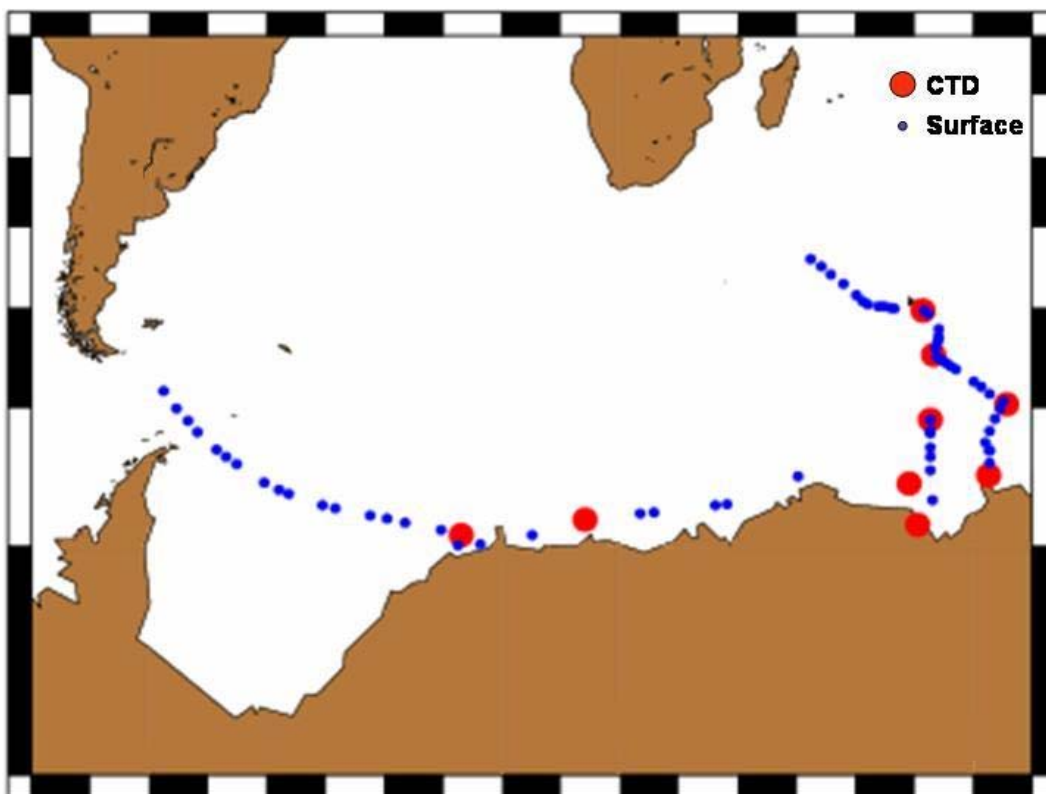


Fig. 5.1: Surface water and CTD sampling localities for trace elements and Si and N isotopes.

While most parameters sampled for will be measured back at the AWI, at IFM-GEOMAR, and Rutgers University, preliminary values for dissolved and total Fe concentrations were measured on board via luminol chemiluminescence in a flow injection analysis (FIA) system. Fe solubility was also measured using the radioisotope, ^{55}Fe , whereby the activity of the isotope was monitored in $0.02\ \mu\text{m}$ filtered and unfiltered samples over an equilibration time of 72 hours.

The preliminary Fe concentration measurements, intended more as a monitor of the cleanliness of sampling conditions (it is difficult to obtain samples that are not contaminated with more metal than they themselves contain naturally), are not presented here. In general, however, they showed expected low concentrations of Fe in Southern Ocean surface waters (roughly $0.5\ \text{nM}$) and much higher concentrations (values off the scale of the FIA) at locations on the Kerguelen Plateau with the shallowest water depths (around $300\ \text{m}$), suggesting Fe fertilization of those waters by the sediments of the plateau itself.

In terms of Fe solubility (i.e. that portion of the Fe truly in solution and available for biological uptake), the highest Fe solubilities (around 5 %) were observed close to the Antarctic continent and on the Kerguelen Plateau (Fig. 5.2). Markedly lower solubilities (around 2.5 %) were observed in the Drake Passage and in the open ocean. This may be due to higher concentrations of organic ligands, produced by phytoplankton (especially under conditions of Fe limitation), in the surface water masses of the Southern Ocean proper. Further,

more complete, comments on this will be made later, following the analyses of nutrient and chlorophyll concentrations and other parameters back on land.

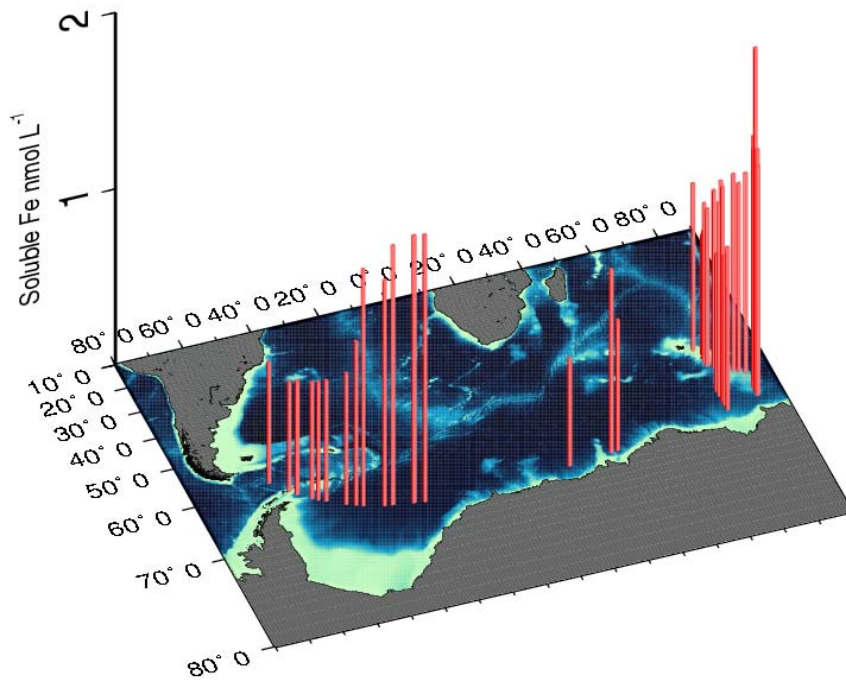


Fig. 5.2: Total amounts of soluble Fe in surface water samples

6. THE CARBONATE SYSTEM AND THE CARBON ISOTOPIC COMPOSITION OF PARTICULATE ORGANIC MATTER IN SOUTHERN OCEAN SURFACE WATERS

Christina L. De La Rocha
Alfred-Wegener-Institut (AWI), Bremerhaven

Objectives

The carbon isotopic composition $\delta^{13}\text{C}$ of organic matter, especially that associated with diatom frustules accumulating in marine sediments, is commonly used to reconstruct oceanographic processes that contribute to variations in atmospheric CO_2 over glacial-interglacial cycles. Large and systematic variations in the $\delta^{13}\text{C}$ of both diatom-bound and bulk organic matter have been observed over glacial-interglacial cycles and between the Atlantic and the other sectors of the Southern Ocean. Organic matter has been observed to have higher values of $\delta^{13}\text{C}$ in Southern Ocean sediments of interglacial age than glacial age. In addition, extremely negative values of $\delta^{13}\text{C}$ occur in the Atlantic sector (up to 8 permil more negative than in the Indian and Pacific sectors). In general, temporal and spatial differences in $\delta^{13}\text{C}$ have been interpreted as indicating everything from changes in primary production, sea surface temperature, and the presence of sea ice. In truth, the $\delta^{13}\text{C}$ of particulate organic carbon is controlled by not one biological or physical factor but a complex set of them, and as yet no consensus has been reached as to which factor plays the key role in setting the $\delta^{13}\text{C}$ of organic matter produced (and sedimenting) in the Southern Ocean.

Identifying the cause of the geographic variability in the $\delta^{13}\text{C}$ of organic matter in the Southern Ocean would go a long ways towards helping us interpret the glacial-interglacial $\delta^{13}\text{C}$ signal. There are several possible candidates, although none very favourable. For example, there is not much regional variation in the $\delta^{13}\text{C}$ of dissolved inorganic carbon (DIC) of surface waters that the phytoplankton are using for the synthesis of the organic matter. Some differences exist, but they are nowhere near the several permil necessary to explain the particulate organic matter and diatom-bound organic matter data. Likewise the higher growth rates of phytoplankton in areas free from Fe-limitation (e.g. the Atlantic sector, which is downwind of South America, a major source of Fe in the form of dust) could explain some of the $\delta^{13}\text{C}$ variability, if only the $\delta^{13}\text{C}$ values in this region were high and not extremely low like they are. Given that the main differences between the Atlantic sector and the other two sectors is the availability of iron, rates of primary production, and the standing

stocks of chlorophyll, it is likely that the cause is of physiological or ecological in origin. There may be unforeseen impacts of Fe-fertilization of carbon isotope fractionation during photosynthesis. Or the $\delta^{13}\text{C}$ differences may have to do with the species of diatoms preserved in the sediments, since the size, surface to volume ratio, growth rate, and specifics of the carbon fixing enzyme, Rubisco, for each species leave room for differences in the $\delta^{13}\text{C}$ of different phytoplankton growing under different conditions.

The objective of this project was to study the carbonate system and carbon isotopes of DIC and particulate organic matter along a large geographic gradient in the Southern Ocean and to compare it with chlorophyll concentrations, Fe availability, and the number and type of phytoplankton present in surface waters. By doing so and combining it with modelling of phytoplankton carbon acquisition and isotope fractionation, light may be shed on the biological factors and biological-physical interactions controlling the $\delta^{13}\text{C}$ of bulk particulate and diatom-bound organic matter in the Southern Ocean. This work is being carried out in conjunction with Dr. Uta Passow and Prof. Dieter Wolf-Gladrow, both of AWI Bremerhaven.

Work at Sea

In conjunction with the surface water sampling carried out by De La Rocha, Anagnostou, and Schlosser on this cruise (see chapter 5), samples of the $\delta^{13}\text{C}$ of particulate organic matter, chlorophyll, and nutrients were collected at every sampling site (see Tab. A.5.1 in the appendix) either using the bow intake line, or the snorkel or fish and teflon membrane pump (for a detailed description of the collection of seawater see De La Rocha et al., chapter 5). In addition, at selected sites (see Tab. A.5.1 in the appendix), samples were taken at 16 sites in the Southern Ocean for alkalinity, dissolved inorganic carbon (DIC), the $\delta^{13}\text{C}$ of DIC, and phytoplankton enumeration. These samples were always taken from the bow intake in order to avoid aeration of the samples (and subsequent addition of dissolved CO_2) by the teflon membrane pump.

Samples for DIC and $\delta^{13}\text{C}$ of DIC were collected gently (without producing bubbles) in a large plastic beaker and filtered immediately (and gently) through an $0.2\ \mu\text{m}$ syringe filter, filling a 4 or 8 ml glass vial without the addition of bubbles to the sample. Samples were allowed to sit very shortly (a few moments) and then they were preserved with the addition of a few μl of $35\ \text{g l}^{-1}$ mercury chloride solution to an end concentration of $140\ \text{mg l}^{-1}$. Alkalinity samples were filtered through GFF filters (the same ones used for the POC, PON samples), poured into an amber glass bottle and also preserved with an end concentration of $140\ \text{mg l}^{-1}$ mercury chloride. Samples for phytoplankton enumeration were preserved (unfiltered) in amber glass bottles with a final concentration of 2 % hexamethylene-buffered formaldehyde.

In addition, at a very small number of sites there was enough time to take a size-fractionated sample of the $\delta^{13}\text{C}$ of particulate organic matter. This involved passing up to 25 liters of water through a series of filters, each of different size, in order to separate the larger phytoplankton from the smaller phytoplankton

from the bacteria and discern which was responsible for the bulk of the $\delta^{13}\text{C}$ signal. The first few attempts at this worked badly and the samples were discarded. Successful samples, splitting the particulate material into $>20\ \mu\text{m}$, $5\text{-}20\ \mu\text{m}$, and $0.2\text{-}5\ \mu\text{m}$, were taken at sites number 25, 28, and 37. These filtrations took a great many hours and there was simply not enough manpower in the lab to obtain a greater number of these samples.

Expected Results

The 71 samples defining the bulk particulate organic matter $\delta^{13}\text{C}$, and the 16 describing the concentrations and isotopic composition of the carbonate system, together with the 3 size-fractionated samples obtained will add greatly to the data set of the carbon isotope system in the Southern Ocean. The bulk of the samples obtained run up from Prydz Bay through the Kerguelen Plateau, allowing for a systematic look at the impact of latitude on the carbon isotopic composition of organic matter. These data from the Indian Sector of the Southern Ocean will then be compared with samples to be obtained on an upcoming *Polarstern* cruise covering transects through the Drake Passage and along the zero meridian, making a comparison of two very different sectors of the Southern Ocean possible.

7. THE INFLUENCE OF SEDIMENT TRANSPORT ON $^{230}\text{Th}_{\text{xs}}$ INVENTORIES AND ^{14}C AGES OF ORGANIC MATTER IN INDIVIDUAL SEDIMENT FRACTIONS

Sven Kretschmer, Gesine Mollenhauer (not on board)
Alfred-Wegener-Institut (AWI), Bremerhaven

Objectives

Different processes of deposition, re-suspension and lateral transport of particles influence depositional patterns and affect the accuracy of sedimentary records. These can be subdivided into pre-depositional processes, such as displacement of suspended particles by advection, and post-depositional processes such as diagenesis, bioturbation and re-suspension by strong bottom currents, so that particles can be transported to another place of deposition.

Lateral transport has the potential to sort sediment particles hydrodynamically according to particle size and sinking velocity. Fine grained particles and organic rich aggregates are more susceptible to lateral transport. This leads to a spatial and temporal decoupling of fine-grained particles and organic matter from coarser sediment constituents and therefore to a decoupling of proxy records residing within these different particle classes. As these processes are poorly understood, the aim of this study is to investigate depositional patterns in detail. It will be investigated the $^{230}\text{Th}_{\text{xs}}$ concentrations in different size fractionated sediment classes for quantifying sediment re-distribution with $^{230}\text{Th}_{\text{xs}}$ -normalized flux rates.

Additionally, the component specific ^{14}C ages will be analysed because ages of distinct sediment components can differ by a wide range depending upon the pre- and post-depositional processes. Laterally transported material is likely to be pre-aged and contain ^{14}C -depleted organic matter. Therefore, the ^{14}C age of organic matter entrained in the fine grain size fraction is expected to be older than bulk organic matter. Reactivity of individual organic compounds during passage through oxygenated water masses is a further control on their ^{14}C -age, as old and refractory material is selectively preserved (Mollenhauer et al. 2006). In this study, the distributions of $^{230}\text{Th}_{\text{xs}}$ and $^{14}\text{C}_{\text{org}}$ in the individual grain size fractions will be compared in sediments from sites where sediment focusing occurs to results from nearby sites without significant amounts of laterally supplied sediments.

This study is part of the Helmholtz Young Investigators Group “Applications of molecular ^{14}C analysis for the study of sedimentation processes and carbon cycling in marine sediments” (Head: Dr. Gesine Mollenhauer).

Work at Sea

Sampling locations

The sampling sites for sediment coring require neighbouring positions which differ strongly in accumulation rates. Small-scaled depositional patterns are likely to be found in the Southern Ocean due to its dynamic bottom water circulation. The Parasound survey makes it possible to locate this depositional pattern. In addition to the sediment coring, surface sediments and bottom water from the nepheloid layer need to be taken, in order to gain additional information about the current situation of sediment re-suspension and transport.

Sites were selected on the basis of the Parasound survey with different thicknesses of sediment layers. Five pairs of neighbouring sites along the seismic profiles between Prydz Bay and Kerguelen Plateau, in water depths between 2,200 and 4,200 meters were sampled using the gravity corer or piston corer, multicorer, and CTD (Tab. 7.1). Information about the coring sites, a station map, and Parasound profiles are included in Diekmann et al. (chapter 4).

Tab. 7.1: List of neighbouring stations that exhibit different depositional patterns observed via Parasound

Pair	Station	Latitude	Longitude	Depth [m]	Gear	depositional pattern
1	PS69/820	60° 56,99' S	72° 43,28' E	4165.0	GC + MUC + CTD	focussed
	PS69/821	60° 55,24' S	72° 43,19' E	4120.0	GC	winnowed
2	PS69/845	61° 51,08' S	72° 43,07' E	4105.0	GC	winnowed
	PS69/846, PS69/847	61° 49,53' S	72° 43,52' E	4124.0	GC + MUC	focussed
3	PS69/852	66° 4,87' S	69° 10,18' E	2271,0	GC	winnowed
	PS69/853	65° 59,89' S	69° 13,18' E	2364,0	GC + MUC + CTD	focussed
4	PS69/890	62° 46,20' S	82° 49,91' E	2258,0	GC	winnowed
	PS69/891	62° 39,55' S	82° 49,93' E	2292,0	GC + MUC + CTD	focussed
5	PS69/898, PS69/899	59° 37,28' S	85° 40,43' E	4124,0	CTD + PC + MUC	focussed
	PS69/900	59° 32,87' S	85° 50,69' E	4116,0	PC	winnowed

Sediment coring

Pairs of sediment cores at neighbouring station were recovered south-west of Kerguelen Plateau (PS69/820, /821, and PS69/845, /846), at southern Kerguelen Plateau (PS69/890, /891), east of Kerguelen Plateau (PS69/899, /900), and at Mac Robertson continental margin (PS69/852, /853). At each location one core with focusing features and a second one with more winnowed layers were retrieved.

The core description and the results of the Multi Sensor Core Logger (P-wave velocity, density, magnetic susceptibility, impedance, porosity) of all sediment cores are included in Diekmann et al. The cores will be sampled after the cruise in the AWI laboratory in Bremerhaven according to stratigraphic information to be made available.

Surface Sediments

Up to 2 parallel multicorer subcores or box-corer subcores per sampling location were sliced in 1 cm intervals. MUC samples were taken at the neighbouring stations (Tab. 7.1). Additional sample material was retrieved from the deep shelf basins for the study of ^{14}C -ages of individual organic biomarkers. Samples were stored frozen aboard ship and during transport. The multicorer was sampled for $^{14}\text{C}_{\text{org}}$ in glass jars and stored frozen at -27°C and for ^{230}Th in plastic bags and stored cooled at 4°C . See Diekmann et al. for a full list of multicorer samples.

Grain size fractionation

The adsorption of ^{230}Th onto particles depends on the material (organic, mineral, siliceous, carbonaceous) and the particle grain size. Grain size fractionation was done with a set of surface sediments that were taken with the multicorer (Tab. 7.2). The sediment was sieved immediately without any pre-treatment using three sieves with mesh sizes $125\ \mu\text{m}$, $63\ \mu\text{m}$ and $20\ \mu\text{m}$. The wet sieving was done with filtered seawater. The use of fresh sediment and of seawater, as well as omitting the disaggregation treatments should ensure that the particles and aggregates were not destroyed and were kept as natural as possible. The cations in the seawater caused a strong flocculation of clay minerals during sieving procedure, so that it was impossible to separate the clay out of the $20\ \mu\text{m}$ fraction. The fractionated samples were centrifuged and stored frozen. The excess water after centrifugation was stored for thorium analyses as well.

Tab. 7.2: Surface sediment up to 5 cm depth from three different sample sites was size-fractionated by wet sieving with mesh sizes 125 μm , 63 μm and 20 μm .

Station	depth [cm]	volume of sediment sample [ml]	volume of seawater used for sieving [l]
PS69/820-2	0-1	10	5,0
	1-2	10	4,7
	2-3	10	7,1
	3-4	10	4,6
	4-5	10	5,3
PS69/847-1	0-1	5	4,8
	1-2	5	4,0
	2-3	5	4,2
	3-4	10	5,4
	4-5	10	5,0
PS69/851-2	0-1	5	2,8
	1-2	5	3,0

Suspended particles

In order to analyse the components of suspended matter in the nepheloid layer, bottom water was sampled with CTD-bottles and was filtered using two different kinds of filters. Glass fibre filters (GF/F) were used for analyses of organic carbon. Polycarbonate filters (PC filter) were used for analyses of particulate ^{230}Th . Filters were stored frozen. The filtrate from the PC filter was collected and acidified for analysis of dissolved ^{230}Th . In addition, two litres were taken for bulk ^{230}Th analyses (Tab. 7.3).

Tab. 7.3: Seawater from CTD sampling was filtered with polycarbonate filters (PC) for particulate $^{230}\text{Th}_{\text{xs}}$ and with glass fibre filters (GF/F) for organic carbon.

Station	Date	Depth [m]	volume filtered seawater [l]		volume unfiltered seawater [l]
			PC-filter	GF/F-filter	
PS69/795-1	24.02.2007	828	-	23,0	-
PS69/820-1	03.03.2007	4165	23,1	23,1	2,0
PS69/853-3	12.03.2007	2200	22,9	22,6	2,0
PS69/878-3	21.03.2007	2900	22,8	22,7	2,0
PS69/891-1	22.03.2007	2140	23,0	23,0	2,0
PS69/898-2	24.03.2007	3950	34,7	46,3	2,0
PS69/907-3	26.03.2007	2064	46,3	46,0	2,0
PS69/912-1	28.03.2007	500	-	45,7	-

Expected results

Grain-size fractionated $^{230}\text{Th}_{\text{xs}}$ and ^{14}C studies will contribute to our understanding of sediment transport and its importance in the formation of deep-sea sediment archives, in particular in the highly dynamic Southern Ocean environment. Time-scales of sediment transport can be derived. The controlling mechanisms for the preservation of organic biomarkers, in particular those derived from Antarctic phytoplankton, will be studied. These findings will have important implications for the use of biomarkers as proxies for past environmental conditions and for cycling of organic carbon in the Southern Ocean. In addition, stratigraphic information for related studies will be made available.

References

Gesine Mollenhauer, Jerry F. McManus, Albert Benthien, Peter J. Müller, Timothy I. Eglinton (2006): Rapid lateral particle transport in the Argentine Basin: Molecular ^{14}C and $^{230}\text{Th}_{\text{xs}}$ evidence. *Deep-Sea Research I* 53, 1224-1243.

8. DOCUMENTATION OF THE HOLOCENE AND PLEISTOCENE VARIABILITY OF PALEO-ENVIRONMENTAL CONDITIONS WITHIN THE ANTARCTIC CIRCUMPOLAR CURRENT (ACC)

Christina L. De La Rocha¹,
Bernhard Diekmann², Peter
Sperlich³, Sven Kretschmer¹,
Norbert Lensch¹

¹ Alfred-Wegener-Institut (AWI),
Bremerhaven

² Alfred-Wegener-Institut (AWI), Potsdam

³ University of Bremen

Objectives

Paleoceanographic studies of the past decade show that physical and biological processes in the Southern Ocean, together with Antarctic ice-sheet dynamics, play a key role in global climate; the leading responses of Southern Ocean sea-surface temperatures (SSTs) and sea ice extent on orbital and suborbital timescales, the correlation between southern hemisphere temperatures and concentrations of CO₂ in the atmosphere, and the export of nutrients from Southern Ocean surface waters to equatorial and coastal upwelling regions all implicate the Southern Ocean as a driver of global climate and ecosystem change. As the largest high-nutrient-low-chlorophyll (HNLC) area in the world, the Southern Ocean has the capacity to be a major CO₂ sink by increasing the efficiency of its biological carbon pump (e.g. through relatively more complete consumption of upwelled nutrients), as has been postulated for the glacial period. Finally, air-sea interactions in the Southern Ocean play a crucial role in closing the global ocean circulation loop and thus Southern Ocean climate may play a key role in setting the rate of global overturning. To understand the Southern Ocean's role in and response to climate development and to link this information with records from continental ice cores (e.g. EPICA cores), high-resolution records from all sectors of the Southern Ocean are required.

Expedition ANT-XXIII/9 presented an excellent opportunity to recover additional sedimentary archives to study Holocene and Pleistocene paleoceanographic variability from a series of sites located on a latitudinal transect across the Indian sector. The latitudinal transect in the Indian sector will help to establish, together with existing transects in the Pacific and Atlantic sector, a circum-Antarctic view of Pleistocene conditions within the ACC.

Work at Sea

Recovery of long (up to 25 - 30 m) piston cores and surface sediments via the multicorer and large box corer along a latitudinal transect along the Kerguelen Plateau was carried out as described in the chapter on marine geology (Diekmann et al., chapter 4) This transect in the Indian sector of the Southern Ocean is intended to document Southern Ocean variability (surface water

temperature and salinity, sea ice, and nutrient availability) between the Antarctic Zone and the northern boundary of the ACC.

Shipboard studies on sediment cores consisted of whole-core measurements of geophysical sediment properties (magnetic susceptibility, P-wave velocity, gamma-ray density) with a GEOTEC Multi-Sensor Core Logger, and to some extent sediment-core splitting, description and sampling, and x-ray imaging of sediment slices from the core sections). This has been described in detail in the section on marine geology (Diekmann et al., chapter 4). In addition, 1 to 2 cm slices were taken from multicores and stored in Whirlpak bags for later work on diatom abundances and transfer functions and on the radiogenic and/or stable isotopic composition of opal back in Bremerhaven.

Results and Expected Results

A considerable amount of work will be done on the sedimentary material recovered on this cruise. Abundances of diatoms and radiolarians from these sediment cores will allow for the reconstruction of physical factors such as sea surface temperatures and sea ice coverage up the latitudinal transect of the Kerguelen Plateau. Through the measurement of particle reactive nuclides, such as thorium isotopes, sediment (and specifically opal) accumulation rates will be tabulated to give a view on the productivity regime and cycling of silicon. This will be coupled, in the case of some cores, with isotopic analysis of trace amounts of organic carbon trapped in the opal matrix of diatoms separated out of the sediments, and with isotopic analysis of the opal itself to gain insight into the cycling and utilization of nutrients, such as silicic acid and nitrate, relative to their supply from deep waters.

All together, these data along the latitudinal transect of sediment cores in the Indian sector will provide new data on Pleistocene sea surface physical and biological variability. It will thus help to establish, together with existing transects in the Pacific and Atlantic sector, a circum-Antarctic view of Pleistocene ACC development, which can be compared with climate records obtained from continental ice cores and with records on continental ice stability from near shore sedimentary archives (see project by Diekmann et al., chapter 4). The collected surface sediments will enlarge our reference database on the distribution of siliceous microfossils (diatoms, radiolarians) in the Southern Ocean and will be used for acquisition of opal isotope data, as well as for flux rate measurements of biogenic and non-biogenic compounds via radionuclide measurements. These studies are essential baseline for paleoceanographic reconstructions.

This work is an important contribution to the marine programme within MARCOPOLI work package, POL6, and the international IPY project "Bipolar Climate Machinery" (BIPOMAC). The research project is being carried out under the direction of Dr. Rainer Gersonde (AWI-Bremerhaven).

9. DEPLOYMENT OF ARGO-FLOATS

Olaf Klatt, Katharina Muhle
Alfred-Wegener-Institut (AWI), Bremerhaven

Objectives

The international Argo-project aims to set on the order of 3,000 profiling floats into the world ocean, to establish a real-time operational data stream of mid- and upper (< 2,000m) ocean temperature and salinity profiles. In addition the array will provide the mid-depth oceanic circulation pattern.

The main objectives of the programme are:

- to increase the understanding of the ice-free ocean and its role in global climate
- to detect and attribute climate change effects on the oceans
- to initialize climate forecast models
- to calibrate and/or validate satellite altimetry data.

Since 2001, the AWI has contributed about 12 floats annually to this programme. During ANT-XXIII/9 floats were provided by two different programmes: 8 floats from the EU MERSEA, and 6 from the German Argo programme.

Work at sea

The instruments were launched at quasi-regular intervals along the southern part of the cruise track, with preference given to undersampled regions and boundary currents (Fig. 9.1 and Tab. 9.1). All floats have already submitted at least one profile. Some of the float launches were preceded by a CTD cast, as indicated in Table 9.1. Further CTD stations have been carried out, primarily to support other groups with water (see Tab. 9.2).

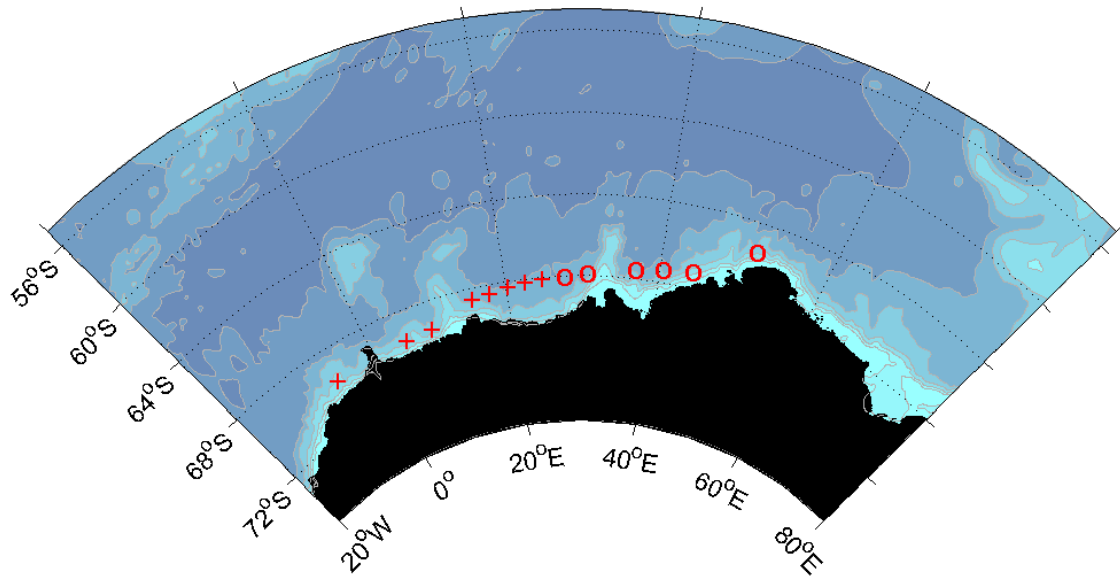


Fig. 9.1: Deployment positions of Argo floats during ANT-XXIII/9. Symbols mark various float types: APEX (o), NEMO (+).

APEX floats

A total of 6 APEX floats were launched. All APEX floats are equipped with RAFOS Navigation System and with Ice Sensing Algorithm (ISA; abort-temperature -1.79°C). Data from profiles aborted due to ISA are lost. The floats were ballasted to drift at a drift depth of 800 m and will acquire profiles from 2000m up. APEX floats are produced by Webb Research Corporation, USA.

NEMO floats

A total of 8 NEMO floats (Navigating European Marine Observer) were deployed. NEMO floats are equipped with RAFOS Navigation System, an adjustable Ice Sensing Algorithm, set to -1.79°C and an 'retarded' response: Once activated, ISA will need to detect 'surfacing conditions' (i.e. the lack of 'abort conditions') for two ascent cycles consecutively, before giving the float permission to completely ascend to the surface on the second cycle. An interim data storage system (iStore), stores any profiles that could not be transmitted in real time due to ISA aborts and transmits these profiles during the period of minimal ice condition (February – 15 March). The floats were ballasted to drift at a drift depth of 800 m and will acquire profiles from 2,000 m up. NEMO floats are produced by Optimare, Germany.

Tab. 9.1: Argo float launch positions and times. APEX and NEMO floats were equipped with Ice Sensing Algorithm, set to -1.79° C. Programme abbreviations: A = German Argo, M = MERSEA.

CTD Station PS69/	AWI – number	ARGOS-DEC	Float type and Serial Nr.	RAFOS	retarded response	Project	Water depth [m]	Latitude [S]	Longitude	Date (UTC)	Time (UTC)
PS69/747-4	106	28045	Nemo 42	y	0	M	2954	69° 24.08'	07° 01.04' W	11.02.07	17:40
PS69/752-1	107	28040	Nemo 37	y	1	M	2897	69° 18.61'	03° 50.58' E	15.02.07	06:53
PS69/754-3	108	28023	Nemo 35	y	1	M	2507	69° 14.86'	07° 39.61' E	15.02.07	17:43
PS69/758-1	109	28022	Nemo 33	y	1	M	3400	68° 25.20'	14° 09.80' E	16.02.07	10:25
PS69/760-1	110	27981	Nemo 32	y	1	M	3577	68° 19.25'	16° 29.78' E	16.02.07	15:38
PS69/763-1	111	28044	Nemo 41	y	1	M	4309	68° 12.99'	19° 01.80' E	16.02.07	23:20
PS69/765-1	112	28042	Nemo 38	y	1	M	4222	68° 07.06'	21° 20.01' E	17.02.07	04:31
PS69/769-1	113	28043	Nemo 39	y	1	M	3969	68° 00.88'	23° 45.63' E	17.02.07	09:57
PS69/771-2	114	28107	APEX 1185	y	-	A	4088	67° 54.53'	26° 43.52' E	17.02.07	18:18
PS69/773-1	115	09365	APEX 2558	y	-	A	3868	67° 46.30'	29° 40.80' E	18.02.07	00:28
PS69/775-1	116	26871	APEX 2551	y	-	A	3344	67° 29.94'	35° 48.04' E	18.02.07	14:28
PS69/777-1	117	25650	APEX 2550	y	-	A	3393	67° 20.73'	39° 19.94' E	18.02.07	21:39
PS69/780-1	118	26735	APEX 2548	y	-	A	2661	67° 10.69'	43° 10.06' E	19.02.07	05:38
PS69/785-1	119	25925	APEX 2549	y	-	A	2239	65° 24.93'	50° 02.90' E	20.02.07	06:31

Tab. 9.2: Positions of CTD-casts during ANT-XXIII/9

Station	Date	Time UTC	Latitude	Long.	Water depth (m)	Remarks
PS69/747-1	11/02/07	13:07	69° 24.04' S	06° 59.84' W	2976	Float 106
PS69/754-1	15/02/07	14:28	69° 14.81' S	07° 39.52' E	2481	Float 108
PS69/757-1	16/02/07	8:20	68° 24.68' S	14° 09.30' E	3428	Float 109
PS69/762-1	16/02/07	21:39	68° 13.06' S	19° 01.40' E	4293	Float 111
PS69/771-1	17/02/07	16:49	67° 54.50' S	26° 43.00' E	4094	Float 114
PS69/782-1	19/02/07	14:42	66° 57.85' S	46° 35.20' E	263	Test-CTD
PS69/782-4	19/02/07	15:55	66° 35.27' S	46° 35.26' E	260	Test-CTD
PS69/794-8	24/02/07	18:11	68° 43.34' S	76° 40.67' E	881	Geostation
PS69/820-1	02/03/07	18:17	60° 60.00' S	72° 43.61' E	4161	Geostation
PS69/846-1	09/03/07	5:45	61° 43.66' S	72° 43.54' E	4124	Geostation
PS69/853-3	12/03/07	6:37	65° 59.90' S	69° 13.13' E	2363	Geostation
PS69/878-3	21/03/07	9:29	65° 21.04' S	82° 39.44' E	3065	Geostation
PS69/898-2	24/03/07	3:23	59° 37.31' S	85° 40.35' E	4105	Geostation
PS69/907-1	26/03/07	18:33	55° 00.34' S	73° 20.04' E	2237	Geostation
PS69/912-1	28/03/07	9:57	50° 19.50' S	71° 33.37' E	563	Geostation

10. **PHAEOCYSTIS ANTARCTICA IN A WATER TRANSECT FROM SOUTH AMERICA TO SOUTH AFRICA**

Juliane Mondzech, Franziska Jurisch, Sarah Agirgöl, Steffi Gäbler (not on board)
Alfred-Wegener-Institut (AWI), Bremerhaven

Objectives

The biological programme of the cruise was supported by the bathymetry working group. The main aim of the programme was to collect water samples containing *Phaeocystis antarctica* from different locations in the Antarctic region. Here we had the opportunity to take samples in the Antarctic Circumpolar Current (ACC), the Weddell Sea, partly Lazarev Sea, on the transit between Neumayer and Prydz Bay, in Prydz Bay and on the transit to Kerguelen Islands.

These samples are needed to establish new cultures from isolates of *P. antarctica* to estimate the genetic diversity of this polar prymnesiophyte in the Antarctic region. The cosmopolitan and ecologically important genus *Phaeocystis* contains two colony-forming cold water species, *P. pouchetii* in the Arctic and *P. antarctica* in the Antarctic. First results about their genetic diversity have been obtained by molecular biological analyses, showing substantial inter- and intraspecific diversity and first attempts have been made to trace the biogeographical history of strains in Antarctic coastal waters. To gain deeper insights into the population structure and bloom dynamics of this microalga, it is necessary to quantify the genetic diversity within populations of *P. antarctica* (Lange et al. 1997, 2002; Medlin et al. 1994). Two methods are used to quantify the genetic diversity in algae blooms of different locations: AFLPs and microsatellites.

Work at Sea

The surface water samples were usually taken by using a normal bucket and in times of rough sea a so called snorkel (description see report Christina L. De La Rocha, Eleni Anagnostou, Christian Schlosser). The water samples were filled into 250 ml culture flasks which already contained 125 ml GP5 media (Loeblich & Smith, 1968). To allow the phytoplankton to develop, the flasks were stored in a lab container at 0° to 2° C with a day/night rhythm.

Overall 121 samples were taken for the above mentioned project. The last 26 samples were taken for scientific interest only, since the temperature scale suitable for the micro algae wanted was already too high. Water samples and stations are shown in figure 10.1 and table A.5.3 in the appendix.

The samples stayed onboard during transit to Bremerhaven and stored in the ship born cooling room at 3° C, also with a 12 hours day/night rhythm.

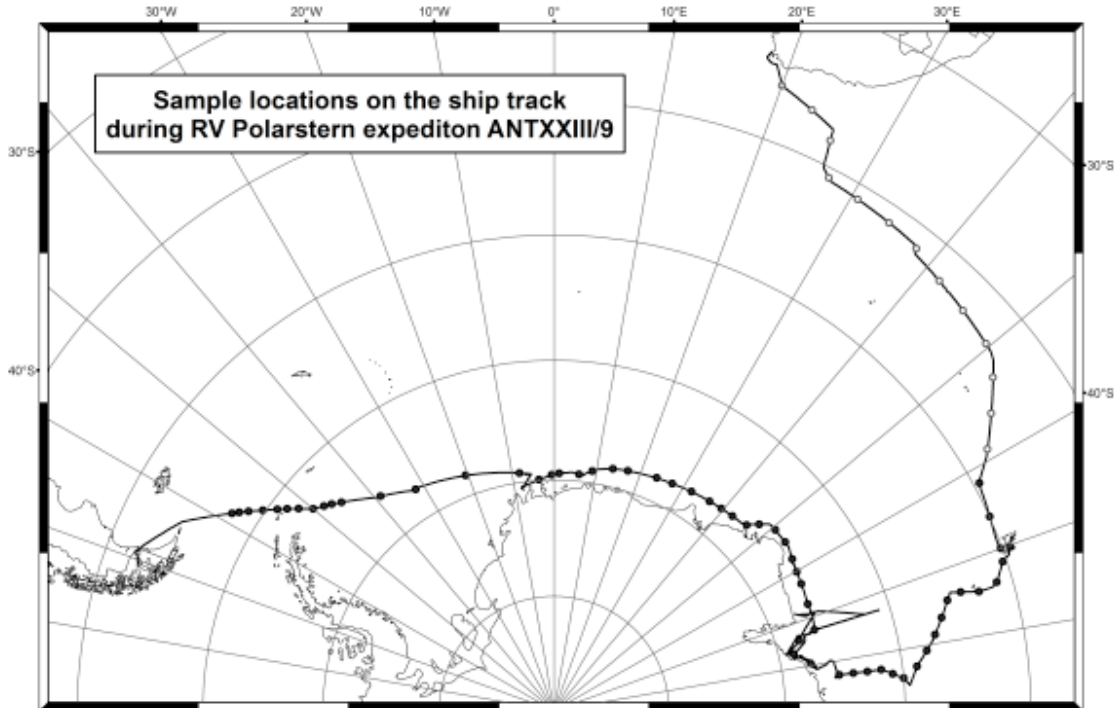


Fig. 10.1: Map of sampling stations

References

- Lange, M. (1997). Molecular genetic investigation within the genus *Phaeocystis* (Prymnesiophyceae). PhD dissertation, University of Bremen, Germany.
- Lange M, Chen Y, Medlin LK (2002), Molecular genetic delineation of *Phaeocystis* species (Prymnesiophyceae) using coding and non-coding regions of nuclear and plastid genomes. *European Journal of Phycology*, **37**, 77-92
- Loeblich AR, Smith VE (1968) Chloroplast pigments of the marine dinoflagellate *Gymnodinium resplendens*. *Lipids* 3: 3-15.
- Medlin, L.K., Lange, M. & Baumann, M.E.M. (1994). Genetic differentiation among three colony-forming species of *Phaeocystis*: further evidence for the phylogeny of the Prymnesiophyta. *Phycologia*, **33**: 199±212.

11. HIGH RESOLUTION BATHYMETRY OF THE PRYDZ BAY AND THE SOUTHERN OCEAN

Juliane Mondzech, Franziska Jurisch, Sarah Agirgöl
Alfred-Wegener-Institut (AWI), Bremerhaven

Objectives

The main objective of the bathymetry working programme was to perform high resolution surveys with the multibeam sonar system Hydrosweep DS2 to support the geological and geophysical working groups by providing precise depth information and bathymetry charts of their research areas. Moreover, the gathering of bathymetric data in Prydz Bay and surroundings is very important because very little high-resolution bathymetric data exists so far for this area.

Depth data have been recorded and processed on board continuously after *Polarstern* left the exclusive economic zone of Argentina on 4 February. These data will be delivered to the International Hydrographic Organisation (IHO) to improve international bathymetric charts. Furthermore, these data will be a valuable contribution to the existing charts GEBCO (General Bathymetric Chart of the Ocean) and IBCSO (International Bathymetric Chart of the Southern Ocean).

Work at sea

The depth measurements were performed using Atlas Hydrosweep DS2, a deep-sea multibeam echo sounding system permanently installed on *Polarstern*. Most of the time, Hydrosweep was operated with a fan aperture of 90°. In this case, with one measurement the sonar system produces a depth profile with 59 depth points and a length of 2 times the water depth.

The measurement accuracy of Hydrosweep DS2 ranges between 0.5 and 1 % water depth. To ensure long-term accuracy, the knowledge of the precise water sound velocity is required to convert travel time into depths. Hydrosweep DS2 has the possibility to calculate the mean sound velocity accomplishing a cross fan calibration. Eight CTD measurements have been carried out in order to achieve best accuracy of depths. The locations of the CTD measurements are shown in Fig. 11.1.

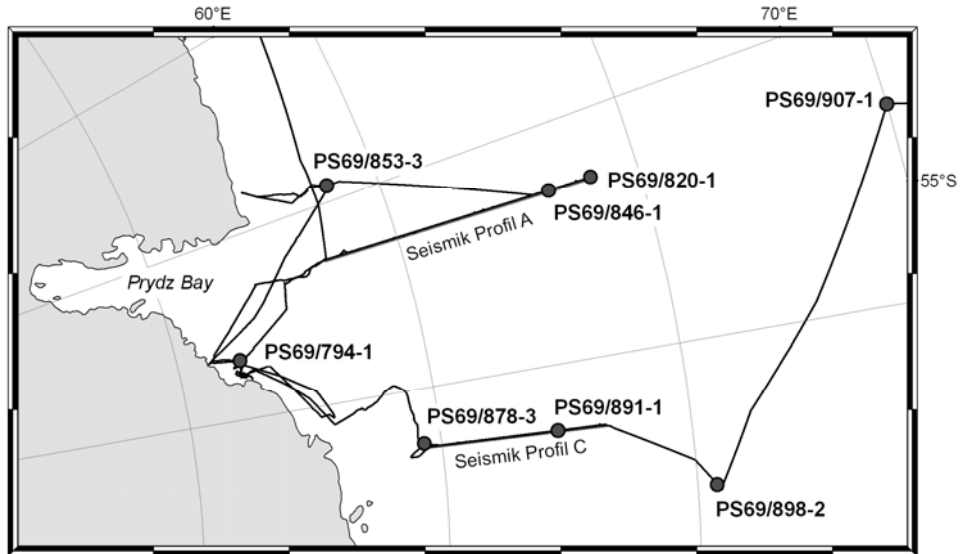


Fig. 11.1: Overview of applied CTD measurements

Whales could be sighted several times during this cruise (Fig. 11.2). To prevent the disturbance of marine mammals the multibeam sonar system was switched off during stations, when there was no scientific necessity for surveying the seafloor. If operation of the multibeam sonar system was necessary during stations, whale watching was conducted. If whales came closer to the ship nearer than 100 m, hydrosweep was switched off till they left this zone. The multibeam sonar system was started in soft start modus after a switch off period of more than an hour. In soft start mode the source level is controlled over 20 minutes in 10 steps from 207 dB to 239 dB.

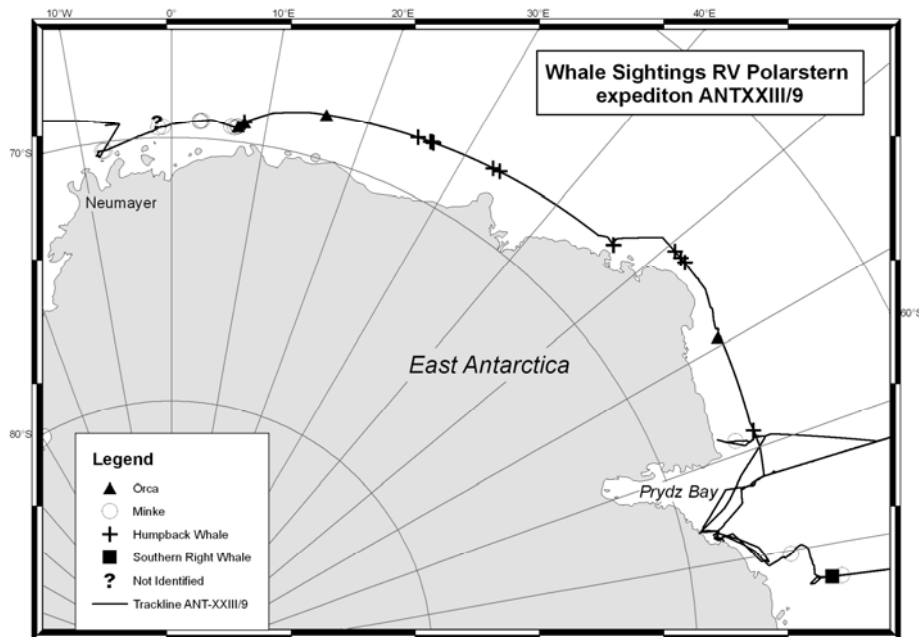


Fig. 11.2: Locations of whale sightings

Beside operating and observing the multibeam sonar system, the data processing was a main part of the work carried out on board. Erroneous depth measurements caused by random, systematic and rough errors need to be cleaned. Using CARIS HIPS & SIPS software about 8 % of raw data have been marked manually to be incorrect and were rejected for further processing.

Within ice-covered areas and in bad weather conditions, the value of rejected beams increased up to 26 %. In such cases, it is difficult to interpret the morphology of the sea floor. An example of such a disturbed profile measured during the cruise through ice-covered areas is shown in figure 11.3.

After data cleaning, the bathymetric data were converted for further processing and archiving. For the interpretation of the seafloor topography, digital elevation models were calculated and presented in preliminary bathymetric maps, using the Generic Mapping Tool (GMT).

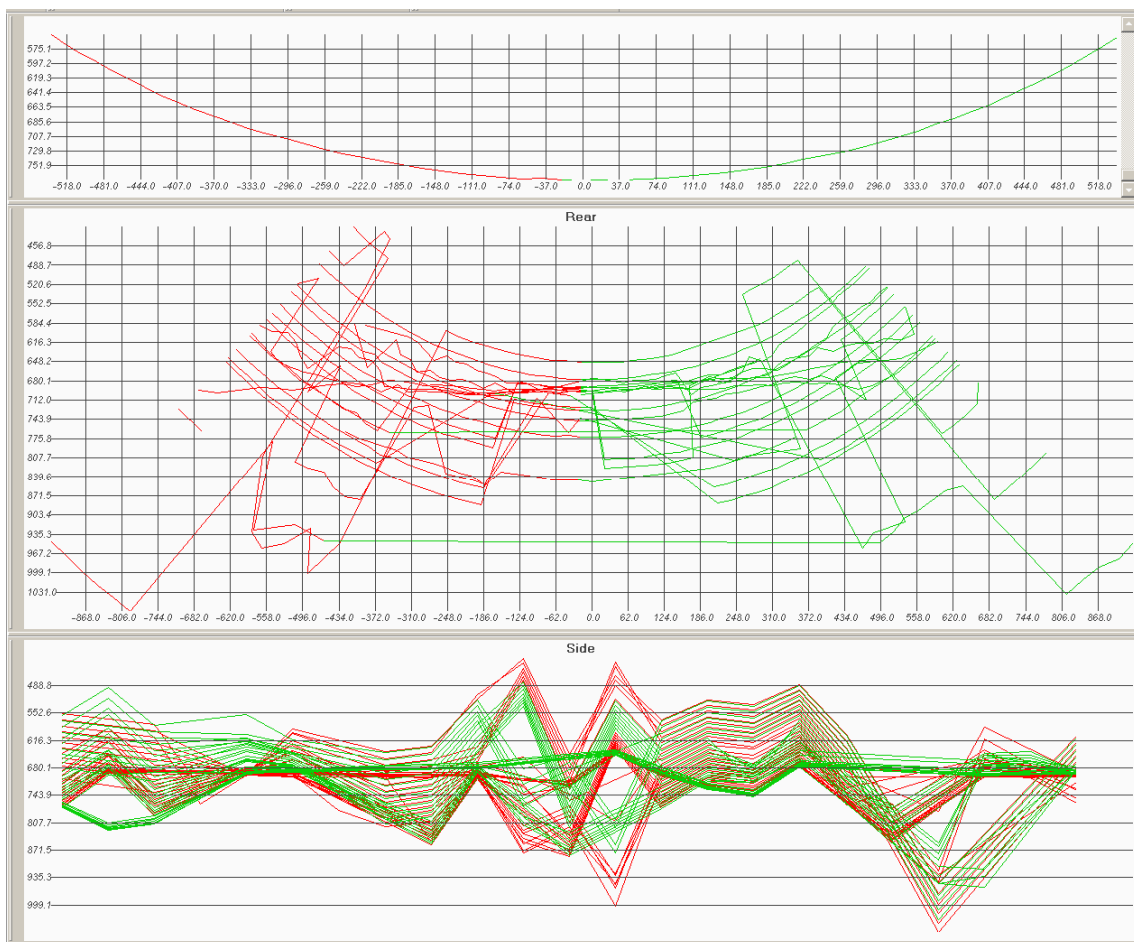


Fig. 11.3: Erroneous depth measurements caused of sea ice

Results

During the whole leg ANT-XXIII/9 bathymetric data were measured and recorded continuously. Apart from small areas in Prydz Bay and covered areas for the search of geological stations, no systematic bathymetric survey with parallel lines was carried out.

On board data processing showed differing seafloor structures in comparison to the existing GEBCO (2003) global data. Using the General Mapping Tool bathymetric charts have been generated based on terrain models that combine GEBCO and recent multibeam data.

In peripheral areas of the Kerguelen Plateau an interesting submarine structure was recorded. This structure is differently displayed in the GEBCO data (Fig. 11.4). The surveyed feature shows a significantly different morphology and a larger height of about 300 m than in the global data sets.

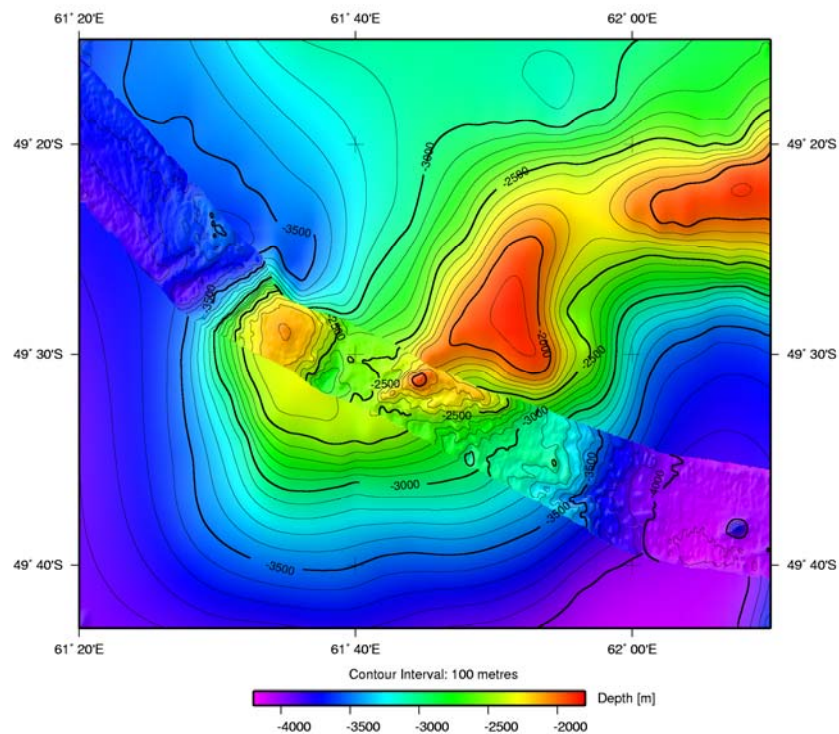


Fig. 11.4: Differences between the GEBCO data and the recent multibeam data

In the Southwest Indian Ridge a seamount was discovered which was previously unknown (Fig. 11.5). It is located in a water depth of about 2,900 metres and is more than 1,350 m high. This seamount has a spatial extend of 9,400 m and the diameter of the crater is about 700 m. This crater like structure suggests a volcanic origin.

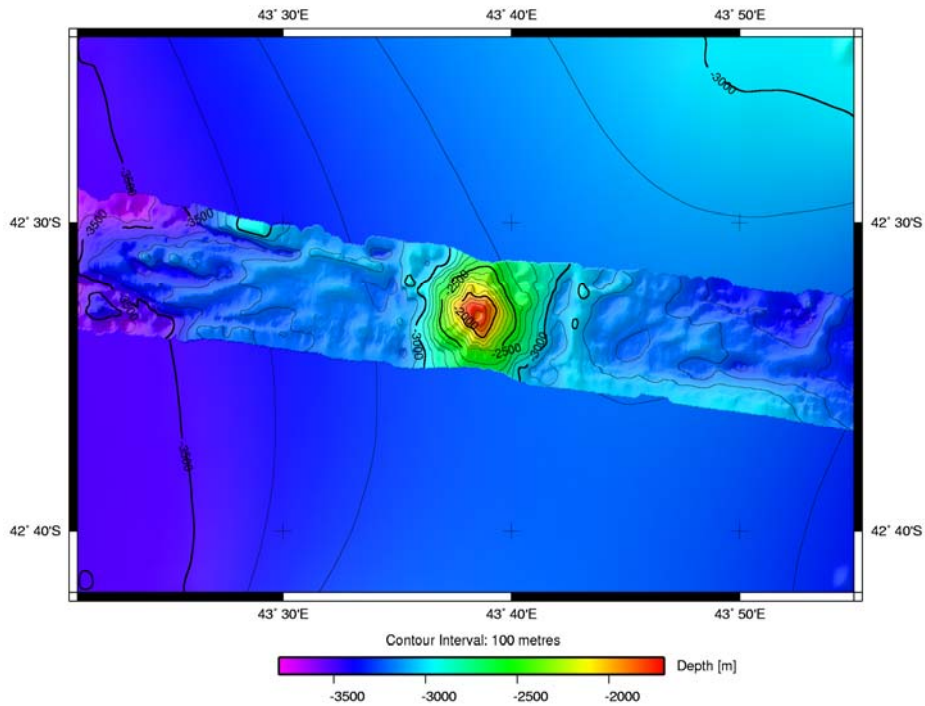


Fig. 11.5: Previously unknown seamount on the Southwest Indian Ridge

This unknown seamount at 42°32,59'S 43°38,37'E will be reported to the International Hydrographic Organisation. According to the guidelines of the GEBCO Sub-Committee on Undersea Feature Names (SCUFN) a name will be suggested for this discovered seamount. In agreement with all participants of this expedition the name proposed is *IPY-Seamount* because *Polarstern* returned from an 18 month long expedition just as the International Polar Year (IPY) begins.

12. LATE QUATERNARY ENVIRONMENTAL HISTORY OF THE RAUER GROUP, PRYDZ BAY REGION, AS DEDUCED FROM LAKE AND MARINE BASIN SEDIMENTS

Bernd Wagner¹⁾, Ole Benneke²⁾,
Sonja Berg¹⁾, Michael Fritz³⁾,
Olaf Klatt⁴⁾, Martin Klug¹⁾,
Katharina Muhle⁴⁾, Sabrina
Ortlepp¹⁾, Hendrik Vogel¹⁾,
Duanne White⁵⁾

¹⁾ University of Cologne, Institute for
Geology and Mineralogy, Cologne
²⁾ Geological survey of Denmark and
Greenland (GEUS), Copenhagen, Denmark
³⁾ Ernst-Moritz-Arndt University of Greifs-
wald (EMAU)
⁴⁾ Alfred-Wegener-Institut (AWI), Bremerha-
ven
⁵⁾ Macquarie University, Dept. of Physical
Geography, Australia

Martin Melles¹⁾ (not on board)

Objectives

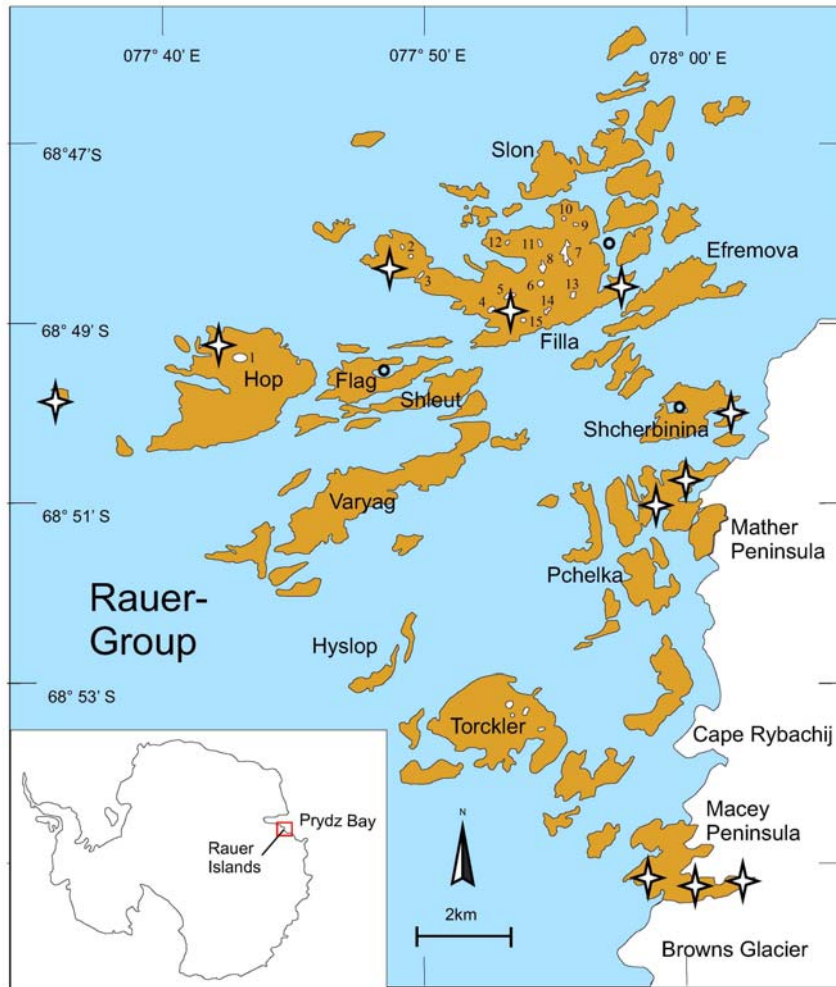
Paleoclimatological and paleoenvironmental investigations in currently ice-free coastal areas (oases) of Antarctica function as a crucial link between investigations on the adjacent Antarctic Ice Sheet and the Southern Ocean. From the oases, comprehensive information can be obtained on the natural variability of the local ice sheet extension, ice sheet altitude, climate, and relative sea level. A detailed reconstruction of these variabilities throughout the recent geological past, allowing the identification of their interdependencies is a precondition for a thorough understanding of ice-sheet stability during future climate changes.

Dating of the timing of the last deglaciation and reconstructions of the climate history, and the relative sea-level changes in the oases around Prydz Bay indicate a high variability in this region, which is supported by investigations of marine records and ice core records from East Antarctica. The Rauer Group, located between the Vestfold Hills and the Larsemann Hills in the south-eastern Prydz Bay region (Fig. 12.1), may provide crucial information about which of the extant reconstructions reflect more local or regional influences.

The Rauer Group is a coastal archipelago of ice-free islands and skerries (or rocks), which cover an area of ca. 300 km². They consist of low hills with a maximum altitude of 137 m a.s.l. The Precambrian gneiss bedrock is partly overlain by glacial, marine, and eolian sediments of Late Pleistocene and Holocene age. Climate records do not exist from Rauer Islands, but the climate is likely similar to that recorded at the nearby Australian Davis Station 30 km to the north. There, the monthly mean temperatures range from 0.5 to -18.0° C.

The annual mean cloud cover is 60 % and there are only ca. 60 days per year with more than 1 mm precipitation. The relatively dry climate is the result of dominating dry katabatic winds from the ice sheet. Snowfall occurs throughout the year, but ablation or melting means that the islands are essentially snow-free in summer. The fauna in the Rauer Group is dominated by birds, mainly skuas and Adélie penguins, with the latter occurring particularly in the outer parts. Seals are sporadically observed along the shorelines. The flora of the islands is comparatively rich, consisting mainly of microbial mats in littoral zones of depressions, mosses at places, which are moist from melting snow, and a few lichens on rocks.

For a better understanding of the paleoglaciology, the relative sea-level history, and the paleoclimatology of the Rauer Group, comprehensive fieldwork including the recovery of sediment sequences from lakes and marine basins and of rock samples for exposure dating was carried out. The main working area was on and around Filla Island, which is the largest island of the Rauer Group and located in its central northern part (Fig. 12.1). Filla Island has a number of lake basins, which had, however, dried out at the end of austral summer 2006/07. Those basins, which had some water, were brackish to hypersaline. There are several marine basins around Filla Island, which likely contain long and relatively undisturbed sediment sequences. However, only some of these basins were accessible during the field season, since the sea around Filla Island, particularly towards the east, was partly covered by ice of various ages, including thin new ice. Therefore, in addition to a marine basin east of Filla Island, two basins near Flag Island and near Shcherbinina Island were selected for the recovery of marine sediment sequences. Helicopter support from the *Polarstern* and the Australian Antarctic Division enabled the transfer of the coring equipment between the coring locations. Rock samples for exposure dating were recovered from several islands in the Rauer Group with varying distance to the present ice-sheet margin. Shell samples were collected from raised marine and littoral deposits, as well as a few samples of bones.



- ★ cosmogenic samples
- coring site

- | | | |
|-------------------|----------------|---------------------|
| 1 Big Hop Lake | 6 Shell Lake | 11 Lagoon Lake |
| 2 Penguin Lakes | 7 Skua Lake | 12 Bronze Lake |
| 3 Shallow Channel | 8 Big Lake | 13 Skua Lake |
| 4 Aquamarin Lake | 9 Mud Lake | 14 Fork Valley Lake |
| 5 Desert Lake | 10 Hidden Lake | 15 Big Rock Lake |

Fig. 12.1: Map of Rauer Group with its location in the south-eastern Prydz Bay (insert). Sampled lakes are indicated by numbers. Coring sites in marine basins are marked by black circles. Stars indicate cosmogenic sampling sites.

Field work & preliminary results

Lake sediment coring

Hendrik Vogel¹⁾, Ole Bennike²⁾,
Sabrina Ortlepp¹⁾

¹⁾ University of Cologne, Institute for Geology
and Mineralogy, Cologne

²⁾ Geological survey of Denmark and Greenland
(GEUS), Copenhagen, Denmark

Overall 25 sediment cores were recovered from 10 lake basins using various coring techniques. Nine of the lake basins were situated on Filla Island, and one on Hop Island (Fig. 12.1, Tab. 12.1).

Prior to coring, water samples were collected from lakes, which were not completely dried out. Hydrological measurements were carried out using a multi-parameter probe (WTW 197), but hypersaline lakes were excluded from the measurements to avoid damaging the probe. During the period of sampling most lakes had low water levels or were dried out. Brackish water lakes were ice covered, whereas hypersaline lakes were ice free.

Indications of seasonal lake level fluctuations were observed at all lake basins, in the form of water level marks at 20 - 30 cm above the present lake level. We also noted that snow fall on 7 March led to a ca. 5 cm increase in lake level in several basins.

Most of the sediment cores were collected using the spade coring technique (SCT). A hole was dug with a spade, and near the hole two PVC-liner halves were pressed into the sediment. The liners were then taped together above the sediment surface and dug out carefully in order to avoid disturbance of the sediment. Other cores were sampled using an Eijkelkamp corer, an Eijkelkamp Russian peat corer with a 0.5 m long chamber, a 2 m long Eijkelkamp piston corer or PVC liners. In the dried-out lake basins the thickness of the active layer was 80 - 100 cm. Further penetration was inhibited by permafrost.

Aquamarine Lake (Fig. 12.2) is situated in the south-western part of Filla Island. The lake surface is situated 1.0 m below the present sea level. The lake occupies the south-western part of the basin and has a maximum depth of 1.2 m within small circular depressions. An alluvial fan is found in the north-eastern part of the basin. Up to 3 cm thick salt crusts on the lake bottom and along the present shoreline are indicators for the hypersaline character of Aquamarine Lake. Two sediment sequences (Co1005-1, -2) were recovered. One core was taken from the south-western, water covered part of the lake using an Eijkelkamp corer. This core was sub-sampled in the field at 1 cm intervals. Another core was sampled near the western shore line using the SCT. The sampled sediments consisted of sand and were dark in colour. The sediments recovered near the shoreline also consisted of medium sand but had a light brown colour and a greenish horizon at ca. 10 cm depth.

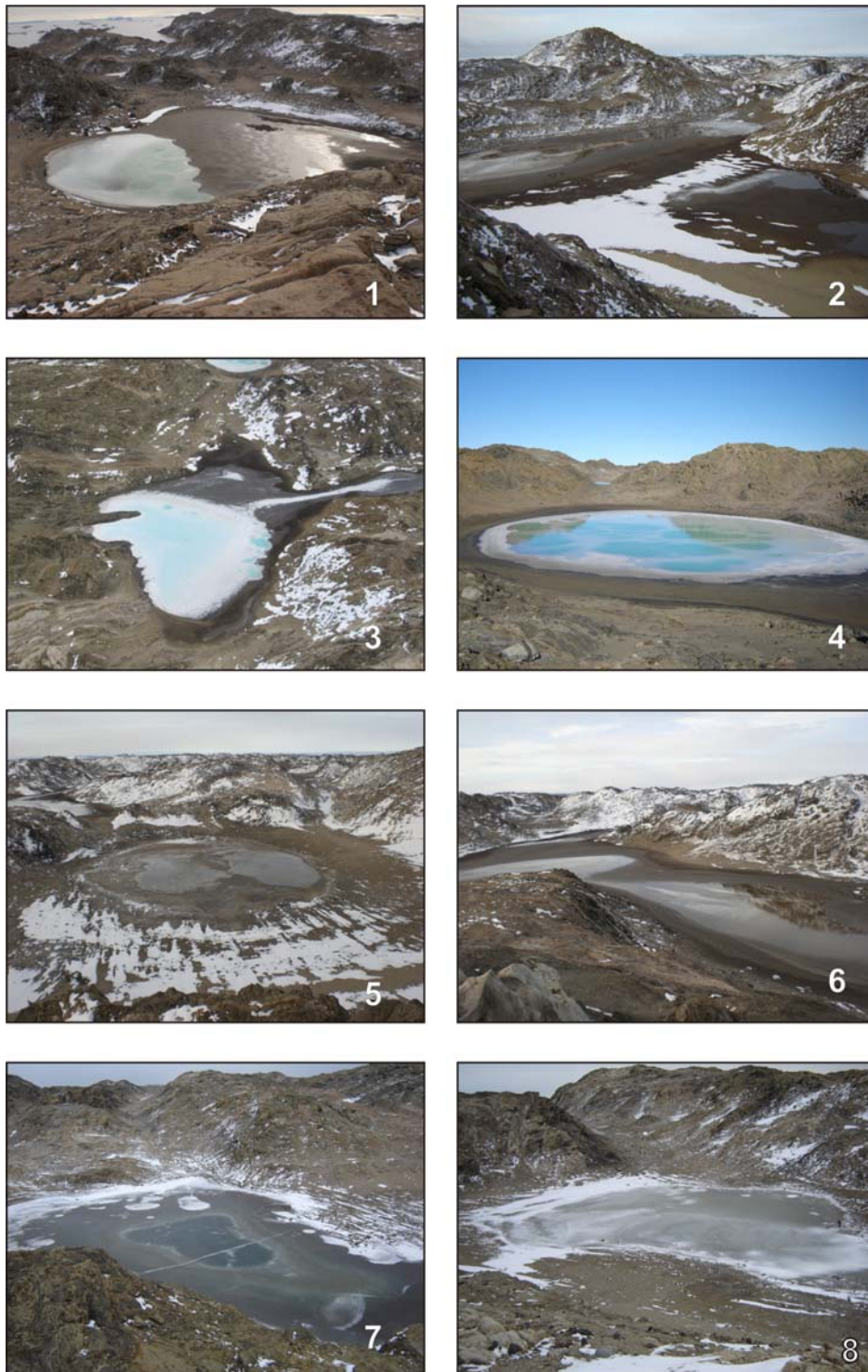


Fig. 12.2: Photos of selected lakes on Filla Island. 1 Aquamarine Lake, 2 Desert Lake, 3 Dead Seal Lake, 4 Lagoon Lake, 5 Shell Lake, 6 Big Lake, 7 Skua Lake, 8 Fork Valley Lake (Photos taken by H. Vogel, S. Ortlepp and L. Ganzert)

Desert Lake (Fig. 12.2) is located in the southern part of Filla Island. The present lake surface is situated 1.5 m a.s.l. and covered at the date of coring a small area of ca. 20 x 20 m in the north-western part of the basin. Here water was covered by a 2 - 3 cm thick salt crust, which indicated the hypersaline

character of the lake. Three sediment cores (Co1000-1, -2, -3) of up to 80 cm lengths were recovered by SCT from a location ca. 10 m south of the extant lake. The sediments consisted of medium sand. The topmost 2 cm of the cores included a red redox layer. Below the redox layer to a depth of about 30 cm a black organic rich horizon was observed. From 30 cm to the core basis relatively homogenous light brown sandy sediments were found.

Shell Lake (Fig. 12.2) is situated in central Filla Island at an elevation of 5.7 m a.s.l. The lake was completely evaporated at the period of sampling. The basin has a circular shape. Three sediment cores (Co1007-1, -2, -3) of 50 cm lengths were taken at the former southern shoreline using an Eijkelkamp Russian peat corer. The topmost 15 cm of the sediment core consist of layered medium grained, light grey to light brown sand. Between 15 and 19 cm the sediment becomes slightly darker in colour and at 19 cm a sharp transition to dark grey and stiff sand with abundant shell fragments occurs.

Dead Seal Lake (Fig. 12.2) is situated in the central part of Filla Island at an elevation of 2.5 m a.s.l. The lake bottom and the shoreline were covered by up to 3 cm thick salt crusts, which is a clear indication of hypersaline conditions. Within the basin small sub-basins with diameters ranging from 1 to 2 m and a maximum depth of 1 m are found. Two 50 cm long sediment cores (Co1015-1, -2) were recovered from the northern, dried out part of the lake using the SCT. The sediment consisted of medium grained sand.

Lagoon Lake (Fig. 12.2) is situated in the northern part of Filla Island at an elevation of 1.2 m a.s.l. The lake has a roughly circular shape. Salt crusts of up to 3 cm in thickness are present along the shoreline and on the lake bottom. Within the water covered part of the basin some smaller depressions of about 1 2 m in diameter and water depths of ca. 1 m occur. One sediment core (Co1009-1) was sampled from the northern, dried out part of the lake basin using SCT. The sediments consist of medium grained sand.

Big Lake (Fig. 12.2) is situated in the north-eastern part of Filla Island. The lake was completely dried out at the period of sampling. The elevation was 3.1 m a.s.l. at the lowest depression of the basin. Salt crusts were present along the former shoreline. Two sediment cores (Co1003-1, -2) with lengths of 80 and 70 cm, respectively, were sampled by SCT in the northern sub-basin. The sediments consisted of medium sand with a redox layer on top and a black organic rich horizon below the redox layer. A second redox layer was found at 60 cm and underlain by dark, organic rich sediments with interspersed grey horizons.

Skua Lake (Fig. 12.2) is situated in the south-eastern part of Filla Island at an elevation of 9.4 m a.s.l. Most of the lake is around 30 cm deep, but in the central part a 120 cm deep basin with steep slopes is found. The shoreline and the shallow areas are covered with red microbial mats. The lake had an 8.5 cm thick ice cover during the period of sampling. The conductivity of 20.1 mS/cm indicates brackish to saline water. The pH value was 8.46 and the oxygen saturation in the surface waters just below the ice cover was 61.9 % (8.91 mg/l).

Six sediment cores (Co1008-1, -2, -3, -4, -5, -6) were taken from the ice surface in the deepest part of the basin. Co1008-1 and -2 with a length of 34 and 33 cm, respectively, were sampled using an Eijkelkamp Russian peat corer. Co1008-3, -4, -5, and -6 were recovered using an Eijkelkamp piston corer. Co1008-3, -4, and -5 include the sediment water interface and reach down to depths of 62, 127, and 153 cm, respectively. The piston of core Co1008-6 was released in 100 cm sediment depth and the coring tube penetrated down to 231 cm sediment depth. Core Co1008-3 was opened in the field. The sediments are dark to light grey in colour and consist mainly of medium to fine grained sand. The sediment is layered with distinct changes in colour and grain size. Distinct layers with gypsum crystals up to 1 cm in diameter were found in the upper 62 cm and probably indicate former evaporation periods. A distinct smell, similar to that of crude oil, was remarked.

Fork Valley Lake (Fig. 12.2) is situated in the southern part of Filla Island at an elevation of 6.6 m a.s.l. The lake has a maximum water depth of only 34 cm and its bottom is covered with brown microbial mats. The waters, taken from directly below the 7.5 cm thick ice cover, had a conductivity of 54.8 mS/cm at the date of sampling, a pH value of 8.4, and an oxygen saturation of 63.2 % (9.09 mg/l). Three sediment cores (Co1013-1, -2, -3) were recovered from the ice in the western part of the lake. Co1013-1 and -2 were sampled using an Eijkelkamp Russian peat corer and reached a sediment depth of 46 and 50 cm, respectively. Co1013-3 was sampled using an Eijkelkamp piston corer and reached a depth of 25 cm. The sediments mainly consist of sandy material. Light brownish sediment in the upper 20 cm is underlain by black coloured more cohesive material containing shell fragments. The sediments show several laminations, such as resulting from redox layers and horizons of enriched gypsum crystals.

Bronze Lake is situated in the north-western part of Filla Island at an elevation of approximately 15 m a.s.l. The lake was up to 15 cm deep and covered by ice with 2 cm thickness. The lake bottom is covered by red microbial mats. The conductivity was 76.8 mS/cm indicating hypersaline waters. The pH value was 8.35 and the oxygen saturation reached 58.9 %. Sediment samples were not recovered from this lake.

Mud Lake is situated in the northern part of Filla Island at an elevation of approximately 15 m a.s.l. The lake was almost completely dried out, but a remnant had a water depth of 10 cm. The lake bottom and the wet shoreline were covered by brown microbial mats. The conductivity of 166.3 mS/cm indicated hypersaline conditions. The pH value was 8.37 and the oxygen saturation was 63 % (9.12 mg/l). Sediment samples were not recovered from this lake.

Hidden Lake is situated in the northern part of Filla Island at an elevation of around 30 m a.s.l. At the date of sampling Hidden Lake consisted of two sub-basins, which were separated by a ca. 15 m wide dried out plain. The northern basin had a maximum water depth of 30 cm and the southern basin was 18 cm deep. Both were covered by 8 cm thick ice. The conductivity was 27.2 mS/cm,

corresponding with brackish to saline water. The pH value was 8.27 and the oxygen saturation reached 47 % (6.64 mg/l). The shoreline was densely covered with dried out, red microbial mats. These mats also cover the bottom of the northern and the southern basin. Two sediment cores were taken from ice using a PVC liner, a 20 cm long core (Co1006-1) from the northern basin and a 25 cm long core (Co1006-2) from the southern basin. Both cores showed red microbial mats on the top and dark organic rich sediments down to a depth of 15 cm. Below 15 cm light grey diamictos were found.

Big Hop Lake is situated on Hop Island at an elevation of around 1 m a.s.l. The lake was completely dried out at the date of sampling. Large shell fragments of the bivalve *Laternula elliptica* were common on the sediment surface. One sediment core (Co1009-1) covering the uppermost 60 cm was sampled from the central part of the basin. The sediment consisted of light brown, homogenous medium grained sand with shell fragments.

The occurrence of apparently marine sediments containing calcareous marine macrofossils in the sediment sequences from Shell Lake and Fork Valley Lake implies that information about past sea-level changes can be obtained by the study of the lake sediment sequences from Filla Island. The elevations of Shell Lake and Fork Valley Lake implies a similar relative sea level history for the Rauer Group as reconstructed for the Vestfold and Larsemann Hills close by, where the maximum relative sea level during the Holocene was 8-9 m above the present sea level (Verleyen et al. 2005). Furthermore, the existence of redox layers and evaporation horizons indicates that the sediment sequences recovered can provide valuable information about paleoenvironmental changes.

Levelling of lakes, sills, and terraces

Sabrina Ortlepp¹⁾, Katharina Muhle²⁾, Duane White³⁾

¹⁾ University of Cologne, Institute for Geology and Mineralogy, Cologne

²⁾ Alfred-Wegener-Institut (AWI), Bremerhaven

³⁾ Macquarie University, Dept. of Physical Geography, Australia

Levelling of lakes, sills, and terraces was carried out on Filla Island in order to reconstruct lake and sea level changes that likely occurred during the Holocene. Measurements were performed in the main valleys, starting from the sea level at the high tide marks and using a surveying instrument (Leica Corp.) and a staff of 5 m in height. Since most lakes on Filla Island had low water levels or were completely evaporated during the field campaign, either the present sediment surface at evaporated basins or the present lake level at basins filled with water were measured for levelling of the lakes. Additional measurements were taken from former lake level highstands, such as indicated by ancient shorelines. Low-lying areas in the west and the southeast of Filla Island, which contained *in-situ Laternula Elliptica* shells and thus were affected by a Holocene marine transgression, were levelled more in detail along cross-cutting profiles (Fig. 12.3).

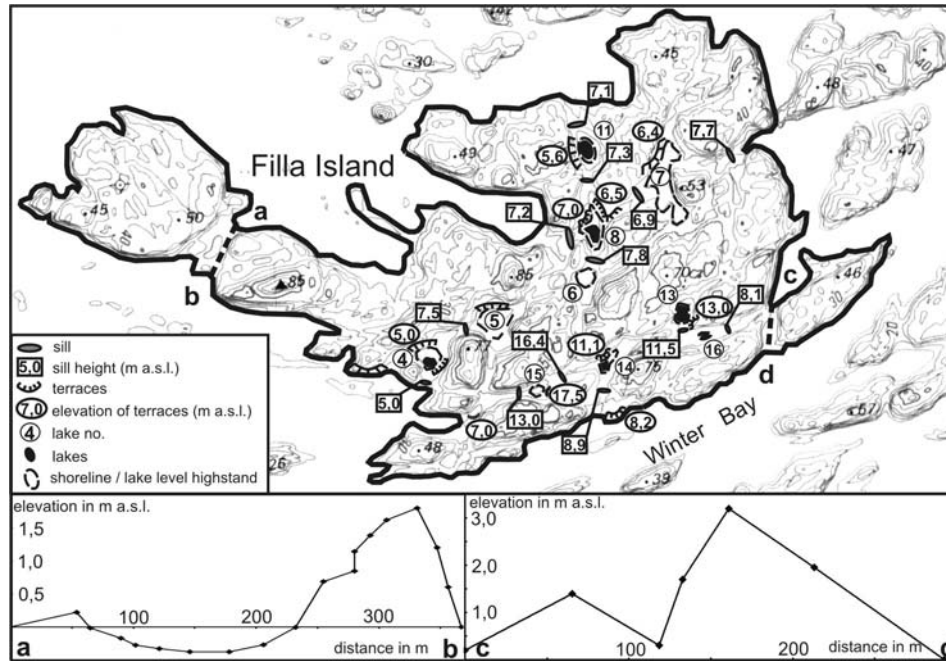


Fig. 12.3: Lake levels and elevations of geomorphological features on Filla Island (map based on Topographical map of the Rauer Group 1:50000; Australian Antarctic Division, 1992)

Coring in marine basins

Bernd Wagner¹⁾, Sonja Berg¹⁾, Michael Fritz²⁾, Olaf Klatt³⁾, Martin Klug¹⁾

¹⁾ University of Cologne, Institute for Geology and Mineralogy, Cologne

²⁾ Ernst-Moritz-Arndt University of Greifswald (EMAU)

³⁾ Alfred-Wegener-Institut (AWI), Bremerhaven

Three marine basins in the Rauer Group were selected according to geomorphological features, water depth, and accessibility in order to obtain long and undisturbed sediment sequences for paleoglaciological and paleoenvironmental reconstructions. The basins were characterized by relatively low water depths, the existence of subaquatic sills separating the basins from the sea, and by a good accessibility, i.e. open water or ice cover of at least 60 cm thickness.

Coring was carried out using gravity and piston corer (both UWITEC Corp., Austria), which were successfully deployed during former expeditions and are in detail described in Wagner (2003).

The first basin selected, here named Romeo Basin, is located east of Filla Island and was covered by ice of ca. 1 m thickness. The water depth in the centre of Romeo Basin, measured by echosounder through a hole in the ice cover, was 38 m. The basin is separated by two sills of 16 and 18 m water depths, respectively, from the sea to the east and by another sill emerging ca. 0.5 m a.s.l. from the adjacent basin to the north. Tidal hub in Romeo Basin was indicated by the angle of ice floes at the shore line and amounted to less than ca. 50 cm.

12. Late Quaternary environmental history of the Rauer Group, Prydz Bay region, as deduced from lake and marine basin sediments

Hydrological measurements along a vertical profile prior to the beginning of the coring process in the centre of Romeo basin were carried out using a water sampler and a WTW Multi 197 probe (WTW Corp., Germany). The measurements revealed temperatures between -0.7 and -1.8° C (Fig. 12.4), and oxygen depletion in the bottom waters. The pH ranges between 7.8 and 9.8 and has its maximum at 15 m water depth, which probably corresponds with a horizon of slightly enhanced productivity. The specific conductivity increases from 32.9 mS/cm in the surface waters to 51.5 mS/cm in the bottom waters. The high conductivity and the oxygen depletion in the lower part of the water column are probably the result of restricted water exchange between the basin and the sea. They also imply lack of bioturbation in the sediment and that the sediments are sapropelic.

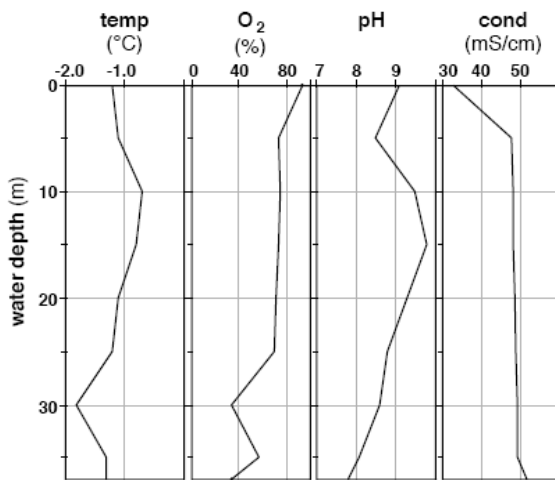


Fig. 12.4: Hydrological profile measured at the coring location in Romeo Basin

Coring in Romeo Basin was carried out between 1 and 8 March. The surface sediments recovered were extremely soft and of gelatinous consistency, and were almost exclusively formed by organic matter. The colour of the sediments was dark greenish to black. An intense smell of H₂S matched the observation of extensive gas formation, particularly in the surface sediment cores, and confirmed that the sediments were sapropelic. With increasing sediment depth, the sediments became dryer and less gas formation occurred. However, remarkable changes in sediment composition and colour were not observed until ca. 20 m sediment depth. From ca. 20 to 22 m sand of greyish colour dominated the sediment composition. Below this horizon, the sediment sequence again was composed of greenish organic sediments, which were, however, very dry and compacted. The coring stopped at 23.32 m sediment depth, when no further penetration was possible.

The second basin selected is located at the northern part of Flag Island (Fig. 12.1). This basin was not ice-covered and is characterized by a maximum water depth of 8 m and a sill height of 4 m below present sea level. The difference between high tide and low tide was determined by observations of the shoreline and amounts ca. 1 m. Since easterly to north-easterly winds prevailed during the complete field season and the outlet opens towards this direction, we assume complete mixture of the water column.

Sediment coring in this basin was carried out from a floating platform between 10 and 13 March. The sediments recovered consisted mainly of organic matter with dark greenish colour. The basis of the sediment sequences, from ca. 10.40 to 10.99 m, was formed by greyish diamicton. Further penetration was not possible.

The third basin selected for coring is located at western Shcherbinina Island. On 15 March, when coring was carried out, the western part of the basin was ice-covered and not accessible. Coring took place at the ice margin, where a water depth of 6.3 m was measured. Tidal hub is assumed to be about 1 m. The sill at the outlet of the basin was very shallow, indicated by several rocks, which evolved above present sea level during the low tide. Hydrological measurements did not take place, but we assume that the water column was completely mixed due to the low water depth. Three gravity cores and three piston cores were recovered from this basin. The cores had a maximum penetration of 2.62 m into the sediment. Further penetration was hampered by technical problems and owing to lack of time.

Geomorphology and Glacial History of the Rauer Group

Duane White¹⁾, Ole Bennike²⁾

¹⁾ Macquarie University, Dept. of Physical Geography, Australia

²⁾ Geological survey of Denmark and Greenland (GEUS), Copenhagen, Denmark

The extent of former glacial overriding across the islands was reconstructed by evaluating the distribution and character of erratics, glacial diamicts and small scale glacial bedforms such as striae and chattermarks. Most of the islands in the northern section of the Rauer Group were investigated through land-based traverses during the three week field campaign. While selected land traverses were carried out in the south, the majority of the observations in the southern section were conducted from boat and helicopter traverses (Fig. 12.5).

12. Late Quaternary environmental history of the Rauer Group, Prydz Bay region, as deduced from lake and marine basin sediments

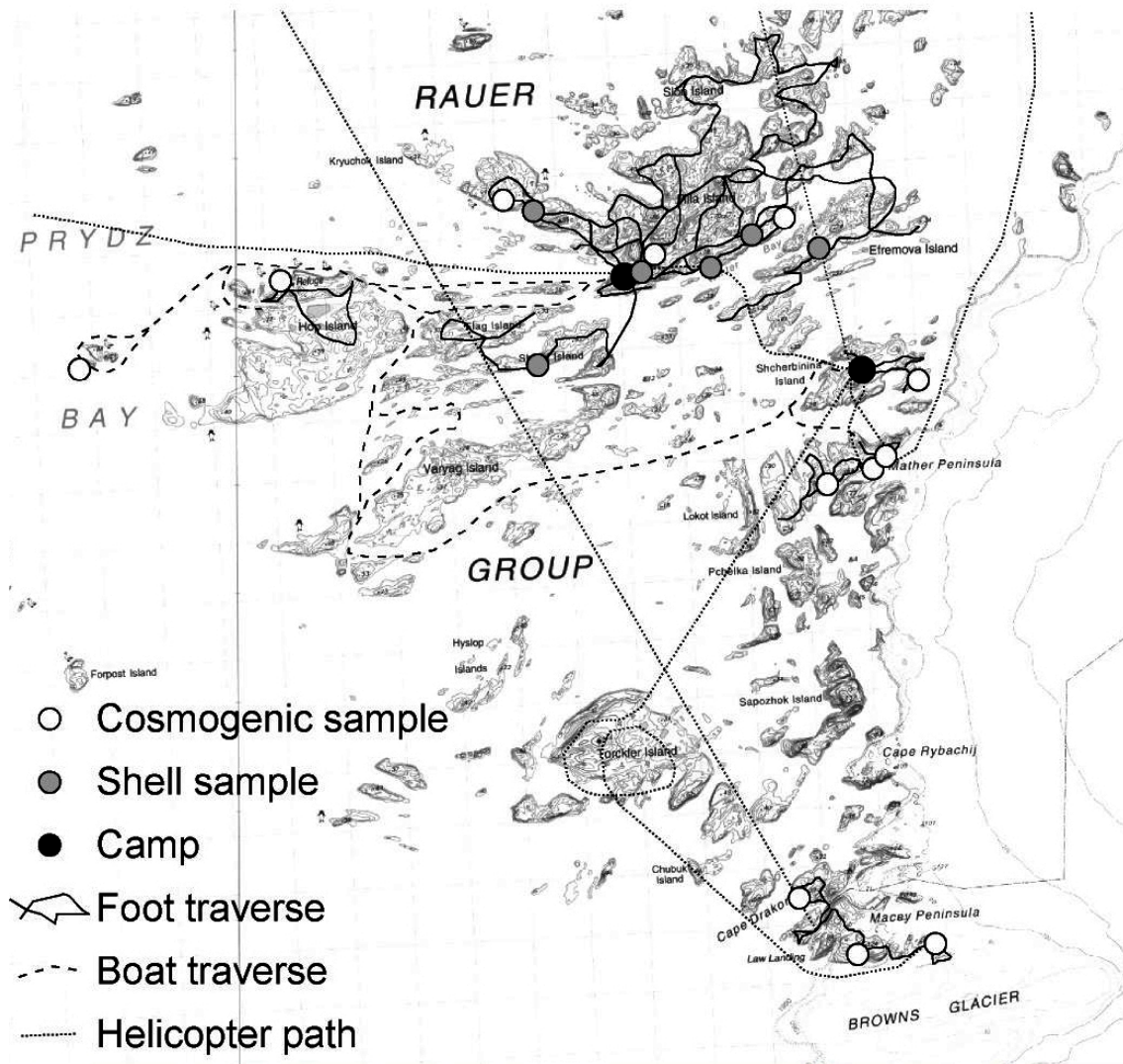


Fig. 12.5: Location of traverse tracks and sample sites

The weathering characteristics of glacial sediments deposited above the marine highstand were mapped to constrain the extent and relative timing of former glacial advances. To provide a semi-quantitative age for each deposit, the Moriwaki index (Moriwaki et al. 1994), and a Schmidt Hammer (Shakesby et al. 2006) were used. The effect of different styles of weathering and different weathering regimes on these data was estimated by recording whether characteristic markers of different weathering styles, namely whether surface features including tafoni, elongated pits, halite accumulations, glacial polish, striae, Fe staining, patterned ground, frost shattered debris, wind polish, sand accumulations and crumbled rock were absent, present or abundant at each site.

Samples for cosmogenic exposure age determinations were collected to provide an absolute timing for the events identified through mapping of the sediment distribution and weathering. As most of the glacial debris more than 1 km from the modern ice margin were extremely weathered, it is unlikely that the degree of surface weathering is sensitive enough to determine the subtle

features of the ice-sheet retreat history across the larger part of the islands (White 2007). Thus, subglacial erratics were collected for cosmogenic exposure dating from summits along a roughly equal spacing along an east-west transect across the central part of the islands. Closer to the present ice-sheet margin, samples were collected from the distinct weathering zones identified. Bedrock samples were also collected to determine how much erosion, if any, occurred during glacial overriding and thus the thermal properties of the ice during these events.

Most of the islands have roche moutonee forms consistent with significant modification by overriding of the ice sheet. Within the islands themselves, the valleys are largely structurally controlled, mostly formed along less resistant paragneisses. Areas of orthogneiss, such as Torckler Island, Hop Island, and the eastern parts of Macey and Mather peninsulas form the highest summits and plateaus, while regions composed of layered gneiss form a mid-point between these extremes.

Quaternary sediments are widely distributed across the islands. Most of these deposits are found in the valleys, and are marine, littoral or glacimarine in character. These deposits are particularly common below the marine limit, and were formed when the relative sea level was higher than at the present. Distinct accumulations of terrestrial glacial deposits are rare, but when present usually take the form of small debris drapes in saddles or high basins. Erratics were found on all the large and also many of the small islands, including the most distal island visited, ~15 km from the present ice edge.

Small sand dunes are common in the lee of bedrock obstacles, or downwind of narrow gaps in valleys. These accumulations were particularly large and abundant on the downwind side of the islands, and also downwind of former marine areas. Quaternary sediments in general, and glacial sediments in particular, are less abundant on the windward side of the islands.

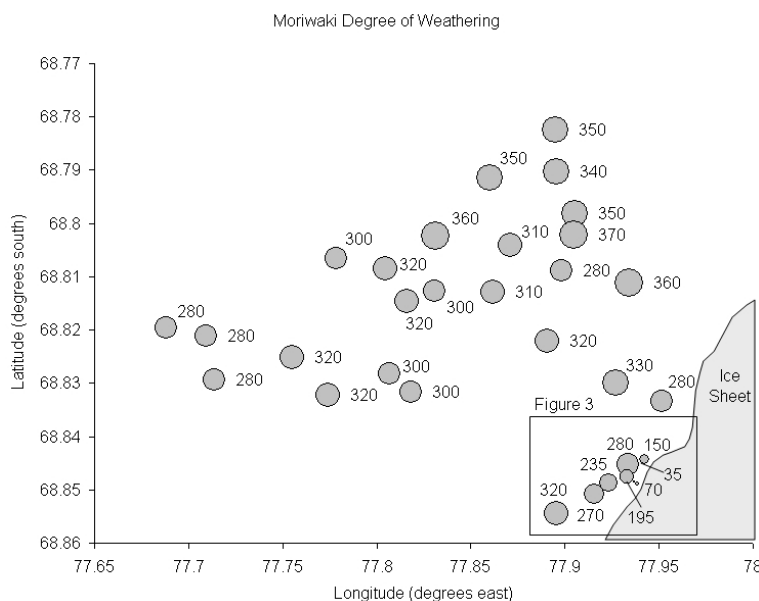


Fig. 12.6: Moriwaki (1994) degree of weathering values across the northern Rauer Islands. Note the lightly weathered deposits close to the ice sheet (shown in detail in Fig. 12.7) and the general increase in index values on the windward portion of the islands.

12. Late Quaternary environmental history of the Rauer Group, Prydz Bay region, as deduced from lake and marine basin sediments

The least weathered glacial deposits are from ice cored moraines within a few hundred meters of the modern ice-sheet margin (Figs 12.6 and 12.7). Next are a group of moderately weathered moraines and erratics within 1 km of the ice margin, which have weathering values consistent with values from Holocene moraines in the Bunger Hills (Augustinus 2002). Lastly, strongly weathered diamict and erratics are present on the remainder of the islands. Within the area not directly downwind of a source of marine salts (including areas below the marine limit), the bedrock surface retains a strong glacial morphology, and patches of striae and glacial polish are occasionally preserved.

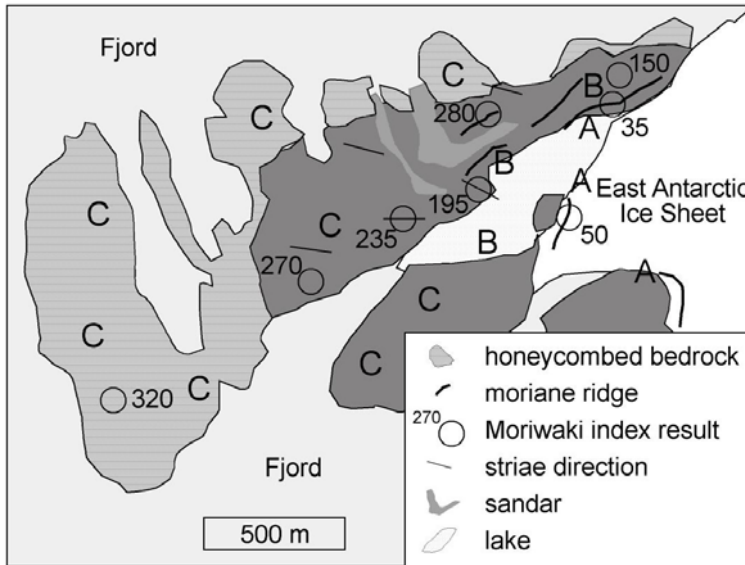


Fig. 12.7: Weathering, moraines and striae directions on Mather Peninsula. A: fresh glacial deposits, B: moderately weathered deposits, C: highly weathered deposits. Note that the areas of honeycomb weathering of bedrock are all downwind of marine salt sources.

However, outside this area the bedrock is highly weathered, with honeycomb weathering present and differential weathering of over one meter common in some places. This difference is likely due to the increased weathering rate seen in areas of abundant marine salts. This inference is reinforced by the general increase in the Moriwaki Index towards the windward side of the islands, perhaps reflecting the influence of increased salt abundance, wind speed, or both in these outer areas.

Tab. 12.1: Elevations of selected lakes on Filla Island (for numbers see Fig. 12.1)

no.	lake	present lake level / lake bottom (m a.s.l.)	lake highstand / shoreline (m a.s.l.)
4	Aquamarin Lake	-1,0	-0,6
5	Desert Lake	1,5	1,9
6	Shell Lake	5,7	5,9
7	Big Lake	3,1	3,3
8	Dead Seal Lake	2,5	2,9
11	Lagoon Lake	1,2	1,4
13	Skua Lake	9,4	9,8
14	Fork Valley Lake	6,6	6,8
15	Big Rock Lake	11,8	/
16	small lake near Skua Lake	2,9	3,2

References

- Augustinus, P.C., 2002. Weathering characteristics of the glacial drifts, Bunge Hills, east Antarctica. *Arctic Antarctic and Alpine Research*, 34: 65-75.
- Moriwaki, K., Iwata, S., Matsuoka, N., Hasegawa, H. and Hirakawa, K., 1994. Weathering stage as a relative age of till in the central Sør-Rondane. *Proceedings of the NIPR Symposium on Antarctic Geoscience*, 7: 156-161.
- Shakesby, R.A., Matthews, J.A., Owen, G., 2006. The Schmidt hammer as a relative-age dating tool and its potential for calibrated-age dating in Holocene glaciated environments *Quaternary Science Reviews*, 25: 2846-2867.
- Verleyen, E., Hodgson, D.A., Milne, G.A., Sabbe, K., Vyvermann, W., 2005. Relative sea-level history from the Lambert Glacier region, East Antarctica, and its relation to deglaciation and Holocene glacier readvance. *Quaternary Research*, 63: 45-52.
- Wagner, B. 2003. The expeditions Amery Oasis, East Antarctica, 2001/02 and Taylor Valley, southern Victoria Land, 2002. *Reports on Polar and Marine Research*, 460: 69 pp.
- White, D., 2007. Cenozoic Glacial History and Landscape Evolution of Mac.Robertson Land and the Lambert Glacier-Amery Ice Shelf System, East Antarctica, Ph.D thesis, Department of Physical Geography, Macquarie University, Australia, pp. 168.

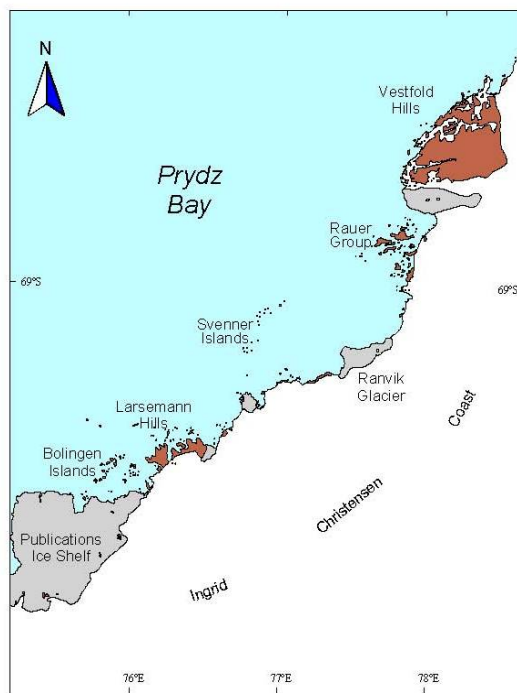
13. FUNCTIONAL MICROBIAL DIVERSITY IN EXTREME ANTARCTIC HABITATS: ABUNDANCE, PHYLOGENY AND ECOLOGY

Lars Ganzert¹, Antje Eulenburg¹, Christina Miller², Dirk Wagner¹

¹) Alfred-Wegener-Institut (AWI), Potsdam
²) Alfred-Wegener-Institut (AWI), Bremerhaven

Objectives

Within the scope of the project, the diversity and ecology of microbial communities and their function in nutrient turnover under extreme conditions in Antarctic periglacial regions will be studied. Polar regions are vast and unique natural laboratories, both because of their geographical isolation and the minor anthropogenic influences active there, for studying microbial life under extreme environmental conditions. For this purpose the diversity and abundance of the microflora in dependence of important site characteristics such as hydrological, thermal and weathering processes will be investigated in different habitats in ice-free areas on Larsemann Hills and Rauer Islands (Prydz Bay, Antarctica, Fig. 13.1 and 13.2).



Universal Mercator Projection Zone 43

0 10 20 30 Kilometers

Fig. 13.1.: Map of the Prydz Bay area (Australian Antarctic Data Center, modified)

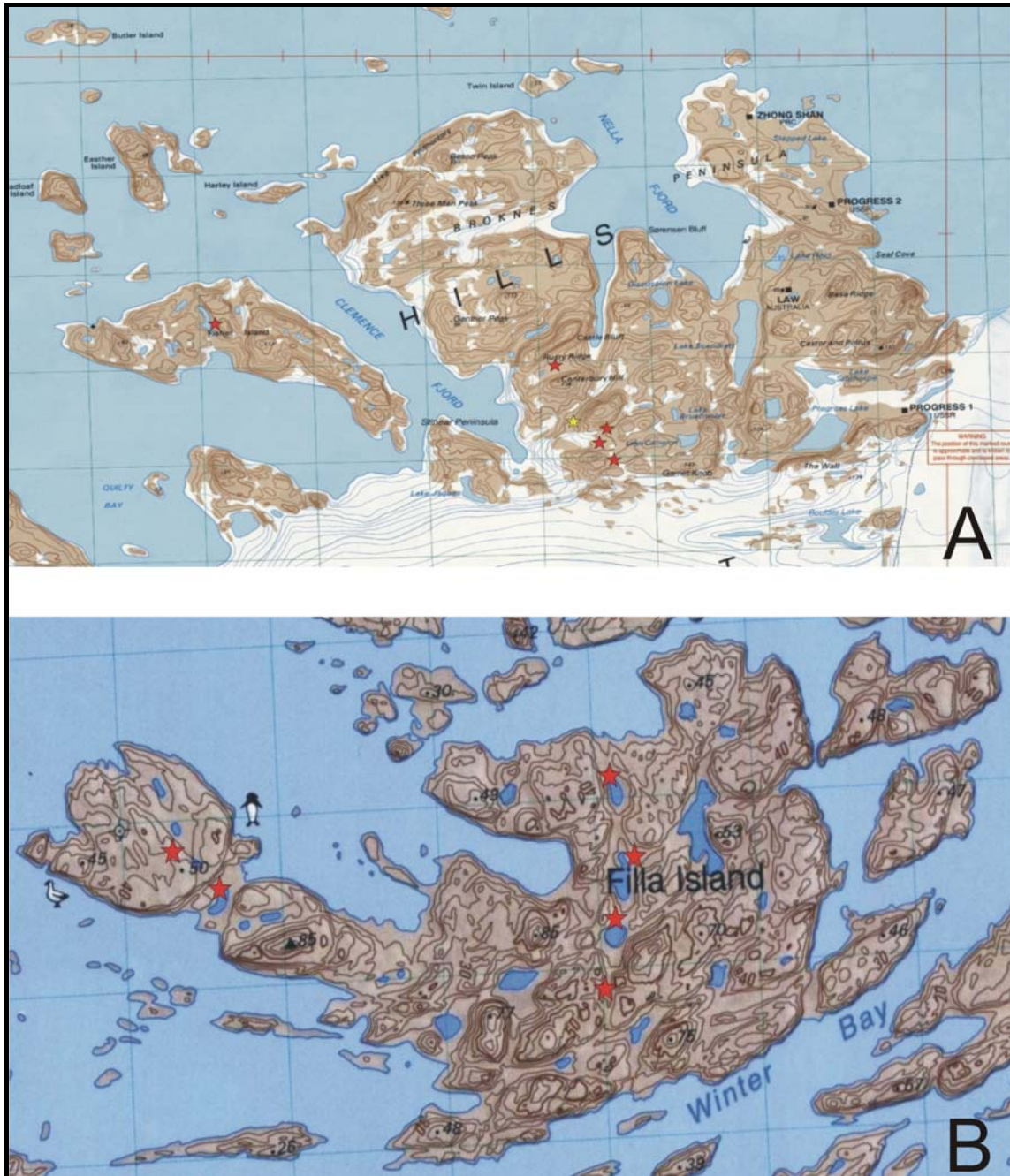


Fig. 13.2: Maps of the investigation sites (Australian Antarctic Data Center, modified). A – Larsemann Hills, B – Filla Island; red stars mark the main sampling sites, the yellow star marks the camp site.

The main objectives are the genotypic and phenotypic characterization of the microbial community by cultivation-independent methods such as lipid profiling and rRNA-based analyses and by physiological characterization of isolated microorganisms. Stable isotope probing will be used to identify the main microbial players in nutrient turnover in the different environments.

The scientific investigations will concentrate on the following goals:

- Soil chemical and physical characterization of the investigation sites regarding microbial life under extreme environmental conditions,
- Cultivation-independent characterization of microbial communities to improve the knowledge of the abundance and biodiversity of the indigenous microflora,
- Understanding of the structure and function relationships of microbial communities in nutrient fluxes in polar habitats.

Field work

The field work on Broknes Peninsula (Larsemann Hills) begun at the end of February with reconnaissance of potential study sites. Sampling of sediments started at March 1 on Broknes Peninsula and was continued on Filla Island (Rauer Group) on 14 March, 2007.

Altogether 36 sediment profiles were excavated, described and 106 samples were taken from defined layers for physico-chemical and microbiological analyses. In addition, 36 surface samples and 2 sediment cores were taken from sites that differ in habitat properties (Fig. 13.3 and 13.4).

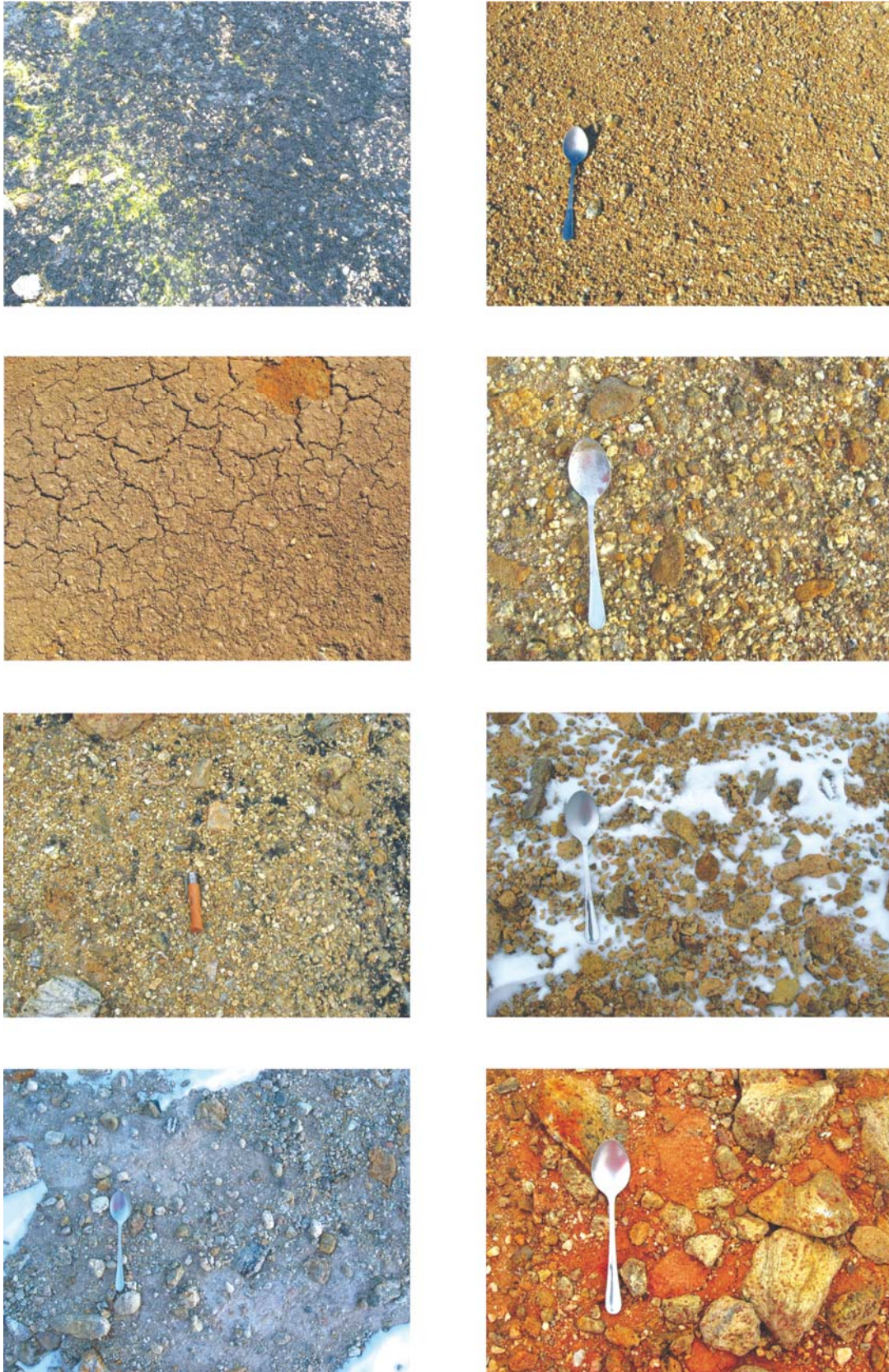


Fig. 13.3: Examples of study sites for sampling of sediments in the Larsemann Hills (photos L. Ganzert)



Fig. 13.4: Study sites on Filla Island (Rauer Group, photos L. Ganzert)

The samples for microbiological analyses were placed in 250 ml sterile Nalgene boxes and have been immediately frozen. Sample transport at -25°C was provided by *Polarstern* from the Prydz Bay area (Antarctica) to Bremerhaven (Germany).

The main study sites in the Larsemann Hills as well as on Filla Island (Rauer Group) were characterized by a marine influenced continental climate which leads to intensive physical weathering processes. No soil formation could be observed in the working area. In certain valleys the presence of large algal

and bacterial mats showed that there must be flowing water during the summer promoting primitive life under these extreme environmental conditions.

During our work in the Larsemann Hills a field lab was established for measuring pH and conductivity and for extracting dissolved organic carbon (DOC) of altogether 89 samples from both the Larsemann Hills and Filla Island (Rauer Group). For the extraction 9 g of sediment material was weighed into 50 ml glass jars and 45 ml of deionized water was added. The suspension was shaken for 1 hour in the dark and filtered through a 45 µm nylon membrane. Measuring of pH and conductivity was done directly in the field whereas the DOC content will be measured in Germany.

Preliminary Results

The results of the pH and conductivity measurements showed differences between the profiles as well as within the depth of the profiles. The pH ranged from slightly acidic to alkaline in the Larsemann Hill sediments with values of pH 6 to 8.7. An exception with pH 4.9 was the upper horizon of a profile that was covered by a moss layer. The conductivity reached the highest values in the upper most layers and then decreased with increasing depth. Here, the values ranged from 4 to 1360 µS cm⁻¹ and the highest values were measured for surface layers. The reason for that could be ocean spray which will be transported into the valleys by storm winds. The results of Filla Island differed from those on Larsemann Hills. Here, we took our samples along the shoreline of different salt lakes. The conductivity was extraordinary high with values of up to 89500 µS cm⁻¹ for the uppermost layer. In the following layers the conductivity was much more lower depending on the investigation site and it became stable throughout the profile. The pH was alkaline from 7.7 to 8.6.

Further investigations, that will be made in our home laboratory at the Alfred Wegener Institute for Polar and Marine Research in Potsdam, will be focused on the physical-chemical properties and on microbial communities of these sediment samples. Grain size, water content, carbon/ nitrogen/ sulphur (CNS), dissolved organic carbon (DOC) and ions (e.g. Na⁺, K⁺, Cl⁻, Fe²⁺) will be analyzed. Further, the structure and the function of the microbial communities will be studied by using molecular-ecological tools such as polymerase chain reaction (PCR), denaturing gradient gel electrophoresis (DGGE) and clone library analyses. Standard microbiological procedures such as plate counting and activity tests will be used to examine who are the main player in nutrient turnover in these cold habitats. Last but not least, the isolation and characterization of micro organisms will also be forced to learn more about how microbes are adapted to these harsh environmental conditions and to have the possibility to find new enzymes or microbial products that could be interesting for biotechnological use. An overview of the analyzes is given in figure 13.5.

13. Functional microbial diversity in extreme Antarctic habitats: abundance, phylogeny and ecology

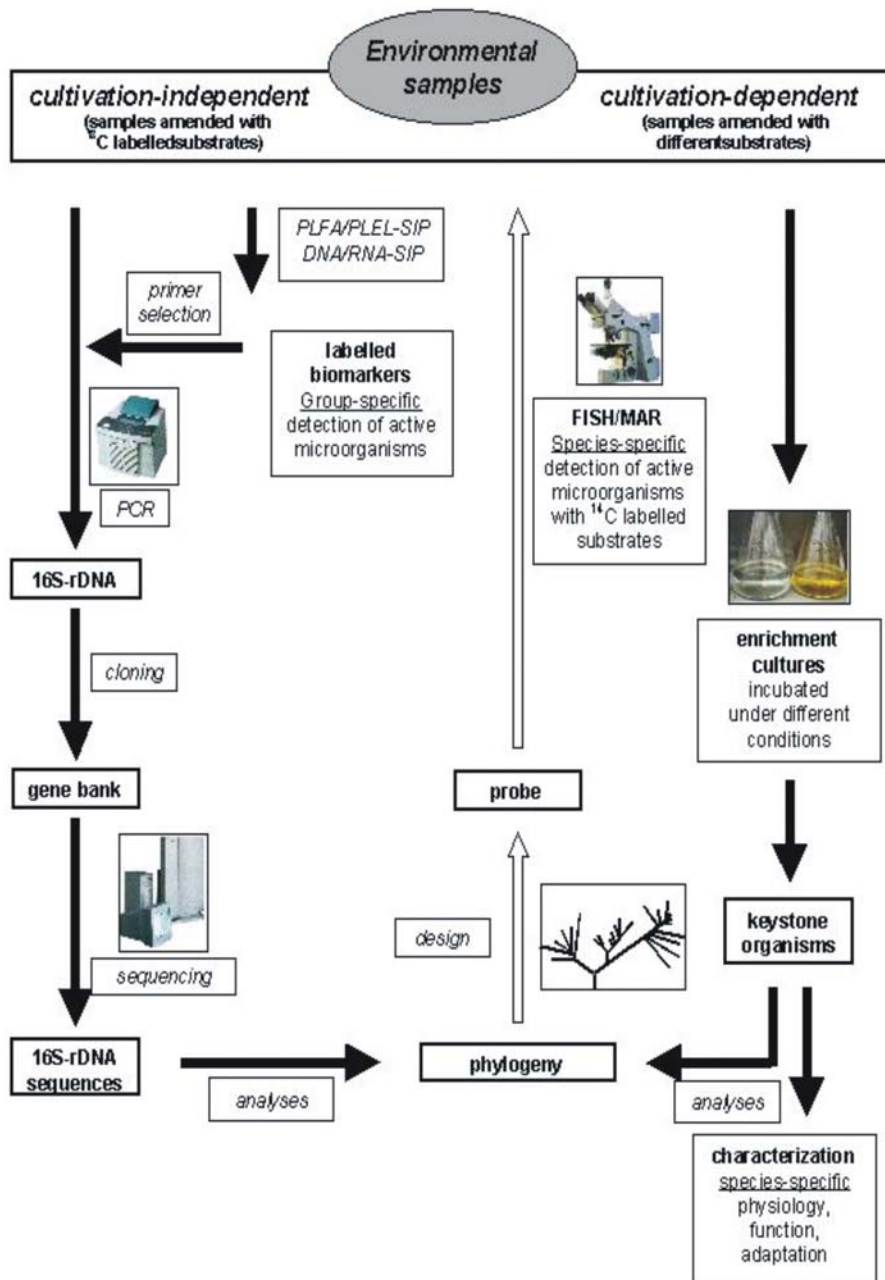


Fig. 13.5: Flow chart summarizing the approach for analyzing structure and function of microbial communities.

14. PETROLOGY OF PRYDZ BAY GRANULITES (Larsemann Hills and Rauer Islands)

Patrick J. O'Brien, Roland Oberhänsli
University of Potsdam, Institute for Geosciences (IGUP), Potsdam

Summary

A variety of granulite-facies metamorphic rocks were sampled from a number of locations from within the exposed Precambrian basement forming the islands and promontories of the Larsemann Hills and Rauer Islands. The main sampling locations from the Larsemann Hills were on Osmar and Fisher islands, and the Stornes, Broknes, Stinear and Brattnevet peninsulas. In the Rauer Islands most samples were from the Mather peninsula with additional material also collected from Filla Island. The main rocks collected were: cordierite-and garnet-rich pods in migmatitic gneisses, lenses of metapelite in migmatitic gneisses, magnetite-rich lenses in quartzo-feldspathic gneisses, B-rich mineral lenses with tourmaline and/or kornepupine, calc-silicate rocks, marble, mafic garnet-clinopyroxene granulites, orthopyroxene-rich gneisses and sapphirine-bearing metapelites.

Objectives

Granulite-facies metamorphic rocks from the Ingrid Christensen Coast of Prydz Bay (Vestfold Hills, Rauer Islands, Brattstrand Bluffs and Larsemann Hills) have been shown to have contrasting metamorphic histories with Archaean, Proterozoic and Pan-African components identified in different places. The region has evolved into a key area for interpreting the construction and destruction of the supercontinent Gondwana as well as the formation of the Antarctic continent itself. Important for constraining the contribution of different metamorphic episodes is a clear relationship between identifiable mineral assemblages yielding pressure-temperature information and minerals yielding ages. In addition, reliable pressure-temperature-time (PTt) paths must be determined in order to test the reliability of postulated isobaric cooling or isothermal decompression paths: paths which imply fundamentally different lithosphere-scale tectonometamorphic processes. For these reasons the aim of the field study was to identify and sample rocks with distinct macroscopically-visible reaction textures which will provide the basis for intensive petrographic and analytical studies to provide such reliable PTt-paths.

Field work & preliminary results

Larsemann Hills

The field campaign in the Larsemann Hills began with a four hour stop on Osmar Island (69°22.490'S 76° 01.022'E) followed by 26 hours on the northern part of Stornes Peninsula (camp: 69°24.308'S 76°07.206'E) before transferring to the Broknes Peninsula (camp: 69°24.081'S 76°19.794'E) (Fig. 14.1). The area is characterised by NE-SW-trending, steep-sided hills and ridges around 100 - 150 m in height rising above a flat platform at around the 50 - 70 m level and incised by NE-SW trending, lake-bearing valleys or roughly NS-trending fjords. Rocks of the hills and ridges are very well exposed (although heavily weathered) whereas much of the platform and lower ground is covered with gravel and boulders.

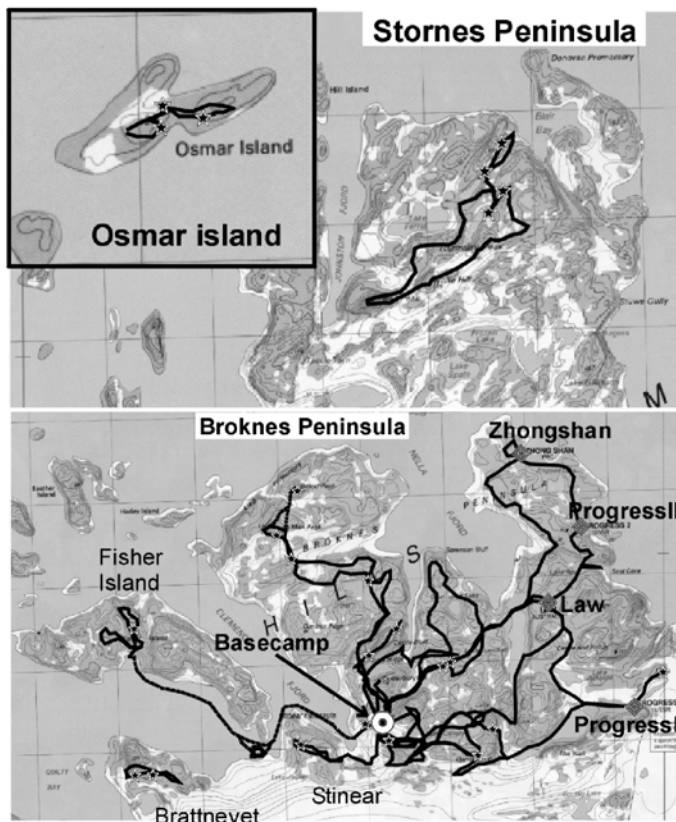


Fig. 14.1: Main routes followed, field camps and main sample locations (stars) in the Larsemann Hills

The ice-free islands and peninsulas of the Larsemann Hills are comprised mostly of multiply-deformed migmatitic semi-pelitic and pelitic gneisses along with less abundant meta-granitic bodies, several generations of pegmatites, and minor strongly-deformed metabasite layers. Partial melting of the precursor rocks has led to the formation of layered migmatites (Fig. 14.2A) or more commonly magmatic migmatites (Fig. 14.2B) or diatexites (Fig. 14.2C) where the amount of restite with residual foliation is small. Fragments of more mafic or restitic material (e.g. Fig. 14.2D) are common in some areas as folded lenses, boudins or blebs within the more quartzo-feldspathic parts of the outcrops.

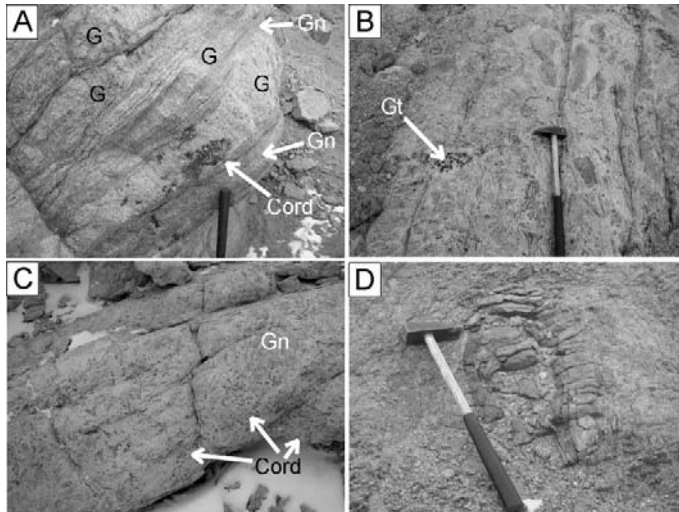


Fig. 14.2: Textural features of migmatic gneisses, Larsemann Hills. A) coarse granitic layers (G) with cm-sized cordierite blebs (Cord) in banded grey gneisses (Gn); B) disaggregated gneiss fragments swimming in melt with some cm-sized garnet (Gt) pods; C) patchy dark cordierite aggregates (Cord) in diatexite preserving only minor remnants of gneissic domains (Gn); D) isolated pod of mafic granulite in migmatic gneiss

Magmatic parts of the rocks commonly contain centimetre- to decimetre-sized aggregates of garnet and/or cordierite commonly also in symplectitic intergrowths with quartz (Fig. 14.3B, C). Many of the quartzo-feldspathic gneisses contain magnetite lenses and masses often several cm in thickness and extent.

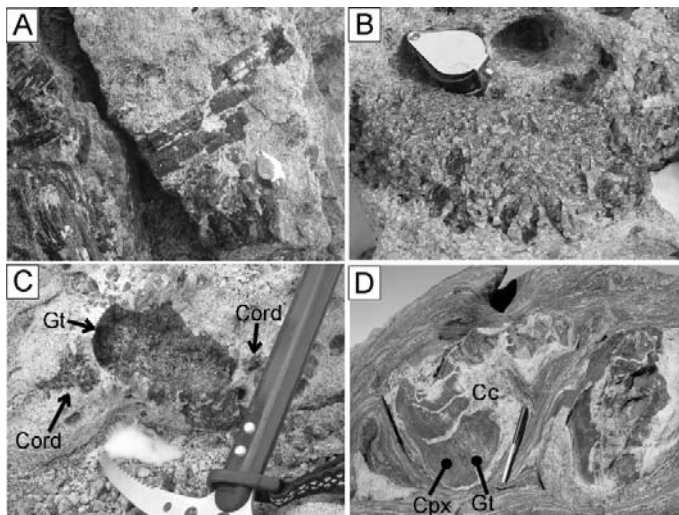


Fig. 14.3: Field photos showing mineralogical features. A) decimetre-sized tourmaline crystals from a B-rich horizon, Stornes; B) cordierite-quartz symplectite from an aluminous pelite band, Broknes; C) garnet-quartz symplectite, Stinear; D) massive garnet (Gt), clinopyroxene (Cpx) and calcite (Cc) from calc-silicate marble pods, Filla Island (Rauer)

Cordierite-rich aggregates were collected from Osmar and Fisher Island, as well as from the Stornes, Brattnevet, and Broknes (especially from Besso peak and SE side of Three Man Peak) peninsulas (Tab. 14). Garnet-rich aggregates were collected from Garnet Knob, Rusty Ridge and from the flat-lying area NE of Gentner Peak. The mechanical weathering of these garnet-rich rocks commonly leads to the formation of garnet sand. Most garnet is brownish red but on the northeast end of Rusty Ridge garnet weathered from pegmatite is very dark red and commonly exhibits stepped growth faces. Unusual yellowish edges were observed on some of these grains. Less common rock types in the Larsemann Hills are horizons extremely rich in tourmaline (and other B-rich minerals such as kornepine). These occur especially on Stornes (where several samples were collected) but also on Fisher Island and Brattnevet Peninsula (Tab. 14).

Rauer Islands

Fieldwork in the area of the Rauer Islands was conducted from *Polarstern* with daily transfer by helicopter (to Filla Island and Mather Peninsula: Fig. 14.4). Relative to the Larsemann Hills it is immediately noticeable in the outer islands that the hills are of lower elevation, valleys wider, lakes highly saline, and ground cover a much more rounded and finer-grained sand indicating a recent shallow marine (beach) environment. On Mather Peninsula widespread ice-scoured pavements were littered with erratics.

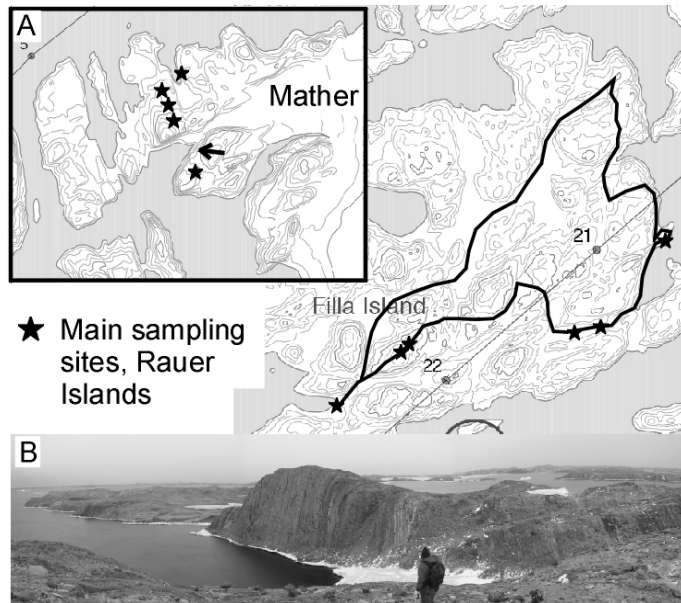


Fig. 14.4: Main routes and sample locations on Filla Island (main picture) and Mather Peninsula (inset A), Rauer Islands. B) View of Mather Peninsula showing steep orientation of main units and lithological contrast (view point and direction shown by arrow in 'A')

The Rauer Islands, dominantly composed of granulite-facies tonalitic orthogneisses intruded by several generations of mafic and ultramafic dykes, locally preserve metasedimentary cover units now represented by pelitic paragneisses, marbles and skarn rocks. These steeply-dipping, more variegated units (Fig. 14.4B) can be followed for several km despite isoclinal folding and boudinage. On Filla Island the paragneiss units trend NE-SW in the west of the island and swing around to run NNW-SSE in the east. Garnet-clinopyroxene (calc-silicate) rocks from this unit were collected. In addition, metabasic garnet-clinopyroxene granulites were sampled from small dykes and lenses. These latter rocks are potentially the best indicators for a high pressure granulite stage in the Rauer Islands. The paragneiss sequences on the Mather peninsula offer a greater variety of rock types including sapphirine-bearing metapelites, garnet+sillimanite-rich metapelites, garnet-orthopyroxene gneisses, orthopyroxene-bearing leucocratic gneisses, forsterite/scapolite/wollastonite-bearing marble, calc-silicate pods and even garnet-bearing quartzites. The sapphirine-bearing rocks, only present as boudinaged lenses a few cm wide and few metres long, exhibit macroscopically-visible reaction textures involving cm-sized sapphirine, garnet, cordierite and biotite grains and so provide highly suitable material for the planned reaction-domain thermodynamic modelling which is necessary to decipher the rock's PTt path. Mafic granulites from the same domain show development of very fine-grained

mm- to cm-wide coronas around cm-sized garnet indicating a clear reaction history relating to a low pressure overprint on a former high pressure assemblage.

Although the rock samples have been collected based on their macroscopically-visible reaction textures, the real test of their suitability for PTt-determination will come when they have been thin-sectioned and examined petrographically, geochemically and isotopically.

Tab. 14: Obtained rock samples

GPS coordinates	Location	Main material
<i>Larsemann</i>		
69°22.700'S 76°01.100'E	Osmar	Crd- & Mt-bearing mig.
69°22.429'S 76°01.186'E	Osmar	Massive Crd and Mt
69°24.200'S 76°06.785'E	Stornes	B-rich mineral layer
69°24.243'S 76°06.676'E	Stornes	Kornerupine-bearing layers
69°24.070'S 76°06.699'E	Stornes	Garnet-rich fels
69°24.020'S 76°06.789'E	Stornes	Mig. with pinitised Crd
69°24.245'S 77°06.589'E	Stornes	Gn. with yellow Grt
69°22.875'S 76°17.763'E	Broknes	Crd-sill gn
69°22.597'S 76°18.174'E	Broknes	Crd-rich pods
69°23.203'S 76°19.646'E	Broknes	Grt-Qz intergrowths
69°23.736'S 76°20.762'E	Broknes	Fresh pelitic granulite
69°24.300'S 76°21.573'E	Broknes	Grt-rich gn.
69°23.668'S 76°19.443'E	Broknes	Pelite boudins in gn.
69°23.519'S 76°19.947'E	Broknes	Pelitic layers in gn., Grt, Fsp
69°23.771'S 76°24.949'E	Broknes	Grt-bearing granitic gn.
69°24.263'S 76°19.885'E	Broknes	Massive crd-sill-grt layers
69°24.081'S 76°19.794'E	Broknes	Grt-bearing (yellow) migmatitic gn.
69°24.185'S 76°18.110'E	Stinear	Garnet sand (100 %)
69°23.434'S 76°15.131'E	Fisher	Opx- & Crd-rich gn.
69°24.437'S 76°15.057'E	Brattnevet	Pegmatite and tourmaline
69°24.418'S 76°15.226'E	Brattnevet	Massive Crd lenses
<i>Rauer Islands</i>		
68°50.991'S 77°54.918'E	Mather	Spr-bearing Mg-metapelites, Opx-gn
68°50.831'S 77°54.734'E	Mather	Spr-bearing Mg-metapelites, Mt, Diop
68°50.746'S 77°55.000'E	Mather	Fo-marble
68°51.101'S 77°55.326'E	Mather	Bronzite, Wo-marble
68°48.987'S 77°49.759'E	Filla	Massive magnetite, semi-pelitic gn.
68°48.818'S 77°52.719'E	Filla	Grt+Cpx (calc-silicate rock)
68°48.869'S 77°52.332'E	Filla	Ultramafic Cpx-Opx rock
68°48.916'S 77°50.554'E	Filla	Mafic Grt+Cpx granulites
68°48.350'S 77°53.387'E	Filla	Grt+Cpx (calc-silicate rock)

15. MABEL: MULTIDISCIPLINARY ANTARCTIC BENTHIC LABORATORY

The First Deep-Sea Observatory in Antarctica. Recovery Mission.

Massimo Calcara¹⁾, Marco Lagalante¹⁾, Haiko de Vries²⁾, Hans W. Gerber³⁾

¹⁾ Istituto Nazionale di Geofisica e Vulcanologia (INGV), Rome
²⁾ Technical University of Berlin (TUB), Berlin
³⁾ University of Applied Sciences Berlin (TFHB), Berlin

Objectives

In the frame of PNRA activities, MABEL project (Multidisciplinary Antarctic Benthic Laboratory), made by INGV, developed a deep sea multidisciplinary observatory for long-term autonomous and continuous observations. From board of *Polarstern* this observatory was deployed on the seafloor of the Weddell Sea at 69° 24.29' S and 5° 32.2' W. 1874 m.w.d on 5 December 2005. It autonomously and automatically registers data for a minimum of one year with the following instruments:

- three component broad band seismometer (100 Hz per channel);
- vectorial current meter (2 Hz);
- conductivity, pressure and temperature recorder (CDT, 1 sample hour);
- light transmissometer (1 data/hour);
- chemical electrode analyser presently equipped with pH and redox electrodes (1 data every two days);
- water sampler (1 sample/week).

All these instruments and service packages are time-referenced with a high precision rubidium clock.

Work at sea

On the evening of 10 February 2007 the observatory recovery operations begun with a dedicated infrastructure developed in the frame of former EU Geostar project (see Fig 15.1): mainly, these are the vehicle MODUS (capable to handle payload up to 30 kN at 4,000 m, 100 kN tested static load, plus safety factors for operation of 5; see Fig 15.2), equipped with sonar and cameras, and the winch equipped with an electro-opticmechanical cable. By using this infrastructure it is possible to recover the observatory with a controlled and accurate procedure. The concept is shown in Figure 15.1.

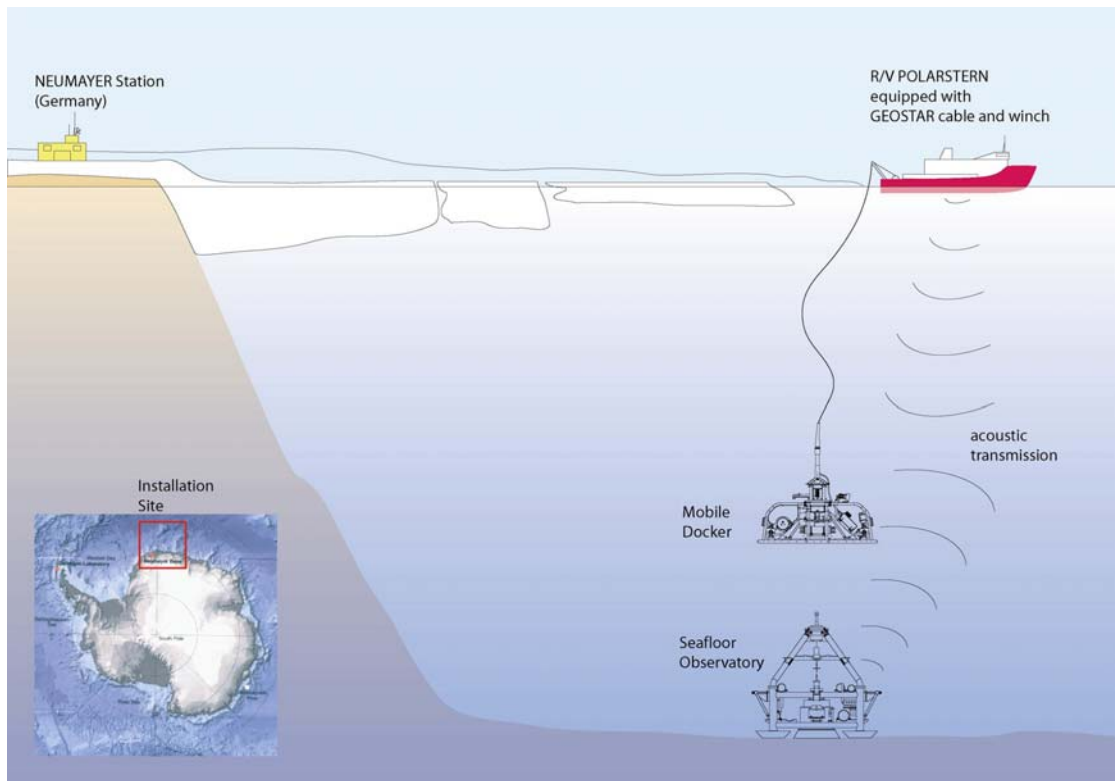


Fig. 15.1: MABEL concept

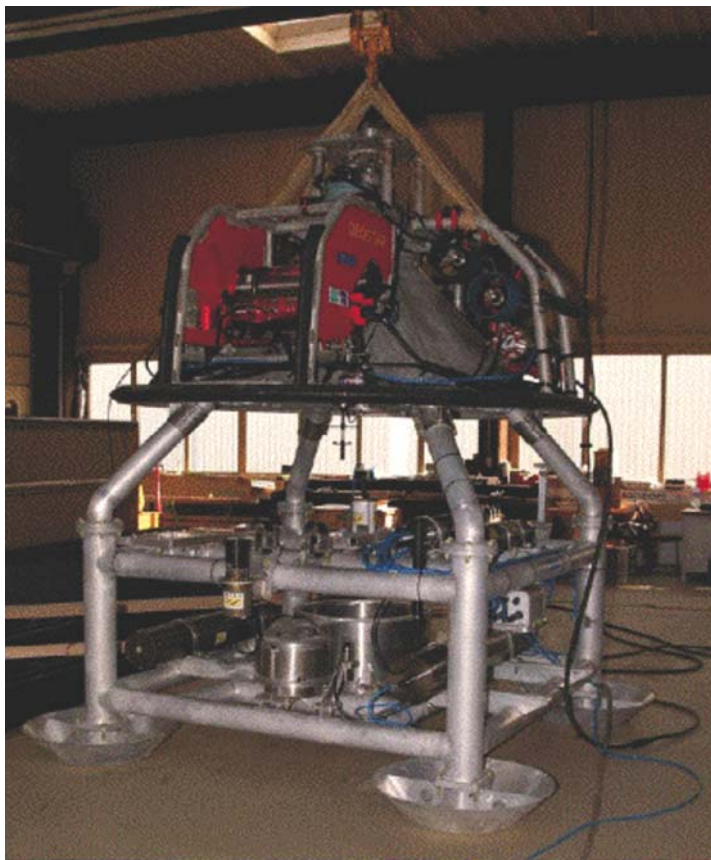


Fig. 15.2: MABEL connected to its deployment/recovery vehicle (MODUS) during tests at HSVA Hamburg

The ship has been positioned at the site of deployment. *Polarstern* has a dynamic positioning system for maintaining the exact position for a long time. Sea state was moderate (three meters swell, almost no wind waves).

Once the depth close to the seafloor had been reached, the sonar and four cameras of the vehicle started to search the exact location of the station, one hour after its water entry at surface. After six hours of continuous and strategic search operation the vehicle had been recovered on board for a pause. Once the vehicle was on board at a first sight it was noticed a displacement between two parts of the termination, then a detailed inspection showed a rupture of outer mechanical layer of the umbilical (optical fibre, power conductors, mechanical load layers) just above the cable itself and the connector (see Figs. 15.3 and 15.4): these damages prevented the prosecution of the recovery mission that for these safety reasons had to be aborted.



Fig. 15.3: Modus before recovery

Detailed inspection of the damage occurred during the recovery trial produced photos and report on the optical fibres state.



Fig. 15.4: After recovery trial. Details on rupture

In the electro-optic mechanical cable three optical fibres are present. Here is a summary of inspection executed after recovery of the vehicle and subsequent interruptions of operations due to the damages:

- *Fibre 1*: no signal loss from winch to termination, strong attenuation signal in the first meters near the termination when measured from termination to winch.
- *Fibre 2*: strong attenuation when measured in both directions.
- *Fibre 3*: quite sufficient conditions when measured in both directions.

These damages were never noted during the over 30 operations performed when reaching deeper sea floor (>3,300 m w.d.) and also with sea state worse than we had during the MABEL recovery.

The following is an extract of an internal file, technical report on what happened: "Deployment of MODUS started at about 2007-02-10-20:00 and ended 2007-02-11-04:00 when the recovery of MODUS began. The position of MABEL had been determined during its deployment with a Posidonia compatible transponder-release-system. This allows the determination of a position of +/- 12 m at the water depth of 1,875 m. *Polarstern* had been positioned with GPS at this spot, coordinates, see above; position in the picture below – white circle.

MODUS reached the operation depth for a search of about 1,800 m within 85 min. In between several checks had been conducted.

The search began at about 21:30 (Fig. 15.5), but MABEL could not be detected with the sonar. The search path is documented until 2007-02-11-01:42 in the picture below.

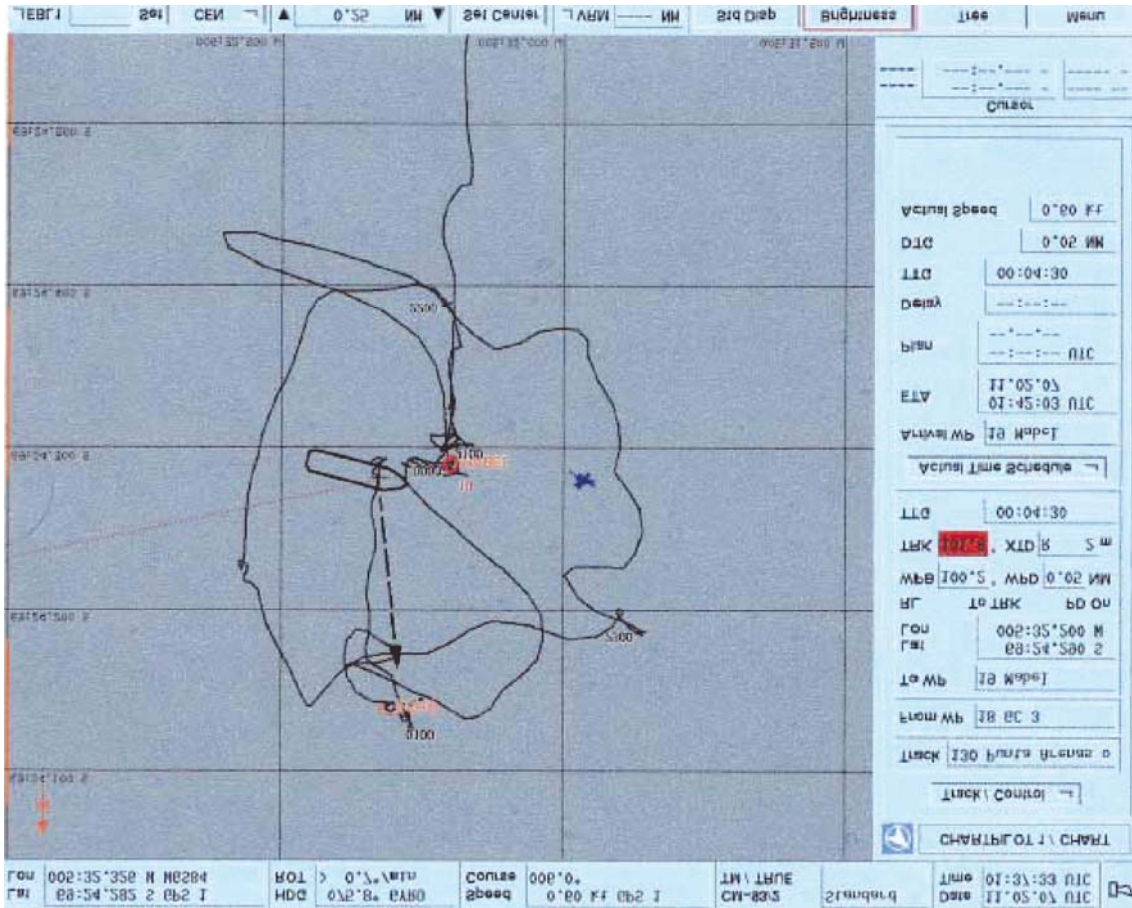


Fig. 15.5: Cruise track during recovery trial

Twice a slight indication of MABEL was given, close to the predetermined spot and north indicated with ECHO. More detailed search did not give verification. At 03:30 a.m. the search was stopped without result and MODUS had been heaved. At about 04:30 a.m. the system was on deck, with the result of damaged termination and cable. The telemetry system still worked properly, in between no unusual events occurred. Pitch and roll seemed to be unusual high once in a while, when noticed, but did not seem plausible.

What can be said about the operation?

- Everything had been prepared and tested as usually.
- The winch was operating properly.
- MODUS was operating properly, there was no failure of any component.
- Long operation of eight hours with monitored conditions caused high bending stress to the umbilical termination and consequently damaged it – outer layer of the umbilical.
- During the final phase intense errors of the protocol can be seen – data transmission errors.
- MABEL was operating since it responded to the modem.
- MABEL is more or less in the position assumed as the modem range is 500 m.
- The sea condition was quite smooth, but above the limit of MODUS design of 3m d-amp.
- No signal of MABEL on the sonar.
- Clear resonance effects with slack and snap loads – after check of the data set, s.a.
- During the operation the preference of one camera was given to the latch. For this there was no view at the cable. Docking first!
- We are lucky not to have lost MODUS and not even worse things occurred.

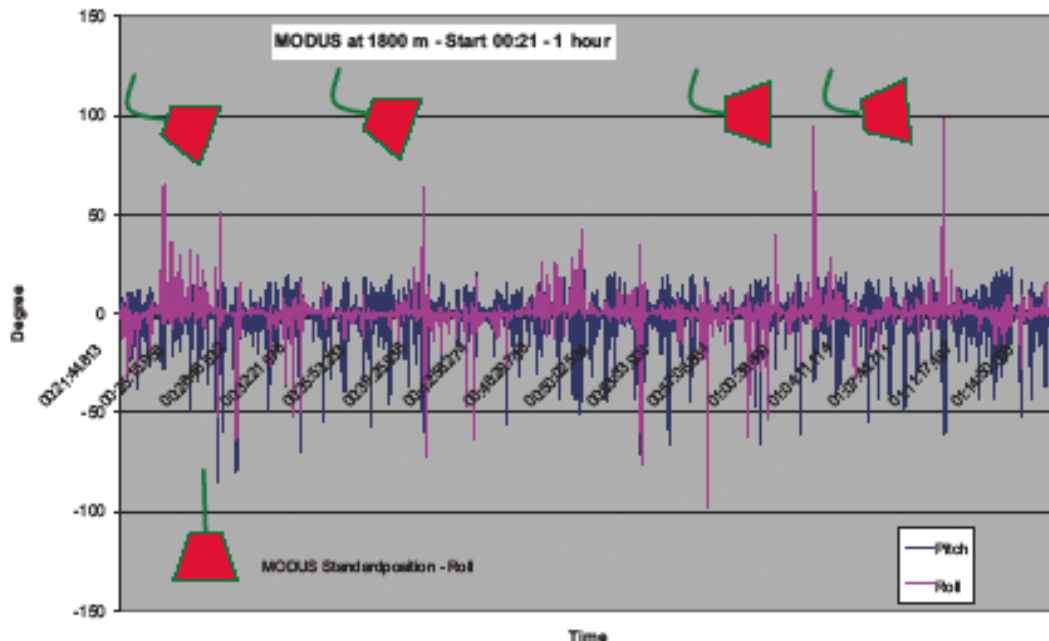


Fig. 15.6: Degree of pitch and roll versus time during recovery trial

What can be discussed?

- Maybe MABEL is exactly on site.
- Maybe MABEL is not exactly on site – systematic error of Posidonia. Unlikely.

- It is not possible to focus MABEL with the acoustic modem. To position the *Polarstern* in different locations, stop the shaft and propeller running is too much effort and not effective.
- No visibility of MABEL because the sonar is too slow for fast motion (pitch and roll, Fig. 15.6) in the meaning that we always missed it – even though we were moving very slowly;
- Automatic levelling of the sonar to compensate pitch motion. Roll – can not be compensated.
- We MUST use a transponder to bring the sub sea position of MODUS on top of a station. Thus, MODUS will be equipped with a transponder, as redundant positioning aid.”

APPENDIX

A.1 Beteiligte Institute / participating institutes

A.2 Fahrtteilnehmer / cruise participants

A.3 Schiffsbesatzung / ship's crew

A.4 Stationsliste / station list PS 69

A.5 List of samples

1. Surface water sample localities
2. Table of depths and locations of water samples from the CTD
3. Sampling overview of water samples for the study area of *Phaeocystis Antarctica* during RV expedition ANT-XXIII/9
4. Samples for exposure dating
5. Lake sediment cores from the Rauer Group
6. List of cores from marine basins in the Rauer Group
7. Microbiological samples

A.6 Graphical Core Description

A.1 BETEILIGTE INSTITUTE / PARTICIPATING INSTITUTES

Adresse / Address

AWI	Alfred-Wegener-Institut für Polar- und Meeresforschung in der Helmholtz-Gemeinschaft Postfach 12 01 61 27515 Bremerhaven, Germany
AWI-P	Alfred-Wegener-Institut für Polar- und Meeresforschung in der Helmholtz-Gemeinschaft Forschungsstelle Potsdam Telegrafenberg A 43 14473 Potsdam, Germany
BGR	Bundesanstalt für Geowissenschaften und Rohstoffe Stilleweg 2 30655 Hannover, Germany
DWD	Deutscher Wetterdienst Seewetterdienst Bernhard-Nocht Strasse 76 20359 Hamburg, Germany
EMAU	Ernst-Moritz-Arndt-Universität Greifswald Institut für Geographie und Geologie Friedrich-Ludwig-Jahnstraße 16 17491 Greifswald, Germany
FHK	Fachhochschule Kiel Sokratesplatz 1 24149 Kiel, Germany
GEUS	De Nationale Geologiske Undersøgelser for Danmark og Grønland Øster Voldgade 10 1350 Copenhagen, Denmark
GMU	Department of Physical Geography Macquarie University, NSW 2109, Australia
GSF	GSF-Forschungszentrum für Umwelt und Ingoldstädter Landstrasse 1 85764 Neuherberg, Germany

Adresse / Address

Heli Service	Heli Service International GmbH Im Geisbaum 2 63329 Egelsbach, Germany
IFM-GEOMAR	Leibnitz-Institut für Meereswissenschaften Düsternbrooker Weg 20 24105 Kiel, Germany
IGUP	Institut für Geowissenschaften der Universität Potsdam Karl-Liebknecht-Strasse 24-25 14476 Golm, Germany
INGV	Instituto Nazionale di Geofisica e Vulcanologia, Via di Vigna Murata 605 00143 Rome, Italy
KUM	K.U.M. Umwelt- und Meerestechnik Kiel GmbH Wischhofstraße 1-3 24148 Kiel, Germany
RUNJ	Institute of Marine & Coastal Sciences Rutgers University 71 Dudley Road, New Brunswick, U.S.A.
TFHB	Technische Fachhochschule Berlin Luxemburger Straße 10 13353 Berlin, Germany
TUB	Technische Universität Berlin Straße des 17. Juni 135 10623 Berlin Germany
University Bremen	Universität Bremen Bibliothekstraße 1 28359 Bremen Germany
University Cologne	Institut für Geologie und Mineralogie Universität Köln Zülpicher Str. 49a 50674 Köln Germany

Adresse / Address

USYD	The University of Sydney NSW 2006, Australia
VNIIOkeangeologia	VNIIOkeangeologia Angliysky Avenue St.Petersburg 190121 Russia

A.2 FAHRTTEILNEHMER / CRUISE PARTICIPANTS

Name/ Last name	Vorname/ First name	Institut/ Institute	Beruf/ Profession
Agirgöl	Sarah	AWI	Student, geodesy
Anagnostou	Eleni	RUNJ	Geologist
Bardenhagen	Janine	AWI	Geologist
Benneke	Ole	GEUS	Geologist
Berg	Sonja	University of Cologne	Geologist
Bienhold	Christina	AWI	Student, biology
Borchers	Andreas	AWI-P	Geologist
Büchner	Jürgen	Heli Service	Pilot
Calcara	Massimo	INGV	Geochemist
Damaske	Detlef	BGR	Geophysicist
Daniel	Kristin	AWI	Student, geology
De la Rocha	Christina	AWI	Geologist
Diekmann	Bernhard	AWI-P	Geologist
Ehlers	Birte-Marie	AWI	Geophysicist
Eulenburg	Antje	AWI-P	Technician
Focke	Lars	FHK	Television
Fritz	Michael	EMAU	Student, geography
Ganzert	Lars	AWI-P	Biologist
Gerber	Hans Walter	TFHB	Physicist
Gohl	Karsten	AWI	Geophysicist
Grobe	Hannes	AWI	Geologist
Hansen	Martin	KUM	Technician
Hubberten	Hans-Wolfgang	AWI-P	Chief-Scientist, mineralogist
Jurisch	Franziska	AWI	Student, geology
Klatt	Olaf	AWI	Physicist
Klug	Martin	University of Cologne	Geologist
Knight	Yoshua	USYD	Student, geophysics
Kopsch	Konrad	AWI-P	Technician
Kretschmer	Sven	AWI	Geoscientist

Name/ Last name	Vorname/ First name	Institut/ Institute	Beruf/ Profession
Lagalante	Marco	INGV	Scientist
Lensch	Norbert	AWI	Technician
Meier	Kristina	AWI	Student, geophysics
Miller	Christina	AWI	Student, medicine
Möllendorf	Karsten	Heli Service	Technician
Mondzsch	Juliane	AWI	Student, bathymetry
Muhle	Katharina	AWI	Student, geography
Oberhänsli	Roland	IGUP	Mineralogist
O'Brien	Patrick	IGUP	Mineralogist
Ortlepp	Sabrina	University of Cologne	Geologist
Parsiegla	Nicole	AWI	Geophysicist
Rudolf	Anton	Heli Service	Pilot
Schlosser	Christian	IfM-GEOMAR	Geologist
Sonnabend	Hartmut	DWD	Technician
Sperlich	Peter	University of Bremen	Student, geology
Stark	Florian	AWI	Student, geophysics
Stimac	Mihael	Heli Service	Technician
Strüfing	Reinhard	DWD	Meteorologist
Trapp	Michael	FHK	Television
Urlaub	Morelia	AWI	Student, geosciences
Vogel	Hendrik	University of Cologne	Geologist
Voigt	Ines	AWI-P	Student, geology
De Vries	Haiko	TUB	Technician
Wagner	Bernd	University of Cologne	Geologist
Wagner	Dirk	AWI-P	Biologist
White	Duanne	GMU	Geologist
Ziegler	Jonas	FHK	Television

A.3 SCHIFFSBESATZUNG / SHIP'S CREW

No.	Name	Rank
1.	Schwarze, Stefan	Master
2.	Spielke, Steffen	1.Offc.
3.	Farysch, Bernd	Ch.Eng.
4.	Becker, Tilo	2. Offc.
5.	Fallei, Holger	2.Offc.
6.	Niehusen, Frank	3.Offc.
7.	Weiß, Volker	Doctor
8.	Hecht, Andreas	R.Offc.
9.	Minzlaff, Hans-Ulrich	1.Eng.
10.	Schnick, Sascha	3.Eng.
11.	Sümnick, Stefan	3.Eng.
12.	Scholz, Manfred	ElecEng.
13.	Himmel, Frank	ELO
14.	Muhle, Helmut	ELO
15.	Nasis, Ilias	ELO
16.	Verhoeven, Roger	ELO
17.	Loidl, Reiner	Boatsw.
18.	Reise, Lutz	Carpenter
19.	Bäcker, Andreas	A.B.
20.	Hagemann, Manfred	A.B.
21.	Reichert, Jörg	A.B.
22.	Rhau, Lars-Peter	A.B.
23.	Schmit, Uwe	A.B.
24.	Stutz, Heinz-Werner	A.B.
25.	Wende, Uwe	A.B.
26.	Winkler, Michael	A.B.
27.	Preußner, Jörg	Storek.
28.	Elsner, Klaus	Mot-man
29.	Hartmann, Ernst-Uwe	Mot-man
30.	Ipsen, Michael	Mot-man
31.	Pinske, Lutz	Mot-man
32.	Voy, Bernd	Mot-man
33.	Müller-Homburg, Ralf-Dieter	Cook
34.	Martens, Michael	Cooksmate
35.	Silinski, Frank	Cooksmate
36.	Jürgens, Monika	1.Stwdess

No.	Name	Rank
37.	Wöckener, Martina	Stwdss/Kr
38.	Czyborra, Bärbel	2.Stwdess
39.	Gaude, Hans-Jürgen	2.Steward
40.	Huang, Wu-Mei	2.Steward
41.	Möller, Wolfgang	2.Stwdess
42.	Silinski, Carmen	2.Steward
43.	Yu, Kwok Yuen	Laundrym.
44.	Felsenstein, Thomas	Apprent.
45.	Grabbert, Steve	Apprent.

A.4 STATION LIST PS 69

Station	Date	Time	Latitude	Longitude	Depth [m]	Gear	Abbrev	Rec [cm]	Comment
PS69/730-1	04.02.07	20:01	57°49.19'S	58°26.56'W	3480	Water Sample Bucket	WSB		
PS69/731-1	04.02.07	23:03	58°18.08'S	57°42.84'W	3823	Water Sample Bucket	WSB		
PS69/732-1	05.02.07	03:00	58°54.57'S	56°46.90'W	3760	Water Sample Bucket	WSB		
PS69/733-1	05.02.07	08:59	59°48.12'S	55°22.50'W	3657	Water Sample Bucket	WSB		
PS69/734-1	05.02.07	13:00	60°53.60'S	36°4.00'W		Water Sample Bucket	WSB		
PS69/735-1	05.02.07	19:03	61°21.63'S	52°49.79'W	1021	Water Sample Bucket	WSB		
PS69/736-1	05.02.07	23:57	62°5.43'S	51°33.96'W	3195	Water Sample Bucket	WSB		
PS69/737-1	06.02.07	06:03	63°1.00'S	49°58.07'W	2667	Water Sample Bucket	WSB		
PS69/738-1	06.02.07	10:52	63°32.85'S	48°16.19'W	3467	Water Sample Bucket	WSB		
PS69/739-1	06.02.07	16:02	63°54.97'S	47°2.61'W	3038	Test	TEST		MABEL-Bergungsglocke
PS69/740-1	06.02.07	15:53	63°54.97'S	47°2.63'W	3041	Water Sample Bucket	WSB		
PS69/741-1	06.02.07	20:58	64°23.45'S	45°30.36'W	4510	Water Sample Bucket	WSB		
PS69/742-1	07.02.07	14:00	66°13.18'S	38°51.20'W	4638	Water Sample Bucket	WSB		
PS69/743-1	08.02.07	10:52	67°27.96'S	31°57.50'W	4671	Water Sample Bucket	WSB		
PS69/744-1	09.02.07	12:59	68°16.14'S	20°33.24'W	4899	Water Sample Bucket	WSB		
PS69/745-1	10.02.07	13:00	69°12.38'S	8°13.33'W	3628	Water Sample Bucket	WSB		
PS69/746-1	10.02.07	19:59	69°24.64'S	5°32.18'W	1880	MABEL	MABEL		Recovery unsuccessful
PS69/747-1	11.02.07	13:51	69°24.03'S	7°0.12'W	2969	CTD/rosette water sampler	CTD/RO		
PS69/747-2	11.02.07	13:33	69°24.01'S	7°0.05'W	2971	Water Sample Bucket	WSB		
PS69/747-3	11.02.07	14:54	69°23.95'S	7°0.06'W	2975	Releaser Test	REL		
PS69/747-4	11.02.07	17:40	69°24.08'S	7°1.04'W	2954	Nemo Float	NFLOAT		
PS69/748-1	14.02.07	01:02	70°21.38'S	8°5.53'W	1096	Magnetic Turn Circle	MTC		Start
	14.02.07	03:00	70°21.27'S	8°5.57'W	1069	Magnetic Turn Circle	MTC		End
PS69/749-1	14.02.07	13:10	69°55.46'S	3°41.94'W	2388	Water Sample Bucket	WSB		
PS69/750-1	14.02.07	21:37	69°34.06'S	0°35.06'W	2283	Water Sample Bucket	WSB		
PS69/751-1	15.02.07	02:13	69°26.16'S	1°17.53'E	2381	Water Sample Bucket	WSB		
PS69/752-1	15.02.07	06:53	69°18.61'S	3°50.58'E	2897	Nemo Float	NFLOAT		
PS69/753-1	15.02.07	11:02	69°25.90'S	6°4.77'E	1662	Water Sample Bucket	WSB		
PS69/754-1	15.02.07	15:11	69°15.07'S	7°39.97'E	2466	CTD/rosette water sampler	CTD/RO		

A.4 Station List

Station	Date	Time	Latitude	Longitude	Depth [m]	Gear	Abbrev	Rec [cm]	Comment
PS69/754-2	15.02.07	16:06	69°15.11'S	7°40.08'E	2462	Releaser Test	REL		
PS69/754-3	15.02.07	17:43	69°14.86'S	7°39.61'E	2507	Nemo Float	NFLOAT		
PS69/754-4	15.02.07	17:53	69°14.71'S	7°39.70'E	2463	Iron Fish	IFISH		Start
	16.02.07	08:11	68°24.71'S	14°8.23'E	3439	Iron Fish	IFISH		End
PS69/755-1	15.02.07	21:10	68°59.08'S	9°4.76'E	3516	Water Sample Bucket	WSB		
PS69/756-1	16.02.07	07:08	68°27.32'S	13°38.92'E	2972	Water Sample Bucket	WSB		
PS69/757-1	16.02.07	09:23	68°24.95'S	14°9.49'E	3407	CTD/rosette water sampler	CTD/RO		
PS69/758-1	16.02.07	10:25	68°25.20'S	14°9.80'E	3400	Nemo Float	NFLOAT		
PS69/759-1	16.02.07	10:30	68°25.46'S	14°10.39'E	3392	Iron Fish	IFISH		Start
	16.02.07	21:25	68°12.92'S	19°0.97'E	4294	Iron Fish	IFISH		End
PS69/760-1	16.02.07	15:38	68°19.25'S	16°29.78'E	3577	Nemo Float	NFLOAT		
PS69/761-1	16.02.07	16:59	68°17.74'S	17°6.02'E	3992	Water Sample Bucket	WSB		
PS69/762-1	16.02.07	22:28	68°13.13'S	19°1.40'E	4295	CTD/rosette water sampler	CTD/RO		
PS69/763-1	16.02.07	23:20	68°12.99'S	19°1.80'E	4309	Nemo Float	NFLOAT		
PS69/764-1	17.02.07	00:04	68°12.15'S	19°19.20'E	4103	Water Sample Bucket	WSB		
PS69/765-1	17.02.07	04:31	68°7.06'S	21°20.01'E	4222	Nemo Float	NFLOAT		
PS69/766-1	17.02.07	07:59	68°3.15'S	22°52.08'E	4135	Iron Fish	IFISH		Start
	17.02.07	16:41	67°54.35'S	26°42.48'E	4096	Iron Fish	IFISH		End
PS69/769-1	17.02.07	09:57	68°0.88'S	23°45.63'E	3969	Nemo Float	NFLOAT		
PS69/770-1	17.02.07	09:59	68°0.89'S	23°46.23'E	3974	Water Sample Bucket	WSB		
PS69/771-1	17.02.07	17:37	67°54.49'S	26°43.57'E	4075	CTD/rosette water sampler	CTD/RO		
PS69/771-2	17.02.07	18:18	67°54.53'S	26°43.52'E	4088	Nemo Float	NFLOAT		
PS69/772-1	17.02.07	20:00	67°51.51'S	27°26.37'E	3869	Water Sample Bucket	WSB		
PS69/773-1	18.02.07	00:28	67°46.30'S	29°40.80'E	3868	Nemo Float	NFLOAT		
PS69/774-1	18.02.07	06:01	67°39.64'S	32°3.61'E	1076	Water Sample Bucket	WSB		
PS69/775-1	18.02.07	14:28	67°29.94'S	35°48.04'E	3344	Nemo Float	NFLOAT		
PS69/775-2	18.02.07	14:30	67°29.92'S	35°48.39'E	3338	Iron Fish	IFISH		Start
	18.02.07	19:52	67°22.98'S	38°27.53'E	4102	Iron Fish	IFISH		End
PS69/776-1	18.02.07	16:02	67°28.00'S	36°32.98'E	3389	Water Sample Bucket	WSB		
PS69/777-1	18.02.07	21:39	67°20.73'S	39°19.94'E	3393	Nemo Float	NFLOAT		
PS69/778-1	18.02.07	22:01	67°20.28'S	39°30.07'E	3113	Water Sample Bucket	WSB		

Station	Date	Time	Latitude	Longitude	Depth [m]	Gear	Abbrev	Rec [cm]	Comment
PS69/779-1	19.02.07	04:01	67°12.58'S	42°26.44'E	3209	Water Sample Bucket	WSB		
PS69/780-1	19.02.07	05:38	67°10.69'S	43°10.06'E	2661	Nemo Float	NFLOAT		
PS69/780-2	19.02.07	05:44	67°10.85'S	43°10.58'E	2650	Iron Fish	IFISH		Start
	19.02.07	08:38	67°7.27'S	44°24.62'E	941	Iron Fish	IFISH		End
PS69/781-1	19.02.07	13:00	66°55.46'S	46°2.34'E	1292	Water Sample Bucket	WSB		
PS69/782-1	19.02.07	14:50	66°57.84'S	46°35.20'E	276	CTD/rosette water sampler	CTD/RO		
PS69/782-2	19.02.07	15:02	66°57.81'S	46°35.24'E	276	Ocean bottom seismometer	OBS		
PS69/782-3	19.02.07	15:38	66°57.75'S	46°35.31'E	276	Giant box grab	GBG	20	
PS69/782-4	19.02.07	16:05	66°57.64'S	46°35.26'E	277	CTD/rosette water sampler	CTD/RO		
PS69/783-1	19.02.07	23:10	66°4.65'S	47°42.80'E	2459	Water Sample Bucket	WSB		
PS69/785-1	20.02.07	06:31	65°24.93'S	50°2.90'E	2239	Nemo Float	NFLOAT		
PS69/786-1	20.02.07	08:07	65°24.61'S	50°40.85'E	2830	Water Sample Bucket	WSB		
PS69/787-1	20.02.07	17:07	65°22.64'S	53°50.12'E	1611	Water Sample Bucket	WSB		
PS69/788-1	21.02.07	05:06	65°42.58'S	57°31.12'E	2789	Water Sample Bucket	WSB		
PS69/789-1	21.02.07	15:02	65°54.60'S	60°8.58'E	3137	Water Sample Bucket	WSB		
PS69/790-1	22.02.07	00:02	66°3.29'S	62°47.63'E	3163	Water Sample Bucket	WSB		
PS69/791-1	22.02.07	11:04	66°17.61'S	67°10.50'E	2860	Water Sample Bucket	WSB		
PS69/792-1	23.02.07	01:00	66°31.48'S	72°40.80'E	1360	Water Sample Bucket	WSB		
PS69/793-1	23.02.07	15:25	68°0.68'S	72°53.27'E	703	Multi corer	MUC	18	
PS69/793-2	23.02.07	16:11	68°0.69'S	72°53.29'E	673	Gravity corer	GC	465	
PS69/794-1	24.02.07	18:35	68°43.34'S	76°40.66'E		CTD	CTD		
PS69/794-2	24.02.07	19:13	68°43.26'S	76°40.75'E		Multi corer	MUC	60	
PS69/794-3	24.02.07	19:58	68°43.28'S	76°40.70'E		Gravity corer	GC	1004	
PS69/795-1	24.02.07	18:06	68°43.38'S	76°40.73'E		Water Sample Bucket	WSB		
PS69/796-1	25.02.07	12:23	68°51.57'S	77°24.10'E	302	Ocean bottom seismometer	OBS		
PS69/797-1	28.02.07	08:57	67°27.05'S	73°14.22'E	614	Releaser Test	REL		POSIDONIA
PS69/798-1	28.02.07	22:14	66°16.24'S	72°43.03'E	2095	Ocean bottom hydrophone	OBH		released
PS69/799-1	01.03.07	00:06	66°2.36'S	72°42.82'E	2539	Ocean bottom hydrophone	OBH		released
PS69/800-1	01.03.07	01:40	65°49.06'S	72°43.07'E	2820	Ocean bottom hydrophone	OBH		released
PS69/801-1	01.03.07	03:55	65°34.71'S	72°43.31'E	2929	Ocean bottom seismometer	OBS		released
PS69/802-1	01.03.07	05:23	65°21.11'S	72°43.10'E	3055	Ocean bottom seismometer	OBS		released

A.4 Station List

Station	Date	Time	Latitude	Longitude	Depth [m]	Gear	Abbrev	Rec [cm]	Comment
PS69/803-1	01.03.07	06:52	65°7.51'S	72°42.90'E	3299	Ocean bottom seismometer	OBS		released
PS69/804-1	01.03.07	08:43	64°53.79'S	72°43.14'E	3464	Ocean bottom seismometer	OBS		released
PS69/805-1	01.03.07	10:57	64°40.08'S	72°43.18'E	3571	Ocean bottom seismometer	OBS		released
PS69/806-1	01.03.07	12:44	64°26.25'S	72°43.26'E	3610	Ocean bottom seismometer	OBS		released
PS69/807-1	01.03.07	14:19	64°12.56'S	72°43.17'E	3614	Ocean bottom seismometer	OBS		released
PS69/808-1	01.03.07	15:57	63°58.76'S	72°43.13'E	3732	Ocean bottom seismometer	OBS		released
PS69/809-1	01.03.07	17:37	63°44.98'S	72°43.23'E	3779	Ocean bottom seismometer	OBS		released
PS69/810-1	01.03.07	19:18	63°31.35'S	72°43.15'E	3861	Ocean bottom seismometer	OBS		released
PS69/811-1	01.03.07	20:58	63°17.58'S	72°43.21'E	3940	Ocean bottom seismometer	OBS		released
PS69/812-1	01.03.07	22:35	63°3.85'S	72°43.20'E	3976	Ocean bottom seismometer	OBS		released
PS69/813-1	02.03.07	00:09	62°50.00'S	72°43.13'E	4002	Ocean bottom seismometer	OBS		released
PS69/814-1	02.03.07	01:43	62°36.13'S	72°43.19'E	4002	Ocean bottom seismometer	OBS		released
PS69/815-1	02.03.07	03:26	62°22.51'S	72°43.19'E	4149	Ocean bottom seismometer	OBS		released
PS69/816-1	02.03.07	05:30	62°8.75'S	72°43.13'E	4057	Ocean bottom seismometer	OBS		released
PS69/817-1	02.03.07	07:32	61°55.04'S	72°43.23'E	4095	Ocean bottom seismometer	OBS		released
PS69/818-1	02.03.07	09:31	61°41.30'S	72°43.18'E	4145	Ocean bottom seismometer	OBS		released
PS69/819-1	02.03.07	11:30	61°27.51'S	72°43.21'E	4155	Ocean bottom seismometer	OBS		released
PS69/820-1	02.03.07	19:29	60°56.97'S	72°43.30'E	4161	CTD/rosette water sampler	CTD/RO		
PS69/820-2	02.03.07	21:26	60°56.98'S	72°43.28'E	4161	Multi corer	MUC	20	
PS69/820-3	02.03.07	23:20	60°56.94'S	72°43.41'E	4160	Gravity corer	GC	1392	
PS69/821-1	03.03.07	01:37	60°55.24'S	72°43.17'E	4117	Gravity corer	GC	938	
PS69/822-1	03.03.07	04:58	60°57.20'S	72°45.50'E	4100	Seismic refraction profile	SEISREFR		Start
	06.03.07	01:00	66°33.17'S	72°43.48'E	1252	Seismic refraction profile	SEISREFR		End
PS69/822-2	04.03.07	04:00	62°50.20'S	72°43.21'E	4003	Hydrophon	HYDRO		
PS69/823-1	06.03.07	03:23	66°18.97'S	72°43.28'E	1988	Ocean bottom hydrophone	OBH		
PS69/824-1	06.03.07	05:50	66°2.35'S	72°43.60'E	2537	Ocean bottom hydrophone	OBH		
PS69/825-1	06.03.07	09:31	65°51.80'S	72°43.12'E	2764	Ocean bottom hydrophone	OBH		
PS69/826-1	06.03.07	12:06	65°37.90'S	72°43.36'E	2898	Ocean bottom hydrophone	OBH		
PS69/827-1	06.03.07	14:41	65°24.19'S	72°43.34'E	2951	Ocean bottom hydrophone	OBH		
PS69/828-1	06.03.07	16:59	65°10.14'S	72°43.24'E	3252	Ocean bottom seismometer	OBS		
PS69/829-1	06.03.07	19:32	64°56.72'S	72°43.08'E	3424	Ocean bottom seismometer	OBS		

Station	Date	Time	Latitude	Longitude	Depth [m]	Gear	Abbrev	Rec [cm]	Comment
PS69/830-1	06.03.07	22:09	64°43.15'S	72°43.01'E	3543	Ocean bottom seismometer	OBS		
PS69/831-1	07.03.07	01:03	64°29.22'S	72°43.10'E	3614	Ocean bottom hydrophone	OBH		
PS69/832-1	07.03.07	03:38	64°15.07'S	72°43.33'E	3585	Ocean bottom seismometer	OBS		
PS69/833-1	07.03.07	06:20	64°1.52'S	72°43.26'E	3706	Ocean bottom seismometer	OBS		
PS69/834-1	07.03.07	09:29	63°48.31'S	72°43.38'E	3759	Ocean bottom seismometer	OBS		
PS69/835-1	07.03.07	12:07	63°34.26'S	72°43.17'E	3833	Ocean bottom seismometer	OBS		
PS69/836-1	07.03.07	14:45	63°20.52'S	72°43.28'E	3911	Ocean bottom hydrophone	OBH		
PS69/837-1	07.03.07	17:25	63°6.62'S	72°43.19'E	3956	Ocean bottom seismometer	OBS		
PS69/838-1	07.03.07	20:03	62°52.87'S	72°43.14'E	4012	Ocean bottom seismometer	OBS		
PS69/839-1	07.03.07	22:38	62°39.45'S	72°42.96'E	3978	Ocean bottom seismometer	OBS		
PS69/840-1	08.03.07	01:10	62°25.56'S	72°42.90'E	4041	Ocean bottom seismometer	OBS		
PS69/841-1	08.03.07	03:52	62°11.63'S	72°43.14'E	4032	Ocean bottom seismometer	OBS		
PS69/842-1	08.03.07	14:48	61°58.00'S	72°43.28'E	4137	Ocean bottom seismometer	OBS		
PS69/843-1	08.03.07	17:41	61°44.12'S	72°43.30'E	4106	Ocean bottom seismometer	OBS		
PS69/844-1	08.03.07	20:34	61°30.85'S	72°43.22'E	4270	Ocean bottom seismometer	OBS		
PS69/845-1	09.03.07	04:17	61°51.08'S	72°43.11'E	4105	Gravity corer	GC	708	bended
PS69/846-1	09.03.07	06:47	61°49.53'S	72°43.54'E	4120	CTD/rosette water sampler	CTD/RO		CTD lost
PS69/846-2	09.03.07	08:42	61°49.53'S	72°43.50'E	4124	Gravity corer	GC	472	
PS69/846-3	09.03.07	10:35	61°49.52'S	72°43.49'E	4123	Multi corer	MUC	0	
PS69/847-1	09.03.07	12:40	61°51.23'S	72°43.88'E	4104	Multi corer	MUC	35	
PS69/848-1	10.03.07	17:15	65°44.79'S	69°15.23'E	2526	HydroSweep/ParaSound profile	HS_PS		Start
	11.03.07	08:00	67°37.47'S	68°0.326'E	535	HydroSweep/ParaSound profile	HS_PS		End
PS69/849-1	11.03.07	08:37	67°35.00'S	68°7.52'E	553	Multi corer	MUC	25	
PS69/849-2	11.03.07	09:46	67°35.03'S	68°7.05'E	559	Gravity corer	GC	379	
PS69/850-1	11.03.07	19:45	66°28.16'S	69°11.49'E	1823	Gravity corer	GC	310	bended
PS69/851-1	11.03.07	22:15	66°22.42'S	69°0.80'E	2035	Gravity corer	GC	874	
PS69/851-2	11.03.07	23:23	66°22.34'S	69°0.70'E	2036	Multi corer	MUC	30	
PS69/852-1	12.03.07	02:56	66°4.69'S	69°10.16'E	2268	Gravity corer	GC	637	
PS69/853-1	12.03.07	04:40	65°59.87'S	69°13.09'E	2364	Gravity corer	GC	939	
PS69/853-2	12.03.07	05:50	65°59.88'S	69°13.07'E	2365	Multi corer	MUC	30	
PS69/853-3	12.03.07	07:18	65°59.89'S	69°13.13'E	2365	CTD/rosette water sampler	CTD/RO		

A.4 Station List

Station	Date	Time	Latitude	Longitude	Depth [m]	Gear	Abbrev	Rec [cm]	Comment
PS69/854-1	13.03.07	00:49	67°59.40'S	73°58.28'E	593	Water Sample Bucket	WSB		
PS69/855-1	13.03.07	18:36	68°41.79'S	76°43.44'E	848	Piston corer BGR	KL	1541	
PS69/855-2	13.03.07	19:54	68°41.80'S	76°43.26'E	848	Multi corer	MUC	60	
PS69/855-3	13.03.07	20:49	68°41.78'S	76°43.37'E	848	Large Box Corer	GKG	40	
PS69/856-1	13.03.07	21:25	68°41.59'S	76°47.65'E	843	Magnetic Turn Circle	MTC		Start
	13.03.07	23:42	68°40.77'S	76°47.69'E	837	Magnetic Turn Circle	MTC		End
PS69/857-1	16.03.07	22:13	67°30.14'S	79°29.88'E	461	Water Sample Bucket	WSB		
PS69/858-1	18.03.07	03:41	65°15.61'S	82°49.99'E	3166	Ocean bottom hydrophone	OBH		
PS69/859-1	18.03.07	05:36	65°1.37'S	82°50.09'E	3341	Ocean bottom hydrophone	OBH		
PS69/860-1	18.03.07	07:08	64°47.11'S	82°49.89'E	3411	Ocean bottom seismometer	OBS		on board
PS69/861-1	18.03.07	08:42	64°32.84'S	82°50.04'E	3590	Ocean bottom seismometer	OBS		on board
PS69/862-1	18.03.07	10:20	64°18.64'S	82°50.08'E	3667	Ocean bottom seismometer	OBS		on board
PS69/863-1	18.03.07	11:48	64°4.40'S	82°50.12'E	3710	Ocean bottom seismometer	OBS		on board
PS69/864-1	18.03.07	13:16	63°50.08'S	82°49.98'E	3712	Ocean bottom seismometer	OBS		on board
PS69/865-1	18.03.07	14:47	63°35.58'S	82°50.11'E	3064	Ocean bottom seismometer	OBS		on board
PS69/866-1	18.03.07	16:11	63°21.38'S	82°50.02'E	2640	Ocean bottom seismometer	OBS		on board
PS69/867-1	18.03.07	17:35	63°7.12'S	82°50.04'E	2554	Ocean bottom seismometer	OBS		on board
PS69/868-1	18.03.07	18:59	62°52.84'S	82°50.05'E	2309	Ocean bottom seismometer	OBS		on board
PS69/869-1	18.03.07	20:24	62°38.60'S	82°49.93'E	2303	Ocean bottom seismometer	OBS		on board
PS69/870-1	18.03.07	21:47	62°24.35'S	82°49.90'E	2387	Ocean bottom seismometer	OBS		on board
PS69/871-1	18.03.07	23:12	62°9.91'S	82°50.04'E	2257	Ocean bottom seismometer	OBS		on board
PS69/872-1	19.03.07	00:41	61°55.80'S	82°50.00'E	2442	Ocean bottom seismometer	OBS		on board
PS69/873-1	19.03.07	02:30	61°45.17'S	82°50.02'E	2376	Water Sample Bucket	WSB		
PS69/874-1	19.03.07	04:22	61°44.99'S	82°50.05'E	2375	Seismic refraction profile	SEISREFR		Start
	20.03.07	22:30	65°19.50'S	82°49.76'E	3079	Seismic refraction profile	SEISREFR		End
PS69/875-1	20.03.07	21:43	65°15.51'S	82°49.94'E	3168	Water Sample Bucket	WSB		
PS69/876-1	20.03.07	23:20	65°18.47'S	82°50.28'E	3101	Ocean bottom hydrophone	OBH		
PS69/877-1	21.03.07	00:15	65°15.73'S	82°50.30'E	3140	HydroSweep/ParaSound profile	HS_PS		Start
	21.03.07	05:55	65°20.93'S	82°40.03'E	3097	HydroSweep/ParaSound profile	HS_PS		End
PS69/878-1	21.03.07	06:56	65°20.99'S	82°39.02'E	3067	Gravity corer	GC	642	
PS69/878-2	21.03.07	08:29	65°21.00'S	82°38.99'E	3068	Multi corer	MUC	0	

Station	Date	Time	Latitude	Longitude	Depth [m]	Gear	Abbrev	Rec [cm]	Comment
PS69/878-3	21.03.07	10:26	65°20.98'S	82°39.48'E	3080	CTD/rosette water sampler	CTD/RO		
PS69/878-4	21.03.07	12:03	65°20.55'S	82°39.37'E	3093	Giant box grab	GBG	42	
PS69/879-1	21.03.07	14:52	65°4.41'S	82°49.15'E	3325	Ocean bottom hydrophone	OBH		
PS69/880-1	21.03.07	16:55	64°49.78'S	82°49.80'E	3414	Ocean bottom seismometer	OBS		
PS69/881-1	21.03.07	19:25	64°35.76'S	82°50.25'E	3529	Ocean bottom seismometer	OBS		
PS69/882-1	21.03.07	22:07	64°21.56'S	82°49.82'E	3650	Ocean bottom seismometer	OBS		
PS69/883-1	22.03.07	00:49	64°7.39'S	82°49.95'E	3694	Ocean bottom seismometer	OBS		
PS69/883-2	22.03.07	01:17	64°4.62'S	82°49.83'E	3697	Water Sample Bucket	WSB		
PS69/884-1	22.03.07	04:12	63°52.71'S	82°49.99'E	3700	Ocean bottom seismometer	OBS		
PS69/885-1	22.03.07	06:34	63°50.23'S	82°52.40'E	3702	Giant box grab	GBG	52	
PS69/886-1	22.03.07	08:45	63°38.70'S	82°50.15'E	3163	Ocean bottom seismometer	OBS		
PS69/887-1	22.03.07	11:06	63°24.55'S	82°49.98'E	2696	Ocean bottom seismometer	OBS		
PS69/888-1	22.03.07	13:15	63°9.94'S	82°49.88'E	2535	Ocean bottom seismometer	OBS		
PS69/889-1	22.03.07	15:25	62°55.51'S	82°50.63'E	2546	Ocean bottom seismometer	OBS		
PS69/889-2	22.03.07	15:36	62°54.79'S	82°50.70'E	2514	Water Sample Bucket	WSB		
PS69/890-1	22.03.07	17:26	62°46.23'S	82°49.91'E	2259	Gravity corer	GC	747	
PS69/891-1	22.03.07	19:38	62°39.49'S	82°49.77'E	2296	CTD/rosette water sampler	CTD/RO		
PS69/891-2	22.03.07	20:50	62°39.39'S	82°49.76'E	2296	Gravity corer	GC	517	bended
PS69/891-3	22.03.07	22:04	62°39.34'S	82°50.16'E	2295	Multi corer	MUC		
PS69/891-4	22.03.07	22:41	62°39.39'S	82°50.06'E	2292	Ocean bottom seismometer	OBS		
PS69/891-5	23.03.07	00:23	62°39.35'S	82°50.39'E	2290	Giant box grab	GBG		
PS69/892-1	23.03.07	02:15	62°27.36'S	82°50.05'E	2441	Ocean bottom seismometer	OBS		
PS69/893-1	23.03.07	04:16	62°12.71'S	82°49.91'E	2191	Ocean bottom seismometer	OBS		
PS69/894-1	23.03.07	06:41	61°58.57'S	82°49.83'E	2470	Ocean bottom seismometer	OBS		
PS69/895-1	23.03.07	09:54	61°41.96'S	82°49.58'E	2352	Multi corer	MUC		
PS69/896-1	23.03.07	16:01	60°51.70'S	83°45.43'E	1606	Water Sample Bucket	WSB		
PS69/897-1	23.03.07	21:36	60°0.89'S	84°38.87'E	2045	HydroSweep/ParaSound profile	HS_PS		Start
	24.03.07	03:19	59°37.27'S	85°40.39'E	4122	HydroSweep/ParaSound profile	HS_PS		End
PS69/898-1	23.03.07	21:42	60°0.21'S	84°40.39'E	2038	Water Sample Bucket	WSB		
PS69/898-2	24.03.07	04:42	59°37.25'S	85°40.52'E	4118	CTD/rosette water sampler	CTD/RO		
PS69/899-1	24.03.07	06:54	59°37.30'S	85°40.42'E	4126	Multi corer	MUC	25	

A.4 Station List

Station	Date	Time	Latitude	Longitude	Depth [m]	Gear	Abbrev	Rec [cm]	Comment
PS69/899-2	24.03.07	09:48	59°37.32'S	85°40.39'E	4128	Piston corer	PC	2263	
PS69/900-1	24.03.07	13:38	59°32.98'S	85°50.57'E	4120	Piston corer	PC	2261	
PS69/901-1	25.03.07	02:51	58°49.54'S	83°0.22'E	1921	Water Sample Bucket	WSB		
PS69/902-1	25.03.07	13:00	57°51.24'S	80°47.80'E	1783	Water Sample Bucket	WSB		
PS69/903-1	25.03.07	19:34	57°13.54'S	79°22.96'E	1713	Multi corer	MUC		
PS69/904-1	25.03.07	22:48	56°58.48'S	78°41.00'E	1819	Water Sample Bucket	WSB		
PS69/905-1	26.03.07	06:37	56°9.61'S	76°26.56'E	2809	Water Sample Bucket	WSB		
PS69/906-1	26.03.07	14:39	55°21.76'S	74°17.70'E	2919	Water Sample Bucket	WSB		
PS69/907-1	26.03.07	19:13	55°0.30'S	73°19.98'E	2248	CTD/rosette water sampler	CTD/RO		
PS69/907-2	26.03.07	21:14	55°0.25'S	73°20.04'E	2253	Piston corer	PC	2289	
PS69/907-3	26.03.07	23:02	55°0.29'S	73°19.99'E	2251	Multi corer	MUC	22	
PS69/908-1	27.03.07	04:37	54°9.32'S	73°42.24'E	2177	Water Sample Bucket	WSB		
PS69/909-1	27.03.07	12:21	52°45.99'S	74°17.71'E	198	Water Sample Bucket	WSB		
PS69/910-1	27.03.07	13:08	52°39.71'S	74°17.25'E	209	Multi corer	MUC	0	
PS69/910-2	27.03.07	13:29	52°39.79'S	74°17.17'E	207	Large Box Corer	GKG	0	box bended
PS69/911-1	27.03.07	22:02	51°12.99'S	73°46.36'E	525	Water Sample Bucket	WSB		
PS69/912-1	28.03.07	10:13	50°19.45'S	71°33.49'E	570	CTD/rosette water sampler	CTD/RO		
PS69/912-2	28.03.07	11:53	50°18.57'S	71°34.14'E	566	Water Sample Bucket	WSB		
PS69/912-3	28.03.07	13:43	50°18.63'S	71°34.06'E	567	Piston corer	PC	2815	
PS69/912-4	28.03.07	16:51	50°18.62'S	71°33.93'E	567	Piston corer	PC	1886	
PS69/912-5	28.03.07	17:46	50°18.64'S	71°33.91'E	565	Multi corer	MUC		
PS69/913-1	29.03.07	05:13	49°21.86'S	70°12.42'E	57	Water Sample Bucket	WSB		
PS69/914-1	29.03.07	17:29	50°7.19'S	69°57.82'E	195	Water Sample Bucket	WSB		
PS69/915-1	30.03.07	07:07	49°58.15'S	65°54.67'E	310	Water Sample Bucket	WSB		
PS69/916-1	31.03.07	06:26	49°32.79'S	61°47.27'E	2459	Water Sample Bucket	WSB		
PS69/917-1	01.04.07	00:14	47°42.59'S	58°49.11'E	4314	Water Sample Bucket	WSB		
PS69/918-1	01.04.07	18:20	45°58.95'S	55°40.86'E	4119	Water Sample Bucket	WSB		
PS69/919-1	02.04.07	14:47	44°17.86'S	52°42.85'E	3478	Water Sample Bucket	WSB		
PS69/920-1	03.04.07	08:48	43°8.93'S	49°33.49'E	2586	Water Sample Bucket	WSB		
PS69/921-1	04.04.07	02:01	42°44.71'S	45°34.41'E	3347	Water Sample Bucket	WSB		
PS69/922-1	04.04.07	05:58	42°39.08'S	44°38.75'E	3354	Test	TEST		airgun kompressor

Station	Date	Time	Latitude	Longitude	Depth [m]	Gear	Abbrev	Rec [cm]	Comment
PS69/923-1	04.04.07	19:16	42°21.49'S	41°46.29'E	3190	Water Sample Bucket	WSB		
PS69/924-1	05.04.07	13:09	41°37.61'S	38°2.32'E	3944	Water Sample Bucket	WSB		
PS69/925-1	06.04.07	07:03	41°16.58'S	34°24.39'E	5195	Water Sample Bucket	WSB		
PS69/926-1	07.04.07	02:32	41°3.49'S	30°37.56'E	4678	Water Sample Bucket	WSB		
PS69/927-1	07.04.07	15:46	40° 52.53' S	27°28.08' E	2719	HydroSweep/ParaSound profile	HS_PS		start
	07.04.07	17:54	40°47.51' S	27°21.80' E	2749	HydroSweep/ParaSound profile	HS_PS		end
PS69/928-1	07.04.07	18:39	40°41.90' S	27°12.25' E	2675	Water Sample Bucket	WSB		
PS69/929-1	07.04.07	22:32	40°12.42' S	26°18.63' E	2482	HydroSweep/ParaSound profile	HS_PS		start
	08.04.07	13:30	37°27.41' S	25°36.68' E	2959	HydroSweep/ParaSound profile	HS_PS		end
PS69/930-1	08.04.07	08:24	38°14.69' S	25°48.42' E	3213	Water Sample Bucket	WSB		
PS69/931-1	09.04.07	00:44	36°49.71' S	23°11.19' E	4758	Water Sample Bucket	WSB		
PS69/932-1	09.04.07	15:45	35°59.73' S	19°59.77' E	184	Water Sample Bucket	WSB		
PS69/933-1	10.04.07	01:20	34°44.82' S	19°0.35' E	154	Magnetic Turn Circle	MTC		start
	10.04.07	03:15	34°44.60' S	19°0.48' E	155	Magnetic Turn Circle	MTC		end

A.5 LIST OF SAMPLES

1. Surface water sample localities

No.	Device	Lat.	Long.	Date	Time (UTC)	Sample type
1	snorkel	58°28.411'S	57°27.075'W	05.02.2007	00:07	a, b
2	snorkel	60°0.749'S	55°23.312'W	05.02.2007	10:22	a, b
3	snorkel	61°3.893'S	53°20.457'W	05.02.2007	17:07	a, b
4	snorkel	62°1.481'S	51°40.494'W	05.02.2007	23:30	a, b
5	snorkel	63°27.574'S	48°32.558'W	06.02.2007	10:04	a, b
6	snorkel	63°56.904'S	46°57.884'W	06.02.2007	17:05	a, b
7	snorkel	64°30.431'S	45°7.126'W	06.02.2007	21:59	a, b
8	snorkel	65°52.512'S	40°25.680'W	07.02.2007	10:07	a, b, c
9	snorkel	66°23.593'S	37°57.292'W	07.02.2007	16:14	a, b
10	snorkel	66°43.472'S	36°13.344'W	07.02.2007	22:08	a, b
11	snorkel	67°28.598'S	30°35.659'W	08.02.2007	14:47	a, b
12	snorkel	67°39.394'S	28°20.771'W	08.02.2007	20:56	a, b
13	snorkel	68°7.068'S	22°29.856'W	09.02.2007	08:59	a, b, d
14	snorkel	68°20.583'S	19°35.899'W	09.02.2007	14:54	a, b, d
15	snorkel	68°34.905'S	16°29.778'W	09.02.2007	20:58	a, b
16	bow intake	69°2.685'S	10°22.879'W	10.02.2007	08:50	a, d
17	bow intake	69°58.824'S	7°26.665'W	10.02.2007	15:06	a
18	bow intake	69°56.683'S	3°47.304'W	14.02.2007	12:57	a, d
19	bow intake	69°20.994'S	5°2.211'E	15.02.2007	09:09	a, d
20	fish	68°1.655'S	23°27.831'E	17.02.2007	09:17	a, b
21	fish	67°55.536'S	25°52.103'E	17.02.2007	14:39	a, b
22	fish	67°28.756'S	36°15.504'E	18.02.2007	15:26	a, b
23	fish	67°23.595'S	38°14.353'E	18.02.2007	19:23	a, b
24	bow intake	65°24.904'S	50°16.729'E	20.02.2007	07:05	a, d
25	bow intake	67°7.792'S	73°10.501'E	23.02.2007	08:48	a, d, e
26	snorkel	61°1.917'S	72°43.182'E	03.03.2007	06:11	a, b
27	snorkel	62°3.437'S	72°43.182'E	03.03.2007	19:20	a, b
28	snorkel	63°16.520'S	72°43.176'E	04.03.2007	08:47	a, b, c, d, e
29	snorkel	63°58.464'S	72°43.163'E	04.03.2007	17:33	a, b, c, d
30	snorkel	64°57.433'S	72°43.178'E	05.03.2007	05:32	a, b, c, d
31	bow intake	62°9.008'S	72°42.485'E	08.03.2007	11:32	a
32	snorkel	61°55.666'S	72°43.232'E	08.03.2007	15:21	a
33	snorkel	64°26.576'S	82°50.000'E	18.03.2007	09:19	a, c, d
34	snorkel	63°32.219'S	82°49.983'E	18.03.2007	15:10	a, b
35	snorkel	61°58.510'S	82°50.000'E	19.03.2007	00:18	a, b, c, d
36	snorkel	63°31.378'S	82°50.0.19'E	22.03.2007	10:14	a, b
37	snorkel	62°50.157'S	82°5.072'E	22.03.2007	16:32	a, b, e
38	snorkel	60°52.840'S	83°44.212'E	23.03.2007	15:56	a, b, c, d
39	snorkel	60°1.172'S	84°38.603'E	23.03.2007	21:34	a, b
40	snorkel	59°22.905'S	85°11.620'E	24.03.2007	17:29	a, b
41	snorkel	58°45.835'S	82°51.532'E	25.03.2007	03:29	a, b, c, d

No.	Device	Lat.	Long.	Date	Time (UTC)	Sample type
42	snorkel	58°4.862'S	81°17.884'E	25.03.2007	10:41	a, b
43	snorkel	57°33.899'S	80°8.255'E	25.03.2007	15:51	a, b
44	snorkel	56°25.234'S	77°9.269'E	26.03.2007	04:13	a, b, c, d
45	snorkel	56°4.457'S	76°12.564'E	26.03.2007	07:25	a, b
46	snorkel	55°48.619'S	75°29.726'E	26.03.2007	10:01	a, b
47	snorkel	55°30.617'S	74°41.338'E	26.03.2007	13:07	a, b, c
48	snorkel	55°13.251'S	73°54.999'E	26.03.2007	16:05	a, b
49	snorkel	54°15.240'S	73°39.660'E	27.03.2007	04:04	a, b
50	snorkel	53°36.995'S	73°56.217'E	27.03.2007	07:34	a, b
51	snorkel	53°10.493'S	74°7.588'E	27.03.2007	09:58	a, b, c, d
52	snorkel	52°18.140'S	74°15.684'E	27.03.2007	15:49	a, b
53	snorkel	50°41.008'S	72°28.141'E	28.03.2007	04:06	a, b
54	snorkel	50°20.694'S	71°39.012'E	28.03.2007	08:57	a, b
55	snorkel	50°2.183'S	66°40.460'E	30.03.2007	04:33	a, b
56	snorkel	49°56.131'S	65°54.456'E	30.03.2007	07:07	a, b
57	snorkel	49°52.890'S	64°55.314'E	30.03.2007	10:22	a, b, c, d
58	snorkel	49°47.330'S	63°52.769'E	30.03.2007	16:09	a, b
59	snorkel	49°37.954'S	62°9.236'E	31.03.2007	04:09	a, b
60	snorkel	49°13.614'S	61°11.971'E	31.03.2007	10:05	b
61	snorkel	48°33.845'S	60°12.758'E	31.03.2007	15:58	a, b
62	snorkel	47°14.653'S	57°57.746'E	01.04.2007	05:10	a, b
63	snorkel	46°6.607'S	55°54.518'E	01.04.2007	17:01	a, b
64	snorkel	45°6.551'S	54°7.895'E	02.04.2007	04:59	a, b
65	snorkel	44°6.767'S	52°23.645'E	02.04.2007	17:11	a, b
66	snorkel	42°57.706'S	47°42.378'E	03.04.2007	16:57	a, b
67	snorkel	42°40.363'S	44°51.495'E	04.04.2007	05:00	a, b
68	snorkel	42°23.293'S	42°4.015'E	04.04.2007	17:56	a, b
69	snorkel	42°5.976'S	39°14.986'E	05.04.2007	06:04	a, b
70	snorkel	41°25.352'S	36°58.382'E	05.04.2007	19:01	a, b
71	snorkel	41°16.799'S	34°28.160'E	06.04.2007	06:47	a, b

a. Samples taken include chlorophyll, biogenic silica, lithogenic silica, dissolved silicon, nitrate, soluble reactive phosphate, POC, PON, $\delta^{13}\text{C}$ of POC, $\delta^{15}\text{N}$ of PON, $\delta^{30}\text{Si}$ of dissolved silicon, $\delta^{15}\text{N}$ of nitrate.

b. Samples taken include pigments, dissolved Fe, particulate Fe, total Fe, Fe solubility, Fe ligands, misc trace elements (Fe, Al, Ti, Zn, Cd, Co, etc) in dissolved, colloidal, and particulate phases, and total intracellular Fe and other intracellular trace metals.

c. Samples taken include diatom morphometrics.

d. Samples taken include phytoplankton number and species composition, alkalinity, DIC, $\delta^{13}\text{C}$ of DIC.

e. Samples taken include size fractionated $\delta^{13}\text{C}$ of POC.

2. Tab. of depths and locations of water samples from the CTD

No.	Station	Date	Time (UTC)	Lat.	Long.	Depth (m)	Sample type
1	PS 69 747 1	11.02.2007	13:51	69°24.03'S	7°0.12'W	20	a
2	PS 69 747 1	11.02.2007	13:51	69°24.03'S	7°0.12'W	40	a
3	PS 69 747 1	11.02.2007	13:51	69°24.03'S	7°0.12'W	60	a
4	PS 69 747 1	11.02.2007	13:51	69°24.03'S	7°0.12'W	80	a
5	PS 69 747 1	11.02.2007	13:51	69°24.03'S	7°0.12'W	200	a
6	PS 69 747 1	11.02.2007	13:51	69°24.03'S	7°0.12'W	300	a
7	PS 69 747 1	11.02.2007	13:51	69°24.03'S	7°0.12'W	500	a
8	PS 69 747 1	11.02.2007	13:51	69°24.03'S	7°0.12'W	1000	a
9	PS 69 747 1	11.02.2007	13:51	69°24.03'S	7°0.12'W	1250	a
10	PS 69 747 1	11.02.2007	13:51	69°24.03'S	7°0.12'W	1500	a
11	PS 69 747 1	11.02.2007	13:51	69°24.03'S	7°0.12'W	1750	a
12	PS 69 747 1	11.02.2007	13:51	69°24.03'S	7°0.12'W	2000	a
13	PS 69 747 1	11.02.2007	13:51	69°24.03'S	7°0.12'W	2250	b
14	PS 69 757 1	16.02.2007	09:23	68°24.95'S	14°9.49'E	20	a
15	PS 69 757 1	16.02.2007	09:23	68°24.95'S	14°9.49'E	40	a
16	PS 69 757 1	16.02.2007	09:23	68°24.95'S	14°9.49'E	60	a
17	PS 69 757 1	16.02.2007	09:23	68°24.95'S	14°9.49'E	80	a
18	PS 69 757 1	16.02.2007	09:23	68°24.95'S	14°9.49'E	200	a
19	PS 69 757 1	16.02.2007	09:23	68°24.95'S	14°9.49'E	300	a
20	PS 69 757 1	16.02.2007	09:23	68°24.95'S	14°9.49'E	500	a
21	PS 69 757 1	16.02.2007	09:23	68°24.95'S	14°9.49'E	1500	a
22	PS 69 757 1	16.02.2007	09:23	68°24.95'S	14°9.49'E	2250	b
23	PS 69 794 1	14.02.2007	18:35	68°43.34'S	70°40.66'E	20	a
24	PS 69 794 1	14.02.2007	18:35	68°43.34'S	70°40.66'E	40	a
25	PS 69 794 1	14.02.2007	18:35	68°43.34'S	70°40.66'E	60	a
26	PS 69 794 1	14.02.2007	18:35	68°43.34'S	70°40.66'E	80	a
27	PS 69 794 1	14.02.2007	18:35	68°43.34'S	70°40.66'E	200	a
28	PS 69 794 1	14.02.2007	18:35	68°43.34'S	70°40.66'E	500	a
29	PS 69 794 1	14.02.2007	18:35	68°43.34'S	70°40.66'E	828	c
30	PS 69 820 1	02.03.2007	19:29	60°56.97'S	72°43.30'E	20	a
31	PS 69 820 1	02.03.2007	19:29	60°56.97'S	72°43.30'E	40	a
32	PS 69 820 1	02.03.2007	19:29	60°56.97'S	72°43.30'E	60	a
33	PS 69 820 1	02.03.2007	19:29	60°56.97'S	72°43.30'E	80	a
34	PS 69 820 1	02.03.2007	19:29	60°56.97'S	72°43.30'E	200	a
35	PS 69 820 1	02.03.2007	19:29	60°56.97'S	72°43.30'E	500	a
36	PS 69 820 1	02.03.2007	19:29	60°56.97'S	72°43.30'E	1000	a
37	PS 69 820 1	02.03.2007	19:29	60°56.97'S	72°43.30'E	1500	a
38	PS 69 820 1	02.03.2007	19:29	60°56.97'S	72°43.30'E	2000	a
39	PS 69 820 1	02.03.2007	19:29	60°56.97'S	72°43.30'E	2250	b
40	PS 69 820 1	02.03.2007	19:29	60°56.97'S	72°43.30'E	2500	a
41	PS 69 820 1	02.03.2007	19:29	60°56.97'S	72°43.30'E	3000	a
42	PS 69 820 1	02.03.2007	19:29	60°56.97'S	72°43.30'E	3500	a
43	PS 69 820 1	02.03.2007	19:29	60°56.97'S	72°43.30'E	4000	a
44	PS 69 820 1	02.03.2007	19:29	60°56.97'S	72°43.30'E	4165	c

No.	Station	Date	Time (UTC)	Lat.	Long.	Depth (m)	Sample type
45	PS 69 853 3	12.03.2007	07:18	65°59.89'S	69°13.13'E	2200	c
46	PS 69 878 3	21.03.2007	10:26	65°20.98'S	82°39.48'E	20	a
47	PS 69 878 3	21.03.2007	10:26	65°20.98'S	82°39.48'E	40	a
48	PS 69 878 3	21.03.2007	10:26	65°20.98'S	82°39.48'E	60	a
49	PS 69 878 3	21.03.2007	10:26	65°20.98'S	82°39.48'E	80	a
50	PS 69 878 3	21.03.2007	10:26	65°20.98'S	82°39.48'E	200	a
51	PS 69 878 3	21.03.2007	10:26	65°20.98'S	82°39.48'E	500	a
52	PS 69 878 3	21.03.2007	10:26	65°20.98'S	82°39.48'E	2250	b
53	PS 69 878 3	21.03.2007	10:26	65°20.98'S	82°39.48'E	2900	c
54	PS 69 891 1	22.03.2007	19:38	62°39.49'S	82°49.77'E	2140	c
55	PS 69 898 2	24.03.2007	04:42	59°37.25'S	85°40.52'E	20	a
56	PS 69 898 2	24.03.2007	04:42	59°37.25'S	85°40.52'E	40	a
57	PS 69 898 2	24.03.2007	04:42	59°37.25'S	85°40.52'E	60	a
58	PS 69 898 2	24.03.2007	04:42	59°37.25'S	85°40.52'E	80	a
59	PS 69 898 2	24.03.2007	04:42	59°37.25'S	85°40.52'E	200	a
60	PS 69 898 2	24.03.2007	04:42	59°37.25'S	85°40.52'E	500	a
61	PS 69 898 2	24.03.2007	04:42	59°37.25'S	85°40.52'E	1000	a
62	PS 69 898 2	24.03.2007	04:42	59°37.25'S	85°40.52'E	1500	a
63	PS 69 898 2	24.03.2007	04:42	59°37.25'S	85°40.52'E	2000	a
64	PS 69 898 2	24.03.2007	04:42	59°37.25'S	85°40.52'E	2250	b
65	PS 69 898 2	24.03.2007	04:42	59°37.25'S	85°40.52'E	2500	a
66	PS 69 898 2	24.03.2007	04:42	59°37.25'S	85°40.52'E	3000	a
67	PS 69 898 2	24.03.2007	04:42	59°37.25'S	85°40.52'E	3500	a
68	PS 69 898 2	24.03.2007	04:42	59°37.25'S	85°40.52'E	3950	c
69	PS 69 907 1	26.03.2007	19:13	55°0.30'S	73°19.98'E	20	a
70	PS 69 907 1	26.03.2007	19:13	55°0.30'S	73°19.98'E	40	a
71	PS 69 907 1	26.03.2007	19:13	55°0.30'S	73°19.98'E	60	a
72	PS 69 907 1	26.03.2007	19:13	55°0.30'S	73°19.98'E	80	a
73	PS 69 907 1	26.03.2007	19:13	55°0.30'S	73°19.98'E	200	a
74	PS 69 907 1	26.03.2007	19:13	55°0.30'S	73°19.98'E	500	a
75	PS 69 907 1	26.03.2007	19:13	55°0.30'S	73°19.98'E	1500	a
76	PS 69 907 1	26.03.2007	19:13	55°0.30'S	73°19.98'E	2064	c
77	PS 69 912 1	28.03.2007	10:13	50°19.45'S	71°33.49'E	20	a
78	PS 69 912 1	28.03.2007	10:13	50°19.45'S	71°33.49'E	40	a
80	PS 69 912 1	28.03.2007	10:13	50°19.45'S	71°33.49'E	60	a
81	PS 69 912 1	28.03.2007	10:13	50°19.45'S	71°33.49'E	80	a
82	PS 69 912 1	28.03.2007	10:13	50°19.45'S	71°33.49'E	200	a
83	PS 69 912 1	28.03.2007	10:13	50°19.45'S	71°33.49'E	500	a
84	PS 69 912 1	28.03.2007	10:13	50°19.45'S	71°33.49'E	500	c

- a. Samples taken include chlorophyll and other pigments, nutrients, BSi and LSi, Si and N isotopes of DSi and nitrate, POC, PON, C and N isotopes on POC and PON, Fe solubility.
b. Samples taken for suspended BSi, LSi, POC, PON, and CaCO₃ only.
c. Samples taken for Th isotopes and radiocarbon only.

3. Sampling overview of water samples for the study area of *Phaeocystis Antarctica* during RV expedition ANT-XXIII/9 (see chapter 10).

No.	Date	Time (UTC)	Latitude	Longitude	Water temp. (° C)	Water depth (m)	Comments
1	04.02.07	20:02	57°49.427'S	58°26.197'W	5.81	3639	PS69/730
2	04.02.07	20:02	57°49.427'S	58°26.197'W	5.81	3639	PS69/730
3	04.02.07	20:02	57°49.427'S	58°26.197'W	5.81	3639	PS69/730
4	04.02.07	23:02	58°17.920'S	57°43.041'W	3.92	3934	PS69/731
5	04.02.07	23:02	58°17.920'S	57°43.041'W	3.92	3934	PS69/731
6	04.02.07	23:02	58°17.920'S	57°43.041'W	3.92	3934	PS69/731
7	05.02.07	02:55	58°53.743'S	56°48.185'W	3.07	3770	PS69/732
8	05.02.07	02:55	58°53.743'S	56°48.185'W	3.07	3770	PS69/732
9	05.02.07	02:55	58°53.743'S	56°48.185'W	3.07	3770	PS69/732
10	05.02.07	08:55	59°47.523'S	55°23.441'W	3.01	3672	PS69/733
11	05.02.07	08:55	59°47.523'S	55°23.441'W	3.01	3672	PS69/733
12	05.02.07	08:55	59°47.523'S	55°23.441'W	3.01	3672	PS69/733
13	05.02.07	14:57	60°43.412'S	53°53.052'W	2.06	2598	PS69/734
14	05.02.07	14:57	60°43.412'S	53°53.052'W	2.06	2598	PS69/734
15	05.02.07	14:57	60°43.412'S	53°53.052'W	2.06	2598	PS69/734
16	05.02.07	18:57	61°20.851'S	52°51.111'W	-0.11	1038	PS69/735
17	05.02.07	18:57	61°20.851'S	52°51.111'W	-0.11	1038	PS69/735
18	05.02.07	18:57	61°20.851'S	52°51.111'W	-0.11	1038	PS69/735
19	06.02.07	00:00	62°05.011'S	51°34.411'W	0.4	3050	PS69/736
20	06.02.07	00:00	62°05.011'S	51°34.411'W	0.4	3050	PS69/736
21	06.02.07	06:05	63°01.298'S	49°57.038'W	-0.1	2645	PS69/737
22	06.02.07	06:05	63°01.298'S	49°57.038'W	-0.1	2645	PS69/737
23	06.02.07	10:49	-	-	-	-	failed; flasks damaged
24	06.02.07	10:49	63°32.517'S	48°17.218'W	0.17	3465	PS69/738
25	06.02.07	10:49	63°32.517'S	48°17.218'W	0.17	3465	PS69/738
26	06.02.07	15:48	63°54.966'S	47°02.631'W	-0.25	3047	PS69/740
27	06.02.07	20:56	64°23.300'S	45°30.793'W	-0.19	4513	PS69/741
28	07.02.07	13:53	66°12.728'S	38°53.503'W	0.2	4534	PS69/742
29	08.02.07	10:50	67°27.900'S	31°57.941'W	-0.21	4671	PS69/743
30	09.02.07	12:53	68°15.936'S	20°35.739'W	0.06	4845	PS69/744
31	09.02.07	12:53	68°15.936'S	20°35.739'W	0.06	4845	PS69/744
32	10.02.07	12:52	69°12.087'S	08°16.803'W	-0.24	3772	PS69/745
33	10.02.07	12:52	69°12.087'S	08°16.803'W	-0.24	3772	PS69/745
34	14.02.07	13:05	69°55.833'S	3°43.533'W	-1.65	2287	PS69/749
35	14.02.07	13:05	69°55.833'S	3°43.533'W	-1.65	2287	PS69/749
36	14.02.07	21:34	69°34.023'S	0°35.982'W	-1.8	2253	PS69/750
37	14.02.07	21:34	69°34.023'S	0°35.982'W	-1.8	2253	PS69/750
38	15.02.07	02:10	69°26.231'S	1°16.362'E	-0.6	2402	PS69/751
39	15.02.07	02:10	69°26.231'S	1°16.362'E	-0.6	2402	PS69/751
40	15.02.07	10:58	69°25.716'S	6°02.396'E	-0.65	1726	PS69/753

No.	Date	Time (UTC)	Latitude	Longitude	Water temp. (° C)	Water depth (m)	Comments
41	15.02.07	10:58	69°25.716'S	6°02.396'E	-0.65	1726	PS69/753
42	15.02.07	21:06	69°59.324'S	9°03.444'E	-0.34	3454	PS69/755
43	15.02.07	21:06	69°59.324'S	9°03.444'E	-0.34	3454	PS69/755
44	16.02.07	07:05	68°27.410'S	13°37.834'E	0.3	2898	PS69/756
45	16.02.07	07:05	68°27.410'S	13°37.834'E	0.3	2898	PS69/756
46	16.02.07	16:55	68°17.800'S	17°4.693'E	0.28	3956	PS69/761
47	16.02.07	16:55	68°17.800'S	17°4.693'E	0.28	3956	PS69/761
48	17.02.07	00:00	68°12.242'S	19°17.055'E	0.23	4045	PS69/764
49	17.02.07	00:00	68°12.242'S	19°17.055'E	0.23	4045	PS69/764
50	17.02.07	09:55	68°00.924'S	23°45.123'E	-0.02	3991	PS69/770
51	17.02.07	09:55	68°00.924'S	23°45.123'E	-0.02	3991	PS69/770
52	17.02.07	19:55	67°51.595'S	27°24.424'E	0.01	3814	PS69/772
53	17.02.07	19:55	67°51.595'S	27°24.424'E	0.01	3814	PS69/772
54	18.02.07	06:00	67°39.686'S	32°02.551'E	-0.08	1071	PS69/774
55	18.02.07	06:00	67°39.686'S	32°02.551'E	-0.08	1071	PS69/774
56	18.02.07	16:01	67°28.009'S	36°32.742'E	-0.34	3386	PS69/776
57	18.02.07	16:01	67°28.009'S	36°32.742'E	-0.34	3386	PS69/776
58	18.02.07	21:56	67°20.385'S	39°27.788'E	0.03	3106	PS69/778
59	18.02.07	21:56	67°20.385'S	39°27.788'E	0.03	3106	PS69/778
60	19.02.07	04:00	67°12.612'S	42°25.639'E	-0.13	3177	PS69/779
61	19.02.07	04:00	67°12.612'S	42°25.639'E	-0.13	3177	PS69/779
62	19.02.07	12:56	66°55.339'S	46°00.745'E	-1.69	1203	PS68/781
63	19.02.07	12:56	66°55.339'S	46°00.745'E	-1.69	1203	PS68/781
64	19.02.07	22:58	66°06.154'S	47°39.501'E	-1.25	2231	PS69/783
65	19.02.07	22:58	66°06.154'S	47°39.501'E	-1.25	2231	PS69/783
66	20.02.07	8:04	65°24.631'S	50°40.485'E	-0.46	2836	PS69/786
67	20.02.07	8:04	65°24.631'S	50°40.485'E	-0.46	2836	PS69/786
68	20.02.07	17:01	65°22.673'S	53°49.600'E	-1.76	1618	PS68/787
69	20.02.07	17:01	65°22.673'S	53°49.600'E	-1.76	1618	PS68/787
70	21.02.07	4:58	65°41.979'S	57°28.585'E	-1.77	2753	PS69/788
71	21.02.07	4:58	65°41.979'S	57°28.585'E	-1.77	2753	PS69/788
72	21.02.07	14:59	65°54.567'S	60°07.889'E	-1.24	3124	PS69/789
73	21.02.07	14:59	65°54.567'S	60°07.889'E	-1.24	3124	PS69/789
74	22.02.07	0:00	66°03.256'S	62°47.040'E	-1.2	2993	PS69/790
75	22.02.07	0:00	66°03.256'S	62°47.040'E	-1.2	2993	PS69/790
76	22.02.07	10:59	66°17.512'S	67°08.709'E	-0.91	2803	PS69/791
77	23.02.07	0:58	66°31.196'S	72°40.685'E	-1.31	1347	PS69/792
78	24.02.07	18:02	68°43.427'S	76°40.580'E	-0.09	851	PS69/794
79	24.02.07	18:02	68°43.427'S	76°40.580'E	-0.09	851	PS69/794
80	13.03.07	0:48	67°59.381'S	73°58.259'E	-1.77	592	PS69/854
81	13.03.07	0:48	67°59.381'S	73°58.259'E	-1.77	592	PS69/854
82	16.03.07	22:11	67°30.200'S	79°29.649'E	-1.8	505	PS69/857

No.	Date	Time (UTC)	Latitude	Longitude	Water temp. (° C)	Water depth (m)	Comments
83	16.03.07	22:11	67°30.200'S	79°29.649'E	-1.8	505	PS69/857
84	19.03.07	2:28	61°45.393'S	82°49.993'E	0.66	2337	PS69/873
85	19.03.07	2:28	61°45.393'S	82°49.993'E	0.66	2337	PS69/873
86	20.03.07	21:42	65°15.373'S	82°49.950'E	-1.33	3175	PS69/875
87	20.03.07	21:42	65°15.373'S	82°49.950'E	-1.33	3175	PS69/875
88	22.03.07	1:17	64°04.789'S	82°50.014'E	-0.94	3695	damaged; rough sea
89	22.03.07	1:17	64°04.789'S	82°50.014'E	-0.94	3695	PS69/883-2
90	22.03.07	15:45	62°54.882'S	82°50.687'E	0.45	2516	damaged; rough sea
91	22.03.07	15:45	62°54.882'S	82°50.687'E	0.45	2516	PS69/889-2
92	23.03.07	15:59	60°52.030'S	83°45.085'E	0.71	1607	PS69/896
93	23.03.07	15:59	60°52.030'S	83°45.085'E	0.71	1607	PS69/896
94	23.03.07	21:41	60°00.121'S	84°40.606'E	0.28	2063	PS69/898
95	23.03.07	21:41	60°00.121'S	84°40.606'E	0.28	2063	PS69/898
96	25.03.07	2:50	58°49.674'S	83°00.672'E	0.95	1930	PS69/901
97	25.03.07	2:50	58°49.674'S	83°00.672'E	0.95	1930	PS69/901
98	25.03.07	13:00	57°51.302'S	80°47.977'E	1.2	1744	PS69/902-1
99	25.03.07	13:00	57°51.302'S	80°47.977'E	1.2	1744	PS69/902-1
100	25.03.07	22:44	56°58.602'S	78°41.310'E	1.51	1817	PS69/904
101	25.03.07	22:44	56°58.602'S	78°41.310'E	1.51	1817	PS69/904
102	26.03.07	6:37	56°09.857'S	76°27.193"E	1.12	2720	PS69/905
103	26.03.07	6:37	56°09.857'S	76°27.193"E	1.12	2720	PS69/905
104	26.03.07	14:37	55°21.926'S	74°18.118'E	2.52	2922	PS69/906
105	26.03.07	14:37	55°21.926'S	74°18.118'E	2.52	2922	PS69/906
106	27.03.07	4:34	54°09.714'S	73°42.072'E	2.43	2143	PS69/908
107	27.03.07	4:34	54°09.714'S	73°42.072'E	2.43	2143	PS69/908
108	27.03.07	12:17	52°46.614'S	74°17.718'E	3.08	199	PS69/909
109	27.03.07	12:17	52°46.614'S	74°17.718'E	3.08	199	PS69/909
110	27.03.07	22:00	51°13.231'S	73°46.784'E	3.43	418	PS69/911
111	27.03.07	22:00	51°13.231'S	73°46.784'E	3.43	418	PS69/911
112	28.03.07	11:51	50°18.553'S	71°34.154'E	4.06	552	PS69/912-2
113	28.03.07	11:51	50°18.553'S	71°34.154'E	4.06	552	PS69/912-2
114	29.03.07	5:08	49°21.857'S	70°12.409'E	6.65	33	PS69/913
115	29.03.07	5:08	49°21.857'S	70°12.409'E	6.65	33	PS69/913
116	29.03.07	17:25	50°06.882'S	69°59.156'E	4.18	189	PSS69/914
117	29.03.07	17:25	50°06.882'S	69°59.156'E	4.18	189	PSS69/914
118	30.03.07	7:04	49°58.218'S	65°55.382'E	4.56	310	PS69/915
119	30.03.07	7:04	49°58.218'S	65°55.382'E	4.56	310	PS69/915
120	31.03.07	6:24	49°32.900'S	61°47.577'E	5.43	2480	PS69/916 - snorkel
121	31.03.07	6:24	49°32.900'S	61°47.577'E	5.43	2480	PS69/916 - snorkel
122	01.04.07	0:10	47°42.976'S	58°49.770'E	8.69	4322	PS69/917
123	01.04.07	0:10	47°42.976'S	58°49.770'E	8.69	4322	PS69/917
124	01.04.07	18:12	45°59.793'S	55°42.308'E	7.8	4123	PS69/918 - snorkel

No.	Date	Time (UTC)	Latitude	Longitude	Water temp. (° C)	Water depth (m)	Comments
125	01.04.07	18:12	45°59.793'S	55°42.308'E	7.8	4123	PS69/918 - snorkel
126	02.04.07	14:44	44°18.080'S	52°43.131'E	9.43	3435	PS69/919
127	02.04.07	14:44	44°18.080'S	52°43.131'E	9.43	3435	PS69/919
128	03.04.07	8:45	43°08.971'S	49°33.901'E	8.51	2562	PS69/920
129	03.04.07	8:45	43°08.971'S	49°33.901'E	8.51	2562	PS69/920
130	04.04.07	2:00	42°44.757'S	45°34.800'E	9.97	3365	PS69/921
131	04.04.07	2:00	42°44.757'S	45°34.800'E	9.97	3365	PS69/921
132	04.04.07	19:08	42°21.662'S	41°48.057'E	13.22	3473	PS69/923
133	04.04.07	19:08	42°21.662'S	41°48.057'E	13.22	3473	PS69/923
134	05.04.07	13:07	41°37.779'S	38°02.423'E	15.58	3921	PS69/924 - snorkel
135	05.04.07	13:07	41°37.779'S	38°02.423'E	15.58	3921	PS69/924 - snorkel
136	06.04.07	7:02	41°16.588'S	34°24.477'E	17.68	4997	PS69/925
137	06.04.07	7:02	41°16.588'S	34°24.477'E	17.68	4997	PS69/925
138	07.04.07	2:25	41°03.587'S	30°39.012'E	17.65	4668	PS69/926
139	07.04.07	2:25	41°03.587'S	30°39.012'E	17.65	4668	PS69/926
140	07.04.07	18:34	40°42.511'S	27°13.370'E	15.72	2671	PS69/928
141	07.04.07	18:34	40°42.511'S	27°13.370'E	15.72	2671	PS69/928
142	08.04.07	8:21	38°15.047'S	25°48.503'E	18.08	3194	PS69/930
143	08.04.07	8:21	38°15.047'S	25°48.503'E	18.08	3194	PS69/930
144	09.04.07	0:44	36°49.938'S	23°12.055'E	23.86	4832	PS69/931
145	09.04.07	0:44	36°49.938'S	23°12.055'E	23.86	4832	PS69/931
146	09.04.07	15:42	36°00.031'S	20°00.096'E	21.05	183,4	PS69/932
147	09.04.07	15:42	36°00.031'S	20°00.096'E	21.05	183,4	PS69/932

4. Samples for exposure dating

Locality	SampleID	Longitude	Latitude	Elevation	Date	Rock	Erratics	Sand	Shell
Mosquito Island	DW-RI07-38	77°36.061' E	68°49.898' S	59	2/03/2007	1	2		
Hop Island	DW-RI07-35	77°41.302' E	68°49.178' S	32	2/03/2007	1	4		
Roadblock Island	DW-RI07-94	77°53.448' E	68°49.320' S	30	10/03/2007			1	
Filla Island	DW-RI07-5	77°46.699' E	68°48.398' S	42	1/03/2007	1	3		
Filla Island	DW-RI07-6	77°47.485' E	68°48.457' S	2	1/03/2007				1
Filla Island	DW-RI07-7	77°50.010' E	68°48.911' S	70	1/03/2007	1	2		
Filla Island	DW-RI07-13	77°53.030' E	68°48.758' S	1	1/03/2007				3
Filla Island	DW-RI07-15	77°53.909' E	68°48.536' S	46	1/03/2007	1	3		
Filla Island	DW-RI07-21	77°49.635' E	68°48.953' S	5	1/03/2007	4			
Filla Island	DW-RI07-69	77°48.608' E	68°48.839' S	18	7/03/2007	1			
Filla Island	DW-RI07-102	77°51.630' E	68°49.010' S	10	12/03/2007			2	3
Filla Island	DW-RI07-103	77°50.987' E	68°48.919' S	15	12/03/2007			1	
Filla Island	DW-RI07-105	77°51.072' E	68°48.755' S	25	12/03/2007			1	
Filla Island	DW-RI07-106	77°50.669' E	68°48.421' S	1	12/03/2007			2	
Romeo Island	DW-RI07-83	77°49.902' E	68°49.148' S	10	9/03/2007			21	
Bravo Island	DW-RI07-85	77°55.351' E	68°48.005' S	40	10/03/2007			1	
Efremova Island	DW-RI07-89	77°57.039' E	68°48.696' S	20	10/03/2007			1	
Efremova Island	DW-RI07-91	77°55.240' E	68°48.866' S	1	10/03/2007				1
Shcherbinina Island	DW-RI07-39	77°57.079' E	68°49.999' S	39	3/03/2007	1	4		
Shcherbinina Island	DW-RI07-109	77°55.867' E	68°49.925' S	18	13/03/2007	2			
Mather Peninsula	DW-RI07-41	77°56.310' E	68°50.720' S	20	3/03/2007		1		

Locality	SampleID	Longitude	Latitude	Elevation	Date	Rock	Erratics	Sand	Shell
Mather Peninsula	DW-RI07-112	77°55.986' E	68°50.851' S	30	14/03/2007	1	2		
Mather Peninsula	DW-RI07-113	77°54.933' E	68°51.048' S	90	14/03/2007	1	3		
Mather Peninsula	DW-RI07-117	77°56.224' E	68°50.914' S	50	14/03/2007		1		
Mace ^o Peninsula	DW-RI07-120	77°57.641' E	68°55.227' S	108	15/03/2007	1	1		
Mace ^o Peninsula	DW-RI07-123	77°55.857' E	68°55.285' S	124	15/03/2007		1		
Mace ^o Peninsula	DW-RI07-131	77°54.148' E	68°54.793' S	30	15/03/2007	1	1		

5. Lake sediment cores from the Rauer Group

code no.	area	latitude	longitude	elevation (m a.s.l.)	WD (cm)	penetration (cm)	date	gear
Co1001-1	Desert Lake, Filla	68°48.747' S	77°50.204' E	1.5	0	0-80	01 March	SCT
Co1001-2	Desert Lake, Filla	68°48.747' S	77°50.204' E	1.5	0	0-85	01 March	SCT
Co1001-3	Desert Lake, Filla	68°48.747' S	77°50.204' E	1.5	0	0-30	01 March	SCT
Co1002-1	Big Lake, Filla	68°48.146' S	77°52.048' E	3.1	0	0-80	01 March	SCT
Co1002-2	Big Lake, Filla	68°48.146' S	77°52.048' E	3.1	0	0-70	01 March	SCT
Co1005-1	Aquamarin Lake, Filla	68°48.901' S	77°49.670' E	-1.0	60	0-50	01 March	russian corer
Co1005-2	Aquamarin Lake, Filla	68°48.901' S	77°49.670' E	-1.0	0	0-30	08 March	SCT
Co1006-1	Hidden Lake, Filla	68°47.803' S	77°52.009' E		30	0-20	03 March	Liner
Co1006-2	Hidden Lake, Filla	68°47.828' S	77°52.021' E		18	0-25	03 March	Liner
Co1007-1	Shell Lake, Filla	68°48.603' S	77°51.161' E	5.7	0	0-60	03 March	russian corer
Co1007-2	Shell Lake, Filla	68°48.603' S	77°51.161' E	5.7	0	0-50	03 March	russian corer
Co1007-3	Shell Lake, Filla	68°48.603' S	77°51.161' E	5.7	0	0-55	03 March	russian corer
Co1008-1	Skua Lake, Filla	68°48.714' S	77°52.173' E	9.4	126	0-34	07 March	russian corer
Co1008-2	Skua Lake, Filla	68°48.714' S	77°52.173' E	9.4	126	0-33	07 March	russian corer
Co1008-3	Skua Lake, Filla	68°48.714' S	77°52.173' E	9.4	126	0-62	08 March	piston corer
Co1008-4	Skua Lake, Filla	68°48.714' S	77°52.173' E	9.4	126	0-127	08 March	piston corer
Co1008-5	Skua Lake, Filla	68°48.714' S	77°52.173' E	9.4	126	0-153	09 March	piston corer
Co1008-6	Skua Lake, Filla	68°48.714' S	77°52.173' E	9.4	126	100-231	10 March	piston corer
Co1009-1	Big Hop Lake, Hop	68°49.417' S	77°42.143' E		0	0-60	02 March	SCT
Co1012-1	Lagoon Lake, Filla	68°48.076' S	77°51.159' E	1.2	0	0-75	04 March	SCT
Co1013-1	Fork Valley Lake, Filla	68°48.892' S	77°51.353' E	6.6	34	0-46	07 March	russian corer
Co1013-2	Fork Valley Lake, Filla	68°48.892' S	77°51.353' E	6.6	34	0-50	07 March	russian corer
Co1013-3	Fork Valley Lake, Filla	68°48.892' S	77°51.353' E	6.6	34	0-25	09 March	piston corer
Co1015-1	Dead Seal Lake, Filla	68°48.338' S	77°51.297' E	2.5	0	0-50	04 March	SCT
Co1015-2	Dead Seal Lake, Filla	68°48.338' S	77°51.297' E	2.5	0	0-50	04 March	SCT

WD – water depth; SCT – spade coring technique

6. List of cores from marine basins in the Rauer Group

core no.	area	latitude	longitude	WD	penetration	date	type
Co1010-1	Filla Island	68°48.142' S	077°53.355' E	38.0 m	0-116 cm	01 March	GC
Co1010-2	Filla Island	68°48.142' S	077°53.355' E	38.0 m	0-111 cm	01 March	GC
Co1010-3	Filla Island	68°48.142' S	077°53.355' E	38.0 m	0-113 cm	01 March	GC
Co1010-4	Filla Island	68°48.142' S	077°53.355' E	38.0 m	0-116 cm	02 March	GC
Co1010-5	Filla Island	68°48.142' S	077°53.355' E	38.0 m	50-345 cm	02 March	PC
Co1010-6	Filla Island	68°48.142' S	077°53.355' E	38.0 m	250-550 cm	02 March	PC
Co1010-7	Filla Island	68°48.142' S	077°53.355' E	38.0 m	450-746 cm	03 March	PC
Co1010-8	Filla Island	68°48.142' S	077°53.355' E	38.0 m	650-948 cm	03 March	PC
Co1010-9	Filla Island	68°48.142' S	077°53.355' E	38.0 m	850-1148 cm	03 March	PC
Co1010-10	Filla Island	68°48.142' S	077°53.355' E	38.0 m	1050-1346 cm	04 March	PC
Co1010-11	Filla Island	68°48.142' S	077°53.355' E	38.0 m	1250-1546 cm	04 March	PC
Co1010-12	Filla Island	68°48.142' S	077°53.355' E	38.0 m	1450-1732 cm	04 March	PC
Co1010-13	Filla Island	68°48.142' S	077°53.355' E	38.0 m	1650-1947 cm	07 March	PC
Co1010-14	Filla Island	68°48.142' S	077°53.355' E	38.0 m	1850-2137 cm	07 March	PC
Co1010-15	Filla Island	68°48.142' S	077°53.355' E	38.0 m	0-112 cm	08 March	GC
Co1010-16	Filla Island	68°48.142' S	077°53.355' E	38.0 m	2050-2332 cm	08 March	PC
Co1011-1	Flag Island	68°49.563' S	077°46.293' E	7.8 m	0-78 cm	10 March	GC
Co1011-2	Flag Island	68°49.563' S	077°46.293' E	7.8 m	0-80 cm	10 March	GC
Co1011-3	Flag Island	68°49.563' S	077°46.293' E	7.8 m	0-296 cm	10 March	PC
Co1011-4	Flag Island	68°49.563' S	077°46.293' E	7.8 m	240-533 cm	10 March	PC
Co1011-5	Flag Island	68°49.563' S	077°46.293' E	7.8 m	480-777 cm	11 March	PC
Co1011-6	Flag Island	68°49.563' S	077°46.293' E	7.8 m	675-969 cm	11 March	PC
Co1011-7	Flag Island	68°49.563' S	077°46.293' E	7.8 m	860-1099 cm	13 March	PC
Co1014-1	Shcherbinina Island	68°49.984' S	077°55.574' E	6.3 m	0-45 cm	15 March	GC
Co1014-2	Shcherbinina Island	68°49.984' S	077°55.574' E	6.3 m	0-56 cm	15 March	GC

core no.	area	latitude	longitude	WD	penetration	date	type
Co1014-3	Shcherbinina Island	68°49.984' S	077°55.574' E	6.3 m	0-47 cm	15 March	GC
Co1014-4	Shcherbinina Island	68°49.984' S	077°55.574' E	6.3 m	0-262 cm	15 March	PC
Co1014-5	Shcherbinina Island	68°49.984' S	077°55.574' E	6.3 m	0-149 cm	15 March	PC
Co1014-6	Shcherbinina Island	68°49.984' S	077°55.574' E	6.3 m	0-253 cm	15 March	PC

WD = water depth, GC = gravity corer, PC = piston corer

7. Microbiological samples

Sample ID	Date	Area	Sample Type	Latitude	Longitude
17005	01.03.07	Larsemann Hills	sediment sample	69°24.135' S	76°20.296' E
17006	01.03.07	Larsemann Hills	sediment sample		
17007	01.03.07	Larsemann Hills	sediment sample		
17008	01.03.07	Larsemann Hills	sediment sample	69°24.137' S	76°20.273' E
17009	01.03.07	Larsemann Hills	sediment sample		
17010	01.03.07	Larsemann Hills	sediment sample		
17011	01.03.07	Larsemann Hills	sediment sample	69°24.137' S	76°20.258' E
17012	01.03.07	Larsemann Hills	sediment sample		
17013	01.03.07	Larsemann Hills	sediment sample	69°24.139' S	76°20.222' E
17014	01.03.07	Larsemann Hills	sediment sample		
17015	01.03.07	Larsemann Hills	sediment sample	69°24.140' S	76°20.178' E
17016	01.03.07	Larsemann Hills	sediment sample		
17017	01.03.07	Larsemann Hills	sediment sample		
17018	01.03.07	Larsemann Hills	sediment sample	69°24.221' S	76°20.813' E
17019	01.03.07	Larsemann Hills	sediment sample		
17020	01.03.07	Larsemann Hills	sediment sample	69°24.245' S	76°20.011' E
17021	01.03.07	Larsemann Hills	sediment sample		
17022	01.03.07	Larsemann Hills	sediment sample	69°24.228' S	76°20.566' E
17023	01.03.07	Larsemann Hills	sediment sample		
17024	01.03.07	Larsemann Hills	sediment sample		
17025	01.03.07	Larsemann Hills	sediment sample	69°24.315' S	76°20.295' E
17026	01.03.07	Larsemann Hills	sediment sample		
17027	01.03.07	Larsemann Hills	sediment sample	69°24.326' S	76°20.273' E
17028	01.03.07	Larsemann Hills	sediment sample		
17029	02.03.07	Larsemann Hills	sediment sample	69°24.104' S	76°20.485' E
17030	02.03.07	Larsemann Hills	sediment sample		
17031	02.03.07	Larsemann Hills	sediment sample		
17032	02.03.07	Larsemann Hills	sediment sample		
17033	02.03.07	Larsemann Hills	sediment sample	69°24.097' S	76°20.448' E
17034	02.03.07	Larsemann Hills	sediment sample		
17035	02.03.07	Larsemann Hills	sediment sample		
17036	02.03.07	Larsemann Hills	sediment sample	69°24.086' S	76°20.403' E
17037	02.03.07	Larsemann Hills	sediment sample		
17038	03.03.07	Larsemann Hills	sediment sample	69°24.076' S	76°20.402' E
17039	03.03.07	Larsemann Hills	sediment sample		
17040	03.03.07	Larsemann Hills	sediment sample		
17041	03.03.07	Larsemann Hills	sediment sample		
17042	03.03.07	Larsemann Hills	sediment sample		
17043	03.03.07	Larsemann Hills	sediment sample		
17044	03.03.07	Larsemann Hills	sediment sample		
17045	03.03.07	Larsemann Hills	sediment sample		
17046	03.03.07	Larsemann Hills	sediment sample		
17047	03.03.07	Larsemann Hills	sediment sample		

Sample ID	Date	Area	Sample Type	Latitude	Longitude
17048	03.03.07	Larsemann Hills	sediment sample		
17049	04.03.07	Larsemann Hills	surface sample	69°23.159' S	76°18.337' E
17050	04.03.07	Larsemann Hills	surface sample	69°23.563' S	76°19.551' E
17051	04.03.07	Larsemann Hills	surface sample		
17052	07.03.07	Larsemann Hills	sediment sample	69°23.808' S	76°19.494' E
17053	07.03.07	Larsemann Hills	sediment sample		
17054	07.03.07	Larsemann Hills	sediment sample	69°23.749' S	76°19.628' E
17055	07.03.07	Larsemann Hills	sediment sample		
17056	07.03.07	Larsemann Hills	sediment sample	69°23.747' S	76°19.622' E
17057	07.03.07	Larsemann Hills	sediment sample		
17058	08.03.07	Larsemann Hills	sediment sample	69°23.680' S	76°19.808' E
17059	08.03.07	Larsemann Hills	sediment sample		
17060	08.03.07	Larsemann Hills	sediment sample	69°23.681' S	76°19.811' E
17061	08.03.07	Larsemann Hills	sediment sample		
17062	09.03.07	Larsemann Hills	sediment sample	69°23.674' S	76°19.894' E
17063	09.03.07	Larsemann Hills	sediment sample		
17064	09.03.07	Larsemann Hills	sediment sample	69°23.671' S	76°19.924' E
17065	09.03.07	Larsemann Hills	sediment sample		
17066	09.03.07	Larsemann Hills	sediment sample	69°23.662' S	76°20.162' E
17067	09.03.07	Larsemann Hills	sediment sample		
17068	09.03.07	Larsemann Hills	sediment sample		
17069	07.03.07	Larsemann Hills	sediment sample	69°23.800' S	76°19.688' E
17070	07.03.07	Larsemann Hills	sediment sample		
17071	07.03.07	Larsemann Hills	sediment sample		
17072	08.03.07	Larsemann Hills	sediment sample	69°23.790' S	76°19.678' E
17073	08.03.07	Larsemann Hills	sediment sample		
17074	07.03.07	Larsemann Hills	sediment sample	69°23.778' S	76°19.665' E
17075	07.03.07	Larsemann Hills	sediment sample		
17076	09.03.07	Larsemann Hills	surface sample	69°23.636' S	76°20.144' E
17077	09.03.07	Larsemann Hills	surface sample	69°23.620' S	76°20.015' E
17078	11.03.07	Larsemann Hills	surface sample	69°23.821' S	76°19.397' E
17079	11.03.07	Larsemann Hills	surface sample	69°23.775' S	76°19.514' E
17080	11.03.07	Larsemann Hills	surface sample	69°23.773' S	76°19.524' E
17081	11.03.07	Larsemann Hills	surface sample	69°23.770' S	76°19.563' E
17082	11.03.07	Larsemann Hills	surface sample	69°23.696' S	76°19.731' E
17083	11.03.07	Larsemann Hills	surface sample	69°23.696' S	76°19.731' E
17084	11.03.07	Larsemann Hills	surface sample	69°23.689' S	76°19.763' E
17085	11.03.07	Larsemann Hills	surface sample	69°23.665' S	76°19.913' E
17086	11.03.07	Larsemann Hills	surface sample	69°23.667' S	76°19.898' E
17087	12.03.07	Larsemann Hills	surface sample	69°24.067' S	76°20.382' E
17088	12.03.07	Larsemann Hills	surface sample	69°24.010' S	76°20.162' E
17089	12.03.07	Larsemann Hills	surface sample	69°24.035' S	76°20.345' E
17090	12.03.07	Larsemann Hills	surface sample	69°24.050' S	76°20.267' E
17091	12.03.07	Larsemann Hills	surface sample	69°24.078' S	76°20.436' E
17092	12.03.07	Larsemann Hills	surface sample	69°24.073' S	76°20.464' E

Sample ID	Date	Area	Sample Type	Latitude	Longitude
17093	12.03.07	Larsemann Hills	surface sample	69°24.128' S	76°20.376' E
17094	12.03.07	Larsemann Hills	surface sample	69°24.276' S	76°20.411' E
17095	12.03.07	Larsemann Hills	surface sample	69°24.356' S	76°20.188' E
17096	12.03.07	Larsemann Hills	surface sample	69°24.361' S	76°20.118' E
17097	11.03.07	Larsemann Hills	surface sample		
17098	11.03.07	Larsemann Hills	surface sample	69°23.440' S	76°15.077' E
17099	11.03.07	Larsemann Hills	surface sample	69°23.601' S	76°15.108' E
17100	11.03.07	Larsemann Hills	surface sample	69°23.605' S	76°15.021' E
17101	11.03.07	Larsemann Hills	surface sample	69°23.605' S	76°15.021' E
17102	11.03.07	Larsemann Hills	surface sample	69°23.561' S	76°15.006' E
17103	14.03.07	Filla Is. (Rauer Group)	sediment sample	68°48.093' S	77°51.165' E
17104	14.03.07	Filla Is. (Rauer Group)	sediment sample		
17105	14.03.07	Filla Is. (Rauer Group)	sediment sample		
17106	14.03.07	Filla Is. (Rauer Group)	sediment sample		
17107	14.03.07	Filla Is. (Rauer Group)	sediment sample		
17108	14.03.07	Filla Is. (Rauer Group)	sediment sample	68°48.415' S	77°51.403' E
17109	14.03.07	Filla Is. (Rauer Group)	sediment sample	68°48.415' S	77°51.381' E
17110	14.03.07	Filla Is. (Rauer Group)	sediment sample		
17111	14.03.07	Filla Is. (Rauer Group)	sediment sample	68°48.412' S	77°51.373' E
17112	14.03.07	Filla Is. (Rauer Group)	sediment sample		
17113	14.03.07	Filla Is. (Rauer Group)	sediment sample		
17114	14.03.07	Filla Is. (Rauer Group)	sediment sample		
17115	14.03.07	Filla Is. (Rauer Group)	sediment sample		
17116	14.03.07	Filla Is. (Rauer Group)	sediment sample		
17117	15.03.07	Filla Is. (Rauer Group)	surface sample	68°48.449' S	77°51.353' E
17118	15.03.07	Filla Is. (Rauer Group)	sediment sample	68°48.555' S	77°51.205' E
17119	15.03.07	Filla Is. (Rauer Group)	sediment sample		
17120	15.03.07	Filla Is. (Rauer Group)	sediment sample		
17121	15.03.07	Filla Is. (Rauer Group)	sediment sample		
17122	15.03.07	Filla Is. (Rauer Group)	sediment sample		
17123	15.03.07	Filla Is. (Rauer Group)	sediment sample		
17124	15.03.07	Filla Is. (Rauer Group)	sediment sample	68°48.642' S	77°51.148' E
17125	15.03.07	Filla Is. (Rauer Group)	sediment sample		
17126	15.03.07	Filla Is. (Rauer Group)	sediment sample	68°48.753' S	77°51.126' E
17127	15.03.07	Filla Is. (Rauer Group)	sediment sample		
17128	15.03.07	Filla Is. (Rauer Group)	sediment sample		
17129	16.03.07	Filla Is. (Rauer Group)	sediment sample	68°48.442' S	77°47.552' E
17130	16.03.07	Filla Is. (Rauer Group)	sediment sample		
17131	16.03.07	Filla Is. (Rauer Group)	sediment sample		
17132	16.03.07	Filla Is. (Rauer Group)	sediment sample		
17133	16.03.07	Filla Is. (Rauer Group)	sediment sample		
17134	16.03.07	Filla Is. (Rauer Group)	sediment sample		
17135	16.03.07	Filla Is. (Rauer Group)	sediment sample		
17136	16.03.07	Filla Is. (Rauer Group)	sediment sample	68°48.444' S	77°47.749' E
17137	16.03.07	Filla Is. (Rauer Group)	sediment sample		

Sample ID	Date	Area	Sample Type	Latitude	Longitude
17138	16.03.07	Filla Is. (Rauer Group)	sediment sample	68°48.455' S	77°47.452' E
17139	16.03.07	Filla Is. (Rauer Group)	sediment sample		
17140	16.03.07	Filla Is. (Rauer Group)	sediment sample	68°48.349' S	77°46.893' E
17141	16.03.07	Filla Is. (Rauer Group)	sediment sample		
17142	16.03.07	Filla Is. (Rauer Group)	surface sample	68°48.338' S	77°46.904' E
Core 1	15.03.07	Filla Is. (Rauer Group)	sediment core	68°48.45' S	77°51.35' E
Core 2	15.03.07	Filla Is. (Rauer Group)	sediment core	68°48.434' S	77°51.338' E
Lake 3	15.03.07	Filla Is. (Rauer Group)	water sample	68°48.45' S	77°51.35' E

A.6 GRAPHICAL CORE DESCRIPTION

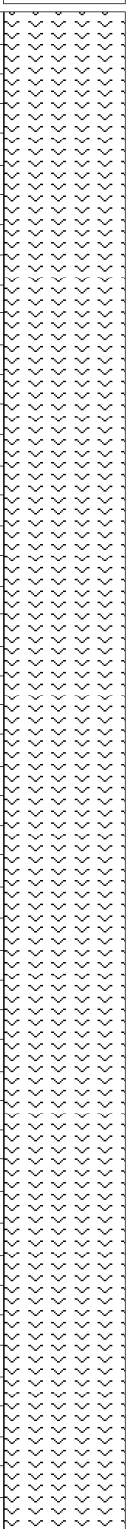

Core ID: PS69/793-2	Latitude: 68° 00.700`S	Cruise: ANT-XXIII/9
Recovery: 4.65 m	Longitude: 72° 53.310`E	Water Depth: 703 m

Lithology	Struct.	Color	Description	Age
			0 - 80 cm: Diatomaceous ooze without stratification and bioturbation Smearslide: 40 cm	
		5Y5/3		
		5Y5/3 to 2.5Y4/1	80 - 100 cm: Transition zone from Diatomaceous ooze to Mud Color ranging from olive to dark gray Smearslide: 90 cm	
		2.5Y4/1	100 - 465 cm: Mud without stratification and bioturbation Smearslide: 280 cm	
			105 cm: dropstone, Ø 50 mm 110 cm: dropstone, Ø 15 mm 177 cm: dropstone, Ø 10 mm 186 cm: dropstone, Ø 5 mm 196 cm: dropstone, Ø 5 mm 207 cm: dropstone, Ø 15 mm 210 cm: dropstone, Ø 10 mm 222 cm: dropstone, Ø 5 mm 237 cm: dropstone, Ø 40 mm 247 cm: dropstone, Ø 30 mm 261 cm: dropstone, Ø 10 mm 298 cm: dropstone, Ø 5 mm 300 cm: dropstone, Ø 5 mm 319 cm: dropstone, Ø 10 mm 362 cm: dropstone, Ø 15 mm 374 cm: dropstone, Ø 20 mm 380 cm: dropstone, Ø 10 mm 384 cm: dropstone, Ø 15 mm 402 cm: dropstone, Ø 20 mm 427 cm: dropstone, Ø 10 mm 451 cm: dropstone, Ø 20 mm	

Core ID: PS69/794-3	Latitude: 68° 43.280`S	Cruise: ANT-XXIII/9
Recovery: 10.04 m	Longitude: 76° 40.700`E	Water Depth: 831 m

Lithology	Struct.	Color	Description	Age
		5Y4/3 to 3Y3/1	0 - 30 cm: Diatomaceous ooze ("Cotton ooze") slightly to moderately mottled	
		5Y4/3	30 - 102 cm: Diatomaceous ooze well laminated	
		5Y5/3 and 5Y4/2	102 - 132 cm: slightly mottled section	
		5Y4/3	132 - 152 cm: laminated to layered section	
		5Y4/3	152 - 187 cm: slightly mottled section	
		and 5Y3/2	187 - 200 cm: moderately mottled section	
		5Y5/3	200 - 230 cm: slightly mottled section	
			230 - 247 cm: moderately mottled with blurred laminations	
			247 - 257 cm: slightly mottled section	
			257 - 270 cm: laminated section	
			270 - 294 cm: slightly mottled section	
			294 - 337 cm: slightly mottled, slightly layered to laminated	
	337 - 369 cm: slightly mottled section			
	369 - 483 cm: laminated to slightly layered section			

Core ID: PS69/794-3	Latitude: 68° 43.280`S	Cruise: ANT-XXIII/9
Recovery: 10.04 m	Longitude: 76° 40.700`E	Water Depth: 831 m

Lithology	Struct.	Color	Description	Age
5			5Y6/3 524 - 1004 cm: Diatomaceous ooze layered to laminated very significant "Cotton ooze" lens at top (524 - 529 cm) "Cotton ooze" layers at: 534 - 538 cm 558 - 564 cm 593 - 611 cm 625 - 629 cm 639 - 645 cm 660 - 685 cm	
6		5Y4/3 and 5Y3/2		
7				
8				
9			872 - 912 cm: "Cotton ooze"	
10		5Y4/3	925 cm: bivalve, Ø 1 mm 936 cm: some bivalve, Ø 1 mm	

Core ID: PS69/820-3	Latitude: 60° 56.940`S	Cruise: ANT-XXIII/9
Recovery: 13.92 m	Longitude: 72° 43.410`E	Water Depth: 4160 m

Lithology	Struct.	Color	Description	Age
	10YR6/3		0 - 14 cm: Diatomaceous mud to Diatomaceous ooze slightly mottled, no stratification Smearslide: 7 cm	
	10YR5/4		14 - 178 cm: Diatomaceous mud slightly to strongly mottled manganese encrusted dropstones at: 35 cm, Ø 35 mm 40 cm, Ø 5 mm 85 cm, Ø 5 mm 128 cm: manganese nodule, Ø 15 mm Smearslide: 60 cm	
	2.5Y8/2		120 - 150 cm: strongly mottled to bioturbated with patches of pale brown	
	10YR6/3			
	10YR7/3		178 - 182 cm: Diatomaceous mud to Diatomaceous ooze slightly mottled	
			182 - 1000 cm: Diatomaceous mud slightly to strongly mottled 200 - 210 cm: moderately mottled 234 cm: manganese nodule, Ø 20 mm 237 cm: manganese nodule, Ø 35 mm	
	10YR5/4			
			338 cm: manganese nodule, Ø 5 mm 345 - 450 cm: moderately mottled 405 cm: manganese nodule, Ø 5 mm 433 cm: manganese nodule, Ø 5 mm 435 cm: manganese nodule, Ø 5 mm	
			466 cm: manganese nodule, Ø 5mm	

Core ID: PS69/820-3	Latitude: 60° 56.940`S	Cruise: ANT-XXIII/9
Recovery: 13.92 m	Longitude: 72° 43.410`E	Water Depth: 4160 m

Lithology	Struct.	Color	Description	Age
5	10YR5/4		182 - 1000 cm: Diatomaceous mud slightly to strongly mottled	
			500 cm: manganese nodule, Ø 35 mm	
			562 cm: manganese nodule, Ø 5 mm	
6			599 cm: manganese nodule, Ø 35 mm	
			648 cm: manganese nodule, Ø 5 mm	
			680 cm: manganese nodule, Ø 15 mm	
7			708 cm: mangan encrusted quartz, Ø 45 mm	
			724 cm: 3 gravels, Ø 5 mm	
			737 cm: dropstone, Ø 5mm	
			752 cm: dropstone, Ø 5 mm	
			756 cm: dropstone, Ø 5 mm	
			770 cm: dropstone, Ø 5 mm	
			772 cm: dropstone, Ø 5 mm	
			777 cm: manganese nodule, Ø 15 mm	
			783 cm: manganese nodule, Ø 10 mm	
8			794 cm: dropstone, manganese encrusted, Ø 35 mm	
			831 cm: manganese nodule, Ø 10 mm	
			860 cm: dropstone, manganese encrusted, Ø 45 mm	
			866 cm: manganese nodule, Ø 5 mm	
			868 cm: manganese nodule, Ø 5 mm	
9				
			901 cm: dropstone, Ø 5 mm	
10				

Core ID: PS69/820-3	Latitude: 60° 56.940`S	Cruise: ANT-XXIII/9
Recovery: 13.92 m	Longitude: 72° 43.410`E	Water Depth: 4160 m

Lithology	Struct.	Color	Description	Age
10	10Y5/4		1000 - 1020 cm: Diatomaceous mud to Diatomaceous ooze "Cotton ooze" slightly mottled	
	2.5Y5/2		Smearslide: 1013 cm	
11	10YR4/4		1020 - 1062 cm: Diatom-bearing mud slightly mottled 1047 cm: mangan-encrusted dropstone, Ø 30 mm 1051 cm: mangan-encrusted dropstone, Ø 30 mm 1057 cm: mangan-encrusted dropstone, Ø 25 mm Smearslide: 1044 cm	
	10YR5/3		1062 - 1392 cm: Diatom-bearing mud slightly to moderately mottled Smearslide: 1083 cm 1122 - 1128 cm: sediment clasts of "Cotton ooze" very pale brown 1128 cm: mangan-encrusted dropstone, Ø 8 mm 1145 cm: mangan-encrusted dropstone, Ø 8 mm 1163 cm: mangan-encrusted dropstone, Ø 5 mm 1177 cm: mangan-encrusted dropstone, Ø 10 mm	
12			1215 cm: dropstone, Ø 3 mm 1222 cm: dropstone, Ø 4 mm 1231 cm: mangan-encrusted dropstone, Ø 10 mm 1243 cm: dropstone, Ø 10 mm 1245 - 1256 cm: sediment clasts of "Cotton ooze" very pale brown 1263 cm: dropstone, Ø 4 mm 1282 cm: dropstone, Ø 4 mm	
			1308 cm: dropstone, Ø 3 mm	
13				
14				
15				

Core ID: PS69/852-1 Latitude: 66° 04.090`S Cruise: ANT-XXIII/9
 Recovery: 6.37 m Longitude: 69° 10.160`E Water Depth: 2268 m

Lithology	Struct.	Color	Description	Age
		<p>5Y5/2</p> <p>5Y5/2 to 10YR4/2 to 2.5Y6/3</p> <p>2.5Y6/3</p> <p>2.5Y4/2</p> <p>10YR3/1</p> <p>2.5Y4/2</p> <p>10YR3/1</p> <p>2.5Y3/2</p> <p>2.5Y4/2</p> <p>2.5Y5/3 to 2.5Y4/2</p>	<p>0 - 78 cm: Sandy mud with some diatoms and radiolarians</p> <p>0 - 58 cm: slightly mottled</p> <p>5, 13, 16, 27 cm: dropstone, ø 10 mm</p> <p style="text-align: right;">Smearslide: 17 cm</p> <p>29 cm: dropstone, ø 25 mm</p> <p>35 cm: dropstone (quartz), ø 5 mm</p> <p>52 cm: dropstone, ø 25 mm</p> <p>58 - 78 cm: Transition zone with color ranging from olive gray to dark grayish brown to light yellowish gray</p> <p style="text-align: right;">Smearslide: 66 cm</p> <p>71 cm: dropstone, ø 20 mm</p> <p>78 - 197 cm: Sandy mud with some diatoms slightly mottled</p> <p style="text-align: right;">Smearslide: 98 cm</p> <p>92 cm: dropstone, ø 10 mm</p> <p>93 cm: dropstone, ø 10 mm</p> <p>98 cm: dropstone, ø 15 mm</p> <p>109 cm: dropstone, ø 20 mm</p> <p>115 cm: dropstone, ø 25 mm</p> <p>123 cm: dropstone, ø 5 mm</p> <p>132 cm: dropstone, ø 15 mm</p> <p>135 cm: dropstone, ø 20 mm</p> <p>140 cm: dropstone, ø 15 mm</p> <p>156 cm: dropstone, ø 30 mm</p> <p>172 cm: dropstone, ø 10 mm</p> <p>177 cm: dropstone, ø 20 mm</p> <p>179 cm: dropstone, ø 30 mm</p> <p>182 cm: dropstone layer (ø 25 mm, 15 mm, 60 mm)</p> <p>186 cm: dropstone, ø 10 mm</p> <p>196 cm: dropstone, ø 15 mm</p> <p>197 - 394 cm: Mud with minor sand</p> <p style="text-align: right;">Smearslides: 248 cm</p> <p>197 - 303 cm: moderately mottled</p> <p style="text-align: right;">261 cm</p> <p>258 - 264 cm: sediment clast (dry and stiff sandy mud)</p> <p>303 - 341 cm: slightly mottled</p> <p>328 cm: dropstone, ø 15 mm</p> <p>330 cm: sediment clast (very dark gray)</p> <p>341 - 357 cm: poorly layered section</p> <p>357 - 394 cm: slightly layered</p> <p>369 cm: dropstone, ø 60 mm</p> <p>377 - 384 cm: section of very dry and stiff sandy mud</p> <p style="text-align: right;">Smearslide: 381 cm</p> <p>384 cm: dropstone, ø 10 mm</p> <p>394 - 418 cm: Mud (silty clay)</p> <p>Transition zone from light olive brown to dark grayish brown</p> <p>slightly to moderately mottled</p> <p>395 cm: dropstone, ø 10 mm</p>	

Core ID: PS69/852-1	Latitude: 66° 04.090`S	Cruise: ANT-XXIII/9
Recovery: 6.37 m	Longitude: 69° 10.160`E	Water Depth: 2268 m

Lithology	Struct.	Color	Description	Age
5			418 - 569 cm: Mud (silty clay) Smearslices: 483 cm 418 - 465 cm: slightly mottled 455 cm 465 - 500 cm: moderately mottled	
	10YR4/2 2.5Y3/2		500 - 525 cm: strongly mottled 501 cm: dropstone, ø 5 mm 521 cm: dropstone, ø 50 mm	
	10YR4/2 to 2.5Y3/2		525 - 544 cm: moderately mottled	
	2.5Y3/1		544 - 549 cm: consolidated section 549 - 569 cm: poorly laminated	
6			569 - 582 cm: Sandy mud Smearslice: 575 cm 569 cm: dropstone, ø 25 mm (quartz)	
	10YR3/2 to 5Y5/2 to 2.5Y4/2		582 - 637 cm: Mud with minor sand Smearslice: 593 cm moderately mottled 582 - 606 cm: Transition from very dark grayish brown to olive gray to dark grayish brown	
	2.5Y5/3		606 cm: very thin black layer	
	2.5Y4/1		625 - 637 cm: disturbed core catcher sediment	
7				
8				
9				
10				

Core ID: PS69/853-1 Latitude: 65° 59.870`S Cruise: ANT-XXIII/9
 Recovery: 9.39 m Longitude: 69° 13.090`E Water Depth: 2364 m

Lithology	Struct.	Color	Description	Age	
			0 - 143 cm: Sandy mud with minor radiolarians slightly to strongly mottled Smearslides: 15 cm 88 cm 20 cm, dropstone, ø 10 mm 35 cm, dropstone, ø 5 mm 38 cm, dropstone, ø 15 mm 41 cm, dropstone, ø 30 mm 48 cm, dropstone, ø 10 mm 86 cm, dropstone, ø 5 mm 111 cm, dropstone, ø 15 mm		
			5Y4/2	111-112 cm: sandy layer, fining upwards	
			▲ 5Y4/2 to 10YR3/2	143 - 208 cm: Mud (silty clay) strongly mottled Smearslide: 155 cm 165 - 171 cm: Sediment clasts (fine sand) 173 - 178 cm Sediment clasts (fine sand) 149 cm: dropstone, ø 5 mm 183 cm: dropstone, ø 5 mm	
			10YR4/2 2.5YR4/1 5Y5/2	208 - 237 cm: Sandy mud slightly to moderately mottled Smearslide: 220 cm 234 cm: dropstone, ø 5 mm 227 - 234 cm: sediment clast (fine sand)	
			5Y4/2	237 - 405 cm: Mud (silty clay) Smearslides: 250 cm 237 - 271: layered section 264 cm 263 - 266 cm: sandy layer 352 cm	
			5Y5/2 5Y3/2 10YR4/2 10YR4/1	271 - 304 cm: slightly mottled 285 cm: dropstone, ø 10 mm	
			2.5Y4/2	304 - 380 cm: poorly layered section 330 cm: sandy layer	
			2.5Y3/1 to 2.5Y4/1	380 - 405 cm: Transition zone from gray to reddish brown to dark brown, sharp boundary at top	
			5Y4/1	381 cm: dropstone, ø 60 mm Smearslide: 394 cm	
			7.5YR4/2	405 - 530 cm: Mud (silty clay), with some sand slightly mottled 465 cm: dropstone, ø 20 mm 513 cm: dropstone, ø 60 mm 528 - 536 cm: sediment clasts (up to ø 20 mm)	
10Y4/2	Smearslide: 483 cm				

Core ID: PS69/853-1		Latitude: 65° 59.870`S		Cruise: ANT-XXIII/9	
Recovery: 9.39 m		Longitude: 69° 13.090`E		Water Depth: 2364 m	
Lithology	Struct.	Color	Description	Age	
		10Y4/2	530 - 615 cm: Sandy mud slightly mottled to poorly layered 576 cm: dropstone, ø 10 mm 589 cm: dropstone, ø 20 mm 590 cm: dropstone, ø 15 mm 593 cm: dropstone, ø 5 mm 597 cm: dropstone, ø 5 mm 602, 603 cm: dropstones, ø 5-10mm 605 cm: dropstone, ø 15 mm	Smearslide: 559 cm	
		10Y4/2 5G4/2 2.5YR5/1	615 - 630 cm: Mud (silty clay) Transition zone from gray to brown to dark gray slightly laminated, sharp boundary at base, normal fault	Smearslide: 622 cm	
		10YR4/1 5YR4/2 10YR3/1	630 - 657 cm: Sandy mud 639 cm: dropstone, ø 10 mm 642 cm: dropstone, ø 10 mm	Smearslide: 635 cm	
		10Y5/2 2.5Y4/1 2.5YR5/3	657 - 670 cm : Transition zone from dark gray to reddish brown, sharp boundary at base, normal fault 662 cm: dropstone, ø 20 mm		
		2.5Y6/3 10Y6/2 2.5Y5/2 2.5YR5/3 2.5YR5/1	670 - 860 cm: Sandy mud 670 - 683 cm: slightly mottled 673 cm: dropstone, ø 5 mm 682 cm: dropstone, ø 10 mm 683 - 729 cm: slightly to moderately mottled 723 cm: dropstone, ø 10 mm 729 - 780 cm: moderately to strongly mottled 758 cm: dropstone, ø 40 mm 762 cm: dropstone, ø 20 mm 780 - 860 cm: slightly to moderately mottled 831 cm: dropstone, ø 25 mm	Smearslide: 710 cm	
		10Y6/2 5Y5/1	860 - 880 cm: Clay Transition zone from reddish gray to very dark gray slightly mottled, poorly laminated sharp boundary at base, normal fault	Smearslide: 876 cm	
		2.5YR5/1 to N3/1 7.5YR5/1 to 5Y4/1 10Y5/2	880 - 915 cm: Transition zone from gray to dark gray slightly mottled, poorly stratified normal fault at base		
			915 - 939 cm: Sandy mud slightly mottled, poorly stratified	Smearslide: 921 cm	

Core ID: PS69/890-1 Recovery: 7.47 m	Latitude: 62° 46.230`S Longitude: 82° 49.910`E	Cruise: ANT-XXIII/9 Water Depth: 2259 m
--	---	---

Lithology	Struct.	Color	Description	Age
	2.5Y8/3 and 2.5Y7/4		0 - 20 cm: Diatom-bearing nannofossil foraminiferal ooze with some radiolarians slightly layered Smear slide: 13 cm	
	2.5Y7/3		20 - 96 cm: Foraminiferal ooze with some diatoms moderately mottled 61 cm: dropstone, Ø 5 mm 81 cm: dropstone, Ø 45 mm 87 cm: dropstone, Ø 10 mm 88 cm: dropstone, Ø 5 mm 94 cm: dropstone, Ø 5 mm Smear slide: 44 cm	
	2.5Y8/2		96 - 536 cm: Diatom-bearing nannofossil foraminiferal ooze no texture to strongly mottled 96 - 223 cm: without texture 102 cm: dropstone, Ø 5 mm 125 cm: dropstone, Ø 5 mm 136 cm: dropstone, Ø 5 mm 174 cm: dropstone, Ø 5 mm	
	2.5Y7/2		204 cm: dropstone, Ø 20 mm 223 - 272 cm: slightly mottled	
	2.5Y8/2 and 2.5Y6/3		267 cm: dropstones, (quartz, mangan-encrusted) with Ø 20 mm, Ø 15 mm 272 - 288 cm: strongly mottled Smear slide: 290 cm 288 - 338 cm: moderately mottled	
	2.5Y8/2 and 2.5Y7/3		306 cm: dropstone, Ø 5 mm 308 cm: dropstone, Ø 10 mm	
	2.5Y7/3		338 - 365 cm: to texture Smear slide: 380 cm	
	2.5Y8/2		365 - 388 cm: slightly mottled	
	2.5Y8/2 and 2.5Y7/3		388 - 433 cm: moderately mottled	
	2.5Y6/3 and 2.5Y8/2		430 cm: dropstone, Ø 30 mm 433 - 459 cm: strongly mottled	
2.5Y7/2		459 - 510 cm: lightly mottled 494 cm: 3 gravels up to Ø 10 mm		

Core ID: PS69/890-1	Latitude: 62° 46.230`S	Cruise: ANT-XXIII/9
Recovery: 7.47 m	Longitude: 82° 49.910`E	Water Depth: 2259 m

Lithology	Struct.	Color	Description	Age
5			513 cm: dropstone, Ø 5 mm 516 cm: dropstone, Ø 60 mm	
	2.5Y7/2		536 - 720 cm: Foraminiferal mud with some diatoms slightly mottled Smear slide: 590 cm	
6			662 cm: dropstone, Ø 5 mm 669 cm: dropstone, Ø 5 mm 700 cm: dropstone, Ø 70 mm 709 cm: dropstone, Ø 10 mm	
	10YR7/3 and 10YR8/2			
7			710 - 720 cm: Transition zone with color ranging from very pale brown to pale brown	
	10YR6/3		731 - 733 cm: gravel horizon with grains up to Ø 40 mm 736 - 747 cm: disturbed core catcher sediment	
8				
9				
10				

Die "Berichte zur Polar- und Meeresforschung"

(ISSN 1866-3192) werden beginnend mit dem Heft Nr. 569 (2008) ausschließlich elektronisch als Open-Access-Publikation herausgegeben. Ein Verzeichnis aller Hefte einschließlich der Druckausgaben (Heft 377-568) sowie der früheren "**Berichte zur Polarforschung** (Heft 1-376, von 1982 bis 2000) befindet sich im Internet in der Ablage des electronic Information Center des AWI (**ePIC**) unter der URL <http://epic.awi.de>. Durch Auswahl "Reports on Polar- and Marine Research" auf der rechten Seite des Fensters wird eine Liste der Publikationen in alphabetischer Reihenfolge (nach Autoren) innerhalb der absteigenden chronologischen Reihenfolge der Jahrgänge erzeugt.

To generate a list of all 'Reports' past issues, use the following URL: <http://epic.awi.de> and select the right frame: Browse. Click on "Reports on Polar and Marine Research". A chronological list in declining order, author names alphabetical, will be produced. If available, pdf files will be shown for open access download.

Verzeichnis der zuletzt erschienenen Hefte:

Heft-Nr. 570/2008 — "The Expedition ARKTIS-XXI/1 a and b of the Research Vessel 'Polarstern' in 2005", edited by Gereon Budéus, Eberhard Fahrbach and Peter Lemke

Heft-Nr. 571/2008 — "The Antarctic ecosystem of Potter Cove, King-George Island (Isla 25 de Mayo). Synopsis of research performed 1999-2006 at the Dallmann Laboratory and Jubany Station", edited by Christian Wiencke, Gustavo A. Ferreyra, Doris Abele and Sergio Marensi

Heft-Nr. 572/2008 — "Climatic and hydrographic variability in the late Holocene Skagerrak as deduced from benthic foraminiferal proxies", by Sylvia Brückner

Heft-Nr. 573/2008 — "Reactions on surfaces of frozen water: Importance of surface reactions for the distribution of reactive compounds in the atmosphere", by Hans-Werner Jacobi

Heft-Nr. 574/2008 — "The South Atlantic Expedition ANT-XXIII/5 of the Research Vessel 'Polarstern' in 2006", edited by Wilfried Jokat

Heft-Nr. 575/2008 — "The Expedition ANTARKTIS-XXIII/10 of the Research Vessel 'Polarstern' in 2007", edited by Andreas Macke

Heft-Nr. 576/2008 — "The 6th Annual Arctic Coastal Dynamics (ACD) Workshop, October 22-26, 2006, Groningen, Netherlands", edited by Pier Paul Overduin and Nicole Couture

Heft-Nr. 577/2008 — "Korrelation von Gravimetrie und Bathymetrie zur geologischen Interpretation der Eltanin-Impaktstruktur im Südpazifik", von Ralf Krockner

Heft-Nr. 578/2008 — "Benthic organic carbon fluxes in the Southern Ocean: regional differences and links to surface primary production and carbon export", by Oliver Sachs

Heft-Nr. 579/2008 — "The Expedition ARKTIS-XXII/2 of the Research Vessel 'Polarstern' in 2007", edited by Ursula Schauer.

Heft-Nr. 580/2008 — "The Expedition ANTARKTIS-XXIII/6 of the Research Vessel 'Polarstern' in 2006", edited by Ulrich Bathmann

Heft-Nr. 581/2008 — "The Expedition of the Research Vessel 'Polarstern' to the Antarctic in 2003 (ANT-XX/3)", edited by Otto Schrems

Heft-Nr. 582/2008 — "Automated passive acoustic detection, localization and identification of leopard seals: from hydro-acoustic technology to leopard seal ecology", by Holger Klinck

Heft-Nr. 583/2008 — "The Expedition ANT-XXIII/9 of the Research Vessel 'Polarstern' in 2007", edited by Hans-Wolfgang Hubberten